Effects of Dual Coating Proteins in Intraosseous Transcutaneous Amputation Prosthesis (ITAP)
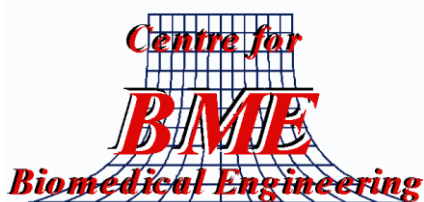
by

Moataz El-Husseiny MB ChB, MRCS

A thesis submitted in fulfillment for the higher degree of

Doctorate in Medicine [MD(Res)]

Institute of Orthopaedics and Musculoskeletal Science, Centre for

Biomedical Engineering, University College London, Royal National

Orthopaedic Hospital Trust, Stanmore, Middlesex,

HA7 4LP

April 2014

Declaration

I, Moataz El-Husseiny, confirm that the work presented in this thesis is my own. Where information has been derived from other sources, I confirm that this has been indicated in the thesis.

Moataz El-Husseiny_____April 2014

Abstract

Intraosseous transcutaneous amputation prostheses (ITAP) provide an alternative method of attaching artificial limbs for amputees. Conventional stump-socket devices are associated with soft tissue complications including pressure sores, neuroma formation and tissue necrosis. ITAP overcomes these problems by attaching the articial limb transcutaneously to the skeleton. In order for ITAP to be successful, it requires an infection-resistant transcutaneous barrier at the skin-implant interface.

Fibronectin (Fn) and Laminin 332 (Ln), are glycoproteins found abundantly in the extracellular matrix. Dual coating proteins ^{125}I-Fn + Ln and ^{125}I-Ln +Fn were covalently bonded to Ti6Al4V through silanization. **The hypothesis tested was: *silanized dual coating protein coatings with fibronectin and laminin, enhances both keratinocyte and fibroblast spreading and increases vinculin focal adhesion plaques on Ti6Al4V in vitro.*** Both remained stable when immersed in foetal calf serum compared with adsorbed dual coating proteins at all time points up to 72 hours ($p<0.05$). There was non-competitive binding of laminin on Ti6Al4V in the presence of fibronectin.

Keratinocytes and fibroblasts were grown on Ti6Al4V surfaces with single coating Fn, Ln, and dual coating FnLn on adsorbed, silanized with passivation and silanized without passivation discs. Vinculin focal adhesion markers and cell size were quantified. Silanized dual coating proteins without passivation (SiFnLn-) produced the largest number of vinculin markers and biggest cell size at all time points upt to 24 hours ($p<0.05$).

Hydroxyapatite (HA) is a naturally occurring osteoinductive mineral in the body. [125] I-Fn coated on HA discs was assessed for optimal time for loading, concentration and durability. Fibroblasts were grown on polished, HA and Fn coated HA discs. Vinculin markers and cell size were quantified. Fn coated HA discs increased fibroblast attachment compared to uncoated controls of Ti6Al4V discs and HA discs ($p < 0.05$).

My thesis demonstrated silanized without passivation dual coating proteins FnLn produced more viculin markers per cell unit and per cell area when compared to uncoated controls and single coating proteins on adsorbed and silanized, passivated discs. Further research is required to establish whether dual coating proteins will produce the same effect *in vivo*. This can be achieved by silanizing ITAP with dual coating FnLn and implanting them in animals. Histopathological analysis at the skin-implant interface would provide valuable information whether this biochemical and physical modification improve soft tissue integration to percutaneous implants.

Acknowledgements

First and foremost I would like to thank God for giving me the power to believe in my passion and pursue my dreams. I could never have done this without the faith I have in You.

I am greatly indebted to Professor Blunn, who has been a great inspiration and provider of continuous help and support, throughout my journey in completing my thesis. This work would have never been finished without him. I would also like to extend my sincere gratitude to Professor Haddad for helping me greatly throughout my career and always being there for guidance. I would like to thank Dr. Pendegrass for her help in this thesis and for performing the experimental work for Chapter 5.

I would like to thank Mr. Mark Harrison, Ms. Rebecca Porter, all staff and students at the Centre for Biomedical Engineering and the Institute of Orthopaedics who taught me the experimental basics in laboratory work and provided invaluable guidance.

I would like to extend my gratitude to Mr Achan, Mr Nolan and all the consultants I worked for. Each one of them has helped me greatly in my career.

I want to especially thank my parents, for always encouraging and supporting me. They are the reason for where I am today. My wife, Sherihan, has been a great asset in my life and I am so grateful for all her help and input together with raising our two beautiful children, Mariam and Yaseen.

I would like to dedicate this thesis to my loving parents, wife and children.

Table of Contents

List of Figures

List of Abbreviations, Formulae and Conventions

^{125}I-Fn	**Radiolabelled Ionized Fibronectin**
^{125}I-Ln	**Radiolabelled Ionized Laminin**
APS	**3-Aminopropyltriethoxylsaline**
BMP	**Bone Morphogenetic Proteins**
CO_2	**Carbon Dioxide**
DMEM	**Dulbecco's Modified Eagle's Medium**
DGEA	**Aspartate- Glycine- Glutamate- Alanine**
ECM	**Extra-Cellular Matrix**
FCS	**Fetal Calf Serum**
FDA	**Fluorescein diacetate**
FITC	**Fluorecein Isothiocyanate**
Fn	**Fibronectin**
FnLn	**Dual coating proteins fibronectin and laminin**
H_2O_2	**Hydrogen peroxide**
ITAP	**Intraosseous transcutaneous amputation prosthesis**
kDa	**Kilo-Dalton**
Ln	**Laminin**
mRNA	**messenger Ribonucleic acid**
PBS	**Phosphate Buffered Saline**
Pol	**Polished uncoated control**

PMMA	**Polymethylmethacrylate**
PPy	**Polypyrrole**
R_a	**Average Roughness**
RDGC	**Arginine- Aspartate- Glycine- Cysteine**
RGD	**Arginine- Glycine- Aspartate**
RGDC	**Arginine- Glycine- Aspartate- Cysteine**
RGDK	**Arginine- Glycine- Aspartate- Phenylalanine- Lysine**
RNA	**Ribonucleic acid**
Si+	**Silanized passivated uncoated control**
Si-	**Silanized non-passivated uncoated control**
SiFn+	**Silanized passivated fibronectin**
SiFn-	**Silanized non-passivated fibronectin**
SiFnLn+	**Silanized, passivated dual coating proteins fibronectin and laminin**
SiFnLn-	**Silanized, non-passivated dual coating proteins fibronectin ad laminin**
SiLn+	**Silanized passivated laminin**
SiLn-	**Silanized non-passivated laminin**
SMP	**N-succinimidyl-3-maleimidopropionate**
Ti	**Titanium**
Ti6Al4V	**Titanium alloy**
YIGSR	**Tyrosyl- Isoleucyl- Glycyl- Seryl- Arginine**

CHAPTER 1

Introduction

1.1 Background, Objectives and Aims of this Thesis

The aim of this thesis is to explore the behaviour of skin keratinocytes and dermal fibroblasts in the presence of dual coating proteins; fibronectin (Fn) and laminin (Ln) on titanium alloy (Ti6Al4V). The hypothesis tested was silanized non-passivated dual coating protein coatings provides a superior surface for cell spreading and provides more focal adhesion vinculin markers This provides a bio- and physicochemical modified Ti6Al4V surface that promotes cell spreading, which can be applied to the design of percutaneous medical devices.

Intraosseous Transcutaneous Amputation Prosthesis (ITAP) is an implant that breaches the skin barrier. For it to be successful, it requires a tight skin-implant seal, which prevents wound down-growth and marsipulization that leads to infection and ultimate failure of the implant.

The objectives are to:

1.   Assess the release kinetics of dual coating radio-labeled Fn and Ln coated on the surface of Ti6Al4V soaked in fetal calf serum (FCS).

2.   Perform cell bioassay to assess the influence of a Ti6Al4V- dual coating protein fibronectin and laminin (FnLn) on keratinocyte attachment though vinculin attachment markers.

3.   Compare fibroblast attachment on silanized dual coating protein FnLn to adsorbed dual coating FnLn, adsorbed and silanized single coating Fn and Ln on Ti6Al4V alloy.

The hypothesis was: *silanized dual coating protein coatings with fibronectin and laminin, enhances both keratinocyte and fibroblast spreading and vinculin markers on Ti6Al4V in vitro* **by modifying the surface both physically and biochemically.**

1.2 Amputation

Amputation comes from the Latin word *amputare*, "to cut away". It has been present with human civilization for thousands of years and remains of prosthetic limbs have been found in preserved human Egyptian mummies.

Removal of a body extremity could be done as a result of congenital deformity, trauma, infection or prolonged vasoconstriction. Nowadays, the main indications for amputation are to relieve intractable pain symptoms and/or to preserve life eg. Gangrene and cancer. In few countries, amputation is implemented as a punishment for criminal actions.

1.2.1 Limb amputation

Amputation of the lower limb is ablation of a leg from below the pelvis at any level. Starting from bottom to top, these include digit amputations, partial foot amputations (Ray, Lisfranc or Chopart's amputations) and ankle disarticulation.

In a similar way, amputations of the upper limb include amputation of digits, metacarpal amputation, wrist disarticulation, forearm amputation (trans-radial), elbow disarticulation, above-elbow amputation (trans-humeral), shoulder disarticulation and forequarter amputation.

The amputation rate in the UK is 5·1 per 100 000 population in major limbs and this figure has not changed from 2003 to 2008 (Moxey et al., 2010). The number of lower limb amputations referrals for prosthesis across the UK was 4957 between April 2006 and March 2007. In the United States, there was 1.6 million people with one limb in 2005 with 1 in 190 individuals affected (Ziegler-Graham et al., 2008).

1.2.2 Amputation Prostheses

Once amputation is established, prosthesis is required for both cosmetic and functional purposes. Prosthesis comes from the Greek word *prostithenai* meaning "to add" or "to put". It is an artificial extension that replaces a missing part.

During the 1980s, advances in lower limb prostheses technology led to the invention of the Sabolich socket for below knee amputees (Sabolich and Guth, 1986). The design held the patient's limb like a glove, locking it and distributing the weight evenly over the stump. The main advantage was to snugly fit the patient's remaining limb allowing rotational stability and comfort. This enabled patients with above knee amputations to walk with a more normal gait, run, step over, step and walk down stairs. On the other hand, despite advances in using thermoplastic and gel liners to accommodate for the prostheses, there remained a large element of skin irritation and need to re-adjust the socket due to changes in stump size.

In 1999, microprocessor-controlled prosthetic knees became available. This made walking feel and look more natural. These prostheses used hydraulic and pneumatic controls and a microprocessor that provided a gait more responsive to change in walking speeds. The hydraulic cylinders controlled knee flexion while moment sensors in the prosthetic limb sent signals to the microprocessor, which in turn sent signals to the hydraulic controls

about the resistance that needed to be supplied. The leg had a knee-angle sensor to measure the angular position and velocity of the flexing joint. The main disadvantage was that it was prone to water damage. It had a learning curve, taking months to accustom to the amputee's gait, during which the patient was susceptible to increased falls and injury. In addition to this, the patient must possess a satisfactory cardiovascular and pulmonary health.

Robotic prostheses have biosensors that detect signals from the amputee's neuromuscular system. These implants utilise surface electromyography (EMG) signals detected by electrodes from normal muscle contraction. A controller in the prosthesis analyzes this information and initiates movement through a motor that mimics the actions of a muscle. In 2003, Jesse Sullivan became the first person to be implanted with this bionic prosthesis. He was an electrician who lost both his arms getting electrocuted. Surgeons reconnected nerves in his arm stump to his chest muscles in a procedure called targeted muscle re-innervation. Surface electrodes were then attached to his chest muscles. He was taught to move his prosthetic limb by contracting his chest muscles (Miller et al., 2008).

1.3 Intraosseous Transcutaneous Amputation Prosthesis (ITAP)

Intraosseous Transcutaneous Amputation Prosthesis (ITAP) is an amputation device that fixes residual long bone of an amputee to an external prosthetic limb. It overcomes problems of conventional stump-socket prostheses; pressure sores, infection, uneven distribution of forces at stump and neuroma formation, through transferring forces normally

encountered by stump-soft tissues directly to the skeleton. It is currently under

development at the Centre of Biomedical Engineering, Stanmore, UK.

© Paul Rogers/The Times

Figure 1.1: Picture of ITAP patient (http://www.dailymail.co.uk/health/article-1092793/Survivor-7-7-bombings-fitted-clip-arm-fuse-skin.html)

ITAP is formed of a Ti6Al4V rod with a flange, where the proximal end is implanted in the

medullary canal of a long bone and the distal end penetrates the skin providing an anchor

to which prosthesis may attach. It depends on the concept of osseointegration at the

proximal end and a tight seal at the skin-implant interface for its success (Figure 1.1).

In 1974, G. Winter at the Centre of Biomedical Engineering, UK published results from

experiments looking at percutaneous implants penetrating porcine skin with a view at

providing an artificial limb that attaches directly to the skeleton (Winter, 1974). He provided

good results to overcome wound down growth and marsupialisation by penetrating skin

with porous polytetraflurethylene implants of 10μm diameter and hydrogen sponge of 40

µm pores. He found the implants became invaded with fibrous tissue and this prevented epidermal down-growth and subsequent infection.

It was not until 2006 where work in the same Centre, identified deer antlers as natural analogues of ITAP (Pendegrass et al., 2006). They studied deer antlers' morphology to determine whether there was a difference in pore size and frequency between antlers and the pedicle bone structures. During the growth phase of deer antlers, a velvet hairy skin covers the antler which is abundant in blood supply. As the deer matures and androgen levels increase, the velvet layer is shed and the antler is left exposed during the mating season. The presence of a subcutaneous pedicle, which is a living bone that undergoes continuous bone remodeling, and attaches to the skin with sufficient strength that prevents wound down-growth and infection.This aided in the development of ITAP by implementing design modifications to mimic deer antlers through providing a flange with pores, coated with hydroxyapatite at the skin penetrating section of the implant. There was a significant decrease in down-growth using these implants, compared with the straight implants (Pendegrass et al., 2006). However, consistent epithelial attachment was not observed and further studies were needed to provide a tight seal around the implant.

In 2008, Pendegrass et al., demonstrated that changing the surface topography of Ti6Al4V affects *in vitro* cell attachment. Attachment is measured by calculating the required force to displace cells from the surface using atom force microscopy. They compared smooth polished, machine finished, sand blasted and acid etched surfaces. They assessed proliferation of keratinocytes on these surfaces using immunofluorescent microscopy. Cell morphology was studied on each surface using scanning electron microscope and cell attachment via vinculin; BP 180 and α6 integrin antibodies were assessed. They found a positive linear correlation between cell attachment and number of vinculin markers

produced. They concluded smooth polished discs provided significantly greater numbers of focal adhesion markers than other surfaces at all time points. They suggested up-regulation of intracellular signalling pathways required for focal adhesion and assembly of hemidesmosomes, may be lacking in surfaces with greater roughness. This is achieved via flattened, spread and well attached cells with high proliferative capacity compared with rounder and more loosely adhered phenotype.(Pendegrass et al., 2008).

Further research was conducted to determine the effect of extracellular matrix components, such as fibronectin, that have a role in regulating assembly of focal adhesions. RGD sequences present on module III of the fibronectin provide attachment sites for transmembrane integrin linkers. These in turn provide attachment arms for actin myoskeleton with the aid of vinculin, talin and pixillin. Adsorbed fibronectin enhanced fibroblast activity and adhesion via focal contacts *in vitro* (Dean et al., 1995, Gallant et al., 2005). However, *in vivo* studies (Pendegrass et al., 2006) histologically assessed the percentage of soft-tissue contact area and cell alignment to the plate. They concluded adsorbed fibronectin does not affect dermal attachment around ITAP implants. This was because of lost adsorbed fibronectin during implantation and competitive binding from other serum proteins. In 2007, Middleton et al., investigated the effect of covalently bonding fibronectin to Ti6Al4V surfaces via silanization *in vitro*. Silanized fibronectin to Ti6Al4V was durable when soaked in protein-rich fluid compared with adsorbed fibronectin and increased early fibroblast adhesion and spreading. They also showed that silanized fibronectin did not affect cell metabolism.

Keratinoctyes have shown to adhere more rapidly in the presence of laminin, a glycoprotein present abundantly in the basement membrane (Fleischmajer et al., 1998). They measured integrins present on the keratinocytes using immunofluorescent

microscopy, and measured total RNA of keratinocytes using Northern Blot. In 2010, Gordon et al. investigated the effect of silanized laminin to titanium alloy, on keratinocyte attachment *in vitro*. They quantified focal adhesions through immunostaining vinculin markers by fluorescent antibody. Their results showed a significant increase in the numbers of vinculin plaques compared with non-treated Ti6Al4V control discs or with adsorbed laminin surfaces.

In epithelial cells, there are two main types of cell-cell attachments, adherens junctions and desmosomes (Lozano & Cano, 1998). In adherens junctions, transmembrane protein E-cadherin, binds to α, β, and γ-catenins, which link the complex to actin cytoskeleton. This complex maintains a tight seal epithelium and prevents epithelial down growth (Hodivala and Watt, 1994). Further research by adsorbing E-cadherins to Ti6Al4V to form cell-cell attachments at the implant interface showed promising results *in vitro* (Pendegrass et al., 2012). They demonstrated that adsorbed E-cadherin on Ti6Al4V discs significantly increased metabolic activity, cell area and vinculin markers in keratinocytes *in vitro* at 24, 48 and 72 hours. In an attempt to enhance fibroblast attachment at the cell-implant interface, fibronectin coated hydroxyapatite discs showed significantly better attachment than hydroxyappatite discs alone or Ti6Al4V controls at 1, 4 and 24 hours (Pendegrass et al., 2012).

In 2011, ITAP was used clinically in the limbs of 4 dogs with malignant neoplasia of distal limbs for limb salvage. Owners and veterinarians assessed functional outcomes, in addition radiographic and histological examinations were conducted. Dermal integration of ITAP was achieved at 3 weeks (based on clinical inspection and palpation of the skin-iplant interface) and dogs were walking pain-free at 8 weeks. ITAP fracture occurred in 1 dog at 10 weeks and an ITAP replacement was done. ITAP-limb interface showed both

osseous and dermal integration at 1 year. Results and information from this study paved the way for using ITAP in humans, namely on an amputated humerus in a survivor of the 7/7 London terrorist attack

1.4 Osseointegration

Osseointegration is the direct integration of artificial implants to living bone. It is defined as a "direct structural and functional connection between ordered living bone and the surface of a load-carrying implant" (Branemark, 1977). An implant is considered osseointegrated when there is no progressive relative movement between the implant and the bone with which it has direct contact. This can be measured indirectly via histologically examination to determine the bone integration with implant. The theory relies on an anchorage mechanism whereby the living bone is incorporated in the implant, so the anchorage can persist under all conditions of loading. In terms of amputation prostheses the concept of osseointegration refers to the bone integration of an implant that is used to attach an external prosthetic device such as an artificial arm or leg. This method provides better muscle control of the prosthesis, allowing ability to use for extended periods of time and for trans-femoral amputees to drive.

In the 1960's, Professor Per-Ingvar Branemark found titanium screws used for implantation in rabbits' bones were difficult to remove (Branemark et al., 1969). He investigated usage of titanium implants in dental tentures. Although his work was initially directed to mandibular reconstruction for malignancy and trauma (Branemark et al. 1975), he later extended it to long bones. In 2010, they reported their results for osseointegrated

titanium implants for limb prostheses' attachments. Out of 39 implants, there was an infection rate of 18% at 3 years follow-up (Tillander et al., 2010).

Branemark's work showed that the living bone could become so fused with the titanium oxide layer of the implant that the two could not be separated without fracture (Branemark, 1983). The main advantage of osseointegrated amputation prosthesis is its ability to avoid pressure loading at the prosthesis-stump interface. This improves stump comfort, eliminates poor prosthetic socket fit and skin problems (Sullivan et al., 2003). Since the prosthesis is skeletally load bearing, the mechanical forces during the gait cycle are transmitted through bone. This allows patients to walk further, be more active and feel as though they use less energy than using a conventional prosthesis. Users feel less disabled and because the alignment of the external components is preserved, they are able to participate in full daily living and activities such as cycling (Sullivan et al., 2003). Amputees also reported improved sensory feedback from the skeletally attached limb through osseoperception (Branemark et al., 2001). This is permitted through for perception of pressure and ground texture (Lundborg et al., 2006).

1.4.1 Applications of osseointegration

1.4.1.1 Dental reconstruction

Osseointegration has been using to replace missing single teeth, for partially edentulous segment of the mouth, and for reconstruction of a completely edentulous patient. Long-term success rates reveal superiority of osseointegration over conventional prosthodontics (Esposito et al., 1998).

1.4.1.2 Facial prostheses

Major maxillofacial defects may utilize an implant that supports prostheses together with bone graft to reconstruct facial defects. Osseointegration implants allowed stabilization of lower partial dentures.

When external ears are removed due to trauma or tumour, successful anchorage of an artificial pinna to the temporal bone is possible by osseointegrated implants. Similarly, orbital prostheses have been anchored to the orbital rim. Bone anchored hearing aids are osseointegrated titanium flanges that aid patients with sensorineural loss. Many patients have benefited from this device designed by Branemark and Kuikka (Branemark et al., 2001), that provided an alternative to hearing aids attached percuataneously.

1.4.1.3 Finger Amputation

Branemark and Lundborg (Lundborg et al., 1996) implanted osseointegrated thumb prostheses in a cohort of 3 patients with traumatic thumb amputation at the metacarpophalangeal joint level . These patients underwent a two-stage reconstruction aimed at fixing a titanium rod within the thumb metacarpal medullary cavity to allow osseointegration. After 3 months of unloading this rod, a second stage involved attaching a skin-penetrating component on top of the titanium rod and modifying the skin graft to decrease relative mobility. Skin healing occurred without any complications. The follow up ranged from 18 months to 3 years. At the final follow up, patients were satisfied with the shape of the prosthesis, felt it was a better tool for fine manipulative tasks and reached excellent results in the Moberg pick-up test, pulp pinch strength, lateral pinch strength, grip strength and grip function.

1.4.1.4 Lower Limb Amputation

In 2001, Branemark implanted lower limb amputation prostheses in rat models. Their results showed excellent intramedullary osseointegration in addition to the presence of nerve endings around titanium implants (Ysander et al., 2001). Pure titanium rods were implanted in femora of 18 rodents for 8 weeks. Microscopic and immunohistochemical observation of the implant-bone interface indicated successful osseointegration with normal remodeled bone. Calcitonin gene-related peptide activity was up-regulated. There was new, normal bone adjacent to and fully occupying the space between fixture threads. Innervation appeared in remodeled bone through the observation of small nerve fibres.

1.5 Infection in Transcutaneous Osseointegrated Implants

Infection has a detrimental effect to osseointegrated transcutaneous amputation implants. For ITAP to be successful, it must have a tight barrier around the skin-implant interface, together with a stable long-term fixation between metal and bone. This has to take into account mobility of adjacent skin, presence of a subcutaneous fatty layer which not only may not integrate with the implant, but also allow the movement of overlying skin against the implant, and attachment properties of keratinocytes, that are different from gingival cells, and hence may nt attach as firmly to dental implants.

Tillander et al., 2010 prospectively followed 39 patients with arm and leg amputations fitted with transcutaneous osseointegrated titanium implants for a mean of 56 months. They reported an infection rate of 5% at inclusion and 18% at 3 years follow-up. In 5 out of the 7 patients with infections, prosthetic use was not affected. Staphylococcus aureus and

coagulase negative staphylococci were the common organisms in the superficial and deep cultures.

Long-term follow-up for dental osseointegrated implants have been reported by Adell et al. 1990. They implanted 4636 standard fixtures in 700 patients with a follow-up for 15 years. More than 95% of maxillae had continuous prosthesis stability at 10 years and 92% at 15 years. For mandibles, stability remained at 99% at 15 years. Estimated survival rates for fixtures in the maxilla and mandible were 78% and 86% respectively at 15 years.

In an attempt to overcome risk of infection, Chou et al., 2010 examined the efficacy of antimicrobial pexiganan acetate in preventing pin tract infection of trancutaneous osseointegrated implants in a rabbit model. They applied topical antibiotic pexiganan acetate 1% daily at the skin-implant interface for 24 weeks (n=8). They found a significant reduction of pin site infection compared to the Ti controls (n=11) at p=0.019 (Chou et al., 2010).

My work tests whether silanized dual coating protein coatings with fibronectin and laminin, enhances both keratinocyte and fibroblast spreading and vinculin markers production on Ti6Al4V in vitro.

1.6 Titanium alloy

Titanium is an element with an atomic number of 22. It is strong, light, corrosion resistant metal. It was first discovered in Cornwall in 1791 and named after the Greek Titans. Due to its high strength-to-weight ratio, it is widely used in aerospace, military, automotive, medical prostheses, dental and orthopaedic implants, mobile phones and jewellery.

Titanium is commonly used as an alloy. Ti6Al4V contains 6% aluminium, 4% vanadium, 0.25% iron, 0.2% oxygen and the remainder is titanium. It has the advantage of being stronger than pure titanium with the same stiffness and thermal properties. It has a density of roughly 4420 kg/m3, Young's modulus of 110 GPa and tensile strength of 1000 MPa. In comparison to stainless steel, which is also used widely in medical implants, Ti6Al4V has greater superior strength under repeated load stresses, withstanding more strain during internal fixation. In addidtion, it is lighter and has a lower modulus of elasticity, making it is less rigid.Titanium is also less prone in generating an immune reaction as it is corrosion resistant compared to stainless steel.(Davies, 2003; Raisanen et al., 2000). Due to its properties, popular use in orthopaedic implants and previous studies on ITAP in our Institute, Ti6Al4V was chosen in my studies.

1.7 Epidermis

The epidermis acts as a physical barrier against pathogens found in the external environment and is arranged in multi-layers. The main cell unit is keratinocyte that produces keratin. They become activated by growth factors and cytokines. This in turn increases keratin gene expression and production of keratin which enables re-epithelialization. The most superficial layer consists of stratum corneum (horny layer), which is acellular and abundant in keratin. Deeper to this is stratum lucidum (clear layer), followed by stratum granulosum (granular layer), then stratum spinosum (prickle cell layer) and finally stratum basal (basal layer). The basal layer produces cuboidal keratinocytes. These attach to the basal layer through hemidesmosomes and to adjacent cells via desmosomes. As keratinocytes mature, they migrate up to more superficial layers. When they reach the stratum spinosum, they attach together via desmosomes and adherens junctions. As they become more superficial, they become flat and die, where keratohyaline

granules combine with intermediate filaments and cell membrane depositing intracytoplasmic keratin within the horny layer. Besides keratinocytes, epidermis also includes basal melanocytes, antigen presenting Langerhan's cells and Merkel cells.

The basement membrane is crucial in maintaining skin integrity and adheres the epidermis to the dermis resisting their separation by shearing forces. The foundation cement that makes this adherence possible are anchoring fibrils, filaments and collagen IV.

The dermis is found deeper to the basement membrane. It is formed of tough elastic connective tissue that contains epidermal appendages as hair follicles, nerve endings, blood and lymphatic vessels. Fibroblasts are found abundantly in this layer, producing collagen and fibronectin. Macrophages, lymphocytes and mast cells are also present in the dermis. The dermis acts as a supportive layer to the overlying epidermis.

1.8 Fibronectin

Fibronectin is a rod-like glycoprotein found abundantly in the body with molecular weight of 440 kilo-Daltons (kDa). It is involved in many cellular processes, including tissue repair, embryogenesis, blood clotting, cell adhesion, growth, migration and differentiation. Fibronectin binds to cell membrane via integrin receptors and to extra-cellular matrix protein such as heparin, fibrin and collagen. This allows fibronectin to act as a cell adhesion molecule by anchoring cells to proteoglycans or collagen. Fibronectin is found in two forms: an insoluble cellular form present in the extracellular matrix produced by fibroblasts, chondrocytes, endothelial cells, macrophages and epithelial cells. The other form is a soluble plasma glycoprotein, formed in the liver and circulates the body in plasma.

Fibronectin is a dimer, formed of two monomers linked by a pair of C-terminal disulfide bonds (Mao et al., 2005). Each monomer is composed of three different types of repeating modules: types I, II and III. Each module is formed of anti-parallel beta strands ().

Type I module is made up of approximately 45 amino acids, found in the amino and carboxy terminal regions of the protein. Two anti-parallel beta strands make up the top sheet, which folds over a bottom sheet that in turn is composed of three anti-parallel beta strands. These sheets interact through hydrophobic and disulfide bonds that stabilize the module. Interactions between adjacent modules are important to fibronectin structure. Twelve type I modules are involved in collagen binding. Two type II modules are found in fibronectin, which are 60 amino acids in length. These are involved in collagen binding. The most abundant module in fibronectin is Type III, where 15-17 modules make up the fibronectin molecule. Each module is composed of 90 amino acids in length. Type III module contains the tripeptide Arg-Gly-Asp (RGD) receptor recognition sequence along with binding sites for other integrins and heparin. The RGD sequence located in Type III module 10 is the site of cell attachment via $\alpha 5\beta 3$ integrins on cell surface. Like other fibronectin modules, type III module cores are made up of overlapping beta sheets. The top sheet contains 4 antiparallel beta strands and the bottom sheet is composed of 3 anti-parallel strands. Unlike types I and II modules, type III are not stabilized by disulphide bonds allowing type III modules to partially unfold under pressure (Erikson 2002). A "variable" V-region exists within fibronectin structure. Its presence and length may vary. This region contains the binding site for $\alpha 4\beta 1$ integrins. The V-region sequence is present in cellular fibronectin but in one of the two subunits in plasma fibronectin.

1.9 Laminin

Laminin is a large 990 kDa glycoprotein that plays a fundamental role in the architectural structure of almost every tissue in the body. This is achieved through its presence in the extracellular matrix, hence interacting with transmembrane integrin linkers to promote cell regulation, adehesion, differentiation and migration. This interaction allows cell cytoskeleton, intermediate filaments and actin to bond to extracellar matrix and organize tissue structuring and adhesion. (Beck et al., 1990). Each laminin protein is formed of α-chain, β-chain and γ-chains, which are found in five, four and three genetic variants respectively (Figure 1.2). The molecules are named according to their chain composition. Thus, laminin-311 contains α3, β1, and γ1 chains. Fifteen chain combinations are present in vivo. The chains intersect to form a cross-like structure that can bind to other cell membrane and extracellular matrix molecules. The long arm binds to cell membrane via integrin receptors anchoring cells to the basement membrane, while the shorter arms are best adapted to binding to other molecules, which allows them to form sheets. RGD complex is located on α chain and is responsible for promoting endothelial cells attachment through their linkage to integrin molecules which triggers the interactin with vinculin, paxillin and actinin. This forms an intracellular adhesion complex which attaches to actin and anchoring filament myoskeleton.

A chain

YIGSR
Cell attachment

RGD
Cell attachment

B1 chain

B2 chain

Cell attachment
Heparin binding

G chain
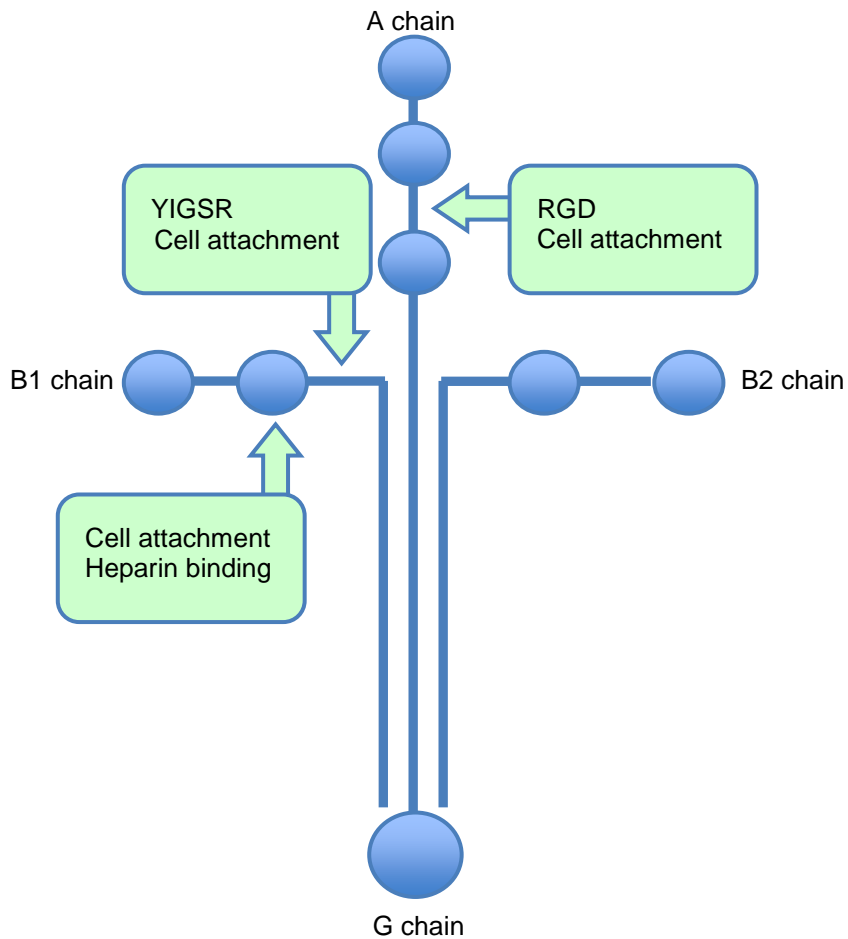
Figure 1.2: Schematic diagram of laminin structure showing locations of biologically active sites (Kleinman and Weeks, 1989)

1.10 Vinculin

Vinculin is a cytoskeletal protein part of focal adhesion complex involved in linking integrin adhesion molecules to actin cytoskeleton. It is 117 kDa with 1066 amino acids. It consists of a globular head domain that contains binding sites for talin, α-actinin as well as a tyrosine phosphorylation site, while the tail region contains binding sites for F-actin, paxillin and lipids (Goldman et al., 2001).

Vinculin is associated with focal adhesion complexes that nucleate actin filaments and cross linkers between the external medium, plasma membrane and actin cytoskeleton.

The complex at the focal adhesions consists of several proteins such as vinculin, α-actin, paxillin, and talin, at the intracellular face of the plasma membrane. Amino-terminal of vinculin binds to talin, which binds to β-integrins and the carboxy-terminal binds to actin, phospholipids, and paxillin-forming homodimers. The binding of vinculin to talin and actin is regulated by polyphosphoinositides and inhibited by acidic phospholipids. The complex then serves to anchor actin filaments to the membrane (Ezzell et al. 1997).

Focal adhesions are macromolecular complexes that mediate mechanical forces and regulatory signals across the cell membrane. They are in a state of constant flux, proteins associate and disassociate with the focal adhesion continuously as signals are transmitted to other parts of the cell, regulating cell activity. Focal adhesions connect to extra-cellular matrix protein via integrins. Integrins bind to extra-cellular proteins through short amino acid sequences such as Arginine- Glycine- Aspartate (RGD), or DGEA and GFOGER sequences in collagen.

The intra-cellular domain of integrin binds to cytoskeleton through adapter proteins such as talin, α-actinin, filamin and vinculin. Many other intracellular signalling proteins, such as focal adhesion kinase, bind to and associate with this integrin-adapter protein–cytoskeleton complex and this forms the basis of a focal adhesion (Ziegler et al., 2006).

1.11 Adhesion markers- Integrins

Integrins are trans-membrane receptors that regulate attachment between the cell and tissues. They play an important role in cell signalling, affecting cell shape, size, motility and cell cycle. Integrins transduce information to and from the cell to the surrounding environment, which affect both cell and the environment. Integrins are responsible for

binding the cell surface to adhesion proteins as fibronectin, laminin, vitronectin and collagen.

Integrins are heterodimers containing two chains, alpha and beta. There are 18 different alpha chains and 8 beta chains. Each chain contains two tails. These tails penetrate the cell membrane into the surrounding matrix. The molecular mass of integrin varies from 90 kDa to 160 kDa. Integrins aid cell attachment, migration, differentiation or death. Integrins are the corner-stone of focal adhesion complexes, which are formed of complexes of integrins, talin, vinculin, paxillin and alpha actinin. The complexes regulate focal adhesion kinase and cause clustering of these complexes. The clusters provide intra-cellular binding sites on the cytoplasmic side of the membrane. The complexes connect the extra-cellular matrix to actin bundles.

Integrins play an important role in cell migration. Cells attach to surrounding substrate through integrins. During cell movement, integrins are moved back from the membrane-substrate contact into the cytoplasm by endocytosis. They are transported through the cell and moved to the new substrate-membrane contact by endocytic cycle.

1.12 Hemidesmosomes

Hemidesmosomes are junctional protein complexes that advocate epithelial cell adhesion of stratified and complex epithelia, as found in skin, cornea, amnion, grastrointestinal and respiratory tracts, to underlying basement membrane or substrate (Borradori and Sonnenberg, 1999). Hemidesmosomes consist of intracellular transmembrane proteins (Koster et al., 2003) and their assembly is vital for the migration of keratinocytes, and adhesion of keratinocytes to basement membrane and titanium implant.

Hemidesmosomes are formed of triangular plaques with a length <0.5μm (Borradori and

Sonnenberg, 1999). Their sub-basal dense plate lies external to the membrane and thin

extra-cellular anchoring filaments extend into basement membrane (Jones et al., 1998).

Their structure is divided into cytoplasmic plaque proteins; plectin and BP 230,

transmembrane proteins; $\alpha6\beta4$ integrins and BP 180 and basement membrane associated

proteins; laminin.

Hemidesmosomes have an important role in cell adhesion through intra-cellular

intermediate filaments attaching to hemidesmosomes. Hemidesmosomes in turn attach to

the basement membrane by anchoring filaments (Rousselle et al., 1995).

They also help in wound repair and cell migration through modulating $\alpha6\beta4$ integrin

expression, stimulating cell migration. In turn, these integrins regulate differentiation,

metabolic activity and apoptosis (Mainiero et al, 1995).

In summary, testing amount of focal adhesion vinculin markers and cell spreading give an

indication of the behavior of keratinocytes and fibroblasts in the presence of bio-chemically

and physically modified surfaces. I understand that the methods used in my thesis do not

directly test attachment of tissues to titanium and should not be treated as such until direct

in vitro methods are used such as atom focus microscopy and *in vivo* studies examining

histological slices for percentage of soft tissue attachment to ITAP.

1.13 Modes of Protein Attachment to Ti6Al4V

Several methods have been used that improve metal surface fixation and subsequent

implant survival. Physicochemical modifications that alter surface charge, composition or

morphology have been used. In addition, biochemical methods have been used to achieve

better cell attachment to metal. Biochemical modification of both organic and inorganic surfaces influences cell adhesion, differentiation and growth (Weetall, 1993). Enzyme immobilization to inorganic materials have been developed (Halling and Dunnill, 1979) and applied to osseointegration successfully (Puleo, 1995).

1.13.1 Adsorption

This represents the simplest form of biochemical modification of inorganic surfaces. It is done by simple immersion of a substrate into a solution of protein without changing the structure of either. They attach by weak H-H bonds, intermolecular van der Waal forces and salt channel bonds. The main advantage of this method is its simplicity; however several studies showed that a large percentage of protein coating is easily washed away from the titanium alloy. There is little control over release, retention and orientation of molecules. Weak bonds retain proteins, which detach from the surface in an uncontrolled fashion. If targeted response is required, an alternative biochemical method is needed to couple proteins on titanium.

1.13.2 Silanization

Silanization is a biochemical process that modifies an inorganic substrate so that bioactive proteins could be immobilized to it. A silicon base group of atoms attach to the substrate surface called the silane complex. This in turn bonds to a spacer arm of glutaraldehyde, which acts an intermediary for protein coupling. This method is biocompatible and improves protein attachment to metal (Rezania, 1997). Puleo, 1995 (48) and Nanci et al., 1998 showed that silanization does not affect enzyme activity of silanized protein.

There are 2 methods of silanization depending on the solvent used: aqueous and organic. Aqueous silanization provides thinner silane layer with greater coverage compared to organic, which provides a thicker layer, loosely bound, but with higher capacity coating (Weetall, 1993). Methoxy-salines and ethoxy-salines are chemical forms that can be used with both solvents whereas chloro-silanes can only be used with organic solvents.

Silanization linkers are required to immobilize protein to the silane complex. Several spacer arms are available and choice depends on silanization complex and reactive groups on the protein. Bifunctional spacer arms are composed of two functional groups on each end, which can be the same (homo-bifunctional) or different (hetero-bifunctional). Gluteraldehyde is a homo-bifunctional spacer arm, used commonly with metal-protein immobilization, with two CHO groups attaching protein to titanium surface with spacer arm of 10 atoms (Weetall, 1976; Halling and Dunnill, 1979; Puleo, 1995; Nanci et al., 1998).

In my thesis, γ-aminopropyltriethoxysilane (APS) is used as a silane complex and gluteraldehyde as a spacer arm. This silane complex was used based on previous work done by the same group, testing single coating fibronectin covalently bonded to titanium alloy in presence of fibroblasts, and testing single coating laminin covalently bonded to titanium alloy in presence of keratinocytes. Weetall first used APS with inorganic substrates in 1976. It has 2 functional groups; the silane group; composed of a silicon atom attached to 3 hydrocarbon (alkyl) chains and an amino group. The silane group attaches to oxidized Ti6Al4V surface, through its silicone based molecule which bonds to Ti_2O, while the amino group bonds to gluteraldehyde spacer arm. APS forms self-assembly polymers, resulting in increased stability and this increases the stimulatory effect of biological molecules (Ito, 1992).

Chemically modifying Ti6Al4V surface will also change the surface roughness (R_a).

Average surface rougness is the measure of texture of a surface. It is based on a

statistical representation of surface deviations (peaks and valleys) from local mean surface

height. It can be measured either by contact, using a probe across the surface; or non-

contact optical method. Surface roughness (R_a) is mathematically defined as:

$$R_a = \frac{1}{n} \sum_{i=1}^{n} |y_i|$$

n represents equally spaced points along the trace, and y_i is the vertical distance from the

mean line to the ith data point. Height is assumed to be positive in the up direction, away from

the bulk material (Degarmo et, 2003).

1.13.3 Plasma Treatment

Plasma techniques can deposit ultra thin, adherent coatings. Glow discharge plasma is

created by filling a vacuum with a low-pressure gas (ex. argon, ammonia, or oxygen). The

gas is excited using microwaves or current. This ionizes the gas within the contained

chamber. The ionized gas is then thrown onto the substrate surface at a high speed where

the energy produced physically and chemically changes the surface. After the changes

occur, the ionized plasma gas is able to react with the surface to make it ready for protein

adhesion. However, the main disadvantage of this method is the surface may lose

mechanical strength or acquire new properties because of the high amounts of energy.

1.14 Thesis aims and Hypothesis

The hypothesis of my study is that *silanized dual coating protein coatings with fibronectin and laminin, enhances both keratinocyte and fibroblast cell spreading and vinculin markers on Ti6Al4V in vitro.*

I will explore this hypothesis by investigating the spreading of skin keratinocytes and dermal fibroblasts and production of vinculin markers in the presence of dual coating proteins; fibronectin (Fn) and laminin (Ln) on titanium alloy (Ti6Al4V). Laminin and fibronectin were selected as they are the most abundant glycoproteins present in the epidermal and dermal layers respectively. My work in this thesis examines the influence of single and dual protein coatings on cell attachment when coated on Ti6Al4V, in order to design a bio- and physicochemical modified Ti6Al4V surface that cells allows cell spreading as measured by cell size and production of focal adhesion vinculin markers by direct counting of these markers on fixed cells, which can be applied to the design of percutaneous medical devices.

Specifically these objectives are to:

1.   Assess the release kinetics of dual coating radio-labeled Fn and Ln coated on the surface of Ti6Al4V soaked in fetal calf serum (FCS).

2.   Perform cell bioassay to assess the effectof a Ti6Al4V- dual coating protein fibronectin and laminin (FnLn) on keratinocyte cell spreading and production of vinculin markers.

3.   Compare fibroblast cell spreading and vinculin markerson silanized dual coating protein FnLn to adsorbed dual coating FnLn, adsorbed and silanized single coating Fn and Ln on Ti6Al4V alloy by measuring cell size and number of vinculin markers

per cell unit and per cell area, use Mann Whitney U test to identify differences

between each 2 independent sample

CHAPTER 2

Kinetics of Radiolabelled Dual Coating Proteins on Titanium Alloy Surface

2.1 Introduction

2.1.1 Background to Chapter

For ITAP to be successful, a soft tissue-implant barrier must be created which prevents wound down-growth, marsupilization, skin breakdown and infection. To promote the formation of this seal, biological adhesion molecules may be used on implant surface (Gordon et al., 2010).

The hypothesis tested was: *There is no significant difference between the quantity of protein attached to titanium surfaces irrespective of whether they were silanized or adsorbed.*

The objectives of this chapter are:

1)   To quantify dual coating proteins ; fibronectin (Fn)   and laminin 332 (Ln) attaching to different substrates (adsorbed and silanized).

2)   To determine the release kinetics of dual protein over time (from 0 up to 72 hours).

3)   To establish whether there is competitive binding between dual protein attaching to these surfaces.

Several studies have shown that using more than one protein enhances cell adhesion and proliferation. Laflamme et al. (2008), showed that pre-coating bone morphogenetic proteins (BMP) 2 and 7 simultaneously on a collagen scaffold, enhanced osteoblast growth, adhesion and proliferation more than single coatings of either BMP2 or BMP 7. Garcia-Nieto et al. (2010), demonstrated that treating dendritic cells with laminin and fibronectin for 48 hours produced higher levels of key endocytic receptors and induced better T cell differentiation compared with controls of no treatment. Middleton et al., 2007, showed that single coating fibronectin enhanced fibroblast adhesion and growth on

Ti6Al4V surfaces. Similarly, Gordon et al. (2010) demonstrated single coating laminin improved keratinocyte adhesion and growth on Ti6Al4V surfaces. Each extracellular protein may influence growth rates of the same cell line in a different manner. Berens et al.(1994), showed fibronectin and vitronectin proteins minimally supported migration of astrocytoma cells *in vitro* compared with laminin and collagen IV. In addition to this, Johansson et al.(1981), showed that the attachment of cells to fibronectin and laminin involves different cellular receptors. This suggests that presence of dual protein coatings may cause a synergistic or inhibitory effect on cell adhesion and growth.   It has been postulated that dual coating fibronectin and laminin mimics the physiological conditions found in extracellular matrix, providing useful information regarding cell signaling and up-regulation and interaction in presence of more than one protein (Johansson et al., 1981). This may be important for both epidermal and dermal layers and could enhance formation of a tight seal around the prosthesis, leading to the long-term success of ITAP.

2.1.2 Adsorption and attachment of proteins to titanium

Modification of the surface's biochemical and physical characteristics affects cell adhesion, differentiation and growth. This has been studied in the past and applications have been successfully applied to orthopaedic implants for osseointegration. Biochemical modification of titanium surfaces utilizes critical organic components to affect tissue response with the goal of immobilizing proteins, enzymes or peptides for the purpose of inducing specific cell and tissue responses (Puleo and Nanci, 1999). Surface modification of titanium implants can by classified into: surface modification by peptides; surface modification by extra-cellular proteins; surface modification by bone morphogenetic proteins and growth factors (Morra, 2006).

Successful tissue genesis relies on the ability of cells to adhere to extra-cellular material, up-regulate, proliferate and organize extra-cellular matrix into a functional tissue (Miyamato et al., 1998). The first step in the sequence of cell attachment depends on integrins found on cell membranes, which are involved in the process of cell adhesion to extracellular matrix (LeBaron et al., 2000). Integrins interact with short amino acid sequences in particular, Arginine-Glycine-Aspartate (RGD) that mediate cell attachment to several plasma and extracellular proteins, including fibronectin, collagen I, vitronectin, osteopontin and sialoprotein (Grzesik and Robey, 1994). Massia and Hubbell (1990), covalently bonded synthetic peptides containing RGD peptide sequences to non-adhesive glass surface using 3-glycidoxypropyltrimethoxysilane. This produced a chemically stable surface that improved fibroblast adhesion.

Xiao et al. (1997), investigated Arg-Gly-Asp-Cys (RGDC) peptide binding to 3-aminopropyltriethoxylsaline (APS) to titanium surfaces. The coupling involved a hetero-bifunctional cross linker, N-succinimidyl-3-maleimidopropionate (SMP), reacting with terminal amino groups on titanium through covalent addition of cysteine thiol groups of the peptide. The surfaces were evaluated by chemico-physical techniques including X-ray photoelectron spectroscopy, radiolabelling and ellipsometry. Peptide surface density was calculated at approximately 0.03 nmol/cm^2 and the growth of N-C+O component indicated introduction of maleimide and peptide bonds on the surface. They produced a cell-adhesive peptide model that covalently bonded to titanium surfaces by silanization, cross-linking and peptide attachment through cysteine thiol group. There study did not assess cell adhesion or protein adsorption to titanium surfaces.

De Giglio et al. (2000), demonstrated an approach of coupling synthetic peptide containing RGD sequence to polypyrrole (PPy) coated titanium substrates. Polypyrole is grown

47

electrochemically on titanium. Cysteine residue is used to graft the peptide to polymer coating. They found higher adhesion of osteoblasts to RGD-modified PPy-coated Ti as compared to unmodified PPy-coated Ti and glass coverslip.

Bearinger et al. (1998), presented a different method of biochemical modification using interpenetrating polymer network coating. This coating is a thin adherent film of 20 nm of acrylamide, ethylene glycol and acrylic acid. It is grafted by photoinitiated free radical polymerization. Osteoblasts attached to RGD modified interpenetrating polymer network coating at levels significantly greater than on clean quartz, RGD coating. Barber et al. (2003), used the same biochemical modification on RGD containing 15 amino acid sequences from rat bone sialoproteins linking interpenetrating polymer network. Significant enhancement in bone mineralization by primary rat osteoblast was identified. Kantlehner et al.(2000), linked cyclic c-(RGDK-) (Arg-Gly-Asp-Phe-Lys) peptide to polymethylmethacrylate (PMMA) using an acrylamide end group. In vitro results showed that PMMA pellets with RGD sequence bind effectively to murine and human osteoblasts. *In vivo* studies showed that peptide-coated PMMA pellets implanted into the patella groove of rabbits were integrated into regenerating bone tissue faster and stronger than uncoated PMMA pellets.

Cavalcanti-Adam et al. (2002), improved osteoblast activity on RGD peptides covalently linked to surface amino groups introduced by silane chemistry. Huang et al. (2003), immobilized two types of peptides, RGDC and RDGC. Cell culture of primary osteoblasts showed that cell attachment was enhanced on RGDC surfaces at 4 and 8 hours. Increased cell spreading and greater cell proliferation was also noted. This coated surface showed osteocalcin mRNA expression significantly earlier compared to controls.

Porte-Durrieu et al. (2004), covalently linked linear and cyclic RGD containing peptides to Ti surfaces. They used silanization with APS, cross-linking with SMP and immobilization via thiol bonding. They found significant improvement of cell adhesion between 1 and 24 hours compared to untreated surface. Pallu et al. (2005), compared cyclic RGD sequence peptides that were covalently bonded to Ti surface using the same methodology to adsorbed peptides. They found a significant improvement in the former group.

Tosatti et al. (2004), cultured osteoblasts on RGD peptide bonded on a co-polymer containing poly-l-lysine as substrate binding component and polyethylene glycol as protein adsorption polymer. This polymer adsorbs spontaneously from dilute aqueous solution onto negatively charged surfaces, yielding water-stable coatings. They found high phenotype expression on RGD binding polymer compared to polymer with no RGD peptide.

Auernheimer et al. (2005), discussed coating Ti implants with cyclic RGD peptide with phosphonic acid groups. Groll et al. (2005), immobilized linear RGD peptides with reactive star-shaped polyethylene glycol prepolymers. Human mesenchymal stem cells adhered only to RGD coated Ti surfaces and not to controls with prepolymers only. Cells showed expression of osteogenic marker genes after 14 days.

Ferris et al. (1999), showed an increased bone formation by RGD coated implants in vivo. Rat femora were implanted with titanium rods coated with RGDC peptides. The peptide was immobilized using gold-thiol chemistry in water-alcohol solutions. Histology analysis revealed a thicker shell of new bone formed around RGD coated implants versus plain implants at 2 weeks (26.2 +/- 1.9 vs. 20.5 +/- 2.9 microm; $p < 0.01$), and at 4 weeks (32.7 +/- 4.6 vs. 22.6 +/- 4.0 microm; $p < 0.02$). Mechanical pull-out at 4 weeks demonstrated

that the average interfacial shear strength of peptide coated rods was 38% greater than control rods.

Kroese-Deutamn et al. (2005), investigated new bone formation using a porous titanium fibre mesh implant, coated with cyclic RGD peptide, immobilized using phosphonate. Titanium mesh was soaked in coating solution and peptide was allowed to immobilize overnight. Implants were inserted in rabbit cranii and compared to Ti implants without RGD peptides. Histological examination at 2, 4 and 8 weeks showed a significant increase in bone formation in the RGD peptide group at 4 and 8 weeks. Elmengaard et al. (2005), examined plasma sprayed titanium implants coated with cyclic RGD peptide inserted in proximal tibia of dogs for 4 weeks. Significant increase in bone growth and at the same time decrease in fibrous tissue on-growth was found in RGD-coated implants. Schliephake et al. (2002), evaluated titanium implants coated with collagen I, implants coated with collagen I and cyclic RGD peptides, with low and high concentrations. Implants were placed in mandibles of dogs. Collagen was bonded to titanium by low voltage anodization, followed by dip coating in collagen and cross linking by carbodiimide chemistry. RGD peptides were UV grafted to collagen coated implants. Bone-implant contact and volume density of newly formed peri-implant bone. After 1 month, there was significantly enhanced bone implant contact in RGD peptide coated implants and no significant difference was detected between groups with collagen and RGD low and high concentrations. Volume density of newly formed bone was significantly higher in all implants with coating. No significant difference was seen between collagen coated implants compared to collagen and RGD low and high implants in volume density at 1 month.

Introduction of chemical stimulants on the surface increase surface wetability or cell affinity to the surface. Moreover, modifying surface topography plays an important role in

increasing adhesion strength. Buser et al. (1991), demonstrated a positive correlation existed between bone-implant contact and roughness values. Ulerich et al. (2007), modified a titanium surface by patterning the implant by direct laser etching with a 10 μm beam diameter and a pulse energy of 50 μJ, to form linear grooves ranging from 10 to 50nm in depth. They found micro-grooves improved osteoblast adhesion on titanium.

A simple method for biochemical modification is through addition of the molecule to the substrate i.e. adsorption. Initially, proteins are retained on the surface by weak forces, then over time they adsorb from the surface in an uncontrolled manner (Nakabayashi et al., 1972).

2.1.3 Silanization of Titanium

Silanization is one method of biochemical modification that allows biological molecules to covalently bond to the surface. This is possible by attaching a silicon-based group of atoms to the substrate surface. A spacer arm is available for protein coupling. Two methods of silanization exist, namely aqueous and organic depending on the solvent used. Organic silanization produces a thicker, uneven, more loosely bound but with higher capacity coating than aqueous silanization, which produces a thinner silane layer with greater coverage (Weetall, 1993). Chloro-silane is used with organic solvents whereas methoxy and ethoxy forms can be coupled to both solvents. Gluteraldehyde is a common spacer arm that is used in silanization for protein coupling. It possesses 2 reactive functional CHO groups, one group reacts with protein and the other with NH_2 group on the silanized surface. Robinson et al. developed organic silanization using γ-aminopropyltriethyoxysilane (APS) and gluteraldehyde in 1971. Since then their protocol has been extensively used by Halling and Dunnill, (1979); Puleo, (1995); Nanci et al.,

(1998); Middleton et al. (2007) and Gordon et al., (2010). APS is a silane that couples substrates silanol, forms self assembly polymers and increases the stimulatory effect of biological molecules (Ito, 1991). Silanization is the process that I have used throughout this theseis to attach proteins to titanium alloy surfaces.

2.1.4 Quantification of Protein

An accurate method of detecting small quantitates of protein is necessary to determine the stability of protein on the surface. It would also aid in determining whether competitive binding is present with the presence of more than one protein type on the surface. Indirect methods for protein quantification by Western Blots exist. Direct methods include radiolabelling proteins. In my study radiolabelled proteins were used because it allowed us to quantify directly protein attachment and desorbtion onto the surface of titanium alloy.

2.1.5 Hypothesis

The null hypothesis tested is:

There is no significant difference between the quantity of protein attached to titanium surfaces irrespective of whether they were silanized or adsorbed.

There is no significant difference between quantities of single coating protein attached to the substrate compared with dual coating protein.

The alternative hypothesis tested is:

Silanized surfaces bonded significantly more protein compared to non silanized surfaces.

Larger quanties of single proteins bonded to silanized titanium surfaces compared to mixed protein solutions. Non-competitive bonding was present when dual coating proteins were silanized on Ti.

The aim of this chapter was to examine whether covalently bonded protein FnLn attached to Ti surfaces in larger quantites than adsorbed protein coating when placed in Foetal Calf Serum (FCS) over time (0 up to 72 hours).

2.2 Materials and Methods

2.2.1 Disc Preparation

10mm diameter, 3mm thick discs were machined from Ti_6Al_4V rods. These were ground by hand with fine grit paper (300, 600, 1200, 2400, 4000) prior to polishing with a Motopol 2000 grinder (Buehler, Germany), MD polishing cloth (Streuers, Denmark) and OP-S colloidal silica suspension (Streuers, Denmark) 10:1 with 30% H_2O_2 (BDH Ltd, UK). Polished discs (Pol) were considered satisfactory when the surface obtained was a mirror surface finish and a R_a value of less than 0.03μm was achieved using a profilometer. Only discs that fit these criteria were used in the experiments.

2.2.1.1 Cleaning

Discs were ultrasonically cleaned for 10 minutes immersed in 10% Decon 90 (Decon Laboratory Ltd, UK). The discs were left to rinse under running distilled water for 10 minutes. They were placed in Acetone (BDH Ltd, UK) for 10 minutes and air dried under a hood.

2.2.1.2 Autoclaving

Discs were placed into autoclave bags and sterilized in a 2100 Classic Clinical Autoclave (Prestige Medical, UK) for 11 minutes at 126^0C at 1.4 bar pressure.

2.2.1.3 Passivation

Discs were passivated by soaking in a 50:50 of 99% sulphuric acid and 30% hydrogen peroxide (BDH, UK) for 2 hours at room temperature. The passivated discs were rinsed 3 times with distilled water and vacuum dried for 2 hours using aseptic technique.

2.2.1.4 Silanization

Polished and passivated discs were submerged in 10% amino-propyltriethoxysilane (APS) for 2 hrs at 21^0C, for the silanized, non-passivated discs group and the silanized, passivated discs group respectively. Discs were dried at 37^0C in the dry incubator. They were then immersed in 1% glutaraldehyde solution for 2 hours at 21^0C. These were rinsed thoroughly with PBS.

2.2.2 Radiolabelling Fn and Ln: ^{125}I-Fn and ^{125}I-Ln Production Method

Fibronectin (F2006, Sigma-Aldrich, UK) and laminin (CC145, Chemicon International Inc., USA) were custom labeled by Perkin-Elmer Inc., (Wellesley, USA). Modified chloramineT procedure was used to incorporate ^{125}iodine to the protein producing ^{125}iodine-fibronectin (^{125}I-Fn) and ^{125}iodine-laminin (^{125}I-Ln). Radiochemical purity for both radiolabelled proteins yielded 95% incorporation by instant thin-layer chromatography, a specific activity of 7.5µCi/µg and a concentration of 500uCi/ml for ^{125}I-Fn; a specific activity of 21.8µCi/µg and a concentration of 400uCi/ml for ^{125}I-Ln.

2.2.3 Radiolabelling Quantification Method

Gamma radiation from radiolabelled protein was detected using Tricarb 2900TR liquid scintillation counter (PerkinElmer Inc., USA) as counts per minute (CPM). Discs were placed in 5ml scintillant tubes. 4.5ml Ultima Gold XR scintillation cocktail (PerkinElmer Inc., USA) was then added. Tubes were placed in the scintillation counter and CPM was obtained from QuantaSmart software (v. 1.31, Packard Instrument, USA). Each sample was counted 3times.

2.2.4 Calibration Curves

Standard Calibration curves were produced for single coating proteins ^{125}I-Fn and ^{125}I-Ln against CPM to allow for quantification of protein in nanograms. 50 μl droplets of 10 μg, 100 μg, 250 μg, 500 μg and 750 μg of each radiolabelled protein were placed on polished discs and CPM was immediately measured thrice.

2.2.5 Release Kinetics for Radiolabelled Proteins in Fetal Calf Serum

In order to coat discs with single coating protein, 50μl droplet of 636.62ng/cm^2 ^{125}I-Fn, was added to non silansized and silanized, non-passivated discs (n=3) at 21^{0}C under sterile conditions using aseptic techniques. For dual coating proteins, 25μl droplet of 636.62 ng/cm^2 ^{125}I-Fn mixed with 25μl droplet of 636.62 ng/cm^2 non-radiolabelled Ln were added to discs in the same method. This was repeated with ^{125}I-Ln in the same manner. This concentration was chosen because previous work showed that this was the maximal amount that covalently bond to titanium alloys (Middleton et al. 2007, Gordon et al. 2010). Discs were placed in 24 well plates and were left for 4 hours to allow proteins to bind.

Distilled water was used to wash discs 3 times to remove unbound protein. Discs were submersed in 1ml of FCS. CPM measurement was done at 0 hour, 1 hour, 24 hours, 48 hours and 72 hours.

2.2.6 Quantification of Amount of Radiolabelled Proteins in nanograms

Using the calibration curves described in section 2.2.4 and CPM data from section 2.2.5, quantification of radiolabelled proteins (^{125}I-Fn and ^{125}I-Ln) both as single and dual coating proteins on adsorbed and silanized, non-passivated discs was calculated in nanograms.

2.2.7 Quantification of Amount per Disc Area Radiolabelled Proteins

Protein remaining on discs against time, measured in nanograms, was divided by the surface area of discs to obtain the quantity of protein expressed as nanograms per centimetre square. Tricarb 2900TR liquid scintillation counter was calibrated and tested by Perkin-Elmer engineers immediately before I carried out my experiments. The accuracy obtained was within 95%.

2.2.8 Statistical Analysis

Data were anaylsed using SPSS software. The data did not fit the assumptions required for parametric testing and therefore, non-parametric tests were used. Pair-wise Mann-Whitney U test was used to compared medians and determine significance between individual groups. All numerical data are stated as median values (with 95%CI). Power calculations were made using previous similar studies at the institute. Identical numbers of

samples were used in all experiments.Results with p-value< 0.05 level were considered significant.

2.3 Results

2.3.1 Calibration Curve

Standard calibration curves were designed to determine the results for loading and release kinetics experiments with correction for the half-life of ^{125}I-Fn and ^{125}I-Ln. Increasing the amount of ^{125}I-labelled protein results in a proportionate increase in the Counts Per Minute (Figures 2.1-2.2).

Chart annotation: $y = 8524.4x + 51288$, $R^2 = 0.99884$
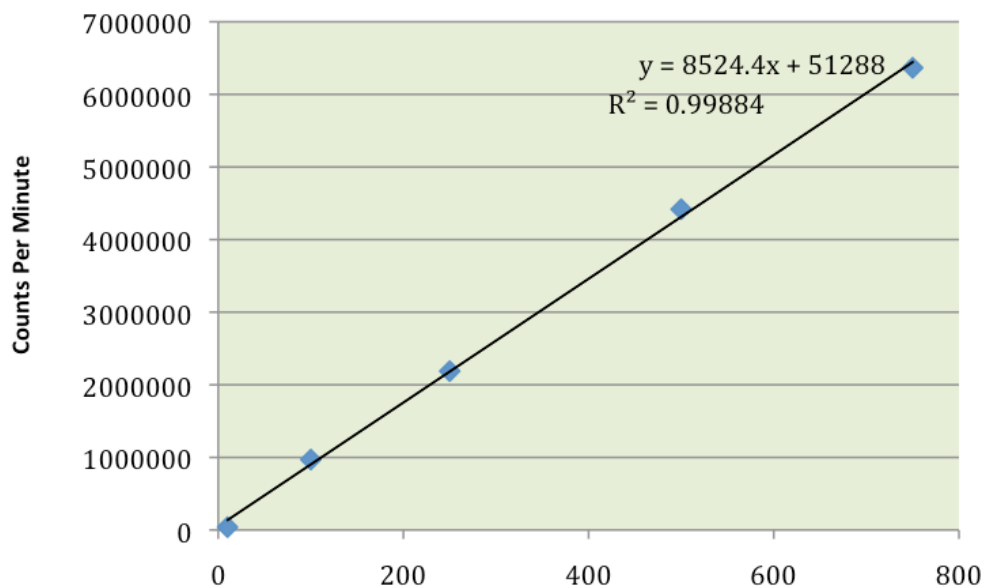
Figure 2.1: Calibration curve for 125I labelled fibronectin in counts per minute (CPM)

The chart shows a calibration curve with the equation $y = 11426x - 151722$ and $R^2 = 0.99767$. The y-axis is labelled "Counts Per Minute" ranging from 0 to 9000000, and the x-axis is labelled "Amount of ^{125}I-Laminin" ranging from 0 to 800.
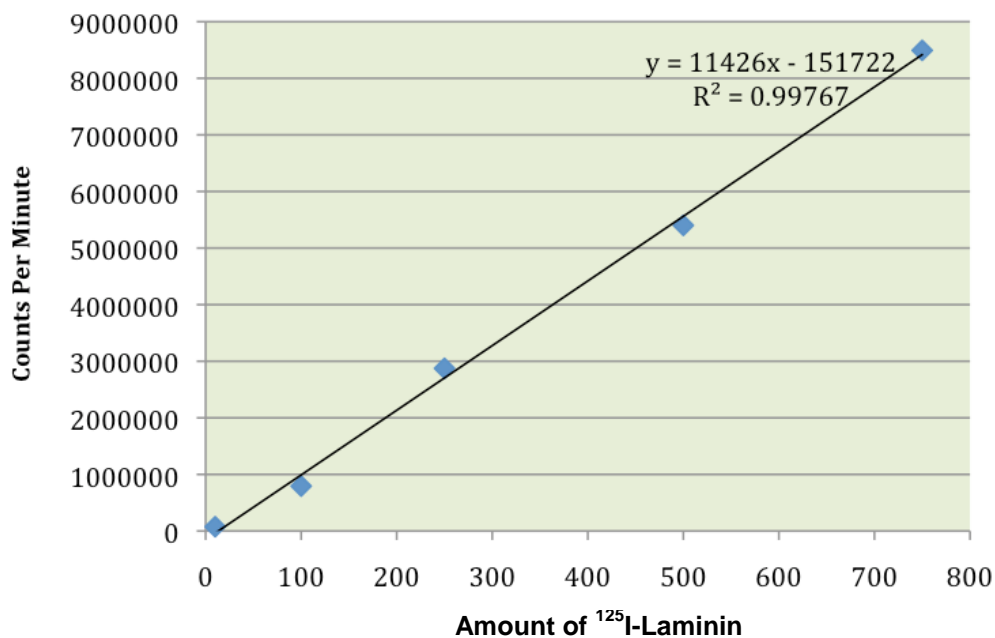
Figure 2.2: Calibration curve for 125I labelled laminin in counts per minute (CPM)

2.3.2 Release Kinetics of ^{125}I-Radiolabelled Proteins

2.3.2.1 Quantification of Proteins

Using the calibration curves and results of release kinetics of different proteins in CPM, quantification of proteins in nanograms and in nanograms/squared centimetres was performed (Figures 2.3-2.28).

2.3.2.2 Durability Kinetics of ^{125}I-Fn and ^{125}I-Ln on Ti discs

There was a significant decrease from a median of 149.54 ng (95% CI 149.76 to 151.32) to 149.63 ng (95% CI 149.21 to 150.62) of silanized Fn was seen within the first hour of incubation in FCS (p=0.024). A significant decrease was seen between 1 and 24 hours to a median amount of 131.65 ng (95% CI 130.52 to 131.90) (p<0.001); and the amount

decreased further significantly by a quarter of its initial loading concentration (median 113.57 ng (95% CI 113.65 to 113.94)) by 48 hours ($p<0.001$). A further decrease in the amount of SiFn was observed between 48 and 72 hours to a median amount of 111.46 ng (95% CI 111.13 to 113.59) ($p=0.047$).

On silanized Ln substrate, there was no significant decrease from a median of 232.58 ng (95% CI 232.32 to 232.87) to 231.67 ng (95% CI 231.27 to 231.95) within the first hour in FCS ($p=0.09$). There was a significant decrease between 1 and 24 hours ($p<0.001$) to a median of 204.45 ng (95% CI 203.91 to 204.87) and a further decrease between 24 to 48 hours, to 183.17 ng (182.91 to 183.67); a fifth of its initial optimal loading concentration ($p<0.001$). No significant decrease in amount of SiLn between 48 and 72 hours to a median on 179.15 ng (95% CI 177.93 to 179.88)($p=0.05$).

On adsorbed Fn, a significant decrease from a median of 27.39 ng (95% CI 26.92 to 27.97) to 25.81 ng (95% CI 22.38 to 26.61) was seen within the first hour of incubation in FCS ($p<0.001$). There was significant decrease between 1 and 24 hours to a median of 3.49 ng (95% CI 2.76 to 4.01) ($p<0.001$). There was no further decrease between 24 and 48 hours to a median of 2.85 ng (95% CI 2.49 to 3.02)($p=0.31$); and no further decrease in the amount between 48 and 72 hours to a median of 2.36 ng (95% CI 2.22 to 2.57) ($p=0.122$).

The median amount of AdLn did not significantly decrease within the first hour of incubation in FCS from 93.41 ng (95% CI 90.55 to 93.62) to 92.71 ng (95% CI 90.81 to 93.21) ($p=0.627$). A significant decrease is seen between 1 and 24 hours, with a median amount of 57.64 ng (95% CI 55.98 to 58.24) and a further decrease between 24 and 48 hours to a median of 50.72 ng (49.16 to 51.35) ($p<0.001$). In addition, a significant further

decrease was observed between 48 and 72 hours, with a median amount of 48.37 ng

(95% CI 46.54 to 48.72) (p=0.047).

No significant difference was seen on silanized dual coating substrate, in the amount of

SiFn within the first hour of incubation from a median of 155.42 ng

(95% CI 155.05 to 155.47) to a median of 155.16 ng (95% CI 154.97 to 155.24) (p=0.102).

From 1 to 24 hours, a significant decrease in the amount of SiFn to a median of 131.75 ng

(95% CI 130.96 to 132.07)(p<0.001). A further decrease was seen between 24 and 48

hours, to a median of 114.94 ng (95% 113.87 to 116.23) (p<0.001). However, no further

decrease was seen between 48 and 72 hours of incubation in FCS, with a median of

114.71 ng (95% CI 113.35 to 115.23(p=0.233).

In addition, silanized Ln on dual coating substrate showed no significant decrease in

median amount from 234.99 ng (95% CI 234.87 to 235.41) to a median amount of 234.63

ng (95% CI 234.43 to 235.59) within one hour of incubation in FCS (p=0.23). A significant

decrease is seen between 1 and 24 hours, with a median amount of 197.72 ng (95% CI

197.56 to 197.79) and a further decrease between 24 and 48 hours to a median of 177.54

ng (177.24 to 178.79) (p<0.001). A further decrease was observed between 48 and 72

hours, with a median amount of 176.38 ng (95% CI 176.20 to 177.85)(p=0.047).

On adsorbed dual coating substrate, the median amount of AdFn did not significantly

decrease within one hour of incubation from 32.80 ng (32.71 to 32.82) to 32.63 ng (95%

CI 32.47 to 32.69) (p=0.06). A significant difference decrease in amount of AdFn to a

median of 16.07 ng (95% CI 15.92 to 16.16) (p<0.001) was seen between 1 and 24 hours.

No further decrease was seen between 24 and 48 hours, with a median amount of 15.51

ng (95% CI 15.48 to 15.83) (p =0.05); however there was a further decrease between 48

and 72 hours to a median amount of 15.30 ng (95% CI 15.29 to 15.30) (p<0.001). In addition, the median amount of AdLn on dual coating substrate, did not significantly decrease within the first hour of incubation in FCS from 71.80 ng (95% CI 71.58 to 73.58) to a median of 71.79 (95% CI 71.46 to 73.52) (p=0.508). A significant decrease is seen between 1 and 24 hours, with a median amount of 47.38 ng (95% CI 47.14 to 47.70) and a further decrease between 24 and 48 hours to a median of 44.54 ng (43.40 to 44.81) (p<0.001). An additional decrease was observed between 48 and 72 hours (p=0.047), to a median amount of 43.40 ng (95% CI 41.61 to 43.56).

On silanized dual coating proteins substrate, similar amounts of Fn and Ln were attached as when used as a single coating (i.e. non competitive binding). Silanized dual coatings bonded to Ti alloy in significantly larger quantities compared with adsorbed coatings (p<0.001). Retention of silanized proteins after incubation in serum was significantly greater than absorbed proteins at all time points. At t=0, silanized single and dual coating fibronectin remained on Ti6Al4V surfaces in larger quantities compared to adsorbed single and dual coating fibronectin, respectively (p<0.001). The same pattern was observed when comparing silanized single and dual coating laminin to adsorbed single and dual coating laminin, respectively (p<0.001).
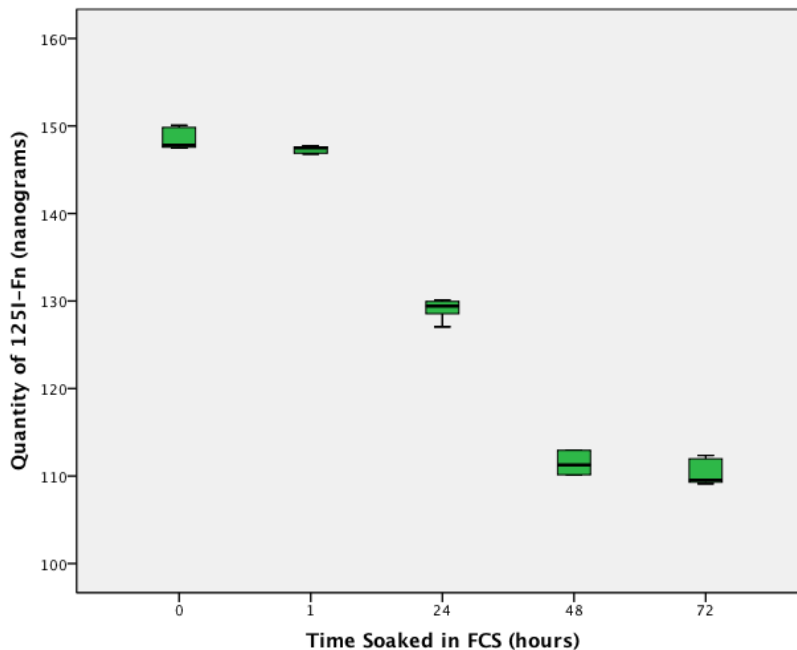
Figure 2.3: Amount of ^{125}I-Fn (nanograms) from single coating protein on Si discs soaked in foetal calf serum over time
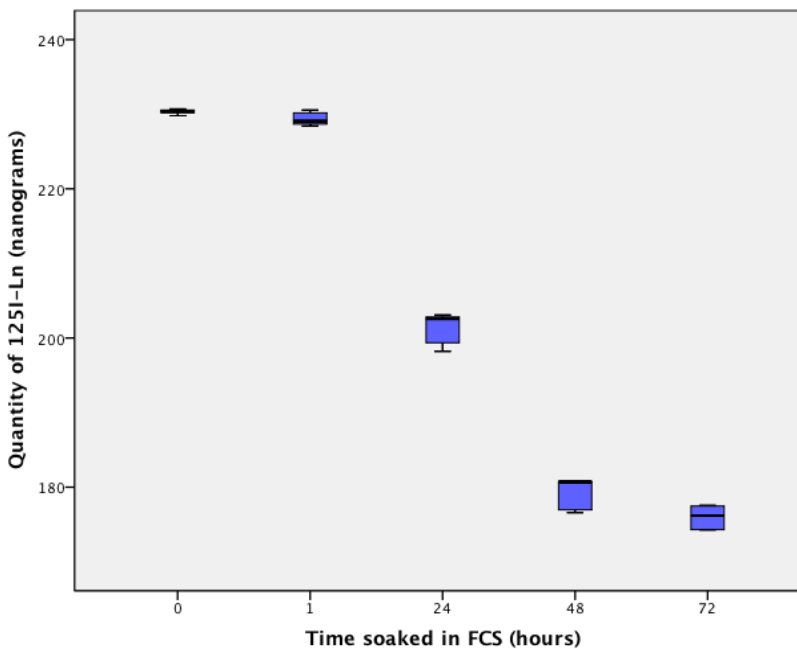
Figure 2.4: Amount of ^{125}I-Ln (nanograms) from single coating protein on Si discs soaked in foetal calf serum over time
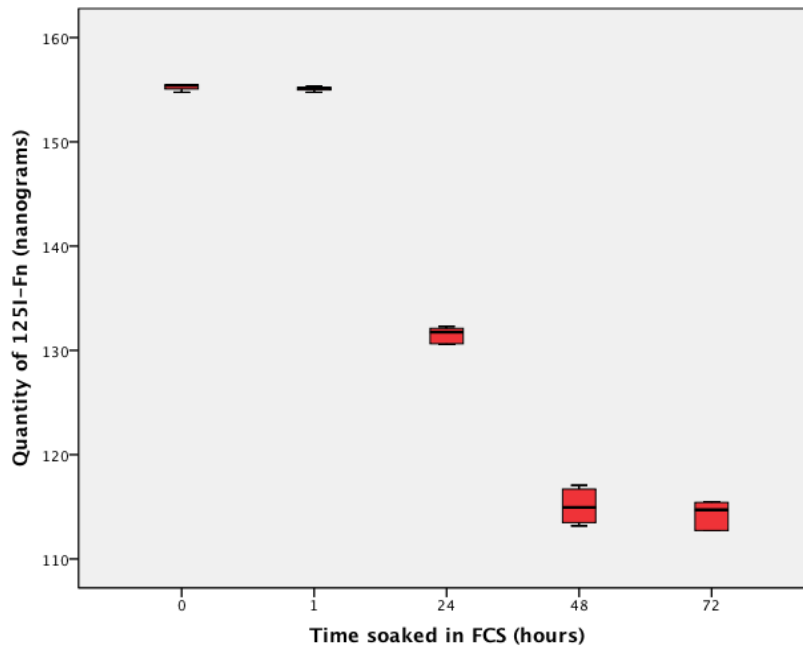
Figure 2.5: Amount of ^{125}I-Fn (nanograms) from dual coating proteins on Si discs soaked in foetal calf serum over time
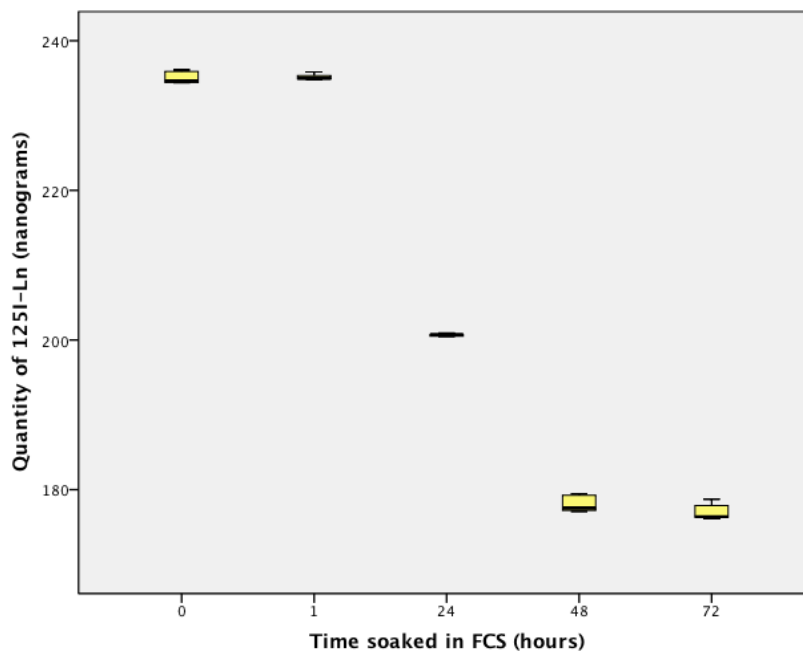
Figure 2.6: Amount of ^{125}I-Ln (nanograms) from dual coating proteins on Si discs soaked in foetal calf serum over time
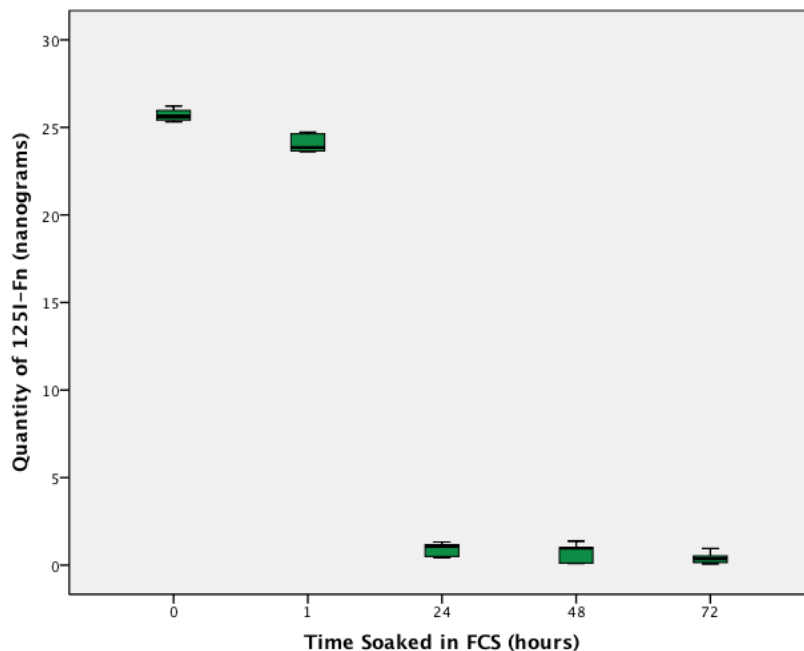
Figure 2.7: Amount of ^{125}I-Fn (nanograms) from single coating protein on Ad discs soaked in foetal calf serum over time
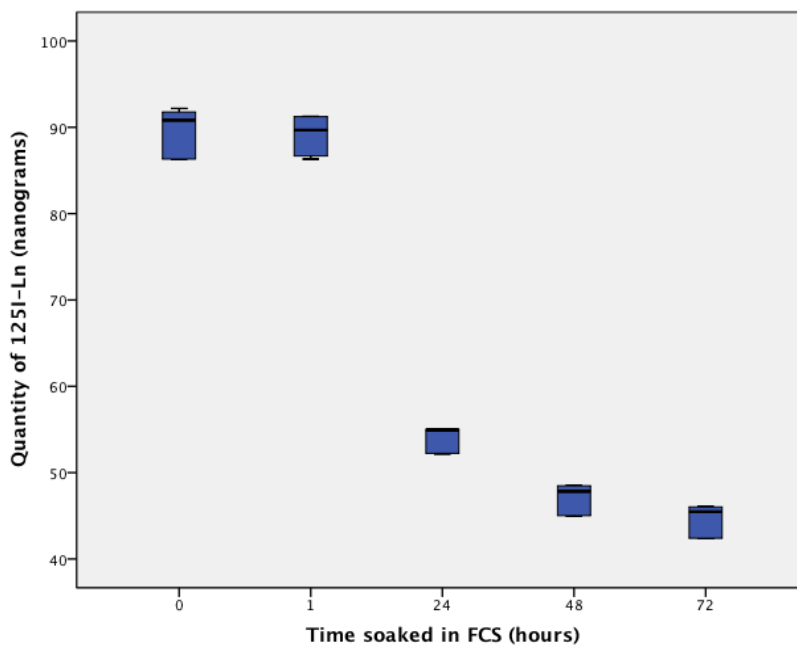
Figure 2.8: Amount of ^{125}I-Ln (nanograms) from single coating protein on Ad discs soaked in foetal calf serum over time
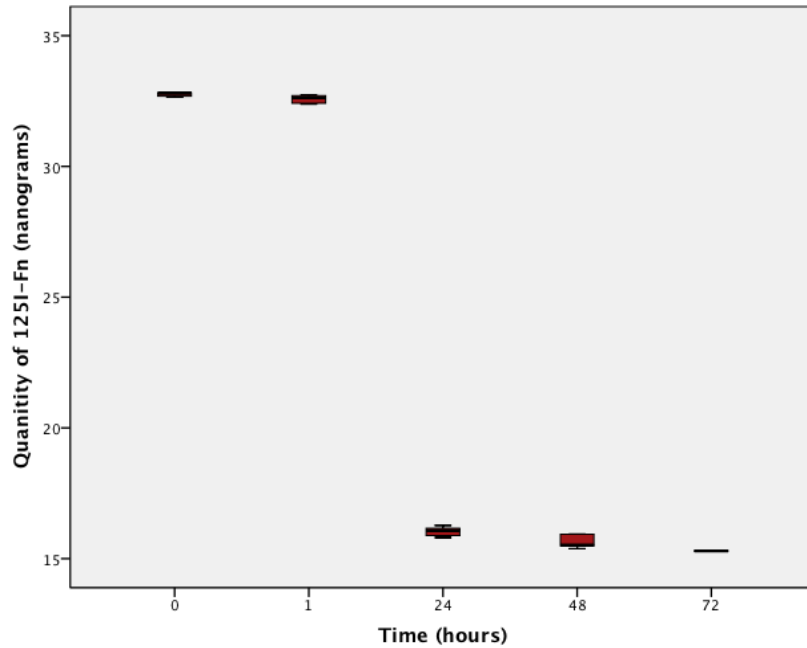
Figure 2.9: Amount of ^{125}I-Fn (nanograms) from dual coating proteins on Ad discs soaked in foetal calf serum over time
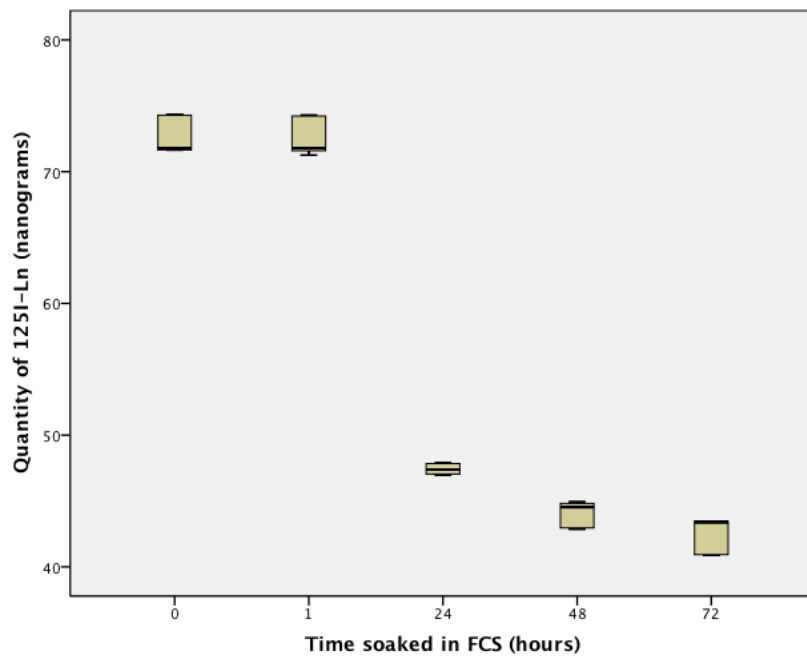
Figure 2.10: Amount of ^{125}I-Ln (nanograms) from dual coating proteins on Ad discs soaked in foetal calf serum over time
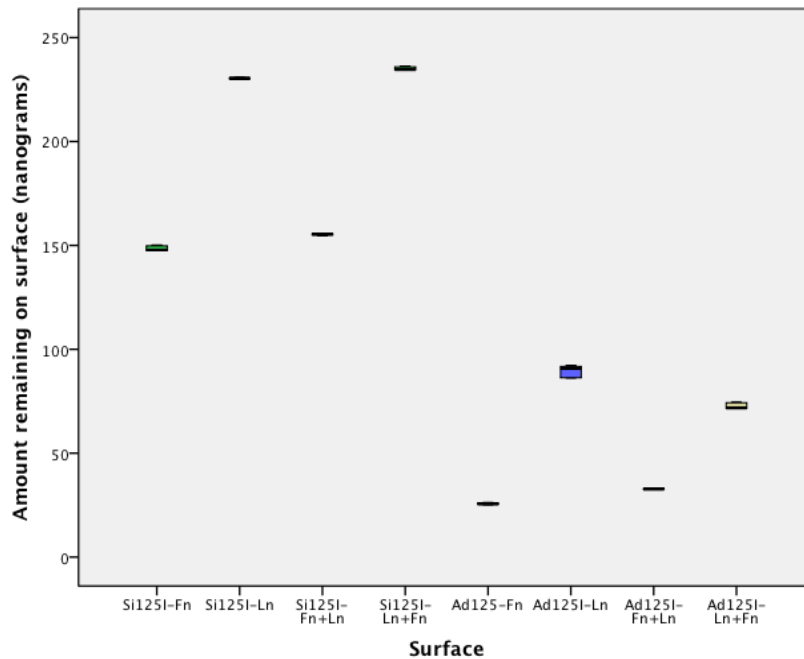
Figure 2.11: Amount of protein (nanograms) remaining on Ti6Al4V surface at 0 hour
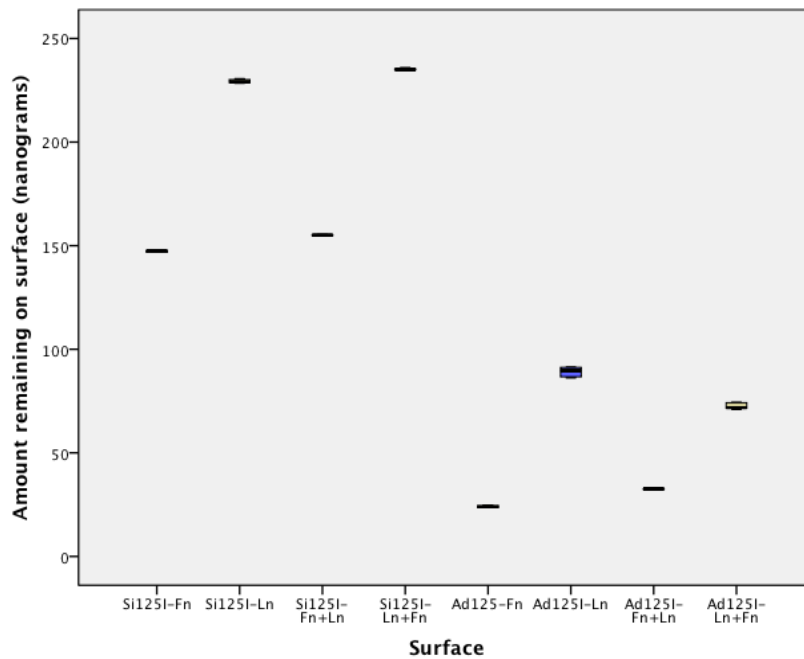
Figure 2.12: Amount of protein (nanograms) remaining on Ti6Al4V surface at 1 hour
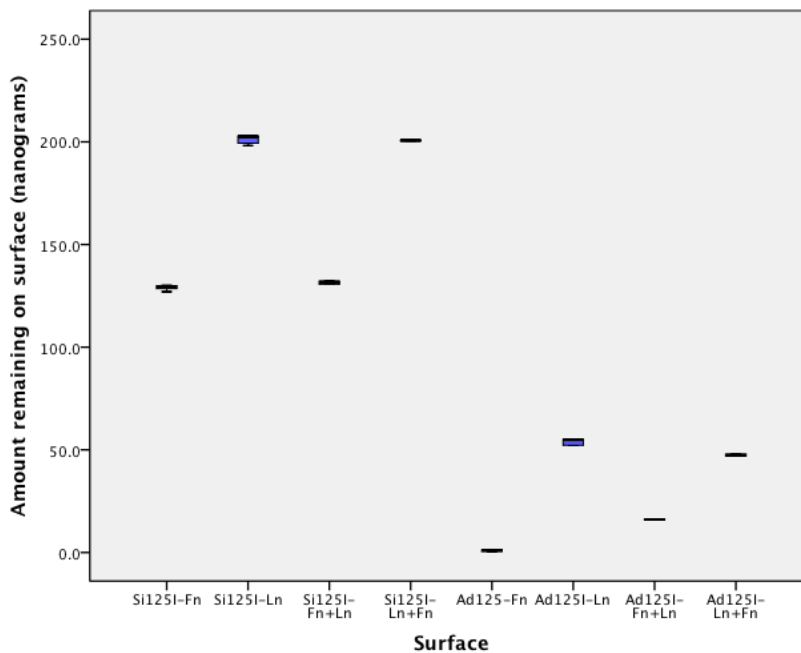
Figure 2.13: Amount of protein (nanograms) remaining on Ti6Al4V surface at 24 hours
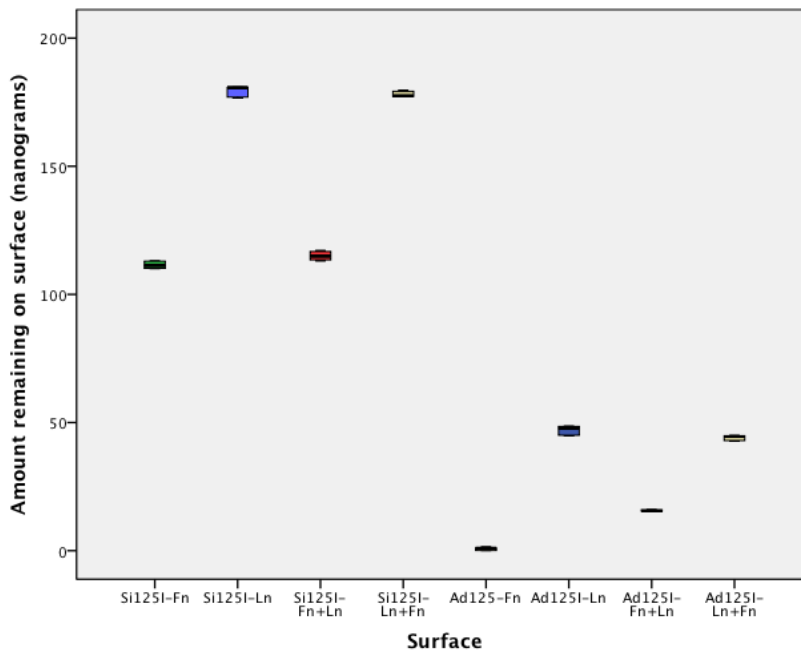
Figure 2.14: Amount of protein (nanograms) remaining on Ti6Al4V surface at 48 hours
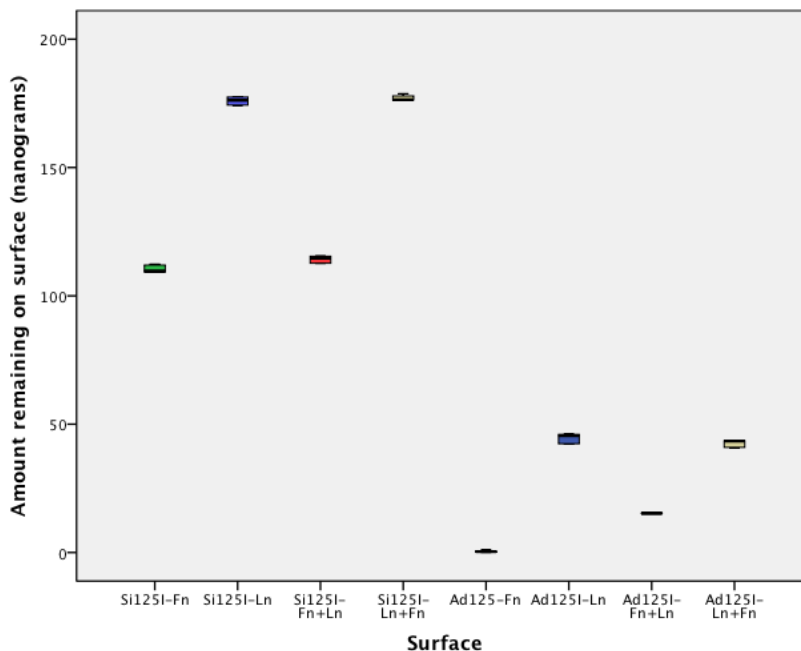
Figure 2.15: Amount of protein (nanograms) remaining on Ti6Al4V surface at 72 hours
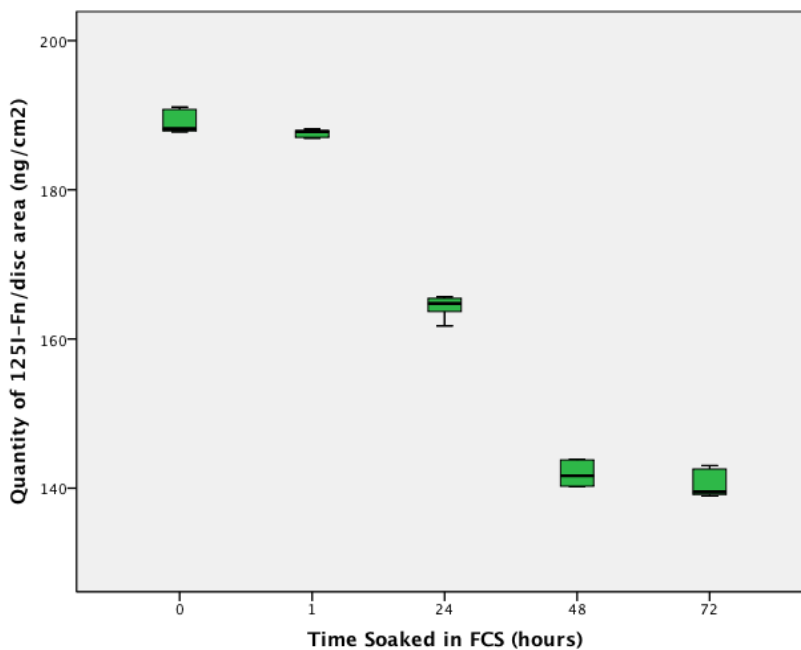
Figure 2.16: Amount of ^{125}I-Fn per disc area (nanograms/cm^2) from single coating protein on Si discs soaked in foetal calf serum over time
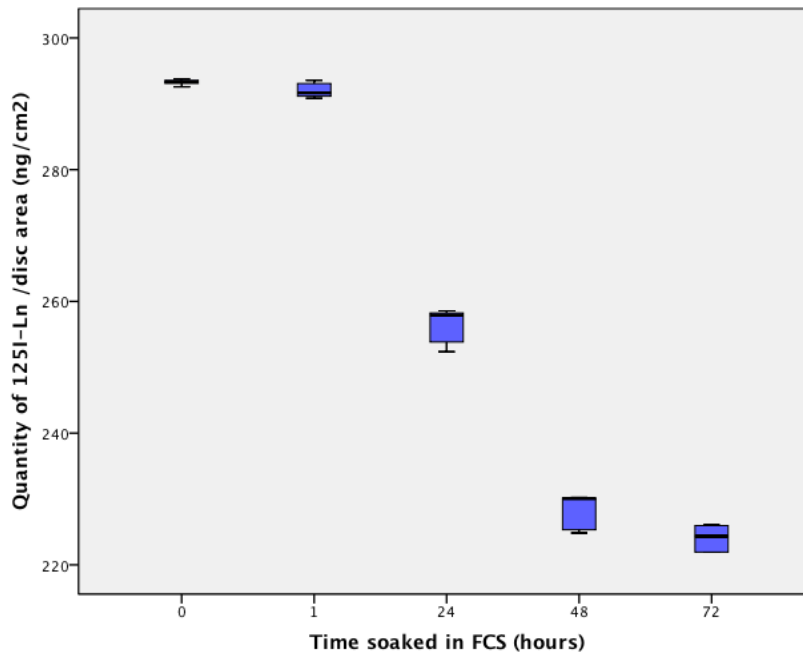
Figure 2.17: Amount of ^{125}I-Ln per disc area (nanograms/cm^2) from single coating protein on Si discs soaked in foetal calf serum over time
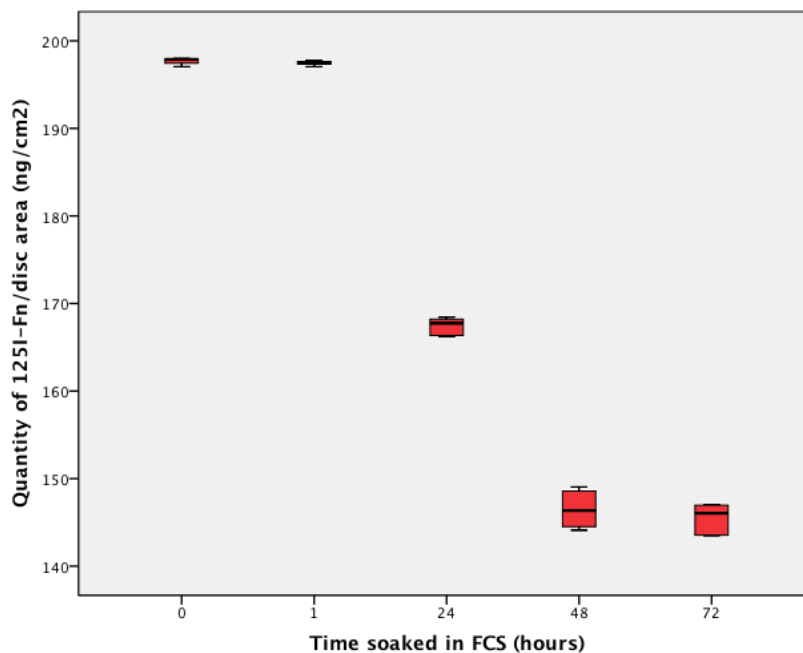
Figure 2.18: Amount of ^{125}I-Fn per disc area (nanograms/cm^2) from dual coating proteins on Si discs soaked in foetal calf serum over time
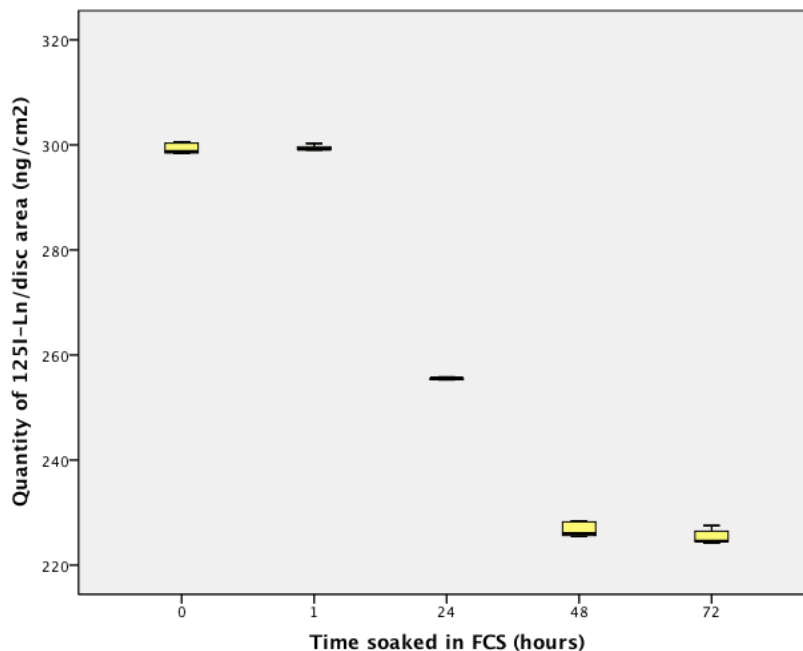
Figure 2.19: Amount of ^{125}I-Ln per disc area (nanograms/cm^2) from dual coating proteins on Si discs soaked in foetal calf serum over time
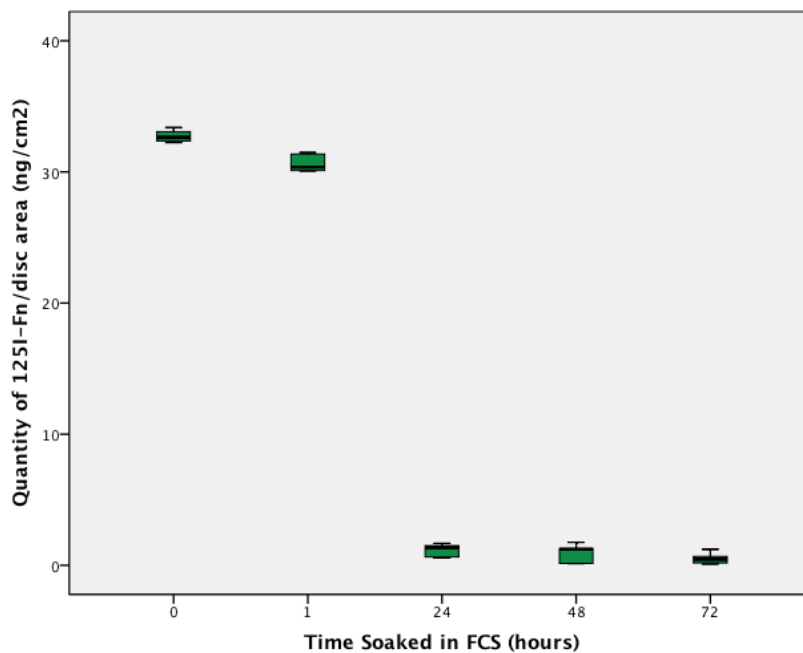
Figure 2.20: Amount of ^{125}I-Fn per disc area (nanograms/cm^2) from single coating protein on Ad discs soaked in foetal calf serum over time
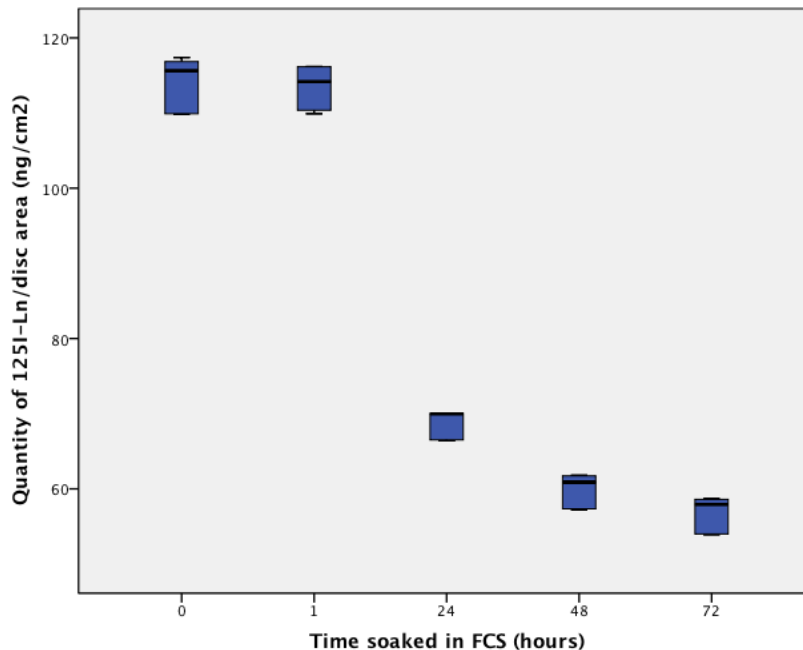
Figure 2.21: Amount of ^{125}I-Ln per disc area (nanograms/cm^2) from single coating protein on Ad discs soaked in foetal calf serum over time
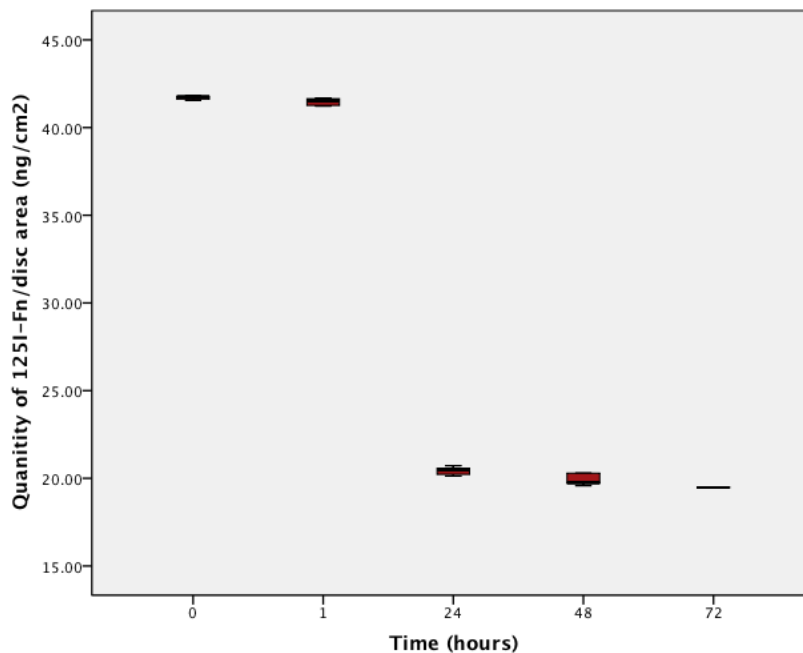
Figure 2.22: Amount of ^{125}I-Fn per disc area (nanograms/cm^2) from dual coating proteins on Ad discs soaked in foetal calf serum over time
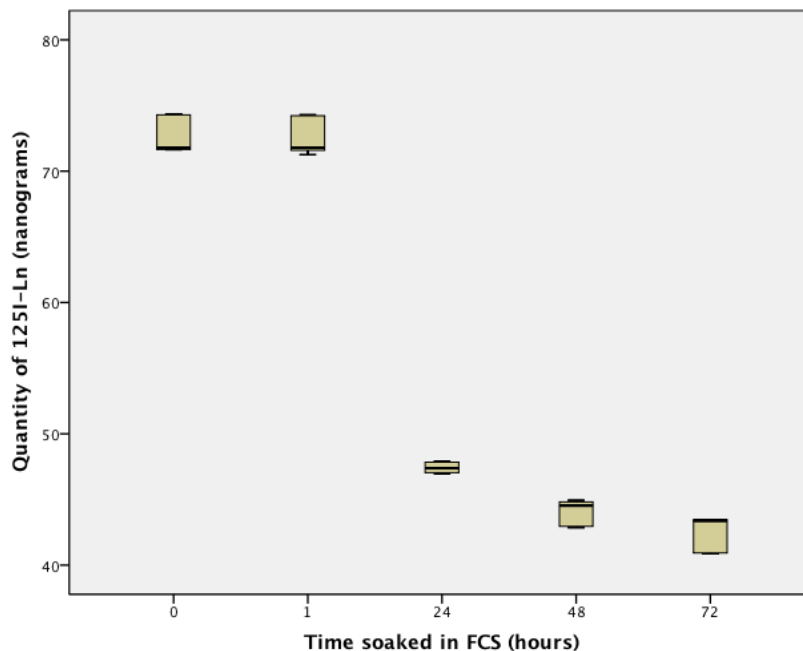
Figure 2.23: Amount of ^{125}I-Ln per disc area (nanograms/cm^2) from dual coating proteins on Ad discs soaked in foetal calf serum over time
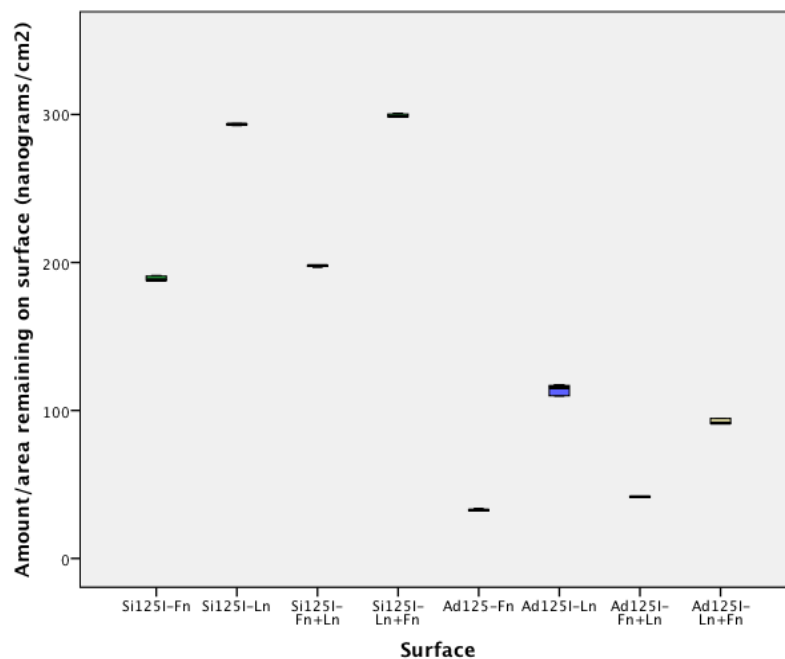
Figure 2.24: Amount of protein/surface area (nanograms/cm^2) remaining on Ti6Al4V surface at 0 hour
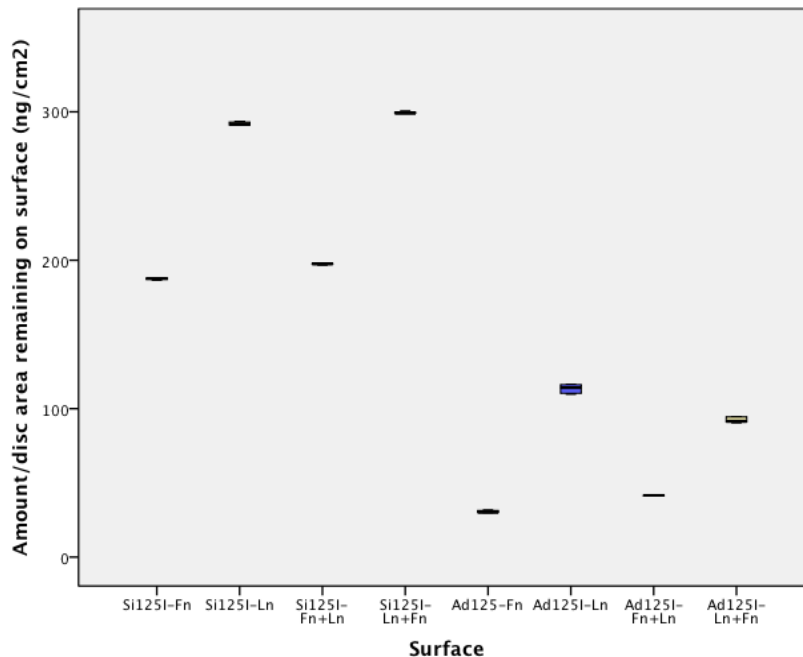
Figure 2.25: Amount of protein/surface area (nanograms/cm^2) remaining on Ti6Al4V surface at 1 hour
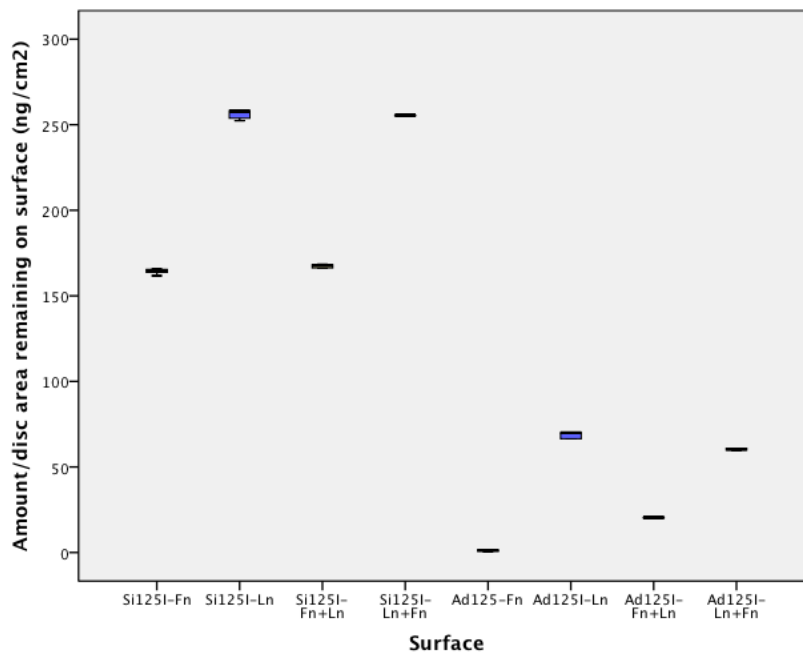
Figure 2.26: Amount of protein/surface area (nanograms/cm^2) remaining on Ti6Al4V surface at 24 hours
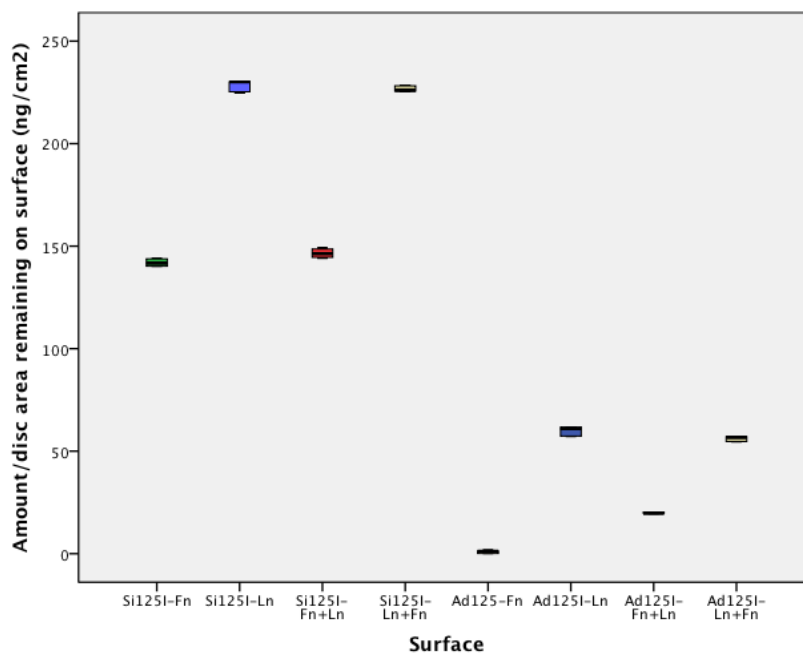
Figure 2.27: Amount of protein/surface area (nanograms/cm^2) remaining on Ti6Al4V surface at 48 hours
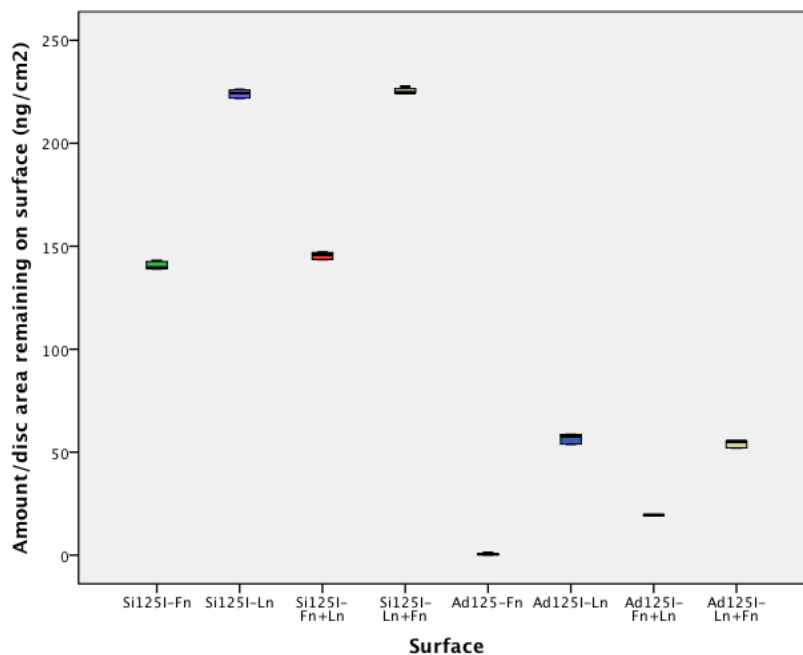
Figure 2.28: Amount of protein/surface area (nanograms/cm^2) remaining on Ti6Al4V surface at 72 hours

2.4 Discussion

2.4.1 Effect of Silanization on Quantity of Protein Attached

Silanized Ti6Al4V significantly binds more protein for both dual and single coatings compared with adsorbed substrates at all time periods. Previous work at our Institute on single coating protein Fn and Ln produced similar results (Middleton et al., 2007; Gordon et al., 2010). In my study, both single coating protein with Fn or Ln separately as well as dual coating proteins with Fn and Ln together attached significantly greater amounts of protein to Ti6Al4V.

Adsorption relies on interaction between protein and Ti6Al4V when the former is placed on its surface. The main advantages of this method are the cost and ease of application which may possibly be carried out in the operating theatre. The process relies mainly on hydrogen bonds, salt channel linkages and Van der Waal's forces for attachment. However, this means it provides weak coupling modalities due to the weak bonding forces. As a result, greater loss of protein occurs from changes in temperature, pH, washing or presence of extra-cellular matrix proteins (Ulbrich et al., 1991). Fluid flow may affect the adsorption process. Middleton et al., 2007 examined the attachment of cells to Ti6Al4V following direct fluid flow directly. They used a novel apparatuts they designed to subject cells attached to Ti6Al4V to a fluid current. They counted the cells that stayed on the surface and from that equation, concluded that fluid flow affects cell attachment. They also found a positive linear correlation between cell attachment and number of focal adhesion vinculin markers.

Immobilization of protein using enzymes can be achieved by inter-molecular cross-linking. This method is both expensive, normally requiring additional means of bonding. However,

since the enzyme is covalently bonded to the support matrix, there is little protein loading loss. Marshall et al. (1973), reported that carbamyl phosphokinase cross linked to alkylamine glass in addition to covalent bonding using glutaraldehyde resulted in a loss of 16% of protein load over 14 days. Occlusion methods where protein is packed within polymerized gels provide an alternative method. This method permits diffusion of protein into the substrate.

Immobilization of proteins on substrates is an effective method of increasing protein loading, thereby decreasing protein loss from the surface due to the strength of protein adhesion. Gluteraldehyde yields an aldehyde that forms a linkage with primary amines on the protein. Ulbrich et al. (1991), compared different types of coupling agents and concluded that gluteraldehyde provided the highest binding yield. The time required to silanize the protein on the surface may be too long for an intra-operative application. However, this time is essential to ensure covalent bonding of protein. Covalent bonding of protein delivers more protein attached to the metal surface compared with adsorbed surfaces and controls. I hope that this would be a suitable micro-environment for early cellspreading and provide more focal adhesion vinculin markers. In my next 2 chapters I will examine whether dual coating protein fibronectin and laminin will affect fibroblast and keratinocyte cell spreading *in vitro.*

Middleton et al.(2007) examined the maximum amount silanized fibronectin to bond to 10 mm diameter Ti6Al4V discs and found that this is 500ng expressed at ng mm^{-2} . They placed loading doses of fibronectin and found saturation of fibronectin was reached at 500ng fibronectin. Gordon et al. (20100 found saturation of silanized laminin was achieved at 500ng on the same diameter discs. Therefore, I used these concentrations of fibronectin and laminin in the release kinetics experiments. My study investigated whether dual

coating protein with these concentrations would result in competitive binding on the Ti6Al4V discs. Interestingly, competitive binding did occur on adsorbed surfaces but non-competitive binding occurred on silanized surfaces. Vroman et al. (1980), described an effect whereby highest mobility proteins arrive first and are later replaced by less motile proteins that have higher affinity for a surface. This competitive binding process showed that highly molecular weight kininogen displaces fibrinogen on bio-polymer surface. I found that fibrinogen and laminin show non-competitive binding when silanized on Ti6Al4V surface. CHO bonds available for protein binding from the silanization process, provide binding arms for more amount of protein to bond. Laurie et al. (1986), showed that there were binding sites on fibronectin and laminin were different on basement membrane. This may explain why there was no increase in the amount of fibronectin bound to the surface in the presence of laminin on either adsorbed or silanized surfaces.

Quantification of immobilized protein has successfully been performed in previous studies. Rodrriguez-Segui et al.(2011), fluorescently labelled fibronectin and stretavidin and used a GenPix fluorescence microarray scanner device to quantify protein on different surfaces. They concluded that certain chemically treated surfaces that allow immobilization of protein are able to retain the protein. Nanci et al. (1998), found similar findings using colloidal gold immunolabelled and silanized albumin.

The quality of silanization can be tested using spectroscopic ellipsometry, atomic force microscopy and water contact angle measurements. A spectropic ellipsometer apparatus measures the spectral variation of ellipsometric angles Ψ and Δ defined through the relation: tgΨe iΔ = Rp Rs (1) where Rp and Rs are the complex reflection coefficients of the light polarized parallel and perpendicular to plane of incidence. Thickness of films present on silicon surface can be determined from the ellipsometric data analysis. Atomic

force microscopy can be used for imaging biofilms. Non-contact mode using silicon-aluminium coated cantilevers with a resonance frequency of 200-400kHz and nominal force contact 40 N/m. Roughness can be calculated on images produced. Sessile drop technique to measure water contact angle with drop shape analysis software.

2.4.2 Effect of Dual Coating Protein on Ti6Al4V

I showed that fibronectin and laminin have non-competitive binding on silanized Ti6Al4V. On the other hand, there is competitive binding between these proteins on adsorbed surfaces. No data in the literature were found to support or challenge this.

2.5 Conclusion

This chapter investigated covalently bonding to dual coating proteins ^{125}I-Fn and ^{125}I-Ln to Ti6Al4V by silanization. I have successfully demonstrated that non-competitive binding of these proteins occurs on silanized surfaces of titanium alloy. This paves the way to *in vivo* studies in which dual coating proteins may be applied to ITAP to improve early tissue spreading onto the alloy.

Silanization process allows for significantly higher quantities of protein to remain on the surface compared with adsorption at all time periods. I have shown that this happens to dual coating proteins as well as single coating protein.

In order to determine whether dual proteins silanized to Ti6Al4 enhance cell adhesion and growth, further experiments are required where cells are grown on dual proteins coatings and their adhesion to the titanium alloy surface is investigated.

CHAPTER 3

Effects of Dual Coating Proteins on Fibroblast Spreading and Number of Focal Adhesion Vinculin Markers

3.1 Introduction

3.1.1 Background

ITAP's success is dependent on early dermal attachment that in turn prevents epithelial down-growth and infection (Pendegrass et al., 2006; Gordon et al., 2010). This can only be achieved through forming an early tight tissue-metal seal.. Couchman et al., 1983 showed dermal fibroblasts have distinct receptors for laminin and fibronectin. In addition, studies have shown fibroblast attachment, spreading and profilereation is enhanced on RGD-modified surfaces (Shu et al., 2003). On the other hand, pretreating keratinocytes with laminin improved epithelial coverage and rate of neobasement membrane formation (Tekada et al., 1999). When ITAP is implanted, cells respond by producing extracellular matrix, which contains proteins that regulate cell proliferation, cell division, cell adhesion and cell migration. Pre-coating the implants with these proteins that contain tripeptide RGD (arginine-glycine-asparnine) sequences may allow the surface to be recognized by integrins enhancing cell adhesion and the formation of a tight seal.

Laminin-332, forms a major component of the basement of the skin and other epithelial tissues. Laminin-332 is a cell adhesion glycoprotein, which interacts with integrin receptors inducing intra-cellular signaling that regulates actin cytoskeleton and gene expression. Laminin-332 interacts with integrin receptors: α3β1, α6β1 and α6β4 integrins, expressed by epithelial cells (Koshikawa et al. 1999, Nguyen et al.200, Nikolopoulos et al.2005). Kariya et al.(2003), found that the major integrin binding site on laminin-332 is located in the LG3 domain of the α3 chains, while the other chains are responsible for the matrix assembly (Hirosaki et al., 2000, Nakashima et al., 2005, Ogawa et al., 2004). The

interaction between laminin-332 and integrin receptors induces intracellular signal transduction to support cell survival and proliferation through gene expression, at the same time supporting cell migration by activating many signal mediators such as focal adhesion kinase, protein kinase C, phosphatidylinositol 3-kinase, Rac and nuclear factor kB. This laminin-332 activity contrasts with fibronectin activity, which induces marked stress fibres and supports stable cell adhesion by activating RhoA via integrin $\alpha5\beta1$. Maschler et al. (2005), showed that cell transformation is accompanied by loss of laminin-332 production and up-regulation of fibronectin and $\alpha5\beta1$ integrin receptor.

Silanizing titanium without passivation not only allows more protein bonding, but also changes the physical surface roughness with that may promote better cell spreading and number of focal adhesion vinculin markers..

In this chapter, I hypothesize that silanized, non-passivated dual coatings of fibronectin and laminin (SiFnLn-) will enhance early fibroblast spreading and number of focal adhesion vinculin markers compared with single coatings (AdFn, AdLn, SiFn-, SiLn-, SiFn+, SiLn+), adsorbed and silanized, passivated dual coatings (AdFnLn, SiFnLn+) and controls (Po, Si-,Si+).

3.2 Materials and Methods

3.2.1 Disc Preparation

10 mm diameter, 3mm thick discs were machined from Ti_6Al_4V rods. These were ground by hand with fine grit paper (300, 600, 1200, 2400, 4000) prior to polishing with a Motopol

2000 grinder (Buehler, Germany), MD polishing cloth (Streuers, Denmark) and OP-S colloidal silica suspension (Streuers, Denmark) 10:1 with 30% H_2O_2 (BDH Ltd, UK). Polished discs (Pol) were considered satisfactory when the surface obtained was a mirror surface finish with an R_a value of less than 0.03 μm measured using a profilometer.

3.2.1.1 Cleaning

Discs were ultrasonically cleaned for 10 minutes immersed in 10% Decon 90 (Decon Laboratory Ltd, UK). The discs were left to rinse under distilled water for 10 minutes. They were placed in Acetone (BDH Ltd, UK) for 10 minutes and air dried under a hood.

3.2.1.2 Autoclaving

Discs were placed into autoclave bags and sterilized in a 2100 Classic Clinical Autoclave (Prestige Medical, UK) for 11 minutes at 126^0C at 1.4 bar pressure.

3.2.1.3 Passivation

Discs were passivated by soaking in a 50:50 of 99% sulphuric acid and 30% hydrogen peroxide (BDH, UK) for 2 hours at room temperature. The passivated discs were rinsed 3 times with distilled water, placed at -70^0C for 30 minutes and vacuum dried for 2 hours.

3.2.1.4 Silanization

Polished and passivated discs were submerged in 10% amino-propyltriethoxysilane (APS) for 2 hrs at 21^0C, for the silanized, non-passivated discs group and the silanized, passivated discs group respectively. Discs were dried at 37^0C in the dry incubator. They

were then immersed in 1% glutaraldehyde solution for 2 hours at 21^0C. These were rinsed thoroughly with PBS.

3.2.2 Protein addition

Surfaces of polished, silanized passivated and silanized non-passivated discs were coated with protein. The protein solution used was either fibronectin (F2006, Sigma-Aldrich, UK) or laminin (CC145, Chemicon International Inc., USA). The dual protein coatings were produced by using equal amounts of fibronectin (F2006, Sigma-Aldrich, UK) and laminin (CC145, Chemicon International Inc., USA).

3.2.2.1 Fibronectin addition method

50μl droplet containing 500ng of fibronectin diluted using sterile PBS, was used to cover the whole disc surfaces. This was left for 4 hours according to the protocol outlined by Middleton et al., 2006. The discs were washed off with distilled water.

3.2.2.2 Laminin addition method

Similar to the steps described above, 500ng laminin in a 50μl droplet was used to cover the disc surfaces. Again, this was left for 4 hours before washing off with distilled water.

3.2.2.3 Dual protein coating addition method

500ng of fibronectin and laminin were diluted with sterile PBS in 25μl droplets separately in Eppindorph tubes. Once prepared, they were immediately mixed to form a 50μl droplet containing 500ng of fibronectin and laminin. The droplet was added to the surface of the discs in a similar method as the single coating protein.

3.2.3 Human Dermal Fibroblasts

1BR.3.G cells derived from a dermal fibroblast, was bought from the European Collection of Cell Cultures supplier (ECACC Catalogue no. 90011801, Lot no. 05G027). Once received, the vial was transferred immediately to gaseous phase liquid nitrogen at -196^{0}C.

3.2.3.1 Resuscitation

Under a tissue culture hood, a tissue soaked in 70% alcohol was used to wipe the cap of the vial. The cap was turned slightly to release any residual liquid nitrogen that may be trapped for 10 seconds and re-tightened. The vial was quickly transferred to a water-bath at 37^{0}C for 1 minute. The rapid thawing was important in minimizing any damage to the cell membrane. The vial was removed from the water-bath and wiped by another 70% alcohol soaked tissue. The contents of the vial were slowly pipetted into a universal tube containing 5ml warm Dulbeccos' Modified Eagle's Media (DMEM) (D6429, Sigma-Aldrich, Ayshire, UK). To remove the cryoprotectant, the tube was centrifuged at 2000 revolutions per minute for 5 minutes. The pellet was resuspended in 35ml DMEM for culture in a 225cm^2 vented flask (Corning Incorporated, New York, USA).

3.3.3.2 Monitoring

Fibroblasts were incubated in DMEM (Sigma-Aldrich, UK) with 4500mg/L, 1% non-essential amino acids, 1% penicillin and streptomycin (Invitrogen, Paisley, UK) and 10% foetal calf serum (First Link Ltd, UK). The flasks were placed in an incubator (Function Line Haraeus Instruments) at 37^{0}C and 5%CO_2. Media was changed every 48 hours until confluence was reached (4 million fibroblasts at 7 days).

3.2.3.3 Trypsinisation

Under tissue culture hood, media was removed, 10mls sterile Phosphate Buffered Saline (PBS) (Oxoid Ltd, Basingstoke,UK) was used to wash the floor of the vented flask to remove any detached dead cells, 10mls of 10% trypsin (T8003, Sigma-Aldrich, UK) was added and the flask was left in the incubator for 5 minutes. Cell detachment was checked under the light microscope (Olympus CkX31) using 10x objective. A gentle tap was required if cells remain attached or incubating for 5 more minutes.

20mls of DMEM was added and the suspension was centrifuged at 2000 revolutions per minute for 5 minutes. The supernatant containing trypsin and DMEM was discarded leaving a pellet containing fibroblasts at the bottom of the tube.

3.2.3.4 Cell Counting

1ml of DMEM was added to re-suspend fibroblasts. 20μl of the suspension and an equal volume of Trypan Blue (T8154, Sigma-Aldrich, UK) were pipetted and mixed into a sterile Eppindorf tube. The mixture was left to stand for 2 minutes. A 10μl droplet of the resultant cell suspension was placed under a glass coverslip attached to a Neubauer haemocytometer counting chamber slide (Sigma-Aldrich, UK). The coverslip was made to attach by placing it on top on the slide and rubbing the 2 surfaces until Newton's rings were seen. The slide was placed under a light microscope (Olympus, Japan), and using 10x objective, the number of cells found in 4 chambers under the slide, were counted. The total number of cells in the original suspension was calculated by multiplying the mean of total number of cells counted, by dilution factor with Trypan Blue (i.e2x since there were equal volumes of cell suspension and Trypan Blue, by volume of cell suspension). Two

independent observers counted each sample and sample was accepted for experiment when identical count was obtained. This follows the same protocol outlined by Middleton et al., 2007, Gordon et al., 2008 while examining single coating protein on Ti6Al4V surface.

3.2.3.5 Cell seeding on discs

5000 fibroblasts in a 50μl droplet were placed on the centre of each disc surface, spread evenly to the margins using the micropipette tip. A 24 well-plate holding the discs was placed in an incubator (Function Line Haraeus Instruments) at 37^{0}C and 5%CO_2, for 1 hour. It was transferred to a sterile fume hood where the discs were submerged with 1ml of Fetal Calf Serum. The well plate was incubated for 1, 4 and 24 hours.

3.2.4 Antibody Detection Method

Discs were washed for 5 minutes in PBS twice. They were fixed in 10% formal saline for 5 minutes. To rehydrate the cells, the discs were washed for 20 minutes in PBS, changing the solution every 5 minutes. 50μl droplet formed using 250nl primary anti-vinculin mouse monoclonal antibody (v9131, Sigma-Aldrich,UK) diluted in 49.625μl PBS + 125nl Triton X-100 (Sigma-Aldrich, UK), was placed on top of each disc, with special care not to drop any solution from the top, for 2 hours at room temperature. The discs were washed 3 times for 10 minutes each in PBS in the dark room, followed by addition of 50μl droplet of Alexa Fluor 488 rabbit anti-mouse IgG secondary antibody (A21441, Invitrogen, UK) diluted in PBS (1:100), for 1 hour. The plates were wrapped in tin foil to prevent exposure of labeled cells to light.

3.2.5 Cell Area and Antibody Analysis

Oil drops were placed on glass cover slips that covered top surfaces of the discs. Each disc was placed on a glass slide and examined under a photomicroscope (Carl-Zeiss x100 lens objective). 15 randomly selected cells were identified for each surface type and anti-vinculin markers were counted by two independent observers who were blinded both to test substrate and to one another. This was following the same protocol used by Middleton et al., 2007, and Gordon et al., 2008 when examining single coating protein on Ti6Al4V surface. Photographs were taken using Carl-Zeiss microscope (Carl Zeiss Ltd, Welwyn Garden City, UK) with x50 and 100x objective lenses. Focal adhesion vinculin markers and the cell area were calculated using Axiovision Image Analysis software (Axioimage 4.4; Carl Zeiss, Gottingen, Germany).

3.2.6 Surface Profilometry

Polished, silanized, non-passivated and silanized, passivated discs (n=6) were tested for average surface roughness (R_a) using a Tesa-Rugosurf 90-G profilometer (TESA Technology, Switzerland), at an angle of incidence of 65∘over the range 300–1600 nm with a resolution of 5 nm. Three readings were obtained for each disc using same protocol outlined by Middleton et al., 2007; Gordon et al., 2008.

3.2.7 Statistical Analysis

SPSS statistical package for Mac (Version 18.0, SPSS Inc, USA) was used for data analysis. Using kappa statistics, kappa scores indicated almost perfect inter-observer reliability (>0.9). The data did not meet assumptions of parametric testing (Kolmogorov-Smirnov p>0.05) and data were analysed using a non-parametric test. Mann-Whitney U

test was used to compare medians. Box plots showing median values, whole and interquartile ranges were plotted. Median values (with 95% CI) were expressed. Results were considered significant at p-value < 0.05 level.

3.3 Results

3.3.1 Box and Whisker Plots

In the graphs, the box length represents the difference between the 25th and 75th percentiles. The horizontal line inside the box represents the median. The whiskers represent the largest and smallest values.

3.3.2 Cell Area

Cell area increased significantly between 1 to 4 and 4 to 24 hours (p<0.05) [Figures 3.1-3.3] on dual coated substrates compared to uncoated controls and single protein coatings (p<0.05) [Figures 3.4-3.6]. On adsorbed substrates, a 4, 3.7 and 3.3-fold increase was seen with AdFnLn compared with Pol substrate alone at 1, 4 and 24 hours, respectively. Cell area was observed to be 1.3-fold greater on AdFnLn than on AdFn at all time points. There was a 1.5, 1.5 and 1.4-fold increase was seen with AdFnLn compared with AdLn alone at 1, 4 and 24 hours, respectively. Cell area was observed to be 3, 1.3 and 1.4-fold greater on SiFnLn- compared with Si- alone at 1, 4 and 24 hours, respectively. In addition there was a 1.3, 1.2 and 1.2-fold greater on SiFnLn- than on SiFn- at 1, 4 and 24 hours, respectively. A 1.5, 1.3 and 1.4- fold increase was seen with SiFnLn- compared with SiLn- at 1, 4 and 24 hours, respectively. On silanized, passivated surfaces a 2, 1.8 and 1.8-fold increase with SiFnLn+ compared with Si+ substrate alone at 1, 4 and 24 hours, respectively. There was a 1.2-fold increase was seen with SiFnLn+ compared with SiFn+

at 1 and 4 hours, respectively. In addition, a 1.4, 1.3 and 1.1-fold increase with SiFnLn+ compared with SiLn+ at 1, 4 and 24 hours, respectively.

At all time points, for dual protein coated surfaces, cell area increased significantly in the order: Si+, Ad, Si-. At 1 hour, there was a 1.5 and 1.2-fold increase seen with SiFnLn- compared with SiFnLn+ and AdFnLn, respectively. At 4 hours, SiFnLn- showed a 1.6 and 1.2-fold increase compared with SiFnLn- and AdFnLn, respectively. At 24 hours, there was a 1.9 and 1.2-fold increase seen with SiFnLn- compared with SiFLn+ and AdFnLn, respectively. A similar pattern was observed for single protein coatings at all time points.
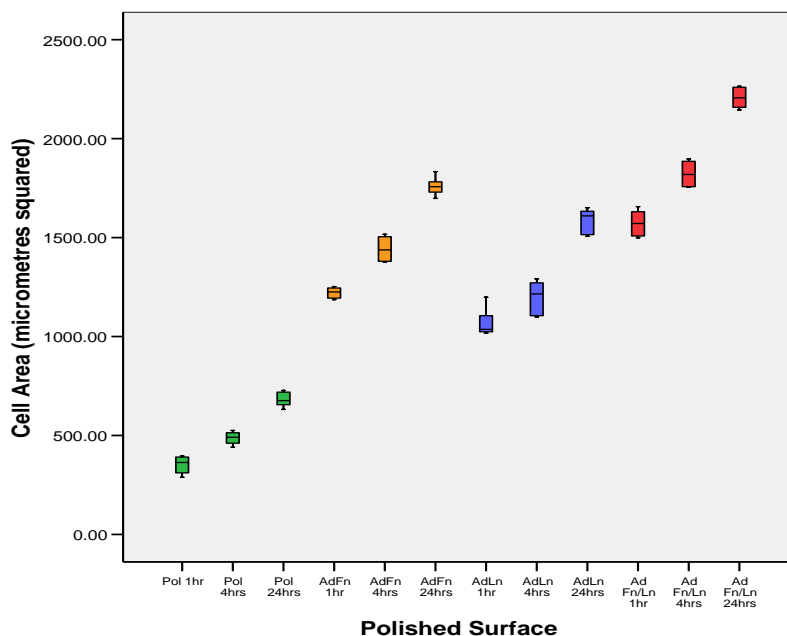
Figure 3.1: Box Plot showing Cell Area (μm^2) at 1, 4 and 24 hours on adsorbed surfaces
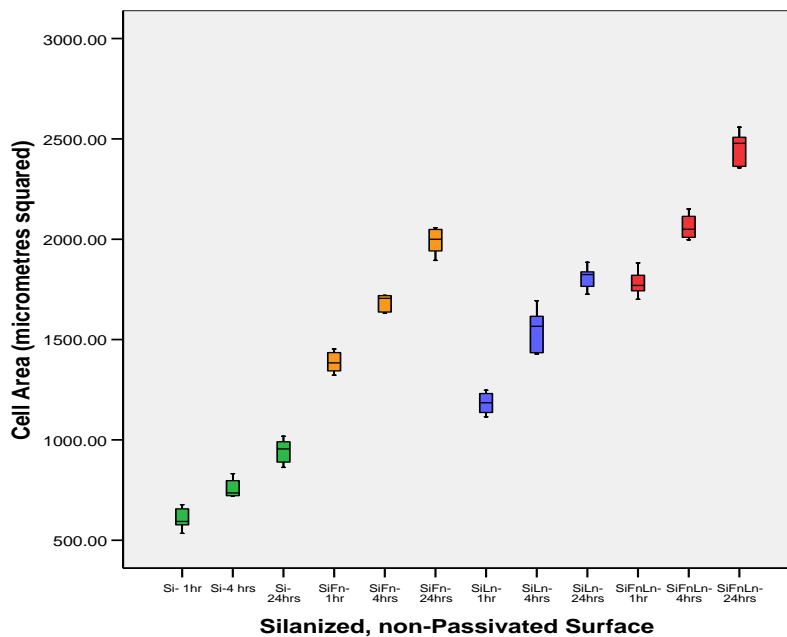
Figure 3.2: Box Plot showing Cell Area (μm^2) at 1, 4 and 24 hours on silanized, non-passivated surfaces
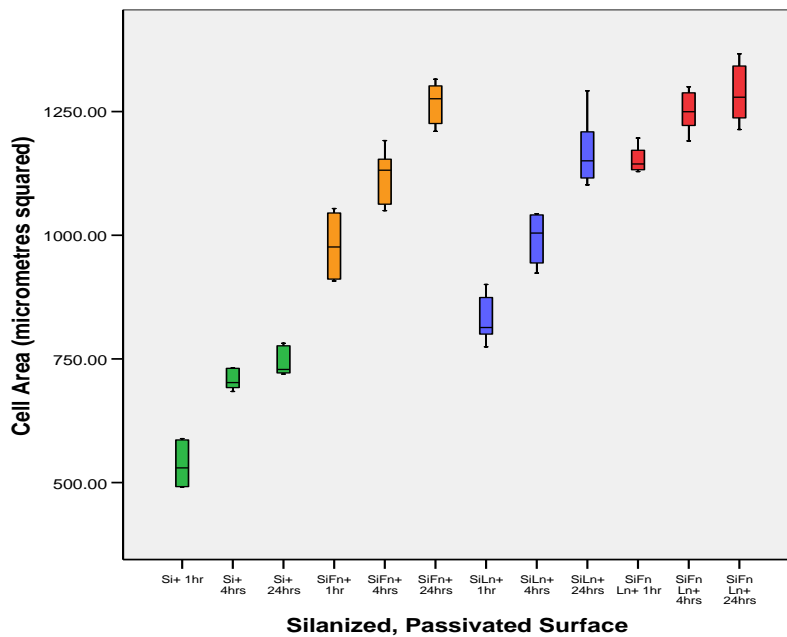
Figure 3.3: Box Plot showing Cell Area (μm^2) at 1, 4 and 24 hours on silanized, passivated surfaces
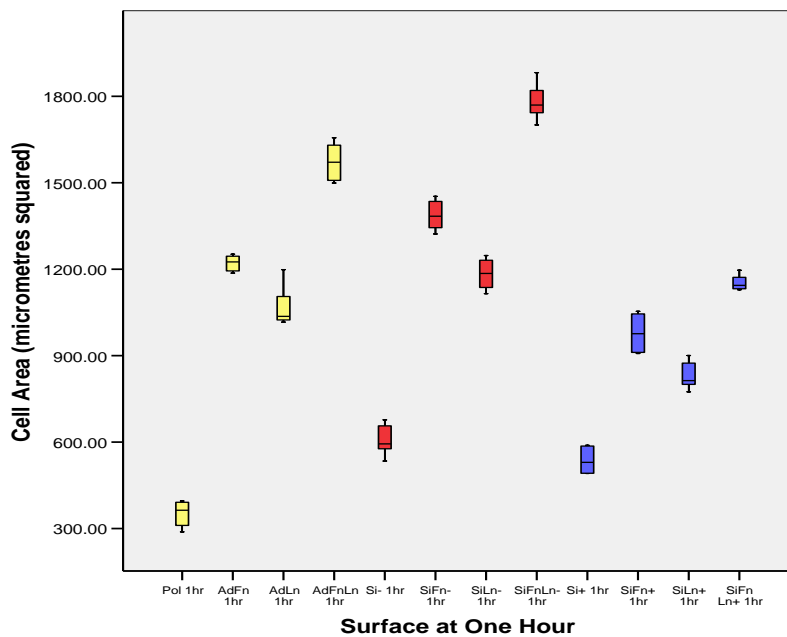
Figure 3.4: Box Plot showing Cell Area (μm2) at 1 hour on different surfaces
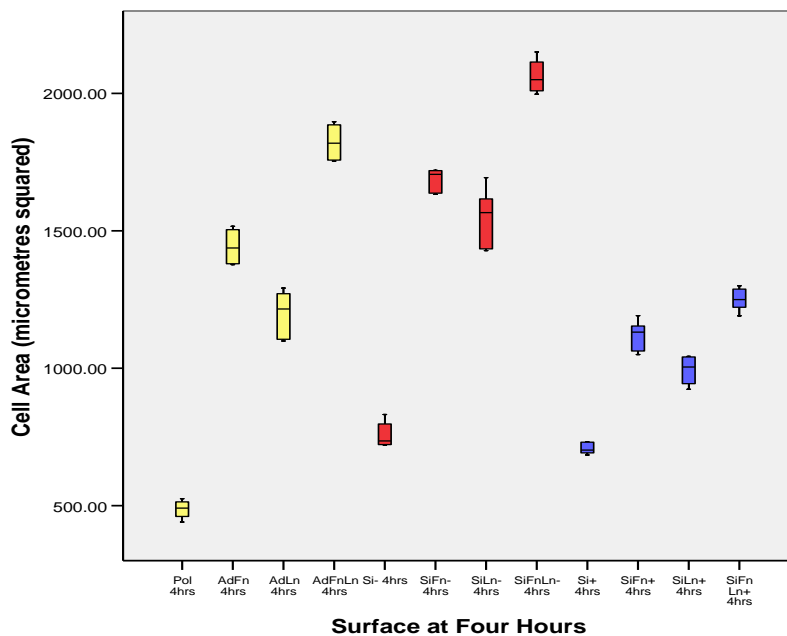
Figure 3.5: Box Plot showing Cell Area (μm^2) at 4 hours on different surfaces
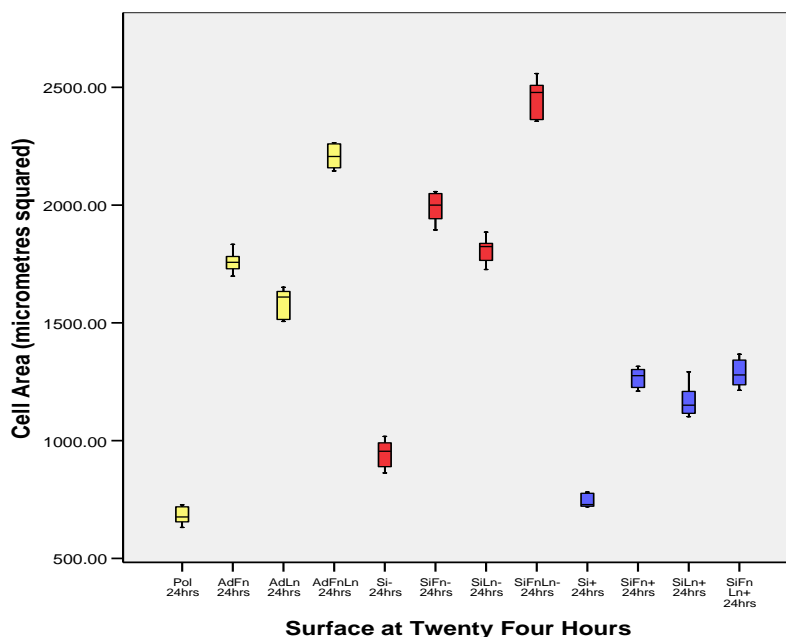
Figure 3.6: Box Plot showing Cell Area (μm^2) at 24 hours on different surfaces

3.3.3 Focal Adhesion Markers Per Cell Unit

Vinculin markers appear as needle shaped markers under the immunofluorescent

microscope. They form during spreading and attachment of cells on surfaces once cell

remodeling has occurred and the cell microenvironment is suitable for cell adhesion over

time. My results show consistency over time of cells on dual coated protein substrate

producing significantly greater numbers of vinculin markers than cells on single coating

proteins or uncoated substrates ($p<0.05$) [Figures 3.7-3.9]. On adsorbed substrates, a

62.7, 23.6 and 25.7-fold increase was seen with AdFnLn compared with Pol substrate

alone at 1, 4 and 24 hours, respectively. Vinculin markers were observed to be 1.7, 1.6

and 1.7-fold greater on AdFnLn than on AdFn at 1, 4 and 24 hours, respectively. There

was a 2.5, 3.2 and 1.8-fold increase was seen with AdFnLn compared with AdLn alone at

1, 4 and 24 hours, respectively. Vinculin markers were observed to be 21.8, 15.6 and

13.5-fold greater on SiFnLn- compared with Si- alone at 1, 4 and 24 hours, respectively. In addition, there was a 1.7, 1.6 and 1.6-fold greater on SiFnLn- than on SiFn- at 1, 4 and 24 hours, respectively. A 2.3, 2.1 and 2.1- fold increase was seen with SiFnLn- compared with SiLn- at 1, 4 and 24 hours, respectively. On silanized, passivated surfaces a 9.8, 6.8 and 6.8-fold increase with SiFnLn+ compared with Si+ substrate alone at 1, 4 and 24 hours, respectively. There was a 1.9, 1.7 and 1.3-fold increase was seen with SiFnLn+ compared with SiFn+ at 1, 4 and 24 hours, respectively. In addition, a 2.7, 1.7 and 2.3-fold increase with SiFnLn+ compared with SiLn+ at 1, 4 and 24 hours, respectively.

In addition to this, adsorbed dual coatings produced less vinculin than silanized, non-passivated single coatings at all time points (p<0.05) [Figures 3.10-3.12].
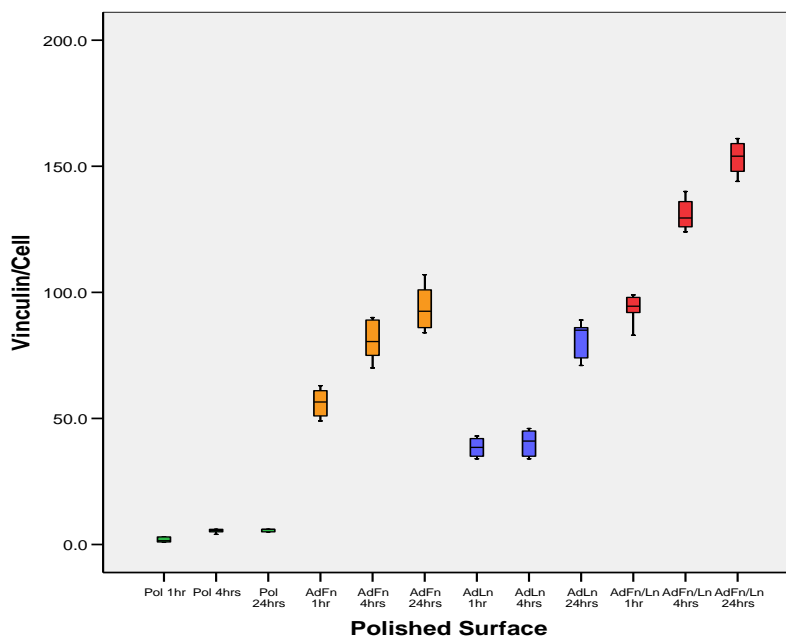
Figure 3.7: Box Plot showing Vinculin marker/Cell unit at 1, 4 and 24 hours on adsorbed surfaces
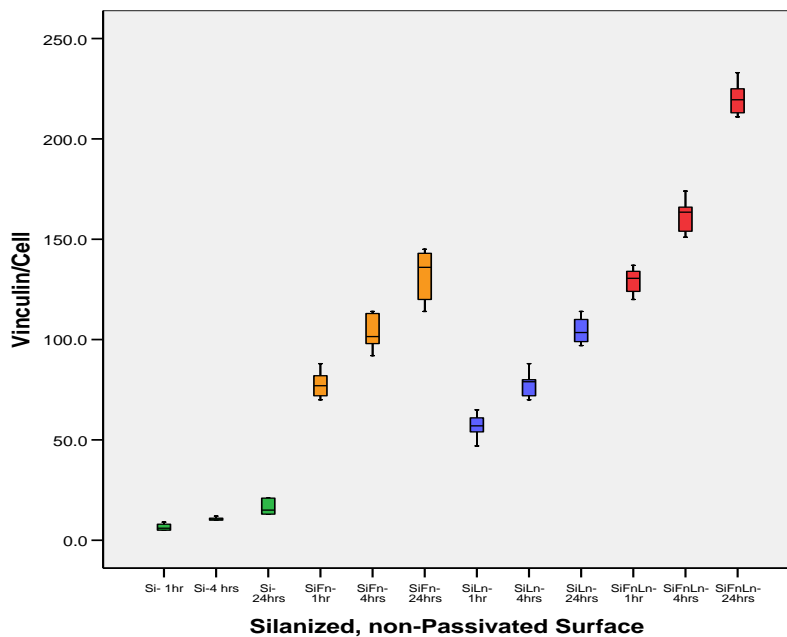
Figure 3.8: Box Plot showing Vinculin marker/Cell unit at 1, 4 and 24 hours on silanized, non-passivated surfaces
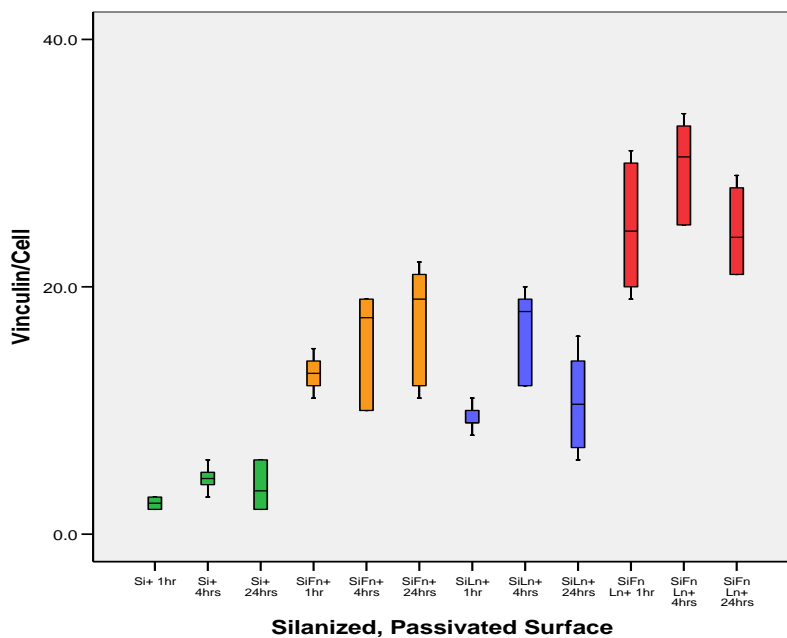
Figure 3.9: Box Plot showing Vinculin marker/Cell unit at 1, 4 and 24 hours on silanized, passivated surfaces
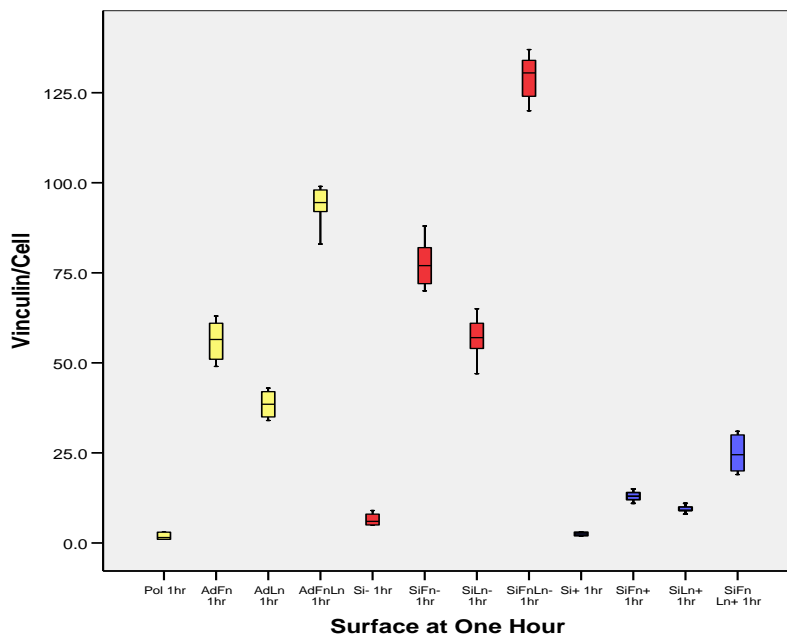
Figure 3.10: Box Plot showing Vinculin marker/Cell unit at 1 hour on different surfaces
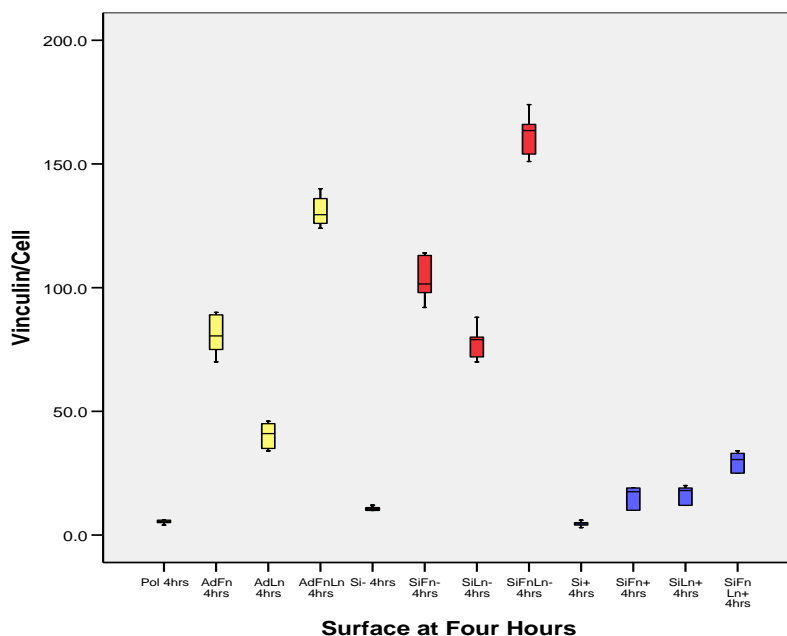
Figure 3.11: Box Plot showing Vinculin marker/Cell unit at 4 hours on different surfaces
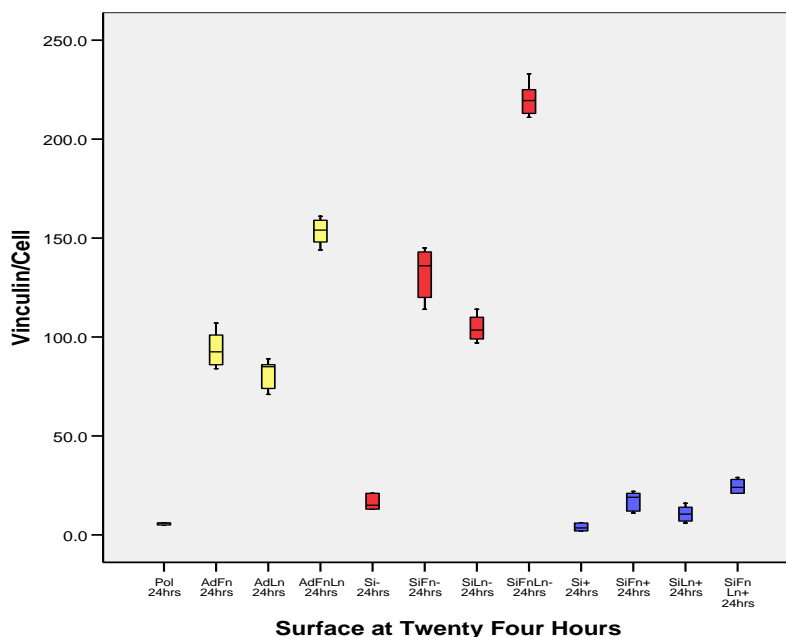
Figure 3.12: Box Plot showing Vinculin marker/Cell unit at 24 hours on different surfaces

3.3.4 Vinculin Markers Per Cell Area

There is a high correlation between cell area and vinculin per cell and cell area (Hunter et al., 1995). My results show that dual coating proteins continued to provide greater vinculin per cell area compared with single coatings on each titanium topography at all time points (p<0.05) [Figures 3.13,3.14,3.15]. This suggests that in the first 24 hours, as fibroblasts grow, more focal adhesion contacts per area are produced on dual coatings substrates. On adsorbed substrates, a 15, 6.3 and 8.3-fold increase was seen with AdFnLn compared with Pol substrate alone at 1, 4 and 24 hours, respectively. Vinculin markers per cell area were observed to be 1.3-fold greater on AdFnLn than on AdFn at all time points. There was a 1.5, 2.2 and 1.3-fold increase was seen with AdFnLn compared with AdLn alone at 1, 4 and 24 hours, respectively. Vinculin per cell area were observed to be 7.4, 5.4 and 5.9-fold greater on SiFnLn- compared with Si- alone at 1, 4 and 24 hours, respectively. In addition, there was a 1.3-fold greater on SiFnLn- than on SiFn- at all time points. A 1.5, 1.6

and 1.6- fold increase was seen with SiFnLn- compared with SiLn- at 1, 4 and 24 hours, respectively. On silanized, passivated surfaces a 4.7, 3.7 and 3.9-fold increase with SiFnLn+ compared with Si+ substrate alone at 1, 4 and 24 hours, respectively. There was a 1.6, 1.5 and 1.2-fold increase was seen with SiFnLn+ compared with SiFn+ at 1, 4 and 24 hours, respectively. In addition, a 1.9, 1.3 and 2-fold increase with SiFnLn+ compared with SiLn+ at 1, 4 and 24 hours, respectively.

Si- surfaces provide the best surface for vinculin per cell area followed by Ad then Si+ surfaces at all time intervals [Figures 3.16-3.21]. A 3.4, 3.3 and 5- fold increase was seen on SnFnLn- compared with SiFnLn+ at 1, 4 and 24 hours, respectively. In a similar pattern, there was a 12, 1.3 and 1.3-fold increase on SnFnLn- compared with AdFnLn at 1, 4 and 24 hours, respectively.
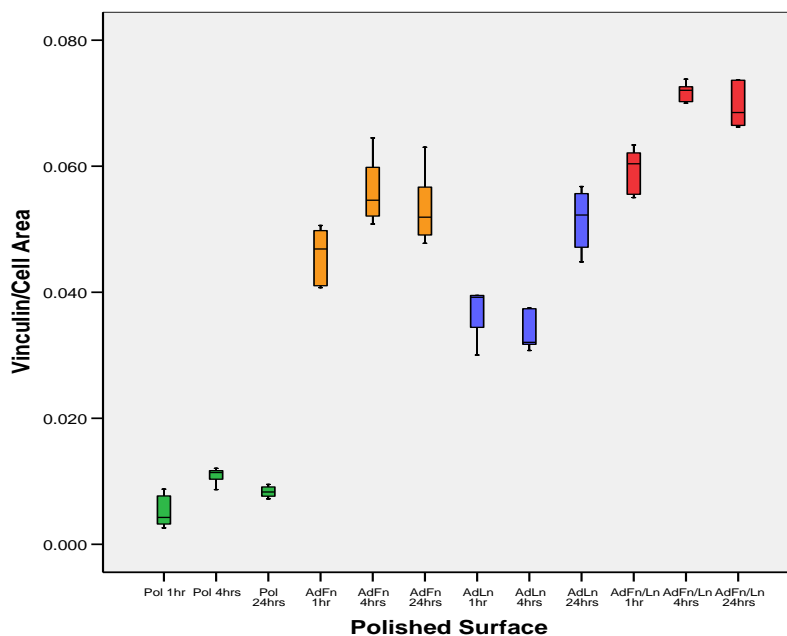
Figure 3.13: Box Plot showing Vinculin marker/Cell area at 1, 4 and 24 hours on adsorbed surfaces
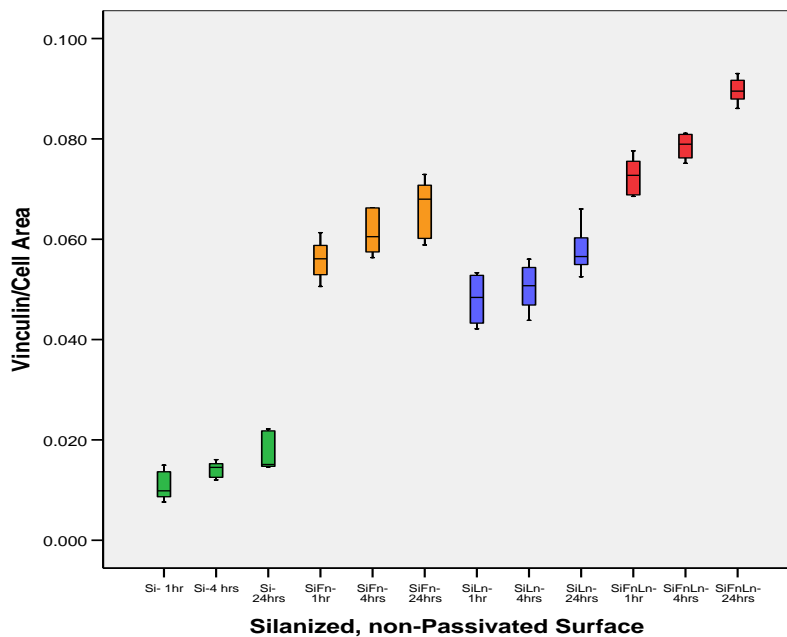
Figure 3.14: Box Plot showing Vinculin marker/Cell area at 1, 4 and 24 hours on silanized, non-passivated surfaces
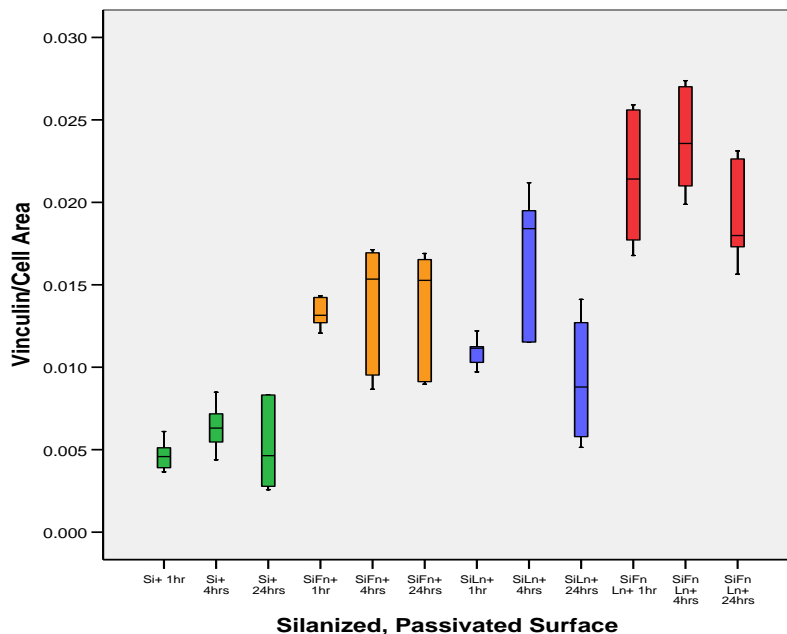
Figure 3.15: Box Plot showing Vinculin marker/Cell area at 1, 4 and 24 hours on silanized, passivated surfaces
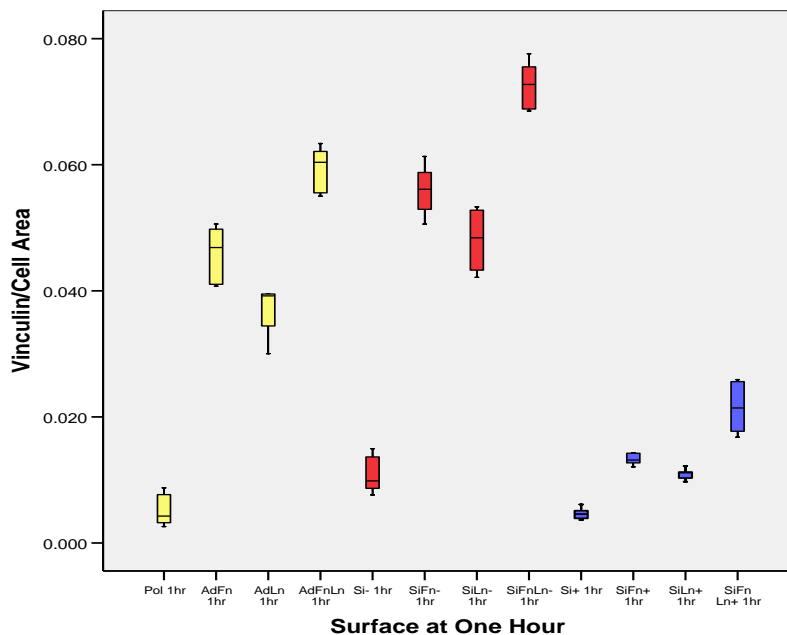
Figure 3.16: Box Plot showing Vinculin marker/Cell area at 1 hour on different surfaces
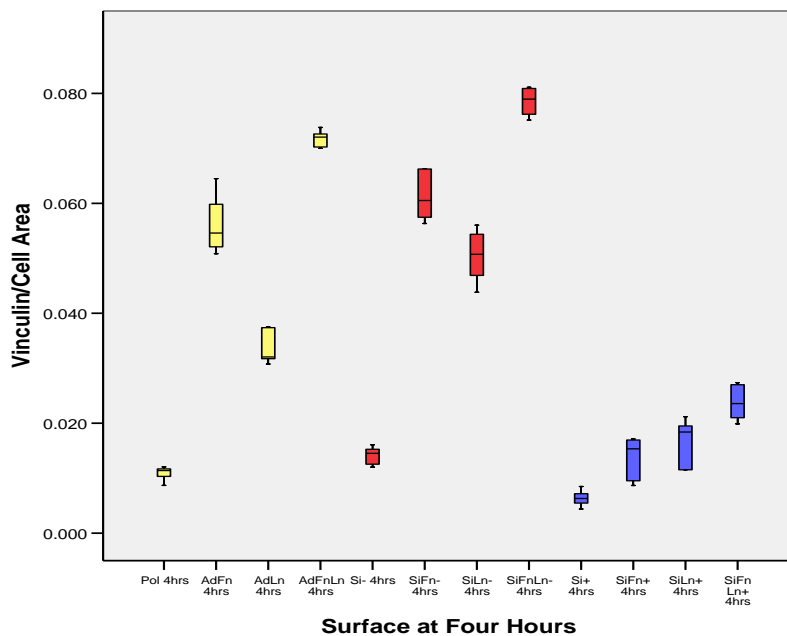
Figure 3.17: Box Plot showing Vinculin marker/Cell area at 4 hours on different surfaces
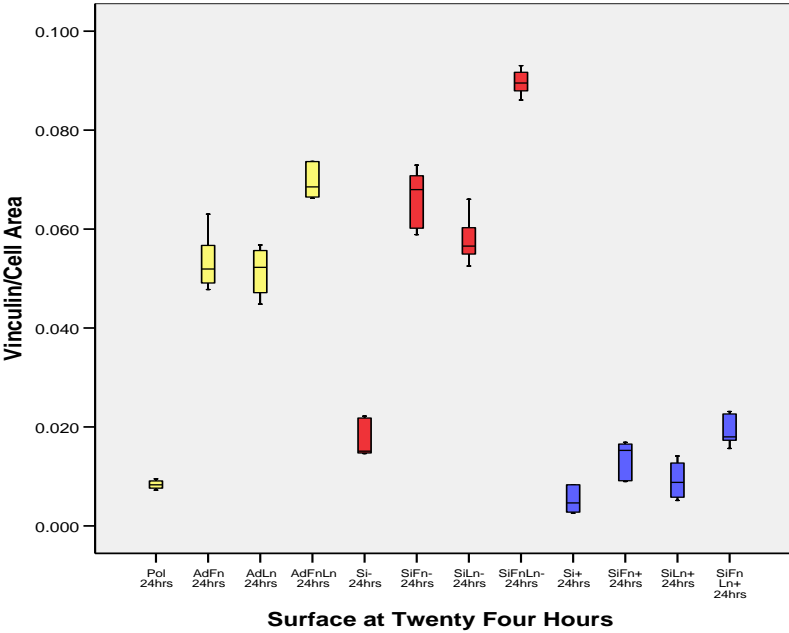
Figure 3.18: Box Plot showing Vinculin marker/Cell area at 24 hours on different surfaces
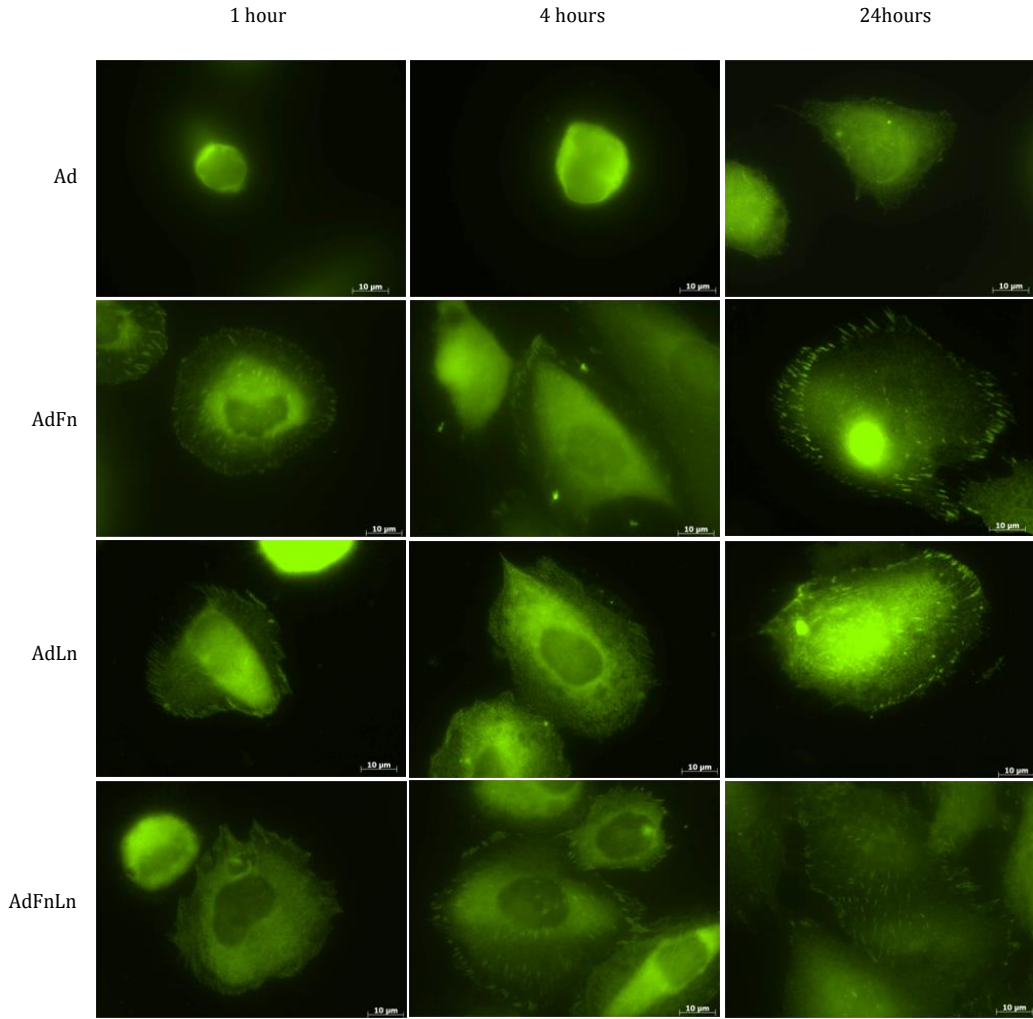
Figure 3.19: Fibroblasts cultured at 1, 4 and 24 hrs on absorbed single and dual coating protein surfaces stained for focal adhesion plaques with anti- vinculin on polished surfaces
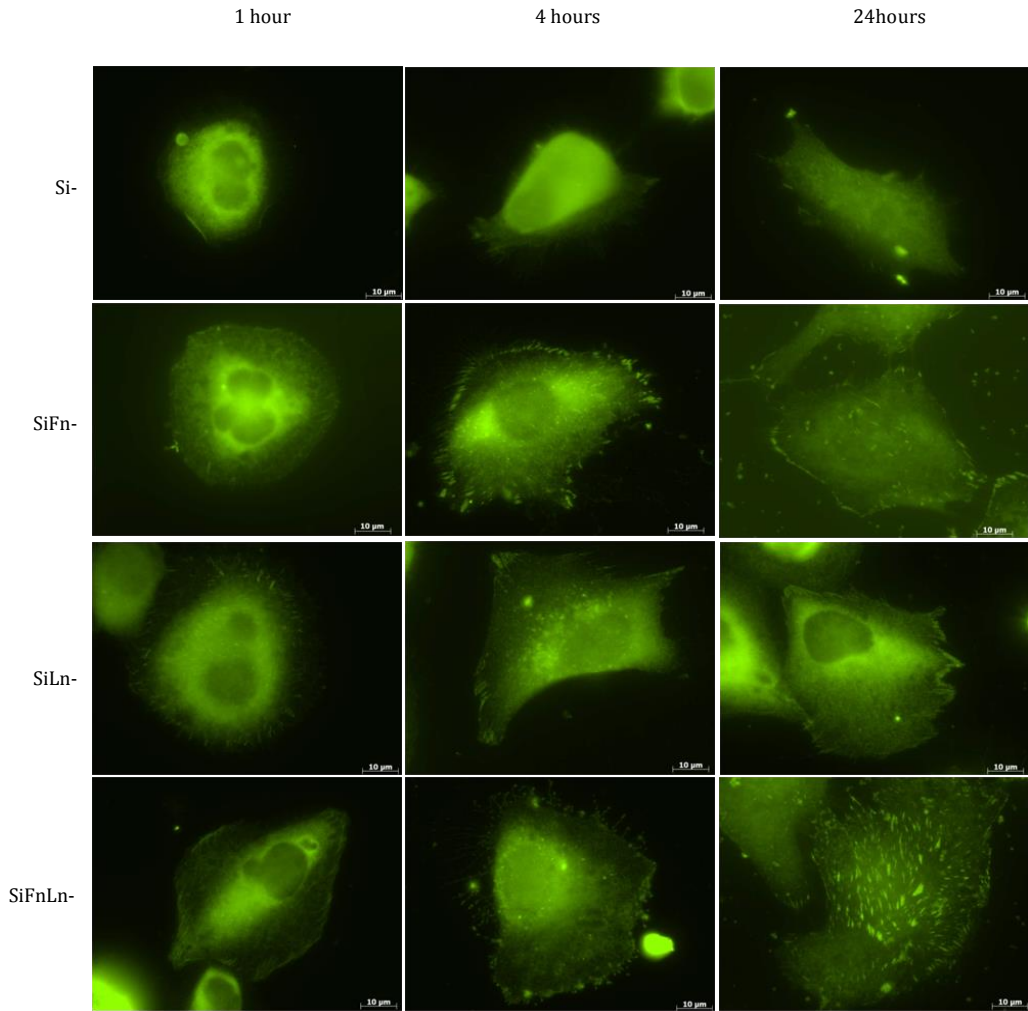
Figure 3.20: Fibroblasts cultured at 1, 4 and 24 hrs on non-passivated, silanized single and silanized dual coating protein surfaces stained for focal adhesion plaques with anti- vinculin
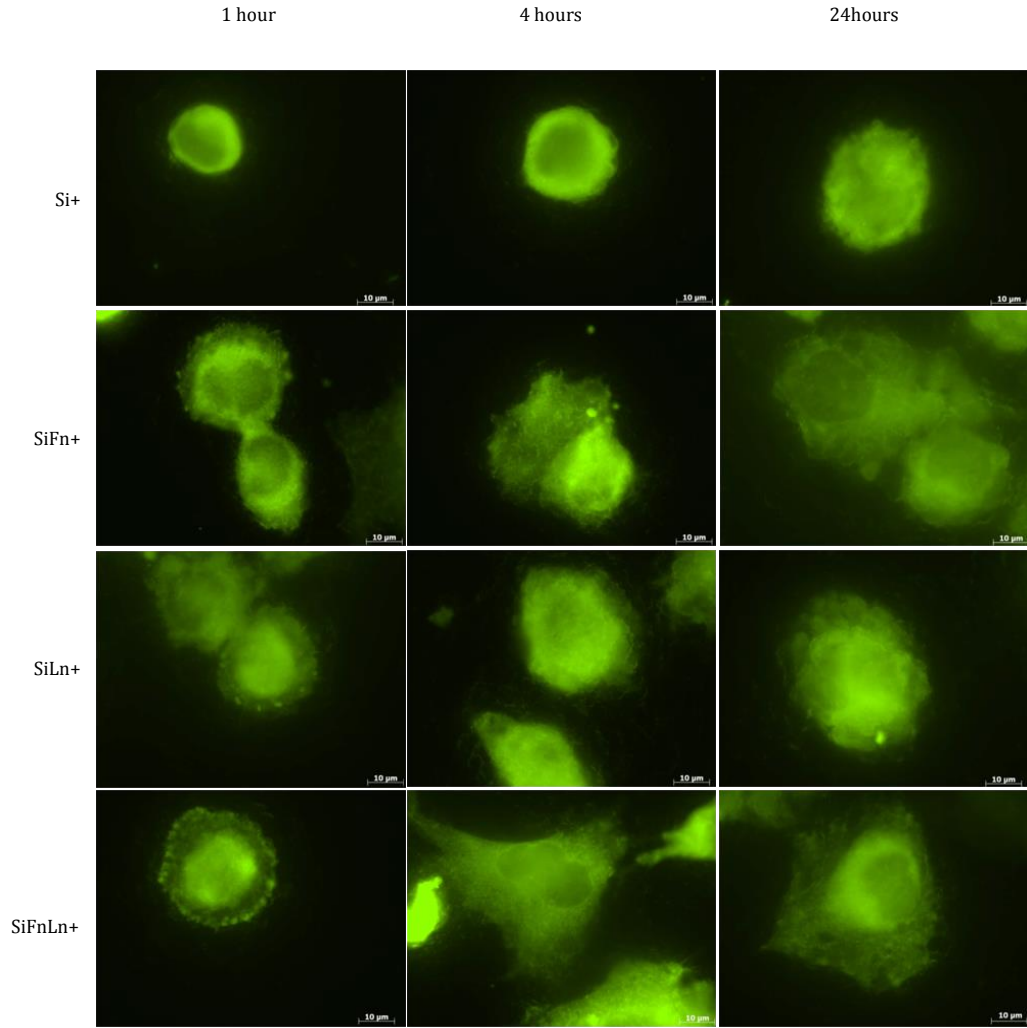
Figure 3.21: Fibroblasts cultured at 1, 4 and 24 hrs on single and dual coating protein surfaces stained for focal adhesion plaques with anti- vinculin on silanized, passivated surfaces

3.3.5 Surface Roughness of different Ti topographies

Silanized, passivated Ti surfaces have the highest average surface roughness, followed by silanized, non-passivated, then polished surfaces ($p<0.05$) [Figure 3.22]. This suggests that surface roughness is a contributing factorto increased number of focal adhesion vinculin markers. .
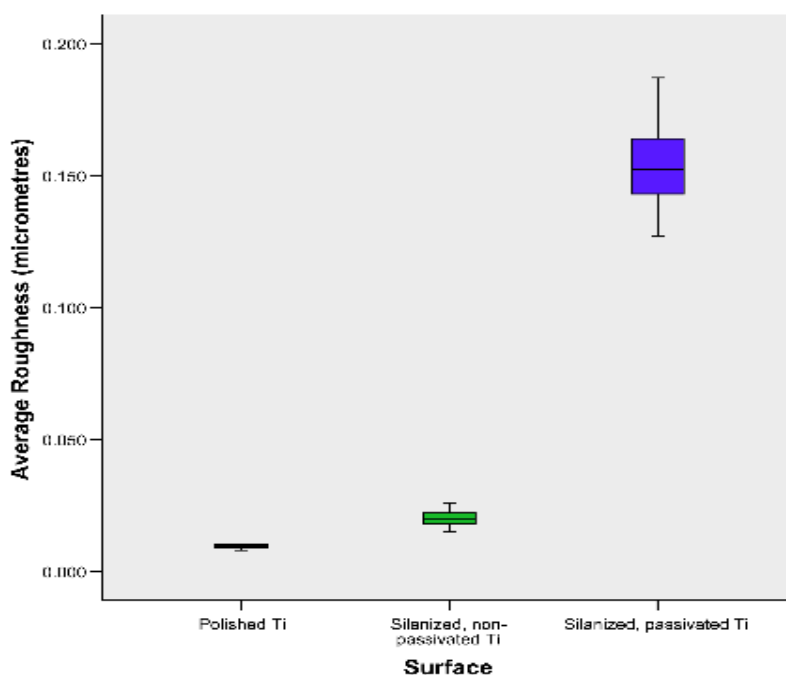
Figure 3.22: Box plot showing average surface roughness (R_a) on polished, silanized, non-passivated,and silanized, passivated titanium surfaces

3.4 Discussion

In my work, I demonstrated that number of focal adhesion vinculin markers and cell spreading increase on dual coating protein surfaces compared with single coatings and controls at all time points. There may be a number of contributing factors that may have

influenced this finding. I postulate that in the presence of dual protein coatings on Ti surface, cells need less adaptation to suit their environment, by secreting ECM proteins, in order to remodel the surface for better attachment and spreading. This is supported by data of cell area, expression of vinculin markers and vinculin per cell area. Other research groups have shown similar findings with dual coatings. For example, Huang et al. (2010), showed that with dual conjugation of fibronectin and collagen I on a platform that supported lipid bilayers, improved fibroblast size and number was observed compared with single coatings alone. They suggested that this might be because fibroblasts did not need to produce endogenous fibronectin to remodel their microenvironment and that as a consequence of this ECM orientation and composition was more similar to that normally encounter by cells in vivo, thus energy required to re-organize and deposit ECM is would be reduced allowing earlier up-regulation of cell attachment. This is also supported by findings by Laflamme et al.(2008), who showed that dual coating proteins with BMP-2/BMP-7 enhanced osteoblast adhesion and growth compared with single coatings with either BMP-2 or BMP-7. They suggested that this may be due to different BMPs acting synergistically to enhance bone regeneration, through improving the expression of type I collagen mRNA and interleukin-6 mRNA expression for which BMP-2 and BMP-7 have a major role in their formation, respectively.

In addition to this, I also suggest that packing the surface with dual proteins produces a construct formed of different sized proteins that looks like a "choppy sea" as opposed to a uniform surface of a "mill pond". More specifically, Biggs et al., 2010 showed that microgrooves greater than 70nm have a detrimental effect on focal contact formation. Hence, it is suggested that cell adhesion is affected when microgrooves are greater than 70nm in height. This in turn, exposes more RGD sequences available for cell adhesion.

Sousa et al. (2008), found that pre-adsorbing equal ratios of fibronectin and albumin on titanium substrates provided better osteoblast adhesion than albumin, 10% plasma or albumin/ fibronectin in the ratio of 200:1. They suggested that the presence of albumin may improve presentation of fibronectin in a more integrin recognized confirmation and provide some degree of molecular packing that prevents loss of integrin binding activity.

It is possible that the observations with fibroblasts on Fn and Ln are a cause of synergistic effect. Cells do not need to organize their matrix accordingly and its more akin to the in vivo situation so these cells upregulate expression of vinculin attachment earlier on dual coatings compared with single coatings. In order to prove this, one would need to further analyze the components of ECM produced by fibroblasts cultured on Ti over time. This would be possible by treating the cells with cycloheximide, which blocks the secretion of endogenous ECM proteins, then comparing the effect of treated and untreated cells on non-coated, single and dual coating protein surfaces.

Van den Dolder et al. (2003), evaluated the effect of fibronectin and collagen I coatings on titanium fibre mesh on the proliferation and osteogenic differentiation of bone marrow rat cells in vitro. They compared single coatings with either fibronectin or collagen I to dual coatings with both over 16 days. Then, they ran a DNA quantification analysis, alkaline phosphatase, calcium and osteocalcin measurements. They found that proliferation of osteogenic cells was not stimulated by single or dual coating of fibronectin or collagen I on titanium fibre meshes. Their results may be different from mine because they did not study the effect of cell adhesion within the first few hours. Moreover, none of the protein added to the titanium was covalently bonded to the surface and the surface roughness was different. It may also be due to the difference in cell type studied. In order to prove the

case, one would need to study the effect of endogenous ECM in remodeling the

environment prior to cell adhesion, by analyzing the protein expression by the cells using

reverse-transcriptase polymerase reaction and quantification of this protein using Western

blotting.

Moreover, my work showed that dual coatings on silanized, non-passivated surface,

improved cell attachment and growth significantly compared with those on adsorbed or

silanized, passivated surfaces at all time points. This may be due to the surface roughness

of Ti. Other research groups have produced similar results with different surface

roughness. Lee et al.(2009), showed that surface microgrooves of 60μm in width and

10μm in depth on acid-etched Ti improved proliferation of human gingival fibroblasts and

increased expression of fibronectin and Rho A proteins, compared with shallower or

deeper microgrooves. Interestingly, Walboomers et al. (1999), showed that fibroblast

attachment to micro-grooved substrates decreased at 1 hour but increased at later time

points. This may be because of absence of pre-coated proteins, which meant that the cells

had to remodel the environment prior to cell adhesion to the surface. This is also evident

from the up-regulation of α5 integrin gene expression and production of fibronectin. They

suggested that the cells migrated into the microgrooves and formed focal adhesion points

at the bottom. They postulated that the depth of the grooves were as important as the

width, since microgrooves with 60μm in width but 5μm in depth showed significantly worse

results.

3.5 Conclusion

I have demonstrated that human dermal fibroblasts are capable of attaching to and growing on Ti6Al4V pre-coated with dual proteins in vitro. I have demonstrated that fibroblasts present significantly higher numbers of vinculin and are larger in size when Ti6Al4V is pre-coated with dual coating proteins when compared with single protein coatings and controls at all time points. I have demonstrated that Ti6Al4V surface topography influences cell attachment and growth. My results have shown that silanized, non-passivated Ti6Al4V re-coated with dual proteins fibronectin and laminin would be the best surface topography to incorporate into ITAP pins in order to promote a dermal seal at this level.

CHAPTER 4

Keratinocyte Spreading and Number of Focal Adhesion Vinculin Markers on Titanium Alloy with Dual Coating Proteins

4.1 Introduction

4.1.1 Background

Early epidermal attachment to titanium alloys allows early cell growth and adhesion (C Middleton et al., 2007). Keratinocytes' ability to bond effectively to an inorganic surface prevents tissue retraction around the metal implant, marsupilization, wound down-growth, infection and subsequent failure (Heaney et al., 1996). In vitro studies investigated adhesion and growth of cells to the implant and interaction between the implant and the biological system. These studies determined a positive influence of fibronectin and laminin on epithelial cells' attachment (Dean III et al, 1995). Distinct preference in adherence was found when fibronectin or laminin were added separately on the titanium surface, to fibroblasts and epithelial cells, respectively. They used adsorbed single coating fibronectin and laminin on substrates composed of plasma-sprayed titanium, hydroxyapatite-coated titanium, and machine finished titanium. They used protein adsorption technique similar to mine. They did not use highly polished titanium substrate as I did. They did not measure the average surface roughness on the substrates they used. Previous studies at our institute showed machine finished tinanium surfaces produced less vinculin markers and had less cell spreading compared with highly polished titanium surface (Gordon et al., 2008).The main difference between their work and mine was the use of single coating proteins, the use of different substrates with different average surface roughness and comparing different covalent bonding to adsorption techniques.

Application of dual coating proteins (FnLn) on titanium surfaces has not been investigated before. In chapter 3, I found that silanized dual coating protein without passivation

provides the optimum media required for fibroblast adhesion and growth in the early phase. The null hypothesis of this chapter is that there is no difference between silanized, non-passivated dual coating proteins (SiFnLn-) on early keratinocyte adhesion and growth compared with dual coating proteins, either silanized, passivated (SiFnLn+), or adsorbed (AdFnLn), single coating Fn, either silanized, non-passivated (SiFn-), or silanized, passivated (SiFn+), or adsorbed (AdFn), or silanized, non-passivated Ln (SiLn-), silanized, passivated Ln (SiLn+) or adsorbed Ln (AdLn), or controls without protein coating (Pol, Si-, Si+).

4.2 Materials and Methods

4.2.1 Disc Preparation and Protein Addition

The same protocol was used to prepare discs, silanized titanium and attach protein as outlined in chapter 3 (Section 3.2.1).

4.2.2 Human Epidermal Keratinoctyes

Human adult low Calcium elevated Temperature (HaCaTs) keratinocytes were given as a gift from Dr. Mee, Department of Dermatology, University College London,UK. This cell line was selected in previous studies in the institute to examine single coating laminin on Ti6Al4V (Gordon et al., 2008). They were compared to primary dermal keratinocytes to study the effect on cell spreading and number of vinculin markers. They produced similar results as primary cell line with no contact inhibition characteristics noted. This cell line was chosen due to ease of maintainance and more visible vinculin markers. They were stored in liquid nitrogen at -70℃. The cells were obtained from the periphery of an excised

melanoma from the back of a 62 year-old male. This cell line is immortal and has been used in experiments outlined in this chapter.

4.2.2.1 Resuscitation, Monitoring, Trypsinization, Cell Counting

The protocols for resuscitation, monitoring, trysinization and counting of HaCaTs were the same as those outlined in chapter 3 (Section 3.2.3).

4.2.2.2 Cell Seeding

20,000 keratinocytes in 50μl droplet was dropped on the top surface of each disc to form a uniform layer covering the whole surface. The discs were carefully placed in a covered 24 wells-plate, which were transferred into an incubator (Function Line Haraeus Instruments) at 37^0C and 5%CO_2, for 1 hour, without disturbing the droplet from the disc top. The plate was removed into a sterile hood and the discs were submerged into 1 ml of Fetal Calf Serum. The well plates were incubated for 1, 4 and 24 hours before fixing with 10% formal saline.

4.2.3 Antibody Detection Method

The same protocol described in chapter 3 was implemented (Section 3.2.4).

4.2.4 Cell Area Measurement and Vinculin Marker Counting

The same technique detailed in chapter 3 (Section 3.2.5), was used to measure the cell surface area and count the immuno-labeled vinculin markers of HaCaT cells.

4.2.5 Statistical Analysis

SPSS statistical package for Mac (Version 18.0, SPSS Inc, USA) was used for data analysis. Kappa statistics indicated excellent inter-observer agreement (>0.9) for both observers.The data did not fit a normal distribution curve for parametric testing (Kolmogorov-Smirnov p> 0.05). Non-parametric Mann-Whitney U test was used to determine differences between individual medians on a pair-wise basis. Results were considered significant at p-value < 0.05.

4.3 Results

4.3.1 Box and Whisker Plots

As previously outlined, the box length represents the difference between the 25th and 75th percentiles. The horizontal line inside the box represents the median. The whiskers represent the largest and smallest values.

4.3.2 Cell Area

The median cell area was significantly greater on dual coated protein surfaces compared with single coated protein surfaces and controls at all time points (p<0.05) [Figures 4.1 - 4.3]. On adsorbed substrates, a 3, 3 and 2-fold increase was seen with AdFnLn compared with Pol substrate alone at 1, 4 and 24 hours, respectively. Cell area was observed to be 1.5, 1.3 and 1.3-fold greater on AdFnLn than on AdFn at 1, 4 and 24 hours, respectively. There was a 2, 1.4 and 1.5-fold increase was seen with AdFnLn compared with AdLn alone at 1, 4 and 24 hours, respectively. Cell area was observed to be 3, 3 and 1.8-fold greater on SiFnLn- compared with Si- alone at 1, 4 and 24 hours, respectively. In addition, there was a 1.4, 1.5 and 1.4 fold greater on SiFnLn- than on SiFn- at 1, 4 and 24 hours,

respectively. A 1.7, 1.4 and 1.2 fold increase was seen with SiFnLn- compared with SiLn- at 1 , 4 and 24 hours, respectively. On silanized, passivated surfaces a 2.8, 3 and 2-fold increase was seen with SiFnLn+ compared with Si+ substrate alone at 1, 4 and 24 hours, respectively. There was a 2.8, 3 and 1.9-fold increase was seen with SiFnLn+ compared with SiFn+ at 1, 4 and 24 hours, respectively. In addition, a 1.8, 1.4 and 1.5-fold increase with SiFnLn+ compared with SiLn+ at 1, 4 and 24 hours, respectively.

For single coating protein, cell area significantly increased on fibronectin-coated surfaces, compared with laminin-coated surfaces on different surface topography, at all time points (p<0.05) [Figures 4.4 - 4.6]. A 1.2, 1.1 and 1.1- fold increase was seen on SnFn- compared with SiLn- at 1, 4 and 24 hours, respectively. In addition there was a 1.1-fold increase on AdFn compared with AdLn at 1, 4 and 24 hours, respectively. In a similar pattern there was a 1.2, 1.1 and 1.2-fold increase with SiFn+ compared with SiLn+ at 1, 4 and 24 hours, respectively.

No significance in size was found between SiFnLn- and AdFnLn at 1 hour and 24 hours time points. For single coatings, there was no significance between AdLn and SiLn+ at 1 hour. Again, no significance difference was found between SiFn- and SiFn+ at 1 hour. Si+ surfaces demonstrated a significantly reduced cell area compared to Si- and Ad surfaces.
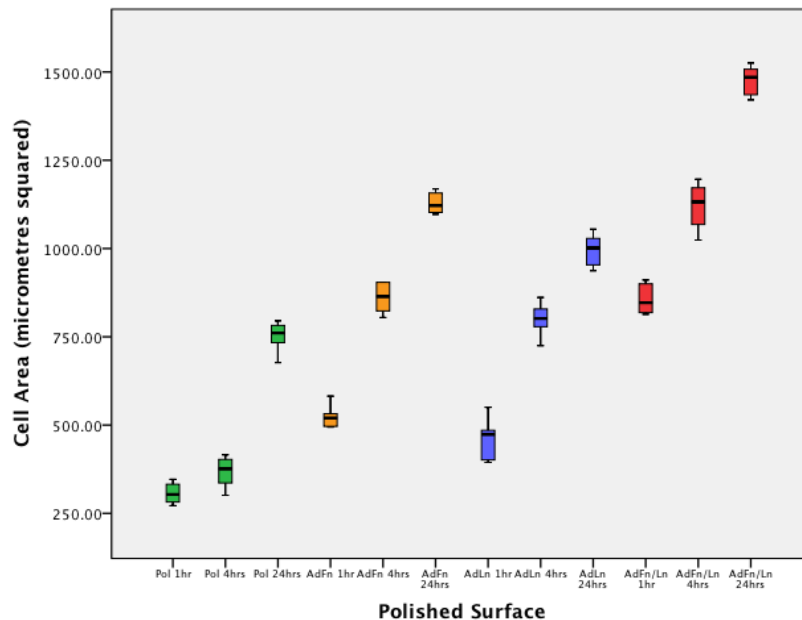
Figure 4.1: Box Plot showing Cell Area (μm^2) at 1, 4 and 24 hours on adsorbed surfaces
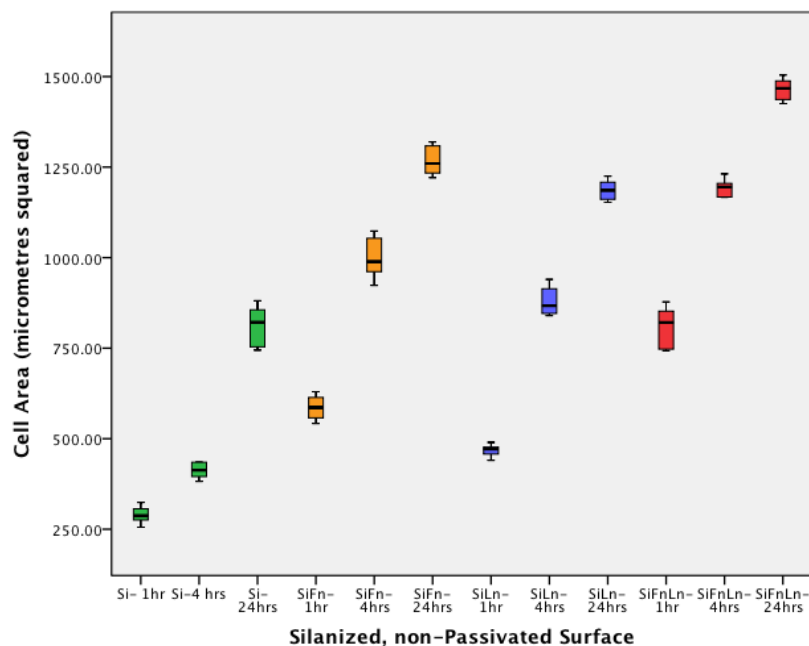
Figure 4.2: Box Plot showing Cell Area (μm^2) at 1, 4 and 24 hours on silanized, non-passivated surfaces
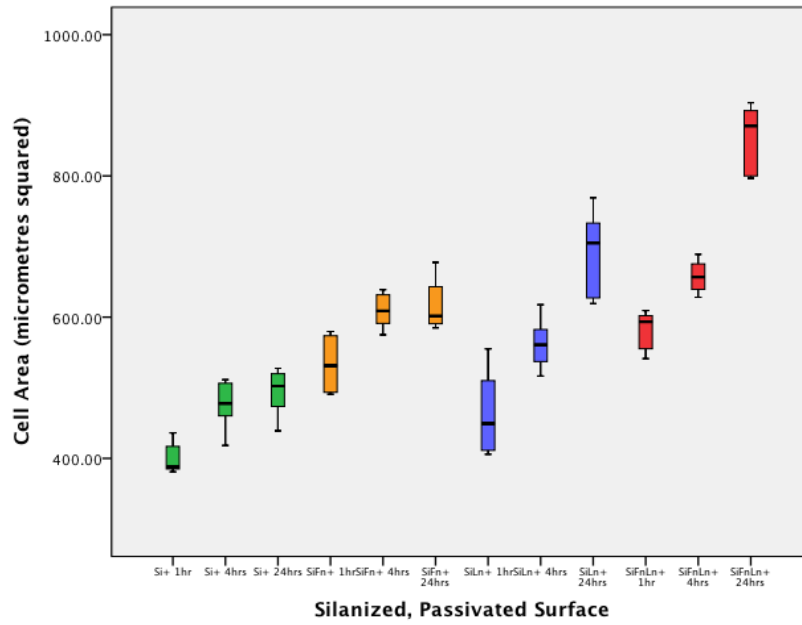
Figure 4.3: Box Plot showing Cell Area (μm^2) at 1, 4 and 24 hours on silanized, passivated surfaces
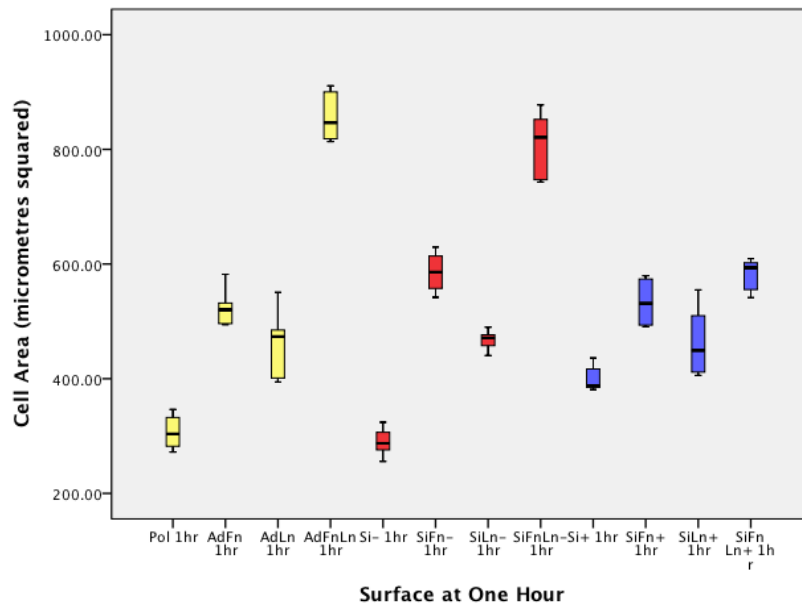
Figure 4.4: Box Plot showing Cell Area (μm^2) at 1 hour on different surfaces

116
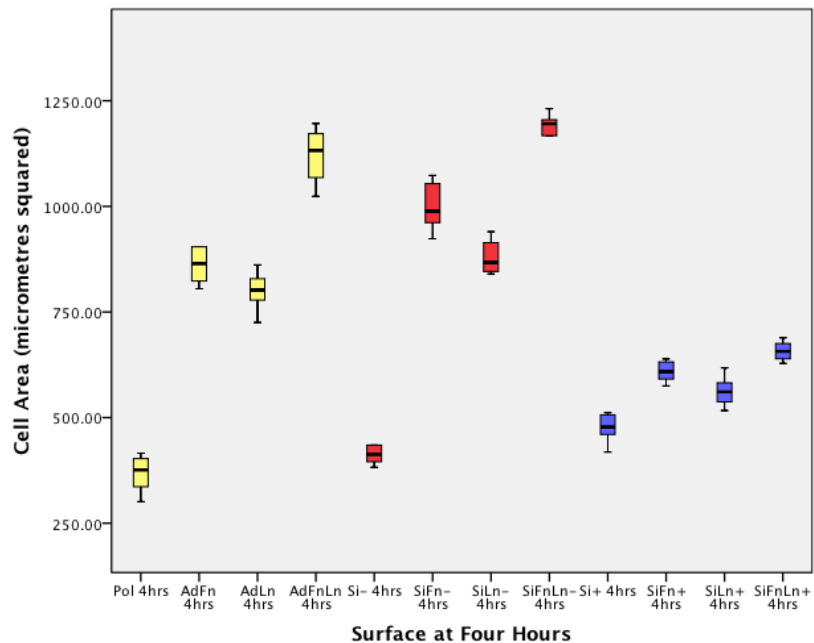
Figure 4.5: Box Plot showing Cell Area (μm^2) at 4 hours on different surfaces
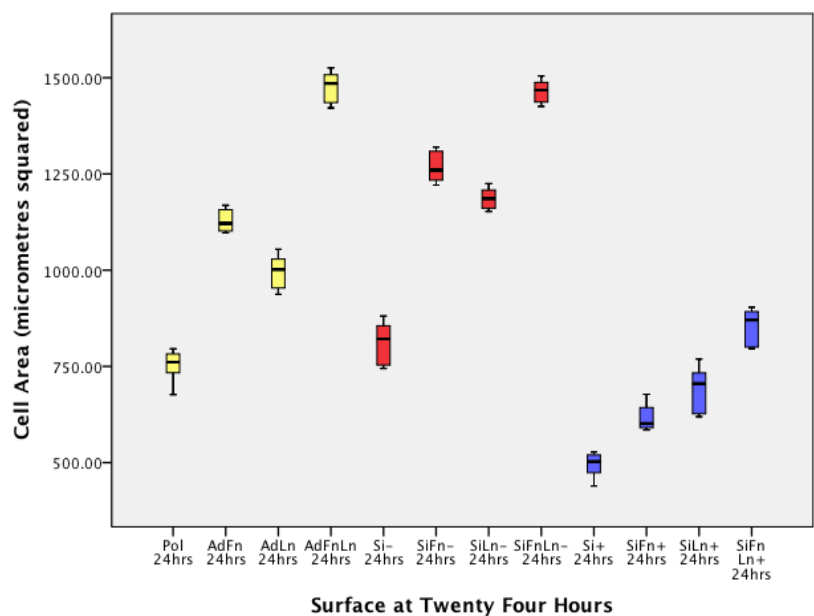
Figure 4.6: Box Plot showing Cell Area (μm^2) at 24 hours on different surfaces

4.3.3 Focal Adhesion Markers Per Cell Unit

At each time point, vinculin markers per cell unit were expressed in significantly greater numbers on dual coated protein surfaces compared with single coated surfaces or controls despite the surface topography ($p < 0.05$). The only exception to this was SiFnLn+ compared with SiFn+ at 24 hours where there was no significant difference ($p = 0.869$) [Figures 4.7- 4.9]. On adsorbed substrates, a 39.5, 35.3 and 23-fold increase was seen with AdFnLn compared with Pol substrate alone at 1, 4 and 24 hours, respectively. Vinculin markers were observed to be 7.2, 3 and 2.4-fold greater on AdFnLn than on AdFn at 1, 4 and 24 hours, respectively. There was a 3.8, 2.1 and 2.1-fold increase seen with AdFnLn compared with AdLn alone at 1, 4 and 24 hours, respectively. Vinculin markers were observed to be 40, 47.7 and 19.6-fold greater on SiFnLn- than on Si- at 1, 4 and 24 hours, respectively. A 5.3, 2.4 and 2-fold increase was seen with SiFnLn- compared with SiFn at 1 , 4 and 24 hours, respectively. In addition, there was a 3.5, 2 and 1.8-fold increase seen with SiFnLn- compared with SiLn- at 1, 4 and 24 hours, respectively. On silanized, passivated surfaces a 39.5, 35.3 and 23-fold increase was seen with SiFnLn+ compared with Si+ subtrate alone at 1, 4 and 24 hours, respectively. There was a 7.2, 1.7 and 1.9-fold increase was seen with SiFnLn+ compared with SiFn+ at 1, 4 and 24 hours, respectively. There was a 2.9, 3.7 and 2.1-fold increase with SiFnLn+ compared with SiLn+ at 1, 4 and 24 hours, respectively.

Keratinocytes showed a similar trend to fibroblasts, where vinculin produced by cells on silanized, non-passivated dual coated substrate was significantly greater than adsorbed surfaces and silanized, passivated surfaces, at 4 hours and 24 hours time points ($p < 0.05$).

During the first hour, more vinculin per cell unit was produced on silanized, non-passivated surfaces and adsorbed surfaces than on silanized, passivated surfaces.

In contrast to the trend seen with cell area, for adsorbed and silanized, non-passivated surfaces, vinculin expression was significantly greater in cells on single coated laminin substrates than on fibronectin coated substrates at all time points (p<0.05).
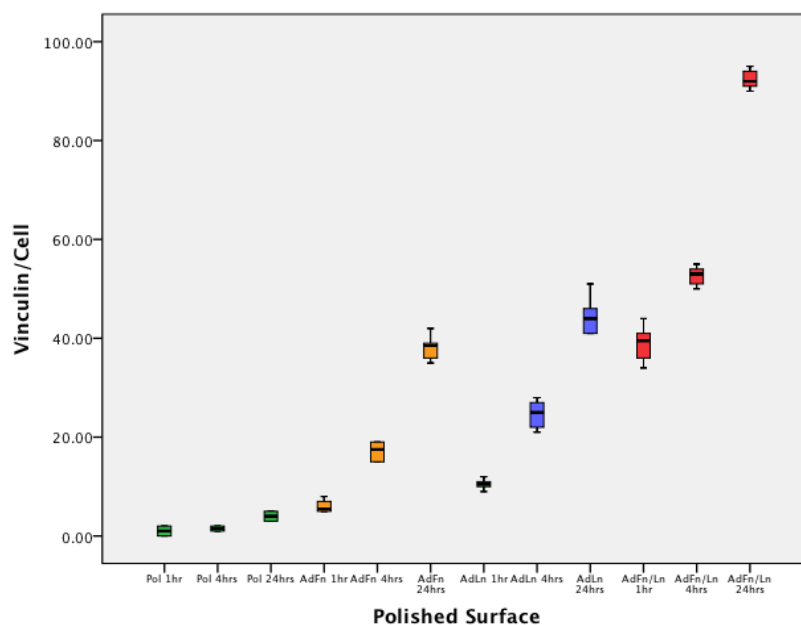
Figure 4.7: Box Plot showing Vinculin marker/Cell unit at 1, 4 and 24 hours on adsorbed surfaces
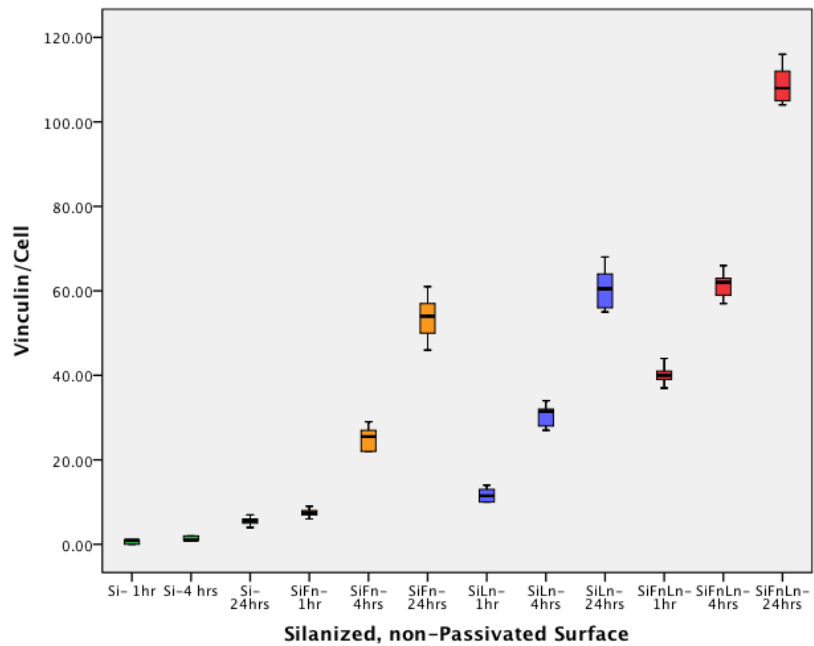
Figure 4.8: Box Plot showing Vinculin marker/Cell unit at 1, 4 and 24 hours on silanized, non-passivated surfaces
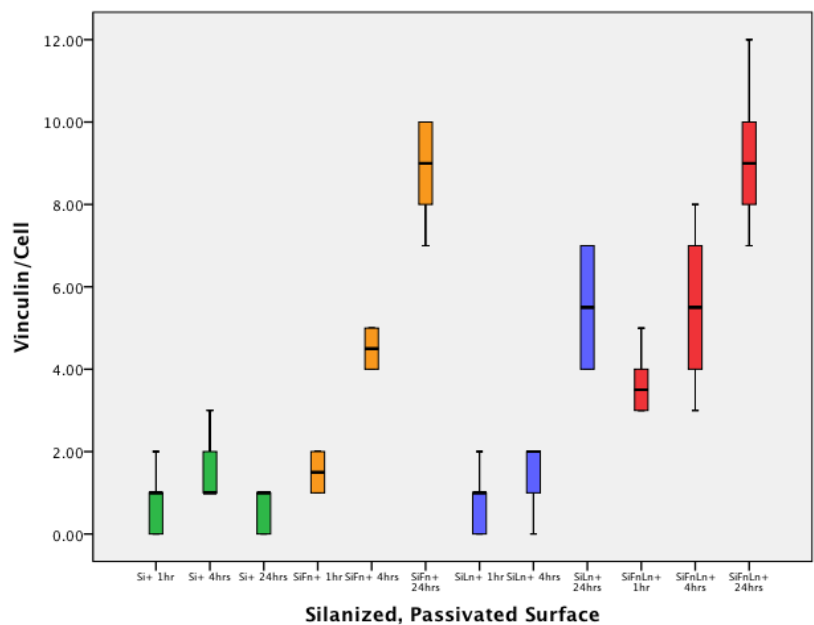
Figure 4.9: Box Plot showing Vinculin marker/Cell unit at 1, 4 and 24 hours on silanized, passivated surfaces
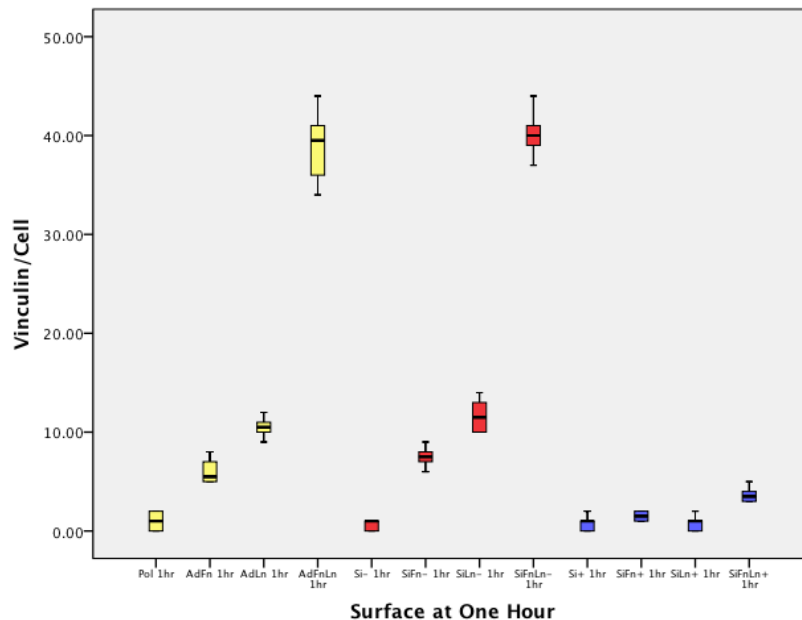
Figure 4.10: Box Plot showing Vinculin marker/Cell unit at 1 hour on different surfaces
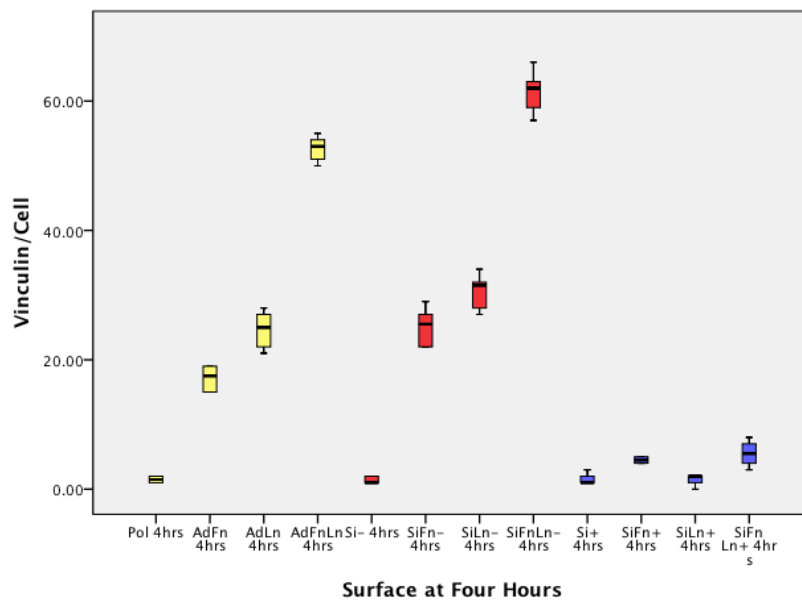
Figure 4.11: Box Plot showing Vinculin marker/Cell unit at 4 hours on different surfaces
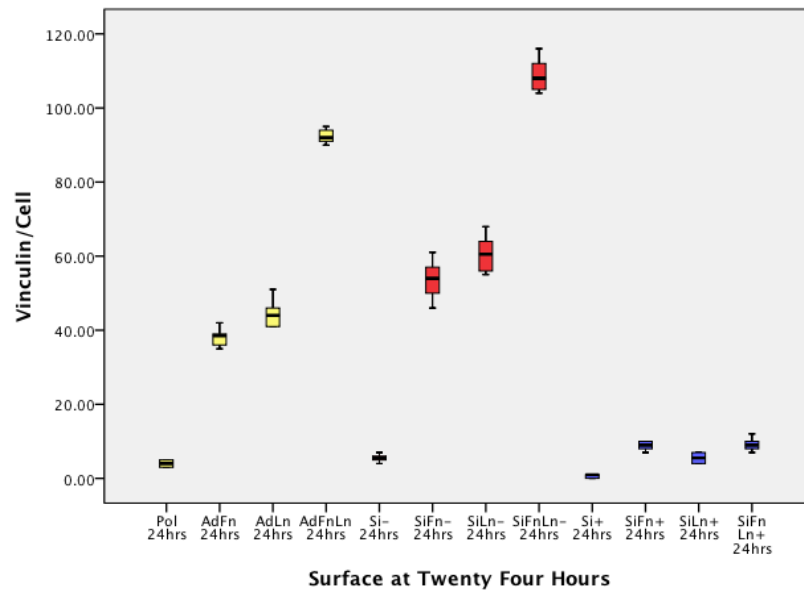
Figure 4.12: Box Plot showing Vinculin marker/Cell unit at 24 hours on different surfaces

4.3.4 Vinculin Markers Per Cell Area

There was greater vinculin per cell area produced on dual coated protein substrates compared with single coated protein on adsorbed and salinized, non-passivated substrates at all time points (p<0.05). As with fibroblasts, this suggests that in the first 24 hours, keratinocytes produce more focal adhesion contacts per area on dual coatings substrates. A 13.2, 11.4 and 12.3-fold increase was seen with AdFnLn compared with Pol substrate alone at 1, 4 and 24 hours, respectively. Vinculin per cell area was observed to be 4.2, 2.3 and 1.8-fold greater on AdFnLn than on AdFn at 1, 4 and 24 hours, respectively. There was a 2, 1.5 and 1.4-fold increase seen with AdFnLn compared with AdLn alone at 1, 4 and 24 hours, respectively. Vinculin per cell area was observed to be 14.6, 21.5 and 10.2-fold greater on SiFnLn- than on Si- at 1, 4 and 24 hours, respectively.

A 4, 2 and 1.7- fold increase was seen with SiFnLn- compared with SiFn- at 1, 4 and 24 hours, respectively. In addition, there was a 2, 1.5 and 1.4-fold increase seen with SiFnLn- compared with SiLn- at 1, 4 and 24 hours, respectively. On silanized, passivated surfaces a 2.9, 3.2 and 5.8-fold increase with SiFnLn+ compared with Si+ subtrate alone at 1, 4 and 24 hours, respectively. There was a 2.2, 1.1-fold increase was seen with SiFnLn+ compared with SiFn+ at 1 and 4 hours, respectively. There was a 2.9, 2.4 and 1.4-fold increase was seen with SiFnLn+ compared with SiLn+ at 1, 4 and 24 hours, respectively.

For surface topography, Si- surfaces provided the best surface for vinculin per cell area followed by Ad then Si+ surfaces at all time intervals [Figures 4.16-4.21]. This is in keeping with the results shown with the fibroblast study.

For single coatings, laminin coated substrates expressed more vinculin markers per cell area than fibronectin at all time points on adsorbed and silanized, non-passivated surfaces independent of surface topography.
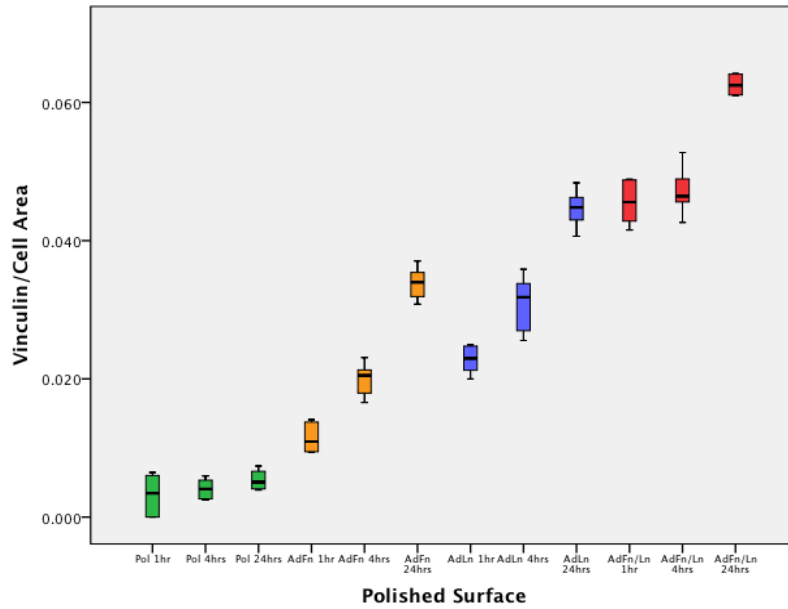
Figure 4.13: Box Plot showing Vinculin marker/Cell area at 1, 4 and 24 hours on adsorbed surfaces
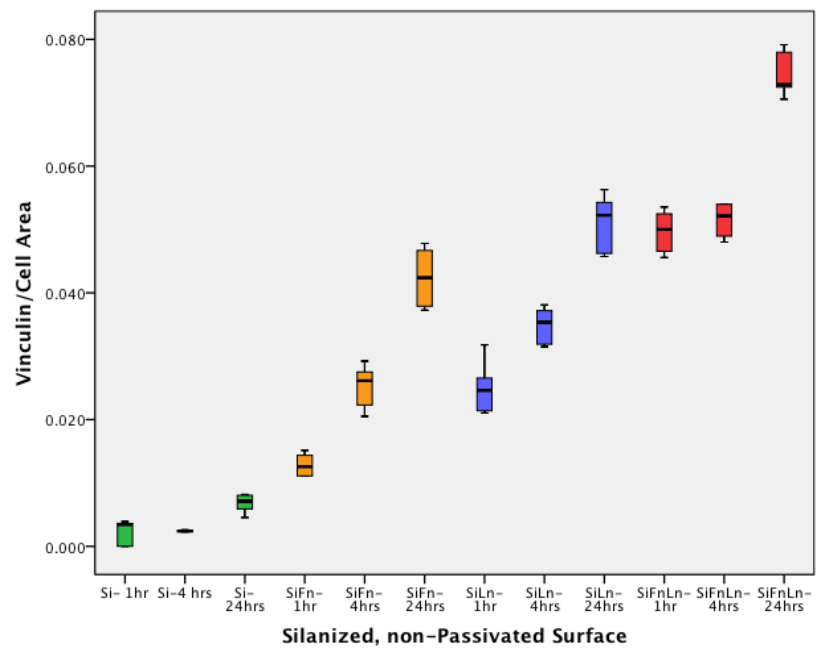
Figure 4.14: Box Plot showing Vinculin marker/Cell area at 1, 4 and 24 hours on silanized, non-passivated surfaces
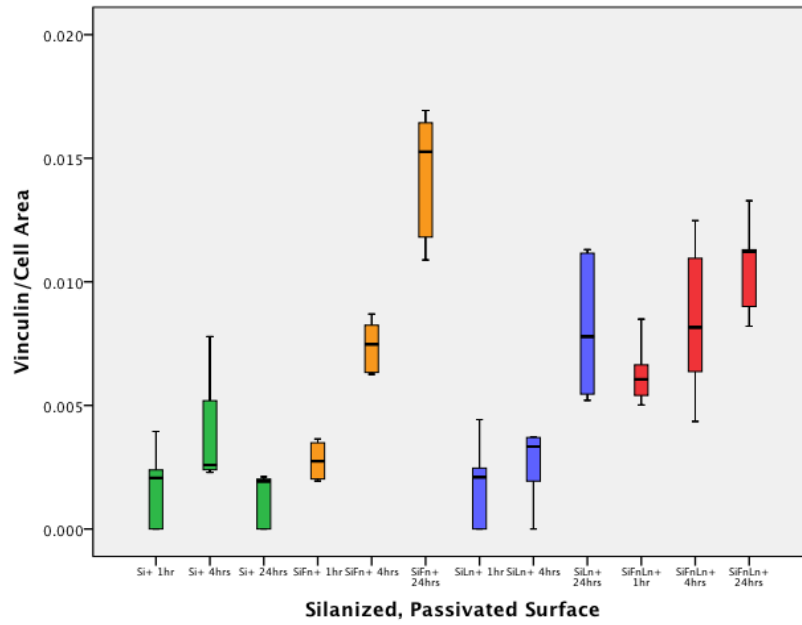
Figure 4.15: Box Plot showing Vinculin marker/Cell area at 1, 4 and 24 hours on silanized, passivated surfaces
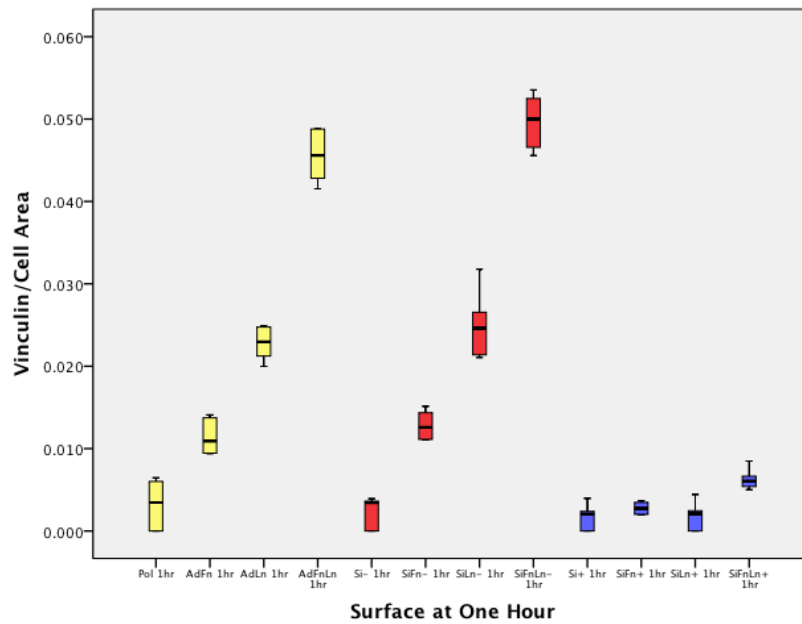
Figure 4.16: Box Plot showing Vinculin marker/Cell area at 1 hour on different surfaces
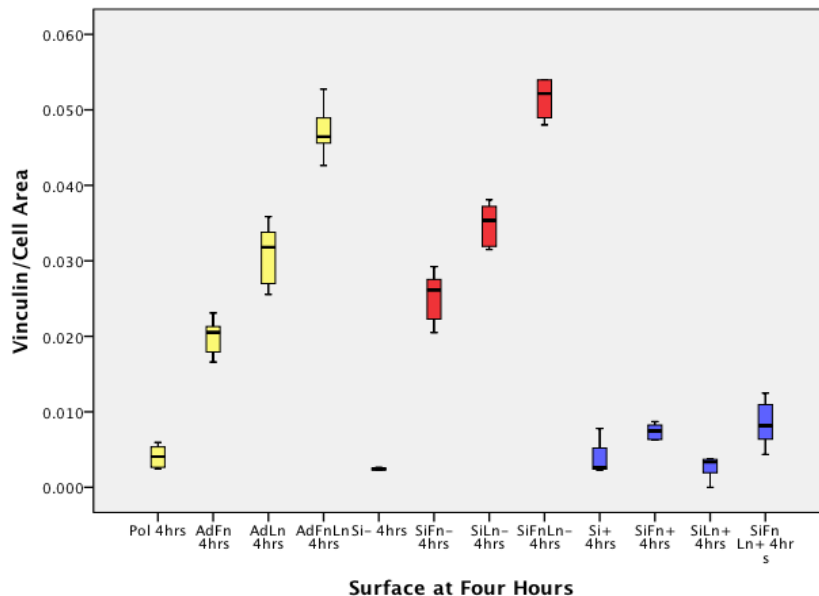
Figure 4.17: Box Plot showing Vinculin marker/Cell area at 4 hours on different surfaces
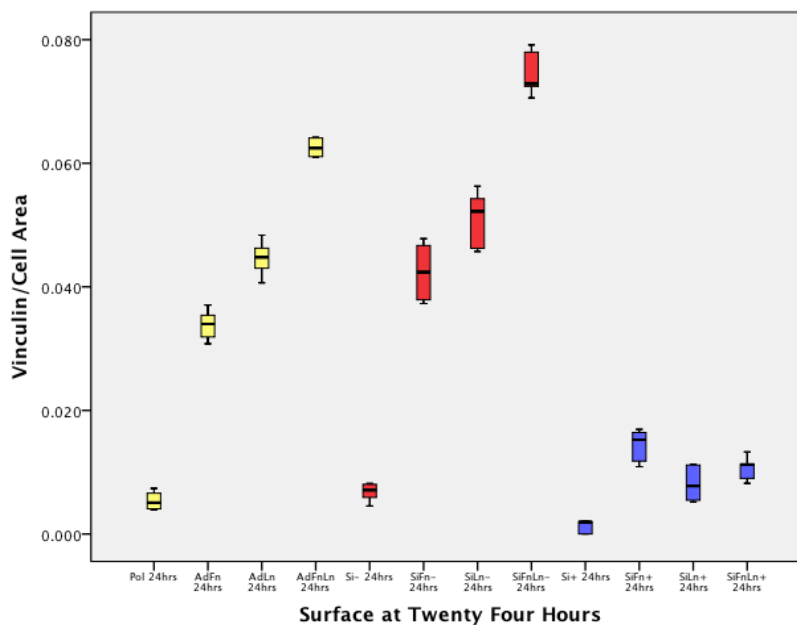
Figure 4.18: Box Plot showing Vinculin marker/Cell area at 24 hours on different surfaces
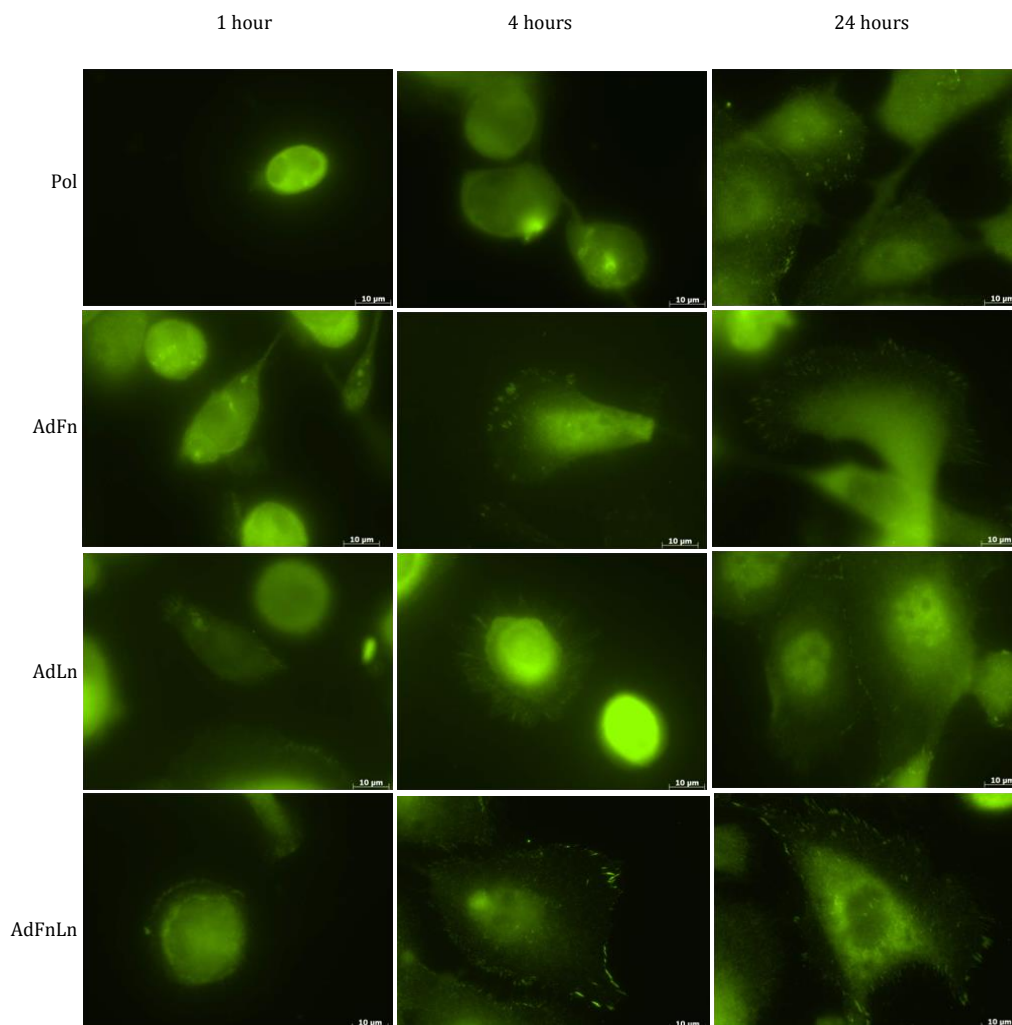
Figure 4.19: Keratinocytes cultured at 1, 4 and 24 hrs on single and dual coating protein surfaces stained for focal adhesion plaques with anti-vinculin on polished surfaces
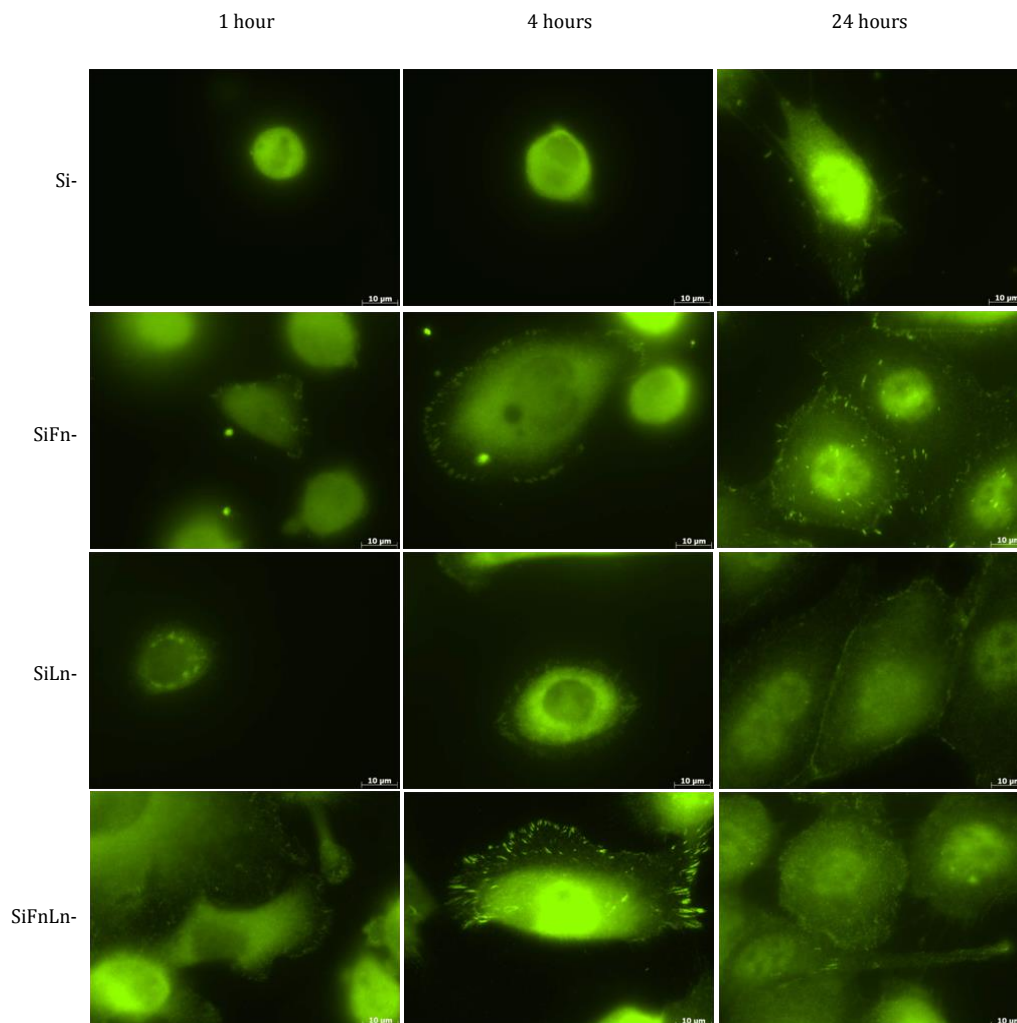
Figure 4.20: Keratinocytes cultured at 1, 4 and 24 hrs on single and dual coating protein surfaces stained for focal adhesion plaques with anti- vinculin on salinized, non-passivated surfaces
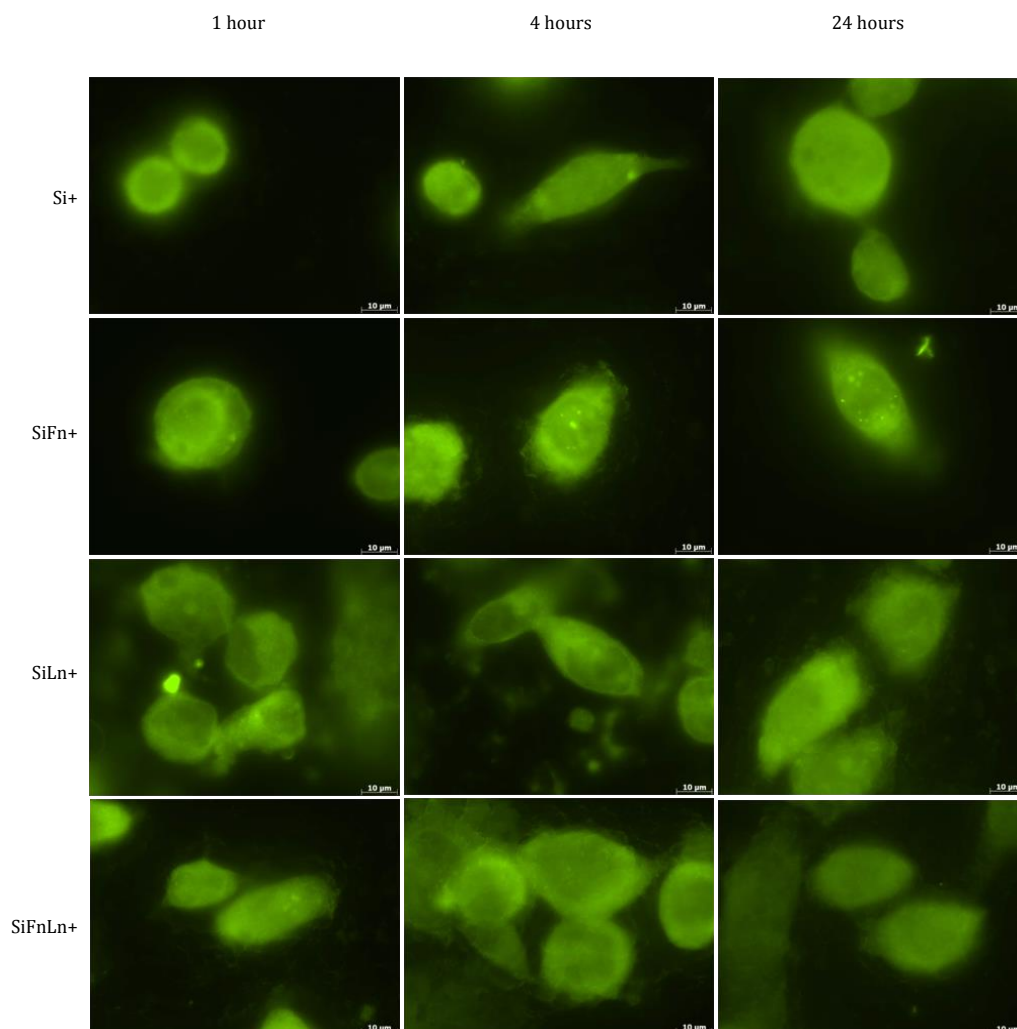
Figure 4.21: Keratinocytes cultured at 1, 4 and 24 hrs on single and dual coating protein surfaces stained for focal adhesion plaques with anti-vinculin on silanized, passivated surfaces

4.4 Discussion

Keratinocytes showed that silanized, non-passivated dual coating protein surface provided the best surface for cell attachment and growth at all time intervals. In addition to this, laminin provided a better coating compared to fibronectin when either adsorbed or silanized on non-passivated titanium alloy for epithelial cells adhesion and growth.

Scheideler et al. (2007), studied effect of silanized fibronectin on titanium surfaces on keratinocyte adhesion and growth. Fibronectin was covalently coupled to titanium (Ti) surfaces via silanization using anthraquinone immobilizer. Impact of initial host-biomaterial keratinocyte adhesion and platelet interactions was studied. Keratinocyte adhesion was studied after 30, 60, 90 and 120 minutes of incubation in Epilife-Medium (TEBU, Offenbach, Germany) at 37^0C and 5% CO_2. Adhering cells were stained using fluorescein diacetate (FDA). Cell surface areas were measured using an epifluorescence microscope equipped with a digital camera. Cell adhesion and spreading was assessed by determination of the mean area of sample surface covered by vital stained cells in each group. They found that covalently bonding fibronectin enhanced both cell adhesion and growth.

Karecla et al. (1994), showed that keratinocytes attached to laminin at three integrin sites. They proved that keratinocytes had specific laminin receptor sites that ensured the binding of the cells to this glycoprotein. $\alpha2\beta1$ is the receptor that mediates the binding to laminin and collagen, while $\alpha3\beta1$ is responsible for binding laminin and Kalinin. On the other hand, $\alpha5\beta1$ is the keratinocyte fibronectin receptor. This shows that fibronectin and laminin could increase cell adhesion to the Ti surface independently since each has different receptor

sites, meaning they do not compete for receptor sites on keratinocytes, making it possible for the cells to bind to both fibronectin and laminin when found together on the surface.

Another factor that may explain the superiority of silanized, non-passivated dual coating surface in providing a better coating for early cell attachment and growth is surface roughness. It is very difficult to control variation of surface roughness at nanoparticle level. This is because even when we silanized the controls, addition of protein will add to roughness that will be difficult to detect. This can be measured using atomic force microscopy but will still be an additional variant. Baharloo et al. (2005), demonstrated as surface roughness increased, epithelial cell surface area decreased. They compared smooth polished Ti surfaces, acid-etched surfaces, grit blasted surfaces. They defined smooth polished Ti surfaces at R_a 0.06 µm. They found that rough surfaces decreased the growth of cells compared with smooth surfaces in cultures up to 28 days. In general, rough surfaces decreased the spreading of cells, as assessed by cell area, with the most pronounced affect for the SLA surface. On the other hand, the strength of cells adhesion was investigated by immunofluorescence staining of vinculin in focal adhesions indicating that cells form a greater number and larger focal adhesions on the smooth polished surface compared with the rougher acid-etched surface. These findings are comparable to mine. We have treated our surfaces with silanization and omitted the passivation step to obtain a smoother surface. We found that this produced favourable results both in terms of cell adhesion and growth, compared with polished surfaces.

Ohji et al. (1993), studied the effect of exogenous laminin and fibronectin on corneal epithelial cell attachment. They found that laminin provided a better medium for cell attachment than fibronectin. They labeled human corneal epithelial cells with ^{3}H-thymidine

and seeded them onto plates coated with laminin or fibronectin. After incubation, the cells that remained attached were lysed with 1ml of 1% sodium dodecyl sulfate and radioactivity of each sample was measured by liquid scintillation counting. Attachment of cells was calculated by dividing the radioactivity in cells that remained attached by the total radioactivity in the original suspension. 69% of human corneal epithelial cells attached to plates coated with human laminin or human fibronectin, with 50% of cells attached to the wells coated with 40ng ml^{-1} of laminin and fibronectin, respectively (p < 0.001). These results are comparable to my findings on single coating proteins on adsorbed and silanized, non-passivated surfaces and prove that exogenous laminin is better for epithelial cells' up-regulation than fibronectin.

El-Ghannam et al. (1998), coated Laminin-5 on Ti6Al4V surface via adsorption and passivation. They showed there was significantly more hemidesmosomes on passivated laminin-5 Ti6Al4V surface than unpassivated laminin-5 coated surface. Hemidesmosomes are small structures found in the inner basal surface of keratinocytes in the epidermis. They act as cell adhesion between cells and extra-cellular matrix. Similar to our results, they showed there was rapid cell attachment and spreading. They suggested the increase in hemidesmosome assembly may reflect better integration between epithelial cells and titanium alloy and may be a predictor to long-term implant stability.

Tamura et al.(1997), investigated epithelial cell attachment to titanium alloy coated with laminin-5. They showed that cells were able to assemble hemidesmoses within 24 hours on laminin-5 coated titanium alloy but not on controls of titanium alloy only. They suggested laminin-5 may have clinical applications as an implant coating that promoted the formation of a biological seal.

In 2008, Pendegrass et al. studied the effect of surface roughness of Ti6Al4V on keratinocyte proliferation and attachment. They compared smooth-polished, machine-finished, sand-blasted and hydrofluoric acid-etched titanium surfaces. Smooth-polished Ti6Al4V surfaces showed significantly better keratinocyte proliferation and cell attachment with vinculin and hemidesmosomes compared with other surfaces. It also provided a substrate for larger more flattened cells compared with the other surfaces. Similar to our results, surface topography influences the morphology of the cells and cell attachment. Keratinocyte attachment was enhanced by addition of fibronectin (Bush et al., 2007).

In conclusion, previous studies have identified addition of protein coating enhances cell spreading and focal contact numbers. Other studies that used dual coating bone morphogenetic proteins found they were superior to single coating on osteoblasts. I have shown that adding dual coating protein fibronectin and laminin improve keratinocyte spreading and number of focal adhesion vinculin markers *in vitro.* This can be validated by examining the effect of dual coating protein fibronectin and laminin on BP180, E-cadherins and hemidesmosomes.

Further *in vitro* studies are required to determine whether hemidesmosome attachment would be enhanced using silanized dual coating fibronectin and laminin. In addition to this, there is a need for *in vivo* studies to determine whether there would be competitive binding from other extra-cellular protein to the covalently bound dual coating protein. This would be done by silanizing the ITAP prostheses, prior to implanting, with single coating fibronectin, single coating laminin and dual coating fibronectin and laminin and comparing these with controls of polished non-silanized prosthesis. After 21 days, histology slides of

ITAP would determine whether there was adequate bonding at the implant-transcutaneous interface and if there was any statistical difference favouring any particular surface, as the in vitro study has with non-passivated silanized dual coating fibronectin-laminin coating on Ti6Al4V surface.

CHAPTER 5

Effect of Fibronectin- Hydroxyapatite Coatings on Fibroblast Focal Adhesion Vinculin Markers

5.1 Introduction

5.1.1 Background

Synthetic hydroxyapatite (HA) coatings have been incorporated in ITAP design to enhance dermal attachment successfully *in vivo* (Pendegrass et al., 2006 (6); Pendegrass et al., 2008, Kang et al., 2010). On the other hand, biological coatings in the form of silanized fibronectin coating improved dermal attachment to titanium alloy *in vitro* (Middleton CA et al., 2007). Both substrates have independently shown promising results in forming a tight seal barrier at the skin-implant barrier, which is crucial for the success of ITAP.

Hydroxyapatite is found abundantly in the bones and teeth, forming the main inorganic component of bone. The crystalline form of calcium apatite is the formula $Ca_{10}(PO_4)_6(OH)_2$. This composite is responsible for the mechanical strength and osteoconduction of bone (Fox et al., 2012). When hydroxyapatite is combined with type 1 collagen fibres and extracellular matrix, it is able to provide support scaffold for bone and teeth (Stigter et al., 2002). Carbonated apatite crystals are the smallest crystals in the human body, with average sizes of 50 x 25 x 2-4nm in bone and 100 x 50 x 50nm in tooth enamel (Weiner et al., 1999). Although hydroxyapaptite has a good compressive strength, it is weak in tension with a high modulus of elasticity. Collagen complements this by providing high tensile strength, hence allowing bone to be strong yet provide some deformation.

Synthetic hydroxyapatite coating of endoprostheses has shown to enhance osseointegration (Cook et al.,1988) and several studies investigated the interaction between extracellular proteins with hydroxyapatite. Shen et al. (2008), investigated the interactions of the 10th type III module of fibronectin with hydroxyapatite surface. They

concluded that the charged –COO(-) and –NH(3)(+) are the strongest groups that interact with hydroxapatite. In addition to this, Dong et al.(2007), studied the bonding of bone morphogenetic protein 2 (BMP-2) on hydroxyapatite. They found three types of functional groups –OH, -NH$_2$ and –COO(-) through which BMP-2 interacts with hydroxyapaptite.

However despite these investigations, the nature of this interaction remains unclear. In this chapter, we investigated the release kinetics and durability of Fn on hydroxyapatite surface in order to establish the optimum Fn coating to improve fibroblast attachment. The second part of the chapter assesses the effect of Fn- functionalized HA on dermal fibroblast attachment *in vitro.* Dr. CJ Pendegrass, performed the cell bioassay experiment and kindly shared the results for use in this chapter.

The hypothesis is that adsorption of Fn on compacted, sintered HA discs would enhance fibroblast attachment when compared with HA alone and Ti controls.

5.2 Materials and Methods

5.2.1 Disc preparation

One gram of hydroxyapatite powder (Apatech, Elstree, UK) was placed into 12 mm casts with 1.5 tonnes of pressure applied over 2 hours at 1250°C (5°C ramp/min). Compacted HA discs 11.7 mm in diameter were compacted in a mould and heated to 500°C. X-ray diffraction analysis (XRD) was performed to assess crystallinity and purity of HA, XRD patterns recorded using X'Pert Pro Diffractometer (PANalytical Ltd, Cambridge, UK) and discs with 95% purity were used.

5.2.2 Fibronectin coating and radiolabelling

Human plasma fibronectin (F2006; Sigma-Aldrich, Gillingham, UK) was custom-labelled by PerkinElmer Inc. (Wellesley, Massachusetts, USA) using the method outlined in chapter 2.2.2. HA discs were coated with 50µl droplets of 125I-Fn, spread evenly on the surface of discs. All techniques were performed at 210C under sterile conditions using aseptic technique.

Gamma radiation from radiolabelled protein was detected using Tricarb 290TR liquid scintillation counter (PerkinElmer Inc., USA) as counts per minute (CPM). Discs were placed facing up in 5ml scintillant tubes and immersed in 4.5ml Ultima Gold XR scintillation liquid (PerkinElmer Inc., USA). QuantaSmart software (v.1.31, Packard Instrument, USA) connected to the counter, provided CPM with correction of 125I half-life, at a count time of 1 minute. Each sample was counted thrice. Six replicates were used for all experiments.

5.2.3 Calibration Curve

A standard calibration curve was generated for 125I-Fn on HA discs against CPM. 50 µl droplets of 10 µg, 100 µg, 250 µg, 500 µg and 750 µg of 125I-Fn protein were placed on HA discs and CPM was immediately measured thrice.

5.2.4 Effect of quantity of 125I-Fn loading on HA discs

In order to determine maximum possible coating concentration, 100ng, 250ng, 500ng, 1000ng and 1500ng of 125I-Fn were placed on disc surfaces for 1 hour before analysis.

5.2.5 Effect of duration on 125I-Fn loading of HA discs

Optimal time to leave 125I-Fn on HA discs was determined by placing 500ng of 125I-Fn on disc surfaces for zero, half an hour, 1 and 2 hours before analysis.

5.2.6 Durability of 125I-Fn on HA discs

$50\mu l$ droplet of 1000ng 125I-Fn was added to HA discs. These were immersed in fetal calf serum (FCS) (First Link Ltd, Birmingham, UK). The discs were analysed immediately after 3washes in sterile PBS at time zero. Remaining discs were left immersed in FCS at $37^{\circ}C$ for 1, 4, 8 and 24 hours.

5.2.7 Disc preparation for dermal fibroblast attachment

Ti6Al4V discs, 10 mm in diameter, were ground, polished and cleaned, to be used as controls (Pol group). Discs were sterilised in a 2100 Classic Clinical Autoclave (Prestige Medical, Blackburn, UK) for 11 minutes at 126°C and a pressure of 1.4 bar. Surface roughness (Ra), mean maximum height of the profile (Rz) and mean spacing of irregularities of the profile (Sm) were measured using a Mitutoyo Surftest SV-400 Surface Profiler (Mitutoyo, War- wick, United Kingdom). Non-functionalised sintered HA discs were prepared as described in section 5.2.1 and represented HA group. 1000ng of Fn were applied to HA discs for 1hour and represented HAFn group.

5.2.8 Fibroblast culture and seeding

Fibroblasts (1BR.3.G cells, ECACC/Sigma-Aldrich) were cultured in Dulbecco's Modified Eagle's medium (DMEM; Sigma- Aldrich) with 4500 mg/l glucose, 1% non-essential amino acids, 1% penicillin/streptomycin (Invitrogen Corporation, Paisley, UK) and 10% FCS (First Link) at 37°C with 5% CO_2; 2500 cells per disc were seeded for 1, 4 and 24 hours on Pol, HA and HAFn discs.

5.2.9 Fibroblast focal adhesion detection method

The discs were washed in PBS and fixed in formal saline for 5minutes. Four five-minute washes in PBS followed. Mouse monoclonal anti-human clone HUV-1 (V9131 Sigma-Aldrich = Anti-vinculin) (1:100) and Triton X-100 (1:500) was added for 2 hours. After 3 washes in PBS the discs were incubated for 45 minutes with fluorescein isothiocyanate (FITC) conjugate in a secondary antibody solution (F2883 Sigma-Aldrich; Anti-mouse) (1:168 in sterile PBS) and then washed 3 times in PBS before analysis.

5.2.10 Fibroblast focal adhesion and cell area quantification

After vinculin staining at 1, 4 and 24 hours, focal adhesion quantification was carried out using a Carl Zeiss microscope (Carl Zeiss Ltd, Welwyn Garden City, UK) with ×50, and ×100 objective lenses. For each disc 15 cells were analysed. A random field of view was selected and the vinculin markers on the cells were manually identified and counted by two independent observers who were blinded both to the test substrate and to one another.

5.2.11 Statistical Analysis

Using kappa statistics, kappa scores indicated almost perfect inter-observer agreement (> 0.90), and so the data presented are those of both observers combined. Cell areas were measured using Axiovision Image Analysis Software (Axioimage 4.4; Carl Zeiss, Gottingen, Germany). The number of vinculin markers per unit and cell area were calculated by dividing the number of vinculin counts by cell unit and cell area, respectively. The data did not fit the assumptions required for parametric testing and were analysed using Mann-Whitney U tests to compare medians. Box plots showing median values, whole and interquartile ranges and median values were expressed with 95% confidence intervals (CI). All numerical data are stated as median values (with

95% CI) unless otherwise stated. Results were considered significant when the p-value < 0.05.

5.3 Results

5.3.1 Calibration Curve

A standard calibration curve was designed and used to determine the results for the loading and release kinetics experiments with correction for the half- life of ^{125}I (R^2 = 0.995) (Figure 5.1).

y = 5893.7x + 111227
R^2 = 0.9946
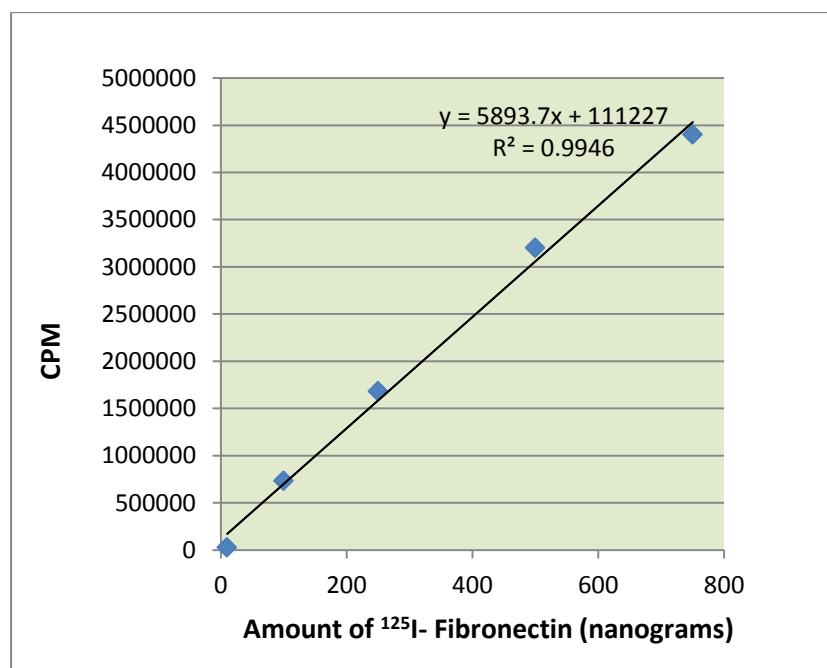
Figure 5.1: Calibration Curve for Correlating Counts Per Minute to 125I-Fn Quantity (nanograms)

5.3.2 Optimisation of loading time for 125I-Fn coating on HA discs

The optimal time for loading of Fn onto HA discs was 1 hour (Figure 5.2 and 5.3). The amount of Fn remaining on HA discs increased significantly between all time points up

to 1 hour (p<0.001), but there was no significant difference between 1 and 2 hours (p = 0.691). The data show that there was no significant increase in the amount of protein retained on the discs after incubation for one hour.

After 1 hour (optimal incubation duration as shown above) the median maximum amount of Fn bound was 255.26ng (95% CI: 253.74 to 264.26ng) from an initial load of 500ng in 50µl.
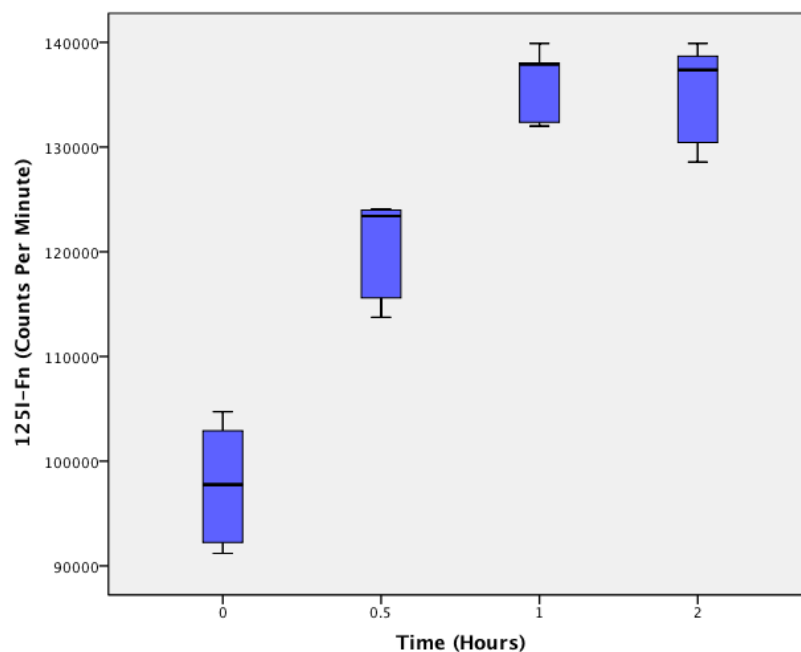
Figure 5.2: Box plot showing Counts Per Minute detected after initial loading with 500ng 125I-Fn on HA discs over time
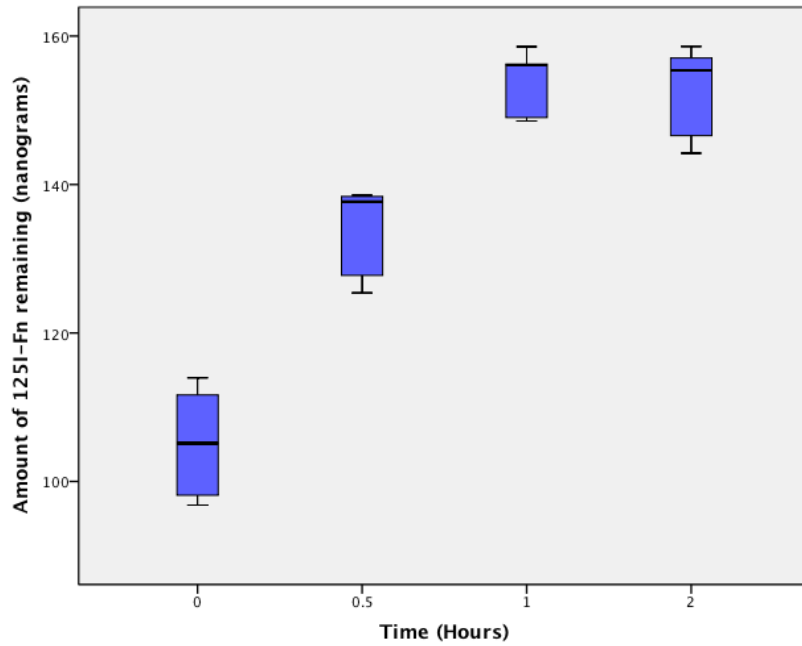
Figure 5.3: Box plot showing amount of 125I-Fn (ng) remaining, after initial loading with 500ng 125I-Fn on HA discs over time

5.3.3 Optimisation of ^{125}I-Fn loading quanitity on HA discs

As the quantity of 125I-Fn added increased (from 100ng to 250ng, and 500ng to 1000ng), a significantly higher quantity of 125I-Fn remained on the discs (all p < 0.001); 50µl droplets containing 1000ng and 1500ng did not produce proportionally more coupled protein (p = 0.085) (Figures 5.4 and 5.5).

The optimal loading concentration and incubation time of 1000ng in 50µl for 1 hour was used to determine the optimum durability.
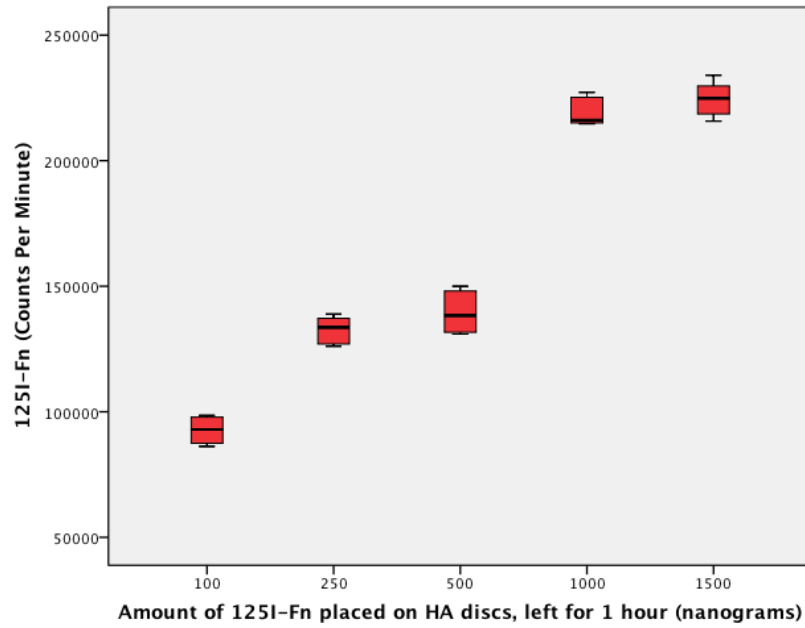
Figure 5.4: Box plot showing CPM detected on HA discs after initial loading between 100ng and 1500ng Fn, incubation for 1 hour
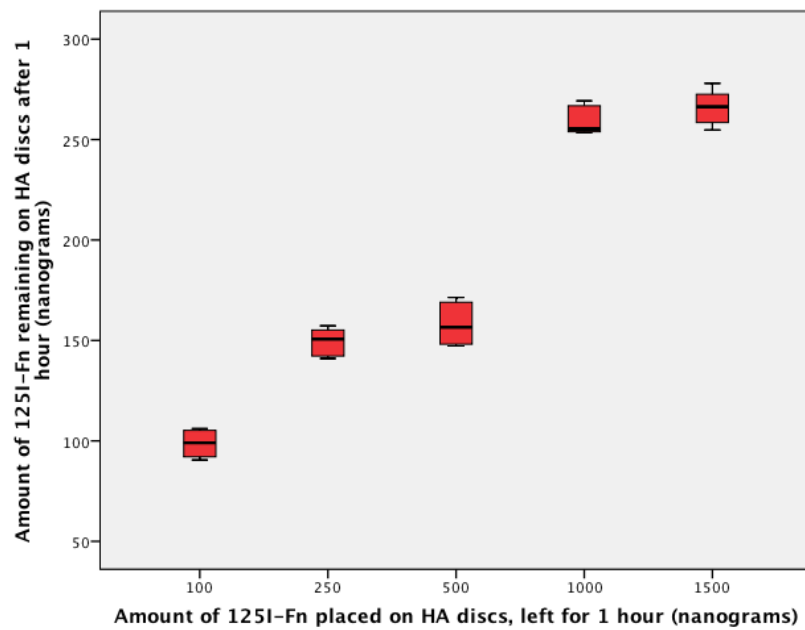
Figure 5.5: Box plot showing amount of ^{125}I-Fn (ng) remaining on HA discs after initial loading between 100ng and 1500ng Fn, incubation for 1 hour

5.3.4: Durability kinetics of ^{125}I-Fn on HA discs

A significant decrease from a median of 249.91ng (95% CI 239.79 to 254.39) to 137.93 ng (95% CI 135.89 to 142.72ng) of Fn coupled to HA was seen within the first hour of incubation in FCS (p < 0.001) (Figures 5.6 and 5.7). There was no further decrease between 1 and 4 hours (p = 0.233), or between four and eight hours (p = 0.1); however, the amount decreased significantly to one-fifth of its initial optimal loading concentration (median 49.99ng (95% CI 43.71 to 51.33)) by 24 hours (p < 0.001). These figures are equivalent to 3.2ng mm-2, 1.8 ng mm-2 and 0.6 ng mm-2 of Fn on HA at zero, 1 to 8, and 24 hours, respectively.
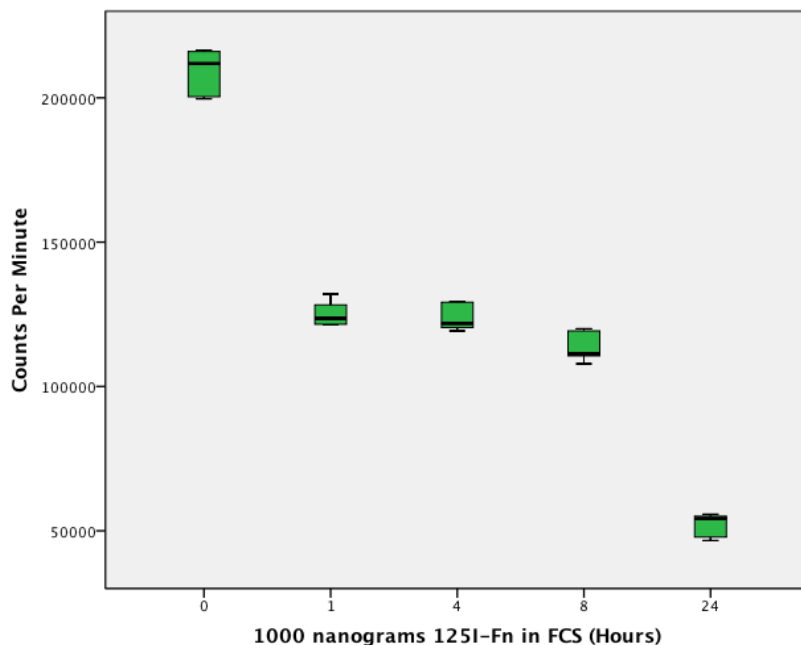
Figure 5.6: Box plot showing CPM detected on HA discs with increasing incubation time (hours) after initial loading of 100 ng 125I-Fn in FCS
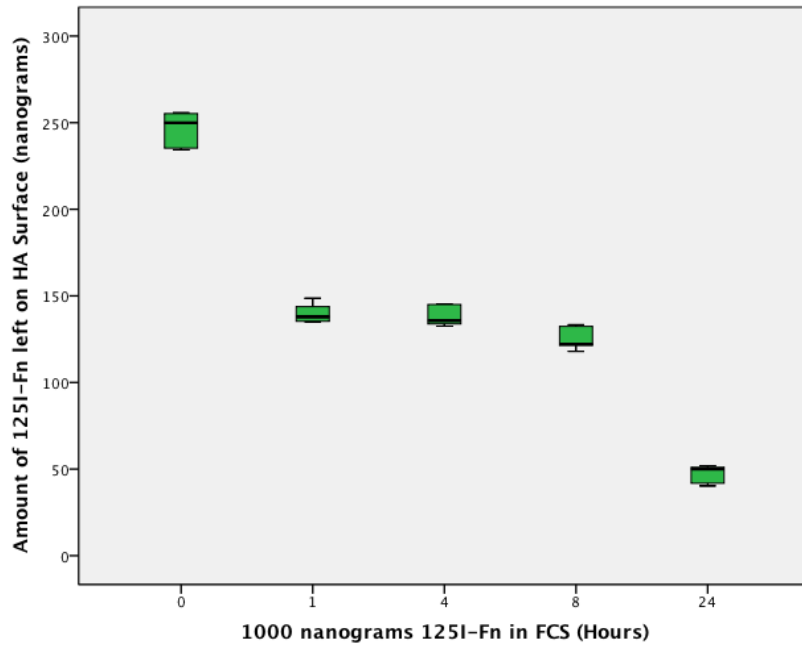
Figure 5.7: Box plot showing amount of125I-Fn (ng) remaining on HA discs with increasing incubation time (hours) after initial loading of 1000ng 125I-Fn in FCS

5.3.5 Surface roughness experiments

Median Ra, Rz and Sm values for Pol were 0.030µm (95% CI 0.011 to 0.048), 0.120µm (95% CI 0.100 to 0.148) and 20.630µm (95% CI 9.804 to 32.701), respectively. The corresponding median values for HA were 0.039 µm (95% CI 0.121 to 0.052), 0.131µm (95% CI 0.107 to 0.159) and 22.005 µm (95% CI 10.020 to 34.653). No statistically significant differences were observed between Pol and HA discs (p = 0.650, p = 0.631 and p = 0.262 for Ra, Rz and Sm, respectively).

5.3.6 Fibroblast focal adhesion and cell area quantification

5.3.6.1 Number of vinculin markers per cell

The number of vinculin markers per cell was significantly greater on HAFn than on the HA and Pol controls at all time-points (HAFn vs HA: p = 0.003, 0.004 and 0.004; HAFn vs Pol: p = 0.003, 0.004 and 0.004; at 1, 4 and 24 hours, respectively). A 15-, 19- and

12-fold increase was seen with HAFn compared with HA alone at 1, 4 and 24 hours, respectively. After one hour the number of vinculin markers per cell was significantly greater with HA than with Pol (p = 0.006), but by 4 and 24 hours the opposite was seen (p = 0.025 and 0.004, respectively).

5.3.6.2 Cell area

At 1 and 4 hours the cell area increased in the order HA < Pol < HAFn. The median cell area on HAFn was significantly greater than those on both HA and Pol controls (HAFn vs HA: p = 0.003 and 0.004; HAFn vs Pol: p = 0.003 and 0.004; at 1 and 4 hours, respectively). At 24 hours the cell areas on both HAFn and Pol were significantly greater than on HA (p = 0.01 and 0.004); there was no significant difference between them (p = 0.631). Cell area was observed to be 5-, 5.5- and 2-fold greater on HAFn than on HA at 1, 4 and 24 hours, respectively.

5.3.6.3 Vinculin marker per cell area

Vinculin adhesion markers were counted and divided by cell area. d . At 1 hour attachment increased significantly between Pol and HA (p = 0.004) and between HA and HAFn (p = 0.003) with a 14- and a three- fold increase, respectively (Fig. 5.8).

A similar pattern was seen at 4 and 24 hours (Fig. 5.8); however, no significant difference was seen between Pol and HA (p = 0.055 and 0.150). Attachment was significantly greater on HAFn than on HA at four and 24 hours (p = 0.004): 4 and 7-fold increases were seen.

On Pol substrates, vinculin per cell area increased significantly between 1 and 4 hours (p = 0.004), after which no significant difference was seen (p = 0.199).

Attachment of cells on HA was not significantly different between 1 and 4 (p = 0.262) or 4 and 24 hours (p = 0.055); however, on HAFn attachment increased significantly between both time points (p = 0.038 and 0.004, respectively) (Figure 5.8). Figure 5.9 shows vinculin staining in cells on Pol, HA and HAFn at 1, 4 and 24 hours. The images show increases in cell area and vinculin markers on HAFn substrates at all times compared to HA and Pol controls. Number of vinculin markers per unit cell area, on HAFn at 1 hour was 3.4 and 4.2 times greater than with HA and Pol at 24 hours (Fig. 5.9).
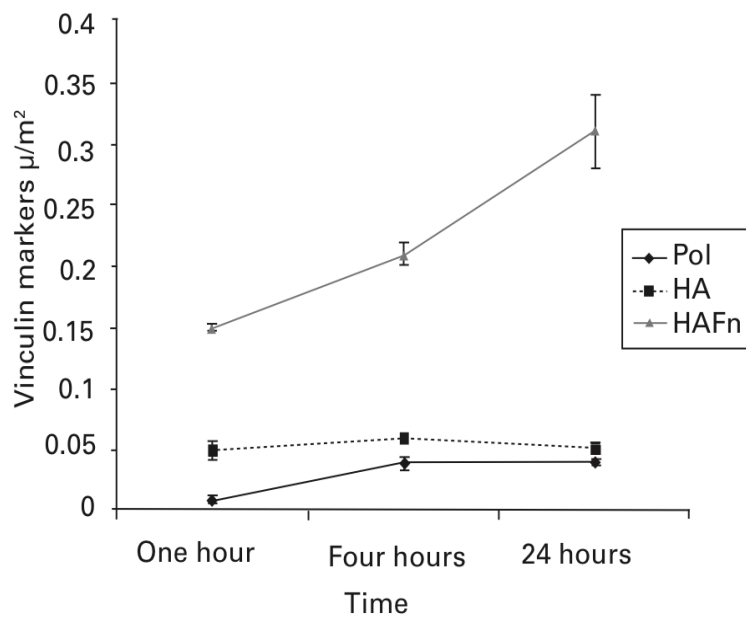
Figure 5.8: Graph showing median number of vinculin markers per unit cell area (count per μm^2) for polished (Pol), HA and HAFn substrates for 1, 4 and 24 hours
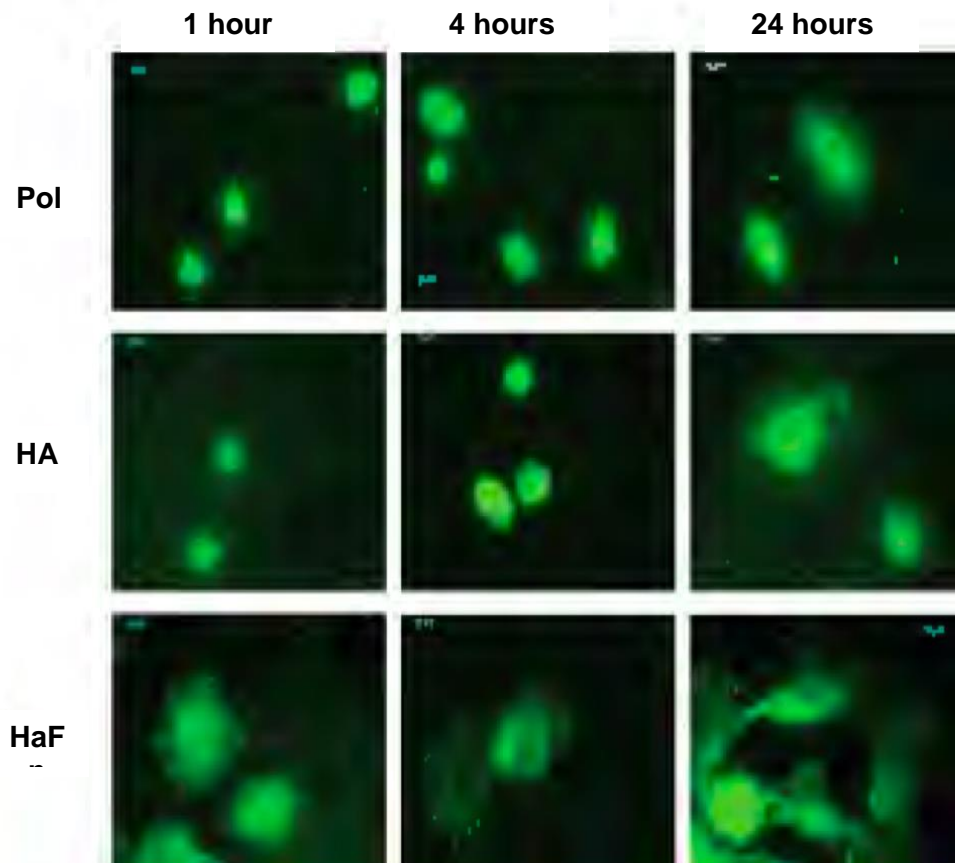
Figure 5.9: Fluorescence microscopy showing appearance of fibroblasts on Pol, HA and HAFn substrates at 1, 4 and 24 hours

5.4 Discussion

In this chapter we have shown that Fn can be adsorbed on HA, and that this procedure increases dermal fibroblasts vincluin markers per unit area of the cell *in vitro*.

Focal adhesions are crucial for cell attachment signalling and regulation (Petit and Thiery, 2000; Sastry and Burridge, 2000). Accurate quantification of cell attachment can be measured through calculating the number of vinculin markers per unit cell area; gives an accurate indication of the biophysical strength of cell attachment (Pendegrass et al.,2010). Previous studies have shown that protein augmentation can increase the attachment of cells *in vitro* (Middleton el al.,2007; El Ghannam et al.,1998), and

attempts to create durable coatings by silanisation have shown promising results (Gordon et al., 2010). My work in chapters 2, 3 and 4 show that silanized dual coating protein on Ti6Al4V is a a durable surface that improves keratinocyte and fibroblast attachment compared to uncoated controls and single coating proteins. Silanisation techniques create –CHO bonds for protein binding, but are laboratory based and subject to considerable variability. The process is time consuming and has a learning curve to master the steps. Protein absorption may be a more consistent technique and, unlike silanisation, could be performed at the time of surgery for ITAP. On HA discs, our findings show that after 1 hour of adsorption with an initial coating concentration of 13 ng mm^{-2} (1000 ng per 10 mm diameter disc), HA substrates are optimally loaded with 3.2 ng mm^{-2}, which significantly increases dermal fibroblast attachment *in vitro*. Given the duration of an ITAP surgical procedure, intra-operative implementation of our adsorption technique would be practicable.

In 2010, Gordon et al., showed that keratinocyte attachment could be increased by a coating of 6 to 7ng/mm^2 of silanised laminin-5. My findings agree with this and show that between 3.2 and 0.6 ng mm^{-2} of Fn have a significant positive effect on fibroblast attachment. The maximum amount of Fn that could be adsorbed was 3.2 ng/mm^2, although we accept that this may not give a maximal increase in the attachment strength of the dermal fibroblasts. In addition to this, *in vivo* studies are still needed to establish whether similar there is a increase in dermal attachment. I noted a decrease in adsorbed Fn on HA, only one-fifth of the initial load remaining by 24 hours. This shows that the stability of the coating is not as robust as that achieved with silanisation. Despite this, a 7-fold increase in fibroblast attachment on Fn-functionalised HA was seen at 24 hours. Further investigations are necessary to determine whether this is directly due to the Fn coating, or whether the initial coating influences the deposition rate and composition of the ECM, which in turn upregulates attachment. In a study assessing the influence of the competitive pre-adsorption of human serum albumin and

Fn on osteoblast adhesion and morphology, Sousa et al. (2008), concluded that the tissue response to implants is dependent on the initial attachment of cells to the substrate and that this is directly related to the ability of cells to interact with the protein layer absorbed on the implant surface. In 2008, Laflamme and Rouabhia showed that BMP-2 and -7 coatings promote osteoblast attachment to collagen scaffolds and concluded that this was due to the substrate mimicking the *in vivo* physiological conditions of the ECM more precisely than uncoated controls. I suggest that Fn-pre-adsorbed HA resembles the adhesion protein component of the fibroblasts' native ECM more closely, enabling them to become attached more quickly and more efficiently than uncoated controls.

In conclusion, our results suggest that Fn-coated HA implants increases vinculin adhesion markers per cell area to ITAP. An adsorption technique that applies Fn to HA-coated implants at the time of surgery may be enough to achieve this without the need for prolonged preparation, which might limit the application of these coatings. Further work is needed to determine whether increased concentrations of Fn result in further upregulation of dermal fibroblast attachment and whether these coatings elicit a similar effect on dermal tissue attachment around an ITAP *in vivo*. The hypothesis would be that Fn applied to HA- coated ITAP would bind to surrounding tissue with more surface area compared to controls on uncoated ITAP and HA coated ITAP without Fn.

CHAPTER 6

Conclusions From My Thesis

6.1 Conclusions from this Thesis

In my thesis, I investigated HaCaT keratinocytes and HDF fibroblasts grown on Ti6Al4V with the overall aim being to increase earlyvinculin markers and cell area. My work aims to help cells form a barrier at the implant- tissue interface that is resistant to infection.This seal may help avoiding cell down-growth, marsupilization, infection and failure of metalwork. This improves longevity and effectiveness of percutaneous devices, which require this seal for their success. Intraosseous Transcutaneous Amputation Prosthesis (ITAP) is a novel percutaneous device that overcomes conventional stump-socket problems. By creating a soft tissue seal around the percutaneous portion of this permanent implant, the hope is that long-term survival can be achieved (Pendegrass et al., 2008).

The overall hypothesis tested in this thesis was that by modifying both the chemical structure and the surface topography of Ti6Al4V, both keratinocyte and fibroblast vinculin markers and cell area would be enhanced. This has been supported.

Since Branemark's design of a percutaneous device for amputees, no attempt to deal with skin-implant interface down-growth and failure was investigated to improve its design. Our research group has attempted to improve this barrier by modifying the chemical structure of Ti6Al4V via covalently bonding laminin to the metal surface, or covalently bonding fibronectin and investigating the behaviour of keratinocytes and fibroblasts on the attachment respectively (Pendegrass et al., 2008). Further work identified that changing the surface topography through oxidation of Ti6Al4V prior to silanization can have a detrimental effect on cell attachment (Pendegrass et al., 2010) that provided the basis for my work.

In order to enhance HaCaT and HDF attachment to Ti6Al4V, I examined the effect of polished surfaces and silanized surfaces on cells. I also examined silanization with and without oxidation as methods to covalently link dual coating proteins of fibronectin and laminin to Ti6Al4V. These surfaces were tested in vitro to assess keratinocyte and fibroblast behaviour, including the expression of adhesion complexes and growth.

In Chapter 2, I hypothesised that silanized dual coating proteins on Ti6Al4V surfaces bonded significantly more and were more durable than on adsorbed surfaces. I also hypothesized that there was non-competitive bonding between laminin and fibronectin when they were silanized on Ti6Al4V. I used radiolabeled protein to quantify the amount of laminin and fibronectin remaining on Ti6Al4V over time in a sensitive and accurate method. I showed that covalent bonding of dual coating proteins ^{125}I-Fn and ^{125}I-Ln to Ti6Al4V through silanization (Weetall, 1993) demonstrated significantly larger amounts of both proteins remaining on the surface compared to adsorbed surfaces at all time periods. There was a 7-fold increase of silanized dual coating fibronectin remaining on Ti6Al4V at 72 hours compared to adsorbed dual coating fibronectin and a 4 -fold increase of silanized dual coating laminin compared to adsorbed dual coating laminin at the same time period. I showed this increase happens in dual coating proteins as well as single coating protein. I also showed that there was non-competitive binding of these proteins on the surface on the substrate. The protocol outlined by Middleton et al. (2007), and Gordon et al.(2010), was implemented where maximum bonded laminin and fibronectin were used respectively, which was 6.366ng/mm^2 for both proteins.

In order to determine whether dual coating protein silanized to Ti6Al4V were sufficient to enhance early cell adhesion and growth, further experiments were required to culture cells on silanized dual coating proteins and test their adhesion properties and size using the same silanization protocols.

In chapter 3, I examined the behaviour of HaCATs on dual coating laminin and fibronectin and single coating laminin and fibronectin on Ti6Al4V surfaces. Silanization allows proteins to couple to metal alloy directly, the protocol outlined by Middleton et al. (2007), requiring metal to be passivated in order to provide a uniform layer of TiO_2. However, passivation leads to creating a rough surface that may have negative effect on cell attachment. I compared dual coating protein on polished surfaces and silanized surfaces with and without passivation. I also ran the same experiments at the same time points using uncoated controls, adsorbed, silanized passivated, silanized non-passivated single coating fibronectin and single coating laminin to determine if there was any significance between them or with dual coating proteins. Cell attachment was determined by measuring vinculin markers and cell growth by measuring cell size. I found that silanized dual coating protein provided the best surface for early cell attachment and growth. Gordon et al. (2008), showed that silanized passivated laminin supported smaller cell area than control discs. There were more vinculin markers per cell and per unit area than controls. However, vinculin markers per cell and cell area were not significantly more than adsorbed laminin at 24 hours. These are similar to my findings; this may be due to the rough surface formed by the passivation step of silanization. When this step is removed, silanized, non-passivated laminin surface supported more cell area, vinculin markers per cell and per unit area than silanized, passivated laminin surface and controls at all time points. No work has investigated silanized, non-passivated dual coating protein fibronectin and laminin. Further studies need to be conducted to validate my results.

In chapter 4, I investigated the effect of dual coating protein fibronectin and laminin on HDF fibroblasts. I compared controls of polished uncoated surface; silanized, non-passivated; silanized passivated, single coating laminin and fibronectin and dual coating protein. I found that silanized, non-passivated dual coating protein surface

expressed significantly more vinculin markers per cell unit and cell area. Middleton et al.(2007), investigated silanized, passivated and non-passivated single coating fibronectin, and concluded that silanized, non-passivated fibronectin surface expressed larger cell areas and vinculin markers at all time periods. No previous studies investigated silanized, non-passivated dual coating protein effect on HDFs.

In chapter 5, I investigated the durability of fibronectin coating on HA discs. Fn attachment peaked at one hour of incubation and the maximum binding efficiency was achieved with a droplet of 1000ng. There was a significant increase in cell attachment at 1, 4 and 24 hours with Fn coating on HA discs to uncoated controls.

6.2 Clinical Relevance of the Experiments

The data presented in this thesis are highly relevant to clinical practice. Intra-osseous transcutaneous amputation prostheses is dependent on the presence of a tight seal at the skin-implant interface to avoiding epithelial downgrowth, marsupialisation, infection, subsequent loosening and failure of the metalwork.

I developed a Ti6Al4V surface that enhances early epithelial attachment and is stable in vitro. By applying this surface in clinical practice, transcutaneous devices may form this barrier that improves the longevity and reduces morbidity in patients with these devices.

This new surface can also be used to coat external pins in treatment of fractures and leg lengthening procedures. Although these devices are temporary, complications of pin site infections can be reduced by forming a seal around the metal alloy.

Research done in my thesis is a step to come closer to developing the ideal surface for ITAP. This will improve the transcutaneous portion of ITAP and will contribute to the ongoing development for this amputation prosthesis.

6.3 Further Work

In vivo, it is not just cell attachment that may be important in producing a seal at the skin-implant interface. Competitive binding from other components within the extracellular matrix such as albumin, cellular activity involved in wound healing in addition to the presence of many other cell types may affect my results in vivo.

Wound healing is a dynamic process that may need other substrates to enhance this environment and may need to be triggered at different time points as the local pH changes. Addition of prophylactic local antibiotics may be necessary to help cells, in case bacteria and other microorganisms attempt to invade the skin-implant barrier and underlying tissues.

Further work needs to investigate synthetic RGD sequences to compare them to dual coating fibronectin and laminin both *in vitro* and *in vivo.* The hypothesis would be synthetic cyclic RGD sequences coated to Ti6Al4V discs produce more vinculin markers and increased cell area on fibroblasts and keratinocytes compared with controls and dual coating FnLn. These would then be tested on animal studies to compare then to controls. Histopathological samples would be examinaed for the percentage of tissue binding to Ti alloy. The following step would be to test the effect of sterilization techniques such as gamma radiation, or ethylene oxide on protein coated ITAP. The hypothesis would be there would be no difference in the vinculin markers and cell area when discs are sterilized using different techniques. This would allow the protein coated implants to be used in operative procedures. The hope is that the

results gained from my studies provide evidence to support the long-term use of ITAP

utilizing biomaterials similar to the ones I used in my thesis and to reach a practical,

commercially available product that can be utilized in normal operating theatres.

SELECTED PUBLICATIONS

■ RESEARCH

The development of fibronectin-functionalised hydroxyapatite coatings to improve dermal fibroblast attachment *in vitro*

C. J. Pendegrass,
M. El-Husseiny,
G. W. Blunn

From University College London, London, United Kingdom

The success of long-term transcutaneous implants depends on dermal attachment to prevent downgrowth of the epithelium and infection. Hydroxyapatite (HA) coatings and fibronectin (Fn) have independently been shown to regulate fibroblast activity and improve attachment. In an attempt to enhance this phenomenon we adsorbed Fn onto HA-coated substrates. Our study was designed to test the hypothesis that adsorption of Fn onto HA produces a surface that will increase the attachment of dermal fibroblasts better than HA alone or titanium alloy controls.

Iodinated Fn was used to investigate the durability of the protein coating and a bioassay using human dermal fibroblasts was performed to assess the effects of the coating on cell attachment. Cell attachment data were compared with those for HA alone and titanium alloy controls at one, four and 24 hours. Protein attachment peaked within one hour of incubation and the maximum binding efficiency was achieved with an initial droplet of 1000 ng. We showed that after 24 hours one-fifth of the initial Fn coating remained on the substrates, and this resulted in a significant, three-, four-, and sevenfold increase in dermal fibroblast attachment strength compared to uncoated controls at one, four and 24 hours, respectively.

■ C. J. Pendegrass, PhD,
Lecturer
■ M. El-Husseiny, MD, Student
■ G. W. Blunn, PhD, Professor
The Centre for Biomedical
Engineering, University
College London, The Royal
National Orthopaedic Hospital,
Brockley Hill, Stanmore,
Middlesex HA7 4LP, UK.

Correspondence should be sent
to Dr C. Pendegrass; e-mail:
c.pendegrass@ucl.ac.uk

Conventional stump–socket prostheses are the treatment of choice for most above-knee amputees; however, a poorly fitting socket will frequently cause pressure sores, infection and an abnormal gait.[1] An intraosseous transcutaneous amputation prosthesis (ITAP) can overcome these problems[2] as well as providing improved proprioception.[3] During normal wound healing, epithelial cells at the margin of the wound migrate to re-establish the protective barrier function of the skin. Around an ITAP this results in downgrowth of the epithelium and pocket formation, which in turn provides a route whereby pathogens can enter and cause infection. For an ITAP to be successful, a tight seal at the skin–implant interface is essential.[4,5]

Deer antlers have been studied as biomimetic models of ITAP[6] and have emphasised the crucial role of dermal tissue adhesion in preventing downgrowth. Surface modifications and synthetic hydroxyapatite (HA) coatings have been incorporated into the design of ITAPs to enhance dermal adhesion,[4-7] and biological coatings have been shown to improve dermal fibroblast attachment both *in vitro* and *in vivo*.[8,9]

Cell adhesion is modulated by the extracellular matrix (ECM). The glycoprotein fibronectin (Fn) is a principal component of ECM, and it contains cell integrin-binding sequences; these include the amino acid sequence arginine-glycine-aspartic acid (RGD in one-letter amino acid code), through which it promotes cell-matrix adhesion.[10] Fn is readily adsorbed onto biomaterials, and enhances fibroblast activity[11] and attachment by upregulation of focal adhesion expression *in vitro*.[8,12] Focal adhesions are specialised electron-dense regions of the plasma membrane which create intimate, discrete contacts of 10 nm to 15 nm with the substratum of cells.[13] Quantification of the number of focal adhesions per unit cell area has been shown to be an accurate way of measuring the direct biophysical strength of dermal fibroblast attachment *in vitro*.[14]

HA is a naturally occurring mineral apatite that comprises 70% of bone.[15] Synthetic HA coating of endoprostheses promotes osseointegration,[16] and Fn functionalisation of HA-coated titanium alloy has been shown to increase dermal tissue attachment *in vivo*.[9] Despite extensive investigations into the interaction of ECM proteins with HA,[17-20] the precise nature of the interaction is not clear. This study investigated the loading and release kinetics of Fn from HA in the hope of providing new data that may enable us to establish an optimal coating regime capable of enhancing dermal fibroblast attachment. This could then be applied to ITAPs in order to enhance the interface between implant and skin. The aim of

this study was to assess the loading, release and durability kinetics of Fn on HA substrates and to assess the effect of Fn-functionalised HA on dermal fibroblast attachment *in vitro*. We hypothesised that adsorption of Fn onto HA would produce a surface that would increase the attachment of dermal fibroblasts compared with HA alone and titanium alloy controls.

Materials and Methods

The study was divided into two parts: the first to determine the loading, release and durability kinetics of Fn coatings on HA, and the second to assess dermal fibroblast attachment to Fn-functionalised HA.

Fn loading, release and durability kinetics experiments. Disc preparation. Sintered HA discs 11.7 mm in diameter and weighing 1 g, made in 12 mm casts with 1.5 tonnes of pressure applied over 2 hours at 1250°C (5°C ramp/min) to HA powder (Apatech, Elstree, United Kingdom), were compacted in a mould and heated to 500°C. X-ray diffraction analysis (XRD) was performed to assess the crystallinity and purity of the HA; XRD patterns recorded using an X'Pert Pro Diffractometer (PANalytical Ltd, Cambridge, United Kingdom) showed that the abundance of calcium phosphate and hydroxyl groups and the crystallinity of HA were identical to those used previously *in vitro* and to the plasma-sprayed HA coating used for ITAPs *in vivo*.[9]

Fibronectin: coating and radiolabelling. Human plasma fibronectin (Fn) (F2006; Sigma-Aldrich, Gillingham, United Kingdom), diluted in phosphate-buffered saline (PBS), was used throughout the experiment. Fn was custom-labelled by PerkinElmer (Waltham, Massachusetts). A modified chloramine-T procedure was used to produce ^{125}I-Fn, which was then used to quantify the amount of Fn remaining on the HA discs. The optimal purification using high-performance liquid chromatography (HPLC) yielded 45% incorporation, > 95% purity, a concentration of 0.27 mCi/ml and a specific activity of 30 μCi/μg. [125]I produces both gamma and beta radiation. HA discs were coated with 50 μl droplets of Fn, which covered the entire surface of each disc to produce ^{125}I-FnHA discs. The ^{125}I-FnHA discs were rinsed with PBS three times before being used in the series of experiments described below. All techniques were performed at 21°C under sterile conditions using aseptic technique. All uncoated control surfaces were treated with equal volumes of PBS for the same period of time.

[125]I-FnHA quantification. A Tricarb 2900TR liquid scintillation counter (PerkinElmer) was used to detect gamma radiation in counts per minute (CPM). Following three washes in sterile PBS, discs were placed face up in 5 ml scintillation tubes and immersed in 4.5 ml of scintillation fluid. QuantaSmart software (PerkinElmer) supplied with the liquid scintillation counter was used, with correction for ^{125}I half-life, at an external standard terminator of 0.5 s and a count time of 1 min. The scintillation counter was calibrated using appropriate standards and each sample was counted twice. The results of the loading and release

kinetics experiments were determined from a standard calibration curve.

Optimisation of ^{125}I-Fn coating of HA. Six replicates were used for all studies unless stated otherwise.

Effect of duration and quantity on ^{125}I-Fn loading of HA. In order to investigate the optimal time to leave ^{125}I-Fn on the HA discs, 500 ng of ^{125}I-Fn was placed on the disc surfaces for zero, 0.5, one and two hours before analysis. In order to determine the maximum possible coating concentration, 100 ng, 250 ng, 500 ng, 1000 ng and 1500 ng of ^{125}I-Fn were placed on the disc surfaces for one hour.

Durability of ^{125}I-FnHA coating. As described above, 1000 ng of ^{125}I-Fn in 50 μl was added to the discs. In order to assess the durability of the ^{125}I-Fn coating, discs were immersed in fetal calf serum (FCS) (First Link Ltd, Birmingham, United Kingdom). The discs were analysed immediately after three washes in sterile PBS (time zero) before immersion in FCS and incubation at 37°C. Samples were removed and washed three times with distilled water, and the amount of ^{125}I-Fn remaining on the discs was measured at one, four, eight and 24 hours.

Dermal fibroblast attachment experiments. Disc preparation and characterisation. Surgical grade titanium alloy (Ti-6Al-4V) discs, 10 mm in diameter, were ground, polished and cleaned to the level required for orthopaedic implant manufacture, and were used as controls (Pol group). Non-Fn-functionalised sintered HA discs (HA group; manufactured as described above) were used to represent the HA that is currently used for ITAPs.[7] To assess the effects of Fn functionalisation of HA on dermal fibroblast attachment, 1000 ng of Fn were then applied to the HA discs (HAFn) for one hour, as described above. The surface roughness (R_a), mean maximum height of the profile (R_z) and mean spacing of irregularities of the profile (S_m) were measured using a Mitutoyo Surftest SV-400 Surface Profiler (Mitutoyo, Warwick, United Kingdom). Discs were sterilised in a 2100 Classic Clinical Autoclave (Prestige Medical, Blackburn, United Kingdom) for 11 minutes at 126°C and a pressure of 1.4 bar.

Dermal fibroblast culture and seeding. Fibroblasts (1BR.3.G cells, ECACC/Sigma-Aldrich) were cultured in Dulbecco's Modified Eagle's medium (DMEM; Sigma-Aldrich) with 4500 mg/l glucose, 1% non-essential amino acids, 1% penicillin/streptomycin (Invitrogen Corporation, Paisley, United Kingdom) and 10% FCS (First Link) at 37°C with 5% CO_2; 2500 cells per disc were seeded for one, four and 24 hours on Pol, HA and HAFn discs.

Fibroblast focal adhesion detection method. The discs were washed twice in PBS and fixed in formal saline for five minutes. Four five-minute washes in PBS were followed by incubation for two hours with a mouse monoclonal anti-human clone HUV-1 (V9131 Sigma-Aldrich = Anti-vinculin) (1:100) and Triton X-100 (1:500) in sterile PBS. After three washes in PBS the discs were incubated for 45 minutes with fluorescein isothiocyanate (FITC) conjugate in a secondary antibody solution (F2883 Sigma-Aldrich = Anti-mouse) (1:168 in sterile PBS), and then washed three times in PBS before analysis.

566   C. J. PENDEGRASS, M. EL-HUSSEINY, G. W. BLUNN
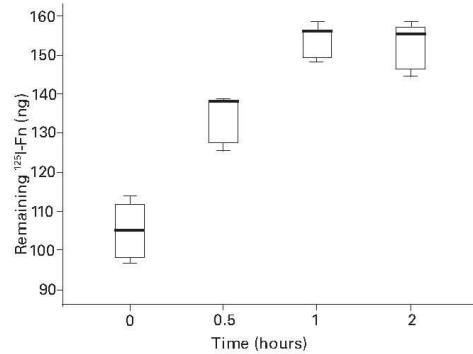
Fig. 1

Box plot showing the amount of ^{125}I-fibronectin (^{125}I-Fn) (in ng) remaining on hydroxyapatite discs after an initial loading with 500 ng, rinsing and detection (as described in text) after incubations of 0, 0.5, one and two hours. The boxes denote the median and interquartile range, and the whiskers denote the full range.
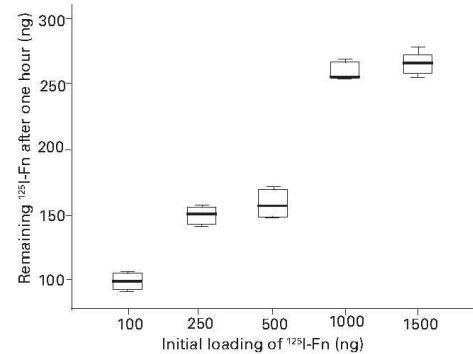
Fig. 2

Box plot showing the amount of ^{125}I-fibronectin (^{125}I-Fn) (in ng) remaining on hydroxyapatite discs after initial loading with between 100 ng and 1500 ng of Fn, incubation for one hour, and rinsing and detection (as described in text). The boxes denote the median and interquartile range, and the whiskers denote the full range.

Fibroblast focal adhesion and cell area quantification. After vinculin staining at one, four and 24 hours, focal adhesion quantification was carried out using a Carl Zeiss microscope (Carl Zeiss Ltd, Welwyn Garden City, United Kingdom) with ×50, and ×100 objective lenses. For each disc 15 cells were analysed. A random field of view was selected and the vinculin markers on the cells (defined as individually distinguishable immunofluorescent markers within the cell, and present at the cell boundaries, as previously described[8,9,14]) were manually identified and counted by two independent observers (CJP, ME) who were blinded both to the test substrate and to one another. Using kappa statistics, kappa scores indicated almost perfect inter-observer agreement (> 0.90), and so the data presented are those of both observers combined. Cell areas were measured using Axiovision Image Analysis Software (Axioimage 4.4; Carl Zeiss, Gottingen, Germany). The number of vinculin markers per unit cell area was calculated by dividing the number of vinculin counts by the cell area.

Statistical analyses. The data did not fit the assumptions required for parametric testing and were analysed using Mann-Whitney U tests to compare medians. Box plots showing median values, whole and interquartile ranges, and median values were expressed with 95% confidence intervals (CI). All numerical data are stated as median values (with 95% CI) unless otherwise stated. Results were considered significant when the p-value ≤ 0.05.

Results

Fn loading, release and durability kinetics experiments.
[125]I-FnHA quantification. A standard calibration curve was generated and used to determine the results for the loading and release kinetics experiments with correction for the half-life of [125]I ($R^2 = 0.995$).

Optimisation of ^{125}I-Fn coating of HA. The optimal time for loading of Fn onto HA discs was one hour (Fig. 1). Significant increases were seen in the amount of Fn remaining on the discs between all time-points up to one hour (all $p < 0.001$), but there was no significant difference between one and two hours ($p = 0.691$). The data show that there was no significant increase in the amount of protein retained on the discs after incubation for one hour.

After one hour (optimal incubation duration as shown above) the median maximum amount of Fn bound was 255.26 ng (95% CI 253.74 to 264.26) from an initial load of 1000 ng in 50 μl.

As the quantity of ^{125}I-Fn added increased (from 100 ng to 250 ng, and 500 ng to 1000 ng), a significantly higher quantity of ^{125}I-Fn remained on the discs (all $p < 0.001$); 50 μl droplets containing 1000 ng and 1500 ng did not produce proportionally more coupled protein ($p = 0.085$) (Fig. 2).

The optimal loading concentration and incubation time of 1000 ng in 50 μl for one hour was used as above to determine the optimum durability. A significant decrease from a median of 249.91 ng (95% CI 239.79 to 254.39) to 137.93 ng (95% CI 135.89 to 142.72 ng) of Fn coupled to HA was seen within the first hour of incubation in FCS ($p < 0.001$). There was no further decrease between one and four hours ($p = 0.233$), or between four and eight hours ($p = 0.1$); however, the amount decreased significantly to one-fifth of its initial optimal loading concentration (median 49.99 ng (95% CI 43.71 to 51.33)) by 24 hours ($p < 0.0001$) (Fig. 3). These figures are equivalent to 3.2 ng mm^{-2}, 1.8 ng mm^{-2} and 0.6 ng mm^{-2} of Fn on HA at zero, one to eight, and 24 hours, respectively.

Dermal fibroblast attachment experiments. For characterisation of the discs, the median R_a, R_z and S_m values for Pol
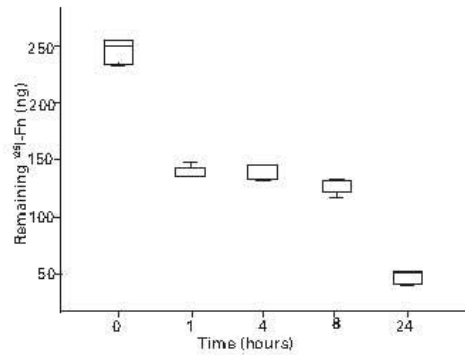
Fig. 3

Box plot showing of the amount of ^{125}I-Fn (in ng) remaining on HA surfaces with increasing incubation time (hours) after an initial loading of 1000 ng of ^{125}I-Fn in FCS. The boxes denote the median and interquartile range, and the whiskers denote the full range.
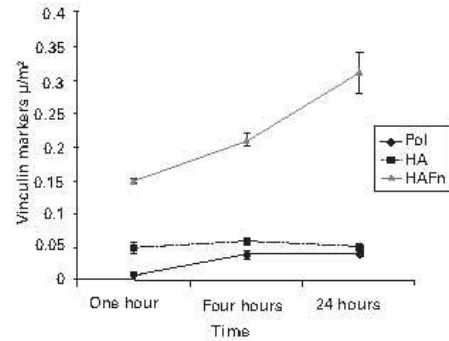
Fig. 4

Graph showing the median (with standard error bars) number of vinculin markers per unit cell area (count per μm^2) for the polished (Pol), hydroxyapatite (HA) and HA-fibronectin (HAFn) substrates at one, four and 24 hours.

were 0.030 μm (95% CI 0.011 to 0.048), 0.120 μm (95% CI 0.100 to 0.148) and 20.630 μm (95% CI 9.804 to 32.701), respectively. The corresponding median values for HA were 0.039 μm (95% CI 0.121 to 0.052), 0.131 μm (95% CI 0.107 to 0.159) and 22.005 μm (95% CI 10.020 to 34.653). No statistically significant differences were observed between Pol and HA discs (p = 0.650, p = 0.631 and p = 0.262 for R_a, R_z and S_m, respectively).

Fibroblast focal adhesion and cell area quantification. Number of vinculin markers per cell. The number of vinculin markers per cell was significantly greater on HAFn than on the HA and Pol controls at all time-points (HAFn vs HA: p = 0.003, 0.004 and 0.004; HAFn vs Pol: p = 0.003, 0.004 and 0.004; at one, four and 24 hours, respectively). A 15-, 19- and 12-fold increase was seen with HAFn compared with HA alone at one, four and 24 hours, respectively. After one hour the number of vinculin markers per cell was significantly greater with HA than with Pol (p = 0.006), but by four and 24 hours the opposite was seen (p = 0.025 and 0.004, respectively).

Cell area. At one and four hours the cell area increased in the order HA < Pol < HAFn. The median cell area on HAFn was significantly greater than those on both HA and Pol controls (HAFn vs HA: p = 0.003 and 0.004; HAFn vs Pol: p = 0.003 and 0.004; at one and four hours, respectively). At 24 hours the cell areas on both HAFn and Pol were significantly greater than on HA (p = 0.01 and 0.004); there was no significant difference between them (p = 0.631). Cell area was observed to be 5-, 5.5- and two-fold greater on HAFn than on HA at one, four and 24 hours, respectively.

The attachment was measured by the number of vinculin markers per unit cell area. At one hour attachment increased significantly between Pol and HA (p = 0.004) and between HA and HAFn (p = 0.003) with a 14- and a threefold increase, respectively (Fig. 4).
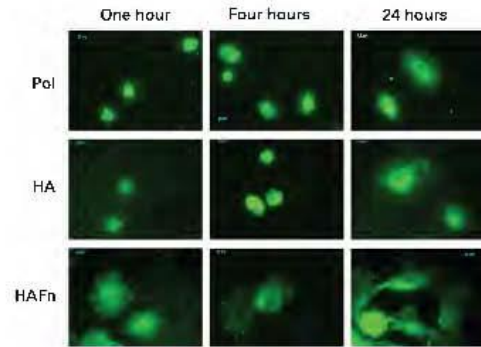
Fig. 5

Fluorescence microscopy images showing the appearance of fibroblasts on the polished (Pol), hydroxyapatite (HA) and HA-fibronectin (HAFn) substrates at one, four and 24 hours.

A similar pattern was seen at four and 24 hours (Fig. 4); however, no significant difference was seen between Pol and HA (p = 0.055 and 0.150). Attachment was significantly greater on HAFn than on HA at four and 24 hours (p = 0.004): four- and sevenfold increases were seen.

On Pol substrates attachment increased significantly between one and four hours (p = 0.004), after which no significant difference was seen (p = 0.199).

Attachment of cells on HA was not significantly different between one and four (p = 0.262) or four and 24 hours (p = 0.055); however, on HAFn attachment increased significantly between both time points (p = 0.038 and 0.004, respectively) (Fig. 4).

Fluorescent microscopy. Figure 5 shows vinculin staining in cells on Pol, HA and HAFn at one, four and 24 hours. The

images show increases in cell area and vinculin markers on HAFn substrates at all times compared to HA and Pol controls. The attachment of cells, measured by the number of vinculin markers per unit cell area, on HAFn at one hour was 3.4 and 4.2 times greater than with HA and Pol at 24 hours (Fig. 5).

Discussion

In this study we have shown that HA can be functionalised by adsorption of Fn, and that optimising this procedure increases the attachment of dermal fibroblasts as measured by the quantification of vinculin markers per unit area of the cell.

Focal adhesions are critical in the regulation of cell attachment,[21,22] and quantification of the number of vinculin markers per unit cell area gives an accurate indication of the biophysical strength of cell attachment.[14]

Previous studies have shown that protein augmentation can increase the attachment of cells *in vitro*,[8,23-25] and attempts to create durable coatings by silanisation have shown promising results.[26] Silanisation techniques create –CHO bonds for protein binding, but are laboratory based and subject to considerable variability. Protein absorption may be a more consistent technique and, unlike silanisation, could be performed at the time of surgery for ITAP. Our findings show that after one hour of adsorption with an initial coating concentration of 13 ng mm^{-2} (1000 ng per 10 mm diameter disc), HA substrates are optimally loaded with 3.2 ng mm^{-2}, which significantly increases dermal fibroblast attachment *in vitro*. Given the duration of an ITAP surgical procedure, clinical implementation of our adsorption technique would be feasible.

In 2010, Gordon et al[26] showed that keratinocyte attachment could be increased by a coating of 6 to 7 ng mm^{-2} of silanised laminin-5. Our current findings agree with this, and show that between 3.2 and 0.6 ng mm^{-2} of Fn have a significant positive effect on fibroblast attachment. The maximum amount of Fn that could be adsorbed was 3.2 ng/mm^2, although we accept that this may not give a maximal increase in the attachment strength of the dermal fibroblasts. Moreover, it may not result in an equivalent increase in attachment *in vivo*, and further studies are needed to investigate this. We noted a decrease in adsorbed Fn on HA, only one-fifth of the initial load remaining by 24 hours. This shows that the stability of the coating is not as robust as that achieved with silanisation.[26] Despite this, a sevenfold increase in fibroblast attachment on Fn-functionalised HA was seen at 24 hours. Further investigations are necessary to determine whether this is directly due to the Fn coating or whether the initial coating influences the deposition rate and composition of the ECM, which in turn upregulates attachment.

In a study assessing the influence of the competitive pre-adsorption of human serum albumin and Fn on osteoblast adhesion and morphology, Sousa et al[27] concluded that the tissue response to implants is dependent on the initial attachment of cells to the substrate, and that this is directly related to the ability of cells to interact with the protein layer absorbed on the implant surface. In 2008, Laflamme and Rouabhia[28] showed that BMP-2 and -7 coatings promote osteoblast attachment to collagen scaffolds, and postulated that this was due to the substrate mimicking the *in vivo* physiological conditions of the ECM more precisely than uncoated controls. We suggest that Fn-pre-adsorbed HA resembles the adhesion protein component of the fibroblasts' native ECM more closely, enabling them to become attached more quickly and more efficiently than uncoated controls.

In conclusion, we propose that Fn-coated HA implants may improve dermal tissue attachment to an ITAP. An adsorption technique that applies Fn to HA-coated implants at the time of surgery may be enough to achieve this without the need for prolonged preparation, which might limit the application of these coatings. Further work is under way to determine whether increased concentrations of Fn result in further upregulation of dermal fibroblast attachment, and whether these coatings elicit a similar effect on dermal tissue attachment around an ITAP *in vivo*.

Supplementary material

ĕ   Box plots showing the number of vinculin markers per cell and cell area for the polished (Pol), hydroxyapatite (HA) and HA-fibronectin (HAFn) substrates at a) one hour, b) four hours and c) 24 hours are available with the electronic version of this article on our website www.jbjs.boneandjoint.org.uk

References

1. **Sullivan J, Uden M, Robinson KP, Sooriakumaran S.** Rehabilitation of the transfemoral amputee with an osseointegrated prosthesis: the United Kingdom experience. *Prosthet Orthot Int* 2003;27:114–120.
2. **Brånemark R, Brånemark PI, Rydevik B, Myers RR.** Osseointegration in skeletal reconstruction and rehabilitation: a review. *J Rehabil Res Dev* 2001;38:175–181.
3. **Ysander M, Brånemark R, Olmarker K, Myers RR.** Intramedullary osseointegration: development of a rodent model and study of histology and neuropeptide changes around titanium implants. *J Rehab Res Dev* 2001;38:183–190.
4. **Pendegrass CJ, Goodship AE, Blunn GW.** Development of a soft tissue seal around bone-anchored transcutaneous amputation prostheses. *Biomaterials* 2006;27:4183–4191.
5. **Pendegrass CJ, Gordon D, Middleton CA, Sun SN, Blunn GW.** Sealing the skin barrier around transcutaneous implants: in vitro study of keratinocyte proliferation and adhesion in response to surface modifications of titanium alloy. *J Bone Joint Surg [Br]* 2008;90-B:114–121.
6. **Pendegrass CJ, Goodship AE, Price JS, Blunn GW.** Nature's answer to breaching the skin barrier: an innovative development for amputees. *J Anat* 2006;209:59–67.
7. **Kang NV, Pendegrass C, Marks L, Blunn G.** Osseocutaneous integration of an intraosseous transcutaneous amputation prosthesis implant used for reconstruction of a transhumeral amputee: case report. *J Hand Surg Am* 2010;35:1130–1134.
8. **Middleton CA, Pendegrass CJ, Gordon D, Jacob J, Blunn GW.** Fibronectin silanized titanium alloy: a bioinductive and durable coating to enhance fibroblast attachment in vitro. *J Biomed Mater Res A* 2007;83:1032–1038.
9. **Pendegrass CJ, Middleton CA, Blunn GW.** Fibronectin functionalized hydroxyapatite coatings: improving dermal fibroblast adhesion in vitro and in vivo. *Adv Eng Mater* 2010;12:365–373.
10. **Clarke RA, An JQ, Greiling D, Khan A, Schwarzbauer JE.** Fibroblast migration on fibronectin requires three distinct functional domains. *J Invest Dermatol* 2003;121:695–705.
11. **Cannas M, Denicolai F, Webb LX, Gristina AG.** Bioplant surfaces: binding of fibronectin and fibroblast adhesion. *J Orthop Res* 1988;6:58–62.

12. **Gallant ND, Michael KE, García AJ.** Cell adhesion strengthening: contributions of adhesive area, integrin binding, and focal adhesion assembly. *Mol Biol Cell* 2005;16:4329–4340.

13. **Räisänen L, Könönen M, Juhanoja J, et al.** Expression of cell adhesion complexes in epithelial cells seeded on biomaterial surfaces. *J Biomed Mater Res* 2000;49:79–87.

14. **Pendegrass CJ, Middleton CA, Gordon D, Jacob J, Blunn GW.** Measuring the strength of dermal fibroblast attachment to functionalized titanium alloys in vitro. *J Biomed Mat Res A* 2010;92:1028–1037.

15. **Kay MI, Young RA, Posner AS.** Crystal structure of hydroxyapatite. *Nature* 1964;204:1050–1052.

16. **Cook SD, Thomas KA, Kay JF, Jarcho M.** Hydroxyapatite-coated porous titanium for use as an orthopaedic biological attachment system. *Clin Orthop* 1998;230:303–312.

17. **Gorbunoff MJ, Timasheff SN.** The interaction of proteins with hydroxyapatite: III: mechanism. *Anal Biochem* 1984;136:440–445.

18. **Sharma CP, Paul W.** Protein interaction with tantalum: changes with oxide layer and hydroxyapatite at the interface. *J Biomed Mater Res* 1992;26:1179–1184.

19. **Dong X, Wang Q, Wu T, Pan H.** Understanding adsorption-desorption dynamics of BMP-2 on hydroxyapatite (001) surface. *Biophys J* 2007;93:750–759.

20. **Shen JW, Wu T, Wang Q, Pan HH.** Molecular simulation of protein adsorption and desorption in HA surfaces. *Biomaterials* 2008;29:513–532.

21. **Petit V, Thiery JP.** Focal adhesions: structure and dynamics. *Biol Cell* 2000;92:477–494.

22. **Sastry SK, Burridge K.** Focal adhesions: a nexus for intracellular signaling and cytoskeletal dynamics. *Exp Cell Res* 2000;261:25–36.

23. **El Ghannam A, Starr L, Jones J.** Laminin-5 coating enhances epithelial cell attachment, spreading, and hemidesmosome assembly on Ti-6A1-4V implant material in vitro. *J Biomed Mater Res* 1998;41:30–40.

24. **Rock MJ, Holden P, Horton WA, Cohn DH.** Cartilage oligomeric matrix protein promotes cell attachment via two independent mechanisms involving CD47 and alphaVbeta3 integrin. *Mol Cell Biochem* 2010;338:215–224.

25. **Hudson AE, Carmean N, Bassuk JA.** Extracellular matrix protein coatings for facilitation of urothelial cell attachment. *Tissue Eng* 2007;13:2219–2225.

26. **Gordon DJ, Bhagawati DD, Pendegrass CJ, Middleton CA, Blunn GW.** Modification of titanium alloy surfaces for percutaneous implants by covalently attaching laminin. *J Biomed Mater Res A* 2010;94:586–593.

27. **Sousa SR, Lamghari M, Sampaio P, Moradas-Ferreira P, Barbosa MA.** Osteoblast adhesion and morphology on TiO2 depends on the competitive preadsorption of albumin and fibronectin. *J Biomed Mater Res A* 2008;84:281–290.

28. **Laflamme C, Rouabhia M.** Effect of BMP-2 and BMP-7 homodimers and a mixture of BMP-2/BMP-7 homodimers on osteoblast adhesion and growth following culture on a collagen scaffold. *Biomed Mater* 2008;3:1–10.

UCL INSTITUTE OF ORTHOPAEDICS & MUSCULOSKELETAL SCIENCE

≜UCL

Coating Proteins Silanized to Titanium Alloy: A Durable Substance enhancing Fibroblast Growth and Adhesion

*El-Husseiny M M, *Pendegrass, C J; Haddad, F S; *Blunn, G W
*Centre for Biomedical Engineering, Institute of Orthopaedics & Musculoskeletal Science, University College London, Stanmore, UK

INTRODUCTION

Intraosseous transcutaneous amputation prostheses (ITAP) provide an alternative means of attaching artificial limbs for amputees [1]. Conventional stump-socket devices are associated with soft tissue complications including; pressure sores and tissue necrosis [2].

ITAP resolves these problems by attaching the exo-prosthesis transcutaneously to the skeleton. Other transcutaneous amputation prosthetics are limited by infection [3,4], however ITAP aims to overcome this by creating an infection-resistant transcutaneous seal.

Previous work has demonstrated that early dermal attachment prevents epithelial downgrowth and infection [5], hence the aim of this study is to increase the attachment of dermal fibroblasts to titanium alloy *in vitro*. Fibronectin (Fn) and laminin 332 (Ln) enhance early cell growth and adhesion [6,7].

Covalent bonding of those proteins to titanium alloy (Ti) through silanization has shown to improve cell attachment [7].

We hypothesize that silanized dual coatings of fibronectin and laminin (SiFnLn) will be more durable when compared with adsorbed dual coating (AdFnLn), and will enhance early fibroblast growth and adhesion compared to single coatings (AdFn, AdLn, SiFn, SiLn).

METHODS

The kinetics of dual single and dual protein coating attachment onto titanium alloy (Al 6%, V 4%) was quantified on silanized 10mm diameter discs using radiolabelled Fn (125I-Fn) and Ln (125I-Ln).

Sixty discs were polished, sterilized and silanized with 636.62 ng/cm^2 of 125I-Fn, 125I-Ln, 125I-Fn+Ln or 125I-Ln+Fn (n=3). Coating durability was assessed when soaked in fetal calf serum (FCS) for 0, 1, 24, 48 and 72hrs.

Data was compared to un-silanized Ti discs with the same coatings. Five thousand human dermal fibroblasts were seeded on discs (n=6) of Ti polished alone (Pol), Ti with adsorbed fibronectin (AdFn), Ti with adsorbed laminin (AdLn), Ti adsorbed dual coating (AdFnLn), Ti silanized (Si), Ti silanized with fibronectin (SiFn), Ti silanized with laminin (SiLn), Ti silanized with a dual coating (SiFnLn) for 24hrs.

Cells were fixed, vinculin stained using mouse vinculin antibody (1:200) for 2hrs and alexa fluor (1:100) for 1hr. Axiovision Image Analysis software was used to measure cell area, vinculin markers per cell and per unit cell area.

Data was analysed in SPSS and significance was assumed at the 0.05 level. The data presented are median values with 95% confidence intervals.

RESULTS

Silanized dual coatings bonded to Ti alloy in significantly larger quantities compared with adsorbed coatings at all time points (Table 1) (all p values < 0.05).

	Silanized discs				Adsorbed discs			
	125I-Fn	125I-Ln	*125I-Fn+Ln	+125I-Ln+Fn	125I-Fn	125I-Ln	*125I-Fn+Ln	+125I-Ln+Fn
0 hr	23.52	36.63	24.71	37.34	4.08	14.45	5.22	11.43
1 hr	23.48	36.46	24.69	37.40	3.80	14.27	5.20	11.43
24 hrs	20.60	32.72	20.97	31.47	0.169	8.75	2.56	7.54
48 hrs	17.71	28.76	18.29	28.26	0.15	7.61	2.47	7.09
72 hrs	17.44	28.04	18.26	28.07	0.06	7.24	2.44	6.89

Table 1. Median amount of protein attached to Ti (ng/cm^2) over time * Dual coating proteins in which Fn was radioactively labelled and measured. + Dual coating proteins in which Ln was radioactively labelled and measured.

Fibroblasts cultured on dual coatings were significantly larger, produced more vinculin markers per cell, and per unit cell area compared with single coatings (Table 2 and Figures 1 & 2). Cells on SiFnLn were larger with more numerous vinculin markers per cell, and per unit cell area compared with AdFnLn (p<0.05).

	Silanized discs				Adsorbed discs			
	Si	SiFn	SiLn	SiFnLn	Pol	AdFn	AdLn	AdFnLn
Cell area	955.2	1999.9	1824.0	2477.9	676.1	1756.9	1609.7	2206.2
Vinculin /Cell	15	136	104	220	6	93	85	154

Table 2. Median cell area and vinculin markers/cell unit at 24 hours
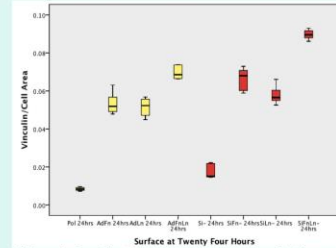
Figure 1. Box Plot showing vinculin markers/cell area at 24 hours

a. Pol Surface   b. AdFn Surface   e. Si Surface   f. SiFn Surface

c. AdLa Surface   d. AdLnFn Surface   g. SiLn Surface   h. SiFnLn Surface
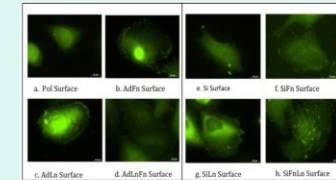
Figure 2. Fibroblasts cultured at 24 hrs

CONCLUSIONS

This study has demonstrated that covalently bonding both fibronectin and laminin to Ti alloy provides a durable dual coating that enhances early fibroblast growth and attachment compared with either protein coating alone *in vitro*. Our study showed that there is non-competitive binding of laminin on Ti surfaces in the presence of fibronectin. Dual coatings may be applied to the skin-penetrating region of transcutaneous devices to improve the skin seal and this may have positive implications for the development of ITAP.

REFERENCES
1. Branemark R. J Rehabil Res Dev 2001; 38; 175-181. 2. Sullivan J. Prosthet Orthot Int 2003; 27: 114-120. 3. Holgers KM. J Invest Surg 1989;2:7–16. 4. Branemark PI. Scand J Plast Reconstr Surg 1982; 16:17–21. 5. Pendegrass CJ. J Biomed Mater Res A 2010;92:1028–1037. 6. Cooke CA. Invest Ophthal- mol Vis Sci 2006;47:2985–2989. 7. Gordon DJ. J Biomed Mater Res Part A: 2010. (Article in Press)

UCL INSTITUTE OF ORTHOPAEDICS & MUSCULOSKELETAL SCIENCE

≜UCL

Sealing the Transcutaneous Skin-Implant Interface by Dual Coating Proteins Chemically Bonded to Titanium Alloy

*El-Husseiny M M, *Pendegrass, C J; Haddad, F S; *Blunn, G W
*Centre for Biomedical Engineering, Institute of Orthopaedics & Musculoskeletal Science, University College London, Stanmore, UK

INTRODUCTION

Following amputation residual stumps used to attach the external prostheses can be associated with sores, infection and skin necrosis. These problems could be overcome by off loading the soft tissues. Intraosseous transcutaneous amputation prostheses (ITAP) attached the external implant directly to the residual bone reducing these complications [1].

However, a tight seal at the skin implant interface is crucial in preventing epithelial down-growth and infection [2]. Fibronectin (Fn) and laminin 332 (Ln), extra-cellular glycoproteins, enhance early cell growth and adhesion of keratinocytes [3,4].

Silanization to titanium alloy (Ti) allows these proteins to bond to the metal directly and has shown to improve cell attachment [2].

We hypothesize that silanized dual coatings of fibronectin and laminin (SiFnLn) will be more durable than absorbed proteins and that keratinocyte adhesion will be increase compared with silanized Ti controls and single silanized proteins.

METHODS

10 mm diameter Ti alloy (Al 6%, V 4%) discs were polished, sterilized and silanized by immersing in 10% aminopropyltriethoxysilane followed by 1% glutaraldehyde for 2 hrs.

The kinetics of silanized single and dual protein coating attachment onto titanium alloy (Al 6%, V 4%) was quantified using radiolabelled Fn (125I-Fn) and Ln (125I-Ln). Sixty discs were silanized with 636.62 ng/cm² of 125I-Fn, 125I-Ln, 125I-Fn+Ln or 125I-Ln+Fn (n=3).Coating durability was assessed when soaked in fetal calf serum (FCS) for 0, 1, 24, 48 and 72hrs. Data was compared to un-silanized Ti discs with the same amount of adsorbed proteins.

In order to study cell attachment twenty thousand human keratinocytes were seeded on the discs (n=6): silanized (Si), silanized fibronectin (SiFn), silanized laminin (SiLn), silanized dual coating (SiFnLn) for 1, 4 and 24hrs. All protein concentrations were the same as used for assessing the kinetics of protein adhesion. Cells were fixed, vinculin stained using mouse vinculin antibody (1:200) for 2hrs and alexa fluor (1:100) for 1hr.

Axiovision Image Analysis software was used to measure cell area, vinculin markers per cell unit and per unit cell area on 15 cells per disc. Data was analysed in SPSS and significance was assumed at the 0.05 level. The data presented are median values with 95% confidence intervals.

RESULTS

Silanized dual coatings bonded to Ti alloy in significantly larger quantities compared with adsorbed coatings (Table 1) (all p values < 0.05). When proteins were combined on silanized discs the same amount of each protein was attached as when used as a single coating (i.e. non competitive binding). Retention of silanized proteins after incubation in serum was significantly greater than absorbed proteins at all time points.

	Silanized discs				Adsorbed discs			
	125I-Fn	125I-Ln	*125I-Fn+Ln	+125I-Ln+Fn	125I-Fn	125I-Ln	*125I-Fn+Ln	+125I-Ln+Fn
0 hr	23.52	36.63	24.71	37.34	4.08	14.45	5.22	11.43
1 hr	23.48	36.46	24.69	37.40	3.80	14.27	5.20	11.43
24 hrs	20.60	32.72	20.97	31.47	0.169	8.75	2.56	7.54
48 hrs	17.71	28.76	18.29	28.26	0.15	7.61	2.47	7.09
72 hrs	17.44	28.04	18.26	28.07	0.06	7.24	2.44	6.89

Table 1. Median amount of protein attached to Ti (ng/cm²) over time * Dual coating proteins in which Fn was radioactively labelled and measured. + Dual coating proteins in which Ln was radioactively labelled and measured.

Keratinocytes cultured on silanized dual coatings were significantly larger, produced more vinculin markers per unit cell area and per cell area compared with single coatings at all time points (Table 2, Figures 1 &2).

		Si	SiFn	SiLn	SiFnLn
Cell area	1 hour	287.4	585.9	471.2	821.1
	4 hours	412.9	988.7	867.4	1195.3
	24 hours	821.3	1260.2	1186.0	1467.8
Vinc/ cell unit	1 hour	1	7.5	11.5	40
	4 hours	1	25.5	31.5	62
	24 hours	5.5	54	60.5	108

Table 2. Median cell area and vinculin/cell unit at 1, 4 and 24 hours
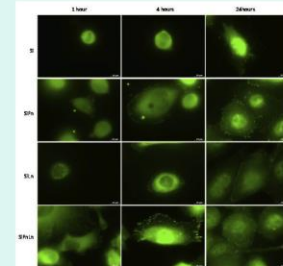
Figure 1. Keratinocytes cultured at 1,4 and 24 hrs on single and dual coating protein surfaces stained for focal adhesion plaques with anti- vinculin
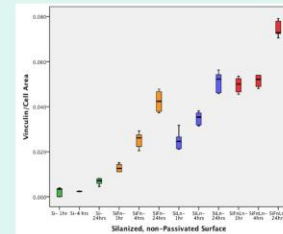
Figure 2. Box Plot showing vinculin markers/ cell area at 1, 4 and 24 hours

CONCLUSIONS

This study has demonstrated that silanized dual coating proteins on Ti alloy enhances early keratinocyte growth and attachment compared with single coating in vitro. It also shows that there is non-competitive binding of laminin to Ti alloys in presence of fibronectin. This may lead to improved epidermal attachment to ITAP creating a tight seal at the implant interface, which will prevent migration of the epithelium and subsequent infection in vivo.

REFERENCES
1. Pendegrass CJ. Biomaterials 2006;27:4183-4191. 2. Pendegrass CJ. J Biomed Mater Res A 2010;92:1028–1037. 3. Cooke CA. Invest Ophthal- mol Vis Sci 2006;47:2985–2989. 4. Gordon DJ. J Biomed Mater Res Part A: 2010. (Article in Press)

REFERENCE LIST

Adell R, Eriksson B, Lekholm U, Branemark PI, Jemt T. Long-term follow-up study of osseointegrated implants in the treatment of totally edentulous jaws. Int J Oral Maxillofac Implants1990 Winter;5(4):347-59.

Auernheimer J, Zukowski D, Dahmen C, Kantlehner M, Enderle A, Goodman SL, et al. Titanium implant materials with improved biocompatibility through coating with phosphonate-anchored cyclic RGD peptides. Chembiochem2005 Nov;6(11):2034-40.

Baharloo B, Textor M, Brunette DM. Substratum roughness alters the growth, area, and focal adhesions of epithelial cells, and their proximity to titanium surfaces. J Biomed Mater Res A2005 Jul 1;74(1):12-22.

Barber TA, Golledge SL, Castner DG, Healy KE. Peptide-modified p(AAm-co-EG/AAc) IPNs grafted to bulk titanium modulate osteoblast behavior in vitro. J Biomed Mater Res A2003 Jan 1;64(1):38-47.

Bearinger JP, Castner DG, Healy KE. Biomolecular modification of p(AAm-co-EG/AA) IPNs supports osteoblast adhesion and phenotypic expression. J Biomater Sci Polym Ed1998;9(7):629-52.

Beck K, Hunter I, Engel J. Structure and function of laminin: anatomy of a multidomain glycoprotein. FASEB J1990 Feb 1;4(2):148-60.

Berens ME, Rief MD, Loo MA, Giese A. The role of extracellular matrix in human astrocytoma migration and proliferation studied in a microliter scale assay. Clin Exp Metastasis1994 Nov;12(6):405-15.

Borradori L, Sonnenberg A. Structure and function of hemidesmosomes: more than simple adhesion complexes. J Invest Dermatol1999 Apr;112(4):411-8.

Branemark PI, Adell R, Breine U, Hansson BO, Lindstrom J, Ohlsson A. Intra-osseous anchorage of dental prostheses. I. Experimental studies. Scand J Plast Reconstr Surg1969;3(2):81-100.

Branemark PI, Hansson BO, Adell R, Breine U, Lindstrom J, Hallen O, et al. Osseointegrated implants in the treatment of the edentulous jaw. Experience from a 10-year period. Scand J Plast Reconstr Surg Suppl1977;16:1-132.

Branemark PI, Lindstrom J, Hallen O, Breine U, Jeppson PH, Ohman A. Reconstruction of the defective mandible. Scand J Plast Reconstr Surg1975;9(2):116-28.

Branemark PI. Osseointegration and its experimental background. J Prosthet Dent1983 Sep;50(3):399-410.

Branemark R, Branemark PI, Rydevik B, Myers RR. Osseointegration in skeletal reconstruction and rehabilitation: a review. J Rehabil Res Dev2001 Mar-Apr;38(2):175-81.

Buser D, Schenk RK, Steinemann S, Fiorellini JP, Fox CH, Stich H. Influence of surface characteristics on bone integration of titanium implants. A histomorphometric study in miniature pigs. J Biomed Mater Res1991 Jul;25(7):889-902.

Bush KA, Downing BR, Walsh SE, Pins GD. Conjugation of extracellular matrix proteins to basal lamina analogs enhances keratinocyte attachment. J Biomed Mater Res A2007 Feb;80(2):444-52.

Canale ST, Beaty JH, eds: Campbell's Operative Orthopaedics, 11th ed,Chapter 11, 2007, Mosby.

Cavalcanti-Adam EA, Shapiro IM, Composto RJ, Macarak EJ, Adams CS. RGD peptides immobilized on a mechanically deformable surface promote osteoblast differentiation. J Bone Miner Res2002 Dec;17(12):2130-40.

Chou TG, Petti CA, Szakacs J, Bloebaum RD. Evaluating antimicrobials and implant materials for infection prevention around transcutaneous osseointegrated implants in a rabbit model. J Biomed Mater Res A Mar 1;92(3):942-52.

Cook SD, Thomas KA, Kay JF, Jarcho M. Hydroxyapatite-coated porous titanium for use as an orthopedic biologic attachment system. Clin Orthop Relat Res1988 May(230):303-12.

Coughlin MJ, Mann RA, eds: Surgery of the foot and ankle, 8th ed, vol 2, St Louis, 2006, Mosby:1370.

De Giglio E, Sabbatini L, Colucci S, Zambonin G. Synthesis, analytical characterization, and osteoblast adhesion properties on RGD-grafted polypyrrole coatings on titanium substrates. J Biomater Sci Polym Ed2000;11(10):1073-83.

Dean JW, 3rd, Culbertson KC, D'Angelo AM. Fibronectin and laminin enhance gingival cell attachment to dental implant surfaces in vitro. Int J Oral Maxillofac Implants1995 Nov-Dec;10(6):721-8.

Dong X, Wang Q, Wu T, Pan H. Understanding adsorption-desorption dynamics of BMP-2 on hydroxyapatite (001) surface. Biophys J2007 Aug 1;93(3):750-9.

El-Ghannam A, Starr L, Jones J. Laminin-5 coating enhances epithelial cell attachment, spreading, and hemidesmosome assembly on Ti-6A1-4V implant material in vitro. J Biomed Mater Res1998 Jul;41(1):30-40.

Elmengaard B, Bechtold JE, Soballe K. In vivo study of the effect of RGD treatment on bone ongrowth on press-fit titanium alloy implants. Biomaterials2005 Jun;26(17):3521-6.

Erickson HP. Stretching fibronectin. J Muscle Res Cell Motil2002;23(5-6):575-80.

Esposito M, Hirsch JM, Lekholm U, Thomsen P. Biological factors contributing to failures of osseointegrated oral implants. (I). Success criteria and epidemiology. Eur J Oral Sci1998 Feb;106(1):527-51.

Ezzell RM, Goldmann WH, Wang N, Parashurama N, Ingber DE. Vinculin promotes cell spreading by mechanically coupling integrins to the cytoskeleton. Exp Cell Res1997 Feb 25;231(1):14-26.

Ferris DM, Moodie GD, Dimond PM, Gioranni CW, Ehrlich MG, Valentini RF. RGD-coated titanium implants stimulate increased bone formation in vivo. Biomaterials1999 Dec;20(23-24):2323-31.

Fleischmajer R, Utani A, MacDonald ED, Perlish JS, Pan TC, Chu ML, et al. Initiation of skin basement membrane formation at the epidermo-dermal interface involves assembly of laminins through binding to cell membrane receptors. J Cell Sci1998 Jul 30;111 (Pt 14):1929-40.

Fox K, Tran PA, Tran N. Recent advances in research applications of nanophase hydroxyapatite. Chemphyschem Jul 16;13(10):2495-506.

Gallant ND, Michael KE, Garcia AJ. Cell adhesion strengthening: contributions of adhesive area, integrin binding, and focal adhesion assembly. Mol Biol Cell2005 Sep;16(9):4329-40.

Garcia-Nieto S, Johal RK, Shakesheff KM, Emara M, Royer PJ, Chau DY, et al. Laminin and fibronectin treatment leads to generation of dendritic cells with superior endocytic capacity. PLoS One;5(4):e10123.

Goldmann WH. Phosphorylation of filamin (ABP-280) regulates the binding to the lipid membrane, integrin, and actin. Cell Biol Int2001;25(8):805-8.

Gordon DJ, Bhagawati DD, Pendegrass CJ, Middleton CA, Blunn GW. Modification of titanium alloy surfaces for percutaneous implants by covalently attaching laminin. J Biomed Mater Res A Aug;94(2):586-93.

Gordon DJ, Bhagawati DD, Pendegrass CJ, Middleton CA, Blunn GW. Modification of titanium alloy surfaces for percutaneous implants by covalently attaching laminin. J Biomed Mater Res A2010 Aug;94(2):586-93.

Groll J, Fiedler J, Engelhard E, Ameringer T, Tugulu S, Klok HA, et al. A novel star PEG-derived surface coating for specific cell adhesion. J Biomed Mater Res A2005 Sep 15;74(4):607-17.

Grzesik WJ, Robey PG. Bone matrix RGD glycoproteins: immunolocalization and interaction with human primary osteoblastic bone cells in vitro. J Bone Miner Res1994 Apr;9(4):487-96.

Halling PJ, Dunnill P. Improved nonporous magnetic supports for immobilized enzymes. Biotechnol Bioeng1979 Mar;21(3):393-416.

Heaney TG, Doherty PJ, Williams DF. Marsupialization of percutaneous implants in presence of deep connective tissue. J Biomed Mater Res1996 Dec;32(4):593-601.

Hirosaki T, Mizushima H, Tsubota Y, Moriyama K, Miyazaki K. Structural requirement of carboxyl-terminal globular domains of laminin alpha 3 chain for promotion of rapid cell adhesion and migration by laminin-5. J Biol Chem2000 Jul 21;275(29):22495-502.

Hodivala KJ, Watt FM. Evidence that cadherins play a role in the downregulation of integrin expression that occurs during keratinocyte terminal differentiation. J Cell Biol1994 Feb;124(4):589-600.

Huang CJ, Tseng PY, Chang YC. Effects of extracellular matrix protein functionalized fluid membrane on cell adhesion and matrix remodeling. Biomaterials Sep;31(27):7183-95.

Huang H, Zhao Y, Liu Z, Zhang Y, Zhang H, Fu T, et al. Enhanced osteoblast functions on RGD immobilized surface. J Oral Implantol2003;29(2):73-9.

Hunter A, Archer CW, Walker PS, Blunn GW. Attachment and proliferation of osteoblasts and fibroblasts on biomaterials for orthopaedic use. Biomaterials1995 Mar;16(4):287-95.

Ito Y, Kajihara M, Imanishi Y. Materials for enhancing cell adhesion by immobilization of cell-adhesive peptide. J Biomed Mater Res1991 Nov;25(11):1325-37.

Johansson S, Kjellen L, Hook M, Timpl R. Substrate adhesion of rat hepatocytes: a comparison of laminin and fibronectin as attachment proteins. J Cell Biol1981 Jul;90(1):260-4.

Jones JC, Hopkinson SB, Goldfinger LE. Structure and assembly of hemidesmosomes. Bioessays1998 Jun;20(6):488-94.

Kang NV, Pendegrass C, Marks L, Blunn G. Osseocutaneous integration of an intraosseous transcutaneous amputation prosthesis implant used for reconstruction of a transhumeral amputee: case report. J Hand Surg Am Jul;35(7):1130-4.

Kantlehner M, Schaffner P, Finsinger D, Meyer J, Jonczyk A, Diefenbach B, et al. Surface coating with cyclic RGD peptides stimulates osteoblast adhesion and proliferation as well as bone formation. Chembiochem2000 Aug 18;1(2):107-14.

Karecla PI, Timpl R, Watt FM. Adhesion of human epidermal keratinocytes to laminin. Cell Adhes Commun1994 Aug;2(4):309-18.

Kariya Y, Tsubota Y, Hirosaki T, Mizushima H, Puzon-McLaughlin W, Takada Y, et al. Differential regulation of cellular adhesion and migration by recombinant laminin-5 forms with partial deletion or mutation within the G3 domain of alpha3 chain. J Cell Biochem2003 Feb 15;88(3):506-20.

Kleinman HK, Weeks BS. Laminin: structure, functions and receptors. Curr Opin Cell Biol1989 Oct;1(5):964-7.

Koshikawa N, Moriyama K, Takamura H, Mizushima H, Nagashima Y, Yanoma S, et al. Overexpression of laminin gamma2 chain monomer in invading gastric carcinoma cells. Cancer Res1999 Nov 1;59(21):5596-601.

Koster J, Geerts D, Favre B, Borradori L, Sonnenberg A. Analysis of the interactions between BP180, BP230, plectin and the integrin alpha6beta4 important for hemidesmosome assembly. J Cell Sci2003 Jan 15;116(Pt 2):387-99.

Laflamme C, Rouabhia M. Effect of BMP-2 and BMP-7 homodimers and a mixture of BMP-2/BMP-7 homodimers on osteoblast adhesion and growth following culture on a collagen scaffold. Biomed Mater2008 Mar;3(1):015008.

Laurie GW, Bing JT, Kleinman HK, Hassell JR, Aumailley M, Martin GR, et al. Localization of binding sites for laminin, heparan sulfate proteoglycan and fibronectin on basement membrane (type IV) collagen. J Mol Biol1986 May 5;189(1):205-16.

LeBaron RG, Athanasiou KA. Extracellular matrix cell adhesion peptides: functional applications in orthopedic materials. Tissue Eng2000 Apr;6(2):85-103.

Lee SW, Kim SY, Rhyu IC, Chung WY, Leesungbok R, Lee KW. Influence of microgroove dimension on cell behavior of human gingival fibroblasts cultured on titanium substrata. Clin Oral Implants Res2009 Jan;20(1):56-66.

Lozano E, Cano A. Cadherin/catenin complexes in murine epidermal keratinocytes: E-cadherin complexes containing either beta-catenin or plakoglobin contribute to stable cell-cell contacts. Cell Adhes Commun1998 Jun;6(1):51-67.

Lundborg G, Branemark PI, Rosen B. Osseointegrated thumb prostheses: a concept for fixation of digit prosthetic devices. J Hand Surg Am1996 Mar;21(2):216-21.

Lundborg G, Waites A, Bjorkman A, Rosen B, Larsson EM. Functional magnetic resonance imaging shows cortical activation on sensory stimulation of an osseointegrated prosthetic thumb. Scand J Plast Reconstr Surg Hand Surg2006;40(4):234-9.

Magnusson MK, Mosher DF. Fibronectin: structure, assembly, and cardiovascular implications. Arterioscler Thromb Vasc Biol1998 Sep;18(9):1363-70.

Mainiero F, Pepe A, Wary KK, Spinardi L, Mohammadi M, Schlessinger J, et al. Signal transduction by the alpha 6 beta 4 integrin: distinct beta 4 subunit sites mediate recruitment of Shc/Grb2 and association with the cytoskeleton of hemidesmosomes. EMBO J1995 Sep 15;14(18):4470-81.

Mao Y, Schwarzbauer JE. Stimulatory effects of a three-dimensional microenvironment on cell-mediated fibronectin fibrillogenesis. J Cell Sci2005 Oct 1;118(Pt 19):4427-36.

Marieb E. Human anatomy and Physiology. 2nd ed, Benjamin-Cummings Publishing,1991:113.

Marshall DL. ATP regeneration using immobilized carbamyl phosphokinase. Biotechnol Bioeng1973 May;15(3):447-53.

Maschler S, Wirl G, Spring H, Bredow DV, Sordat I, Beug H, et al. Tumor cell invasiveness correlates with changes in integrin expression and localization. Oncogene2005 Mar 17;24(12):2032-41.

Massia SP, Hubbell JA. Covalent surface immobilization of Arg-Gly-Asp- and Tyr-Ile-Gly-Ser-Arg-containing peptides to obtain well-defined cell-adhesive substrates. Anal Biochem1990 Jun;187(2):292-301.

Middleton CA, Pendegrass CJ, Gordon D, Jacob J, Blunn GW. Fibronectin silanized titanium alloy: a bioinductive and durable coating to enhance fibroblast attachment in vitro. J Biomed Mater Res A2007 Dec 15;83(4):1032-8.

Miller LA, Lipschutz RD, Stubblefield KA, Lock BA, Huang H, Williams TW, 3rd, et al. Control of a six degree of freedom prosthetic arm after targeted muscle reinnervation surgery. Arch Phys Med Rehabil2008 Nov;89(11):2057-65.

Miyamoto S, Akiyama SK, Yamada KM. Synergistic roles for receptor occupancy and aggregation in integrin transmembrane function. Science1995 Feb 10;267(5199):883-5.

Morra M. Biochemical modification of titanium surfaces: peptides and ECM proteins. Eur Cell Mater2006;12:1-15.

Moxey PW, Hofman D, Hinchliffe RJ, Jones K, Thompson MM, Holt PJ. Epidemiological study of lower limb amputation in England between 2003 and 2008. Br J Surg Sep;97(9):1348-53.

Nakashima Y, Kariya Y, Yasuda C, Miyazaki K. Regulation of cell adhesion and type VII collagen binding by the beta3 chain short arm of laminin-5: effect of its proteolytic cleavage. J Biochem2005 Nov;138(5):539-52.

Nanci A, Wuest JD, Peru L, Brunet P, Sharma V, Zalzal S, et al. Chemical modification of titanium surfaces for covalent attachment of biological molecules. J Biomed Mater Res1998 May;40(2):324-35.

Nguyen BP, Gil SG, Carter WG. Deposition of laminin 5 by keratinocytes regulates integrin adhesion and signaling. J Biol Chem2000 Oct 13;275(41):31896-907.

Nikolopoulos SN, Blaikie P, Yoshioka T, Guo W, Puri C, Tacchetti C, et al. Targeted deletion of the integrin beta4 signaling domain suppresses laminin-5-dependent nuclear entry of mitogen-activated protein kinases and NF-kappaB, causing defects in epidermal growth and migration. Mol Cell Biol2005 Jul;25(14):6090-102.

Ogawa T, Tsubota Y, Maeda M, Kariya Y, Miyazaki K. Regulation of biological activity of laminin-5 by proteolytic processing of gamma2 chain. J Cell Biochem2004 Jul 1;92(4):701-14.

Ohji M, Mandarino L, SundarRaj N, Thoft RA. Corneal epithelial cell attachment with endogenous laminin and fibronectin. Invest Ophthalmol Vis Sci1993 Jul;34(8):2487-92.

Pallu S, Bourget C, Bareille R, Labrugere C, Dard M, Sewing A, et al. The effect of cyclo-DfKRG peptide immobilization on titanium on the adhesion and differentiation of human osteoprogenitor cells. Biomaterials2005 Dec;26(34):6932-40.

Pendegrass CJ, El-Husseiny M, Blunn GW. The development of fibronectin-functionalised hydroxyapatite coatings to improve dermal fibroblast attachment in vitro. J Bone Joint Surg Br Apr;94(4):564-9.

Pendegrass CJ, Goodship AE, Blunn GW. Development of a soft tissue seal around bone-anchored transcutaneous amputation prostheses. Biomaterials2006 Aug;27(23):4183-91.

Pendegrass CJ, Goodship AE, Price JS, Blunn GW. Nature's answer to breaching the skin barrier: an innovative development for amputees. J Anat2006 Jul;209(1):59-67.

Pendegrass CJ, Gordon D, Middleton CA, Sun SN, Blunn GW. Sealing the skin barrier around transcutaneous implants: in vitro study of keratinocyte proliferation and adhesion in response to surface modifications of titanium alloy. J Bone Joint Surg Br2008 Jan;90(1):114-21.

Pendegrass CJ, Middleton CA, Gordon D, Jacob J, Blunn GW. Measuring the strength of dermal fibroblast attachment to functionalized titanium alloys in vitro. J Biomed Mater Res A Mar 1;92(3):1028-37.

Pendegrass CJ, Middleton CA, Gordon D, Jacob J, Blunn GW. Measuring the strength of dermal fibroblast attachment to functionalized titanium alloys in vitro. J Biomed Mater Res A2010 Mar 1;92(3):1028-37.

Pendegrass CJ, Tucker B, Patel S, Dowling R, Blunn GW. The effect of adherens junction components on keratinocyte adhesion in vitro: potential implications for sealing the skin-implant interface of intraosseous transcutaneous amputation prostheses. J Biomed Mater Res A Dec;100(12):3463-71.

Petit V, Thiery JP. Focal adhesions: structure and dynamics. Biol Cell2000 Oct;92(7):477-94.

Porte-Durrieu MC, Guillemot F, Pallu S, Labrugere C, Brouillaud B, Bareille R, et al. Cyclo-(DfKRG) peptide grafting onto Ti-6Al-4V: physical characterization and interest towards human osteoprogenitor cells adhesion. Biomaterials2004 Aug;25(19):4837-46.

Puleo DA, Nanci A. Understanding and controlling the bone-implant interface. Biomaterials1999 Dec;20(23-24):2311-21.

Puleo DA. Activity of enzyme immobilized on silanized Co-Cr-Mo. J Biomed Mater Res1995 Aug;29(8):951-7.

Raisanen L, Kononen M, Juhanoja J, Varpavaara P, Hautaniemi J, Kivilahti J, et al. Expression of cell adhesion complexes in epithelial cells seeded on biomaterial surfaces. J Biomed Mater Res2000 Jan;49(1):79-87.

Rezania A, Thomas CH, Branger AB, Waters CM, Healy KE. The detachment strength and morphology of bone cells contacting materials modified with a peptide sequence found within bone sialoprotein. J Biomed Mater Res1997 Oct;37(1):9-19.

Rodriguez-Segui SA, Pons Ximenez JI, Sevilla L, Ruiz A, Colpo P, Rossi F, et al. Quantification of protein immobilization on substrates for cellular microarray applications. J Biomed Mater Res A Aug;98(2):245-56.

Rousselle P, Golbik R, van der Rest M, Aumailley M. Structural requirement for cell adhesion to kalinin (laminin-5). J Biol Chem1995 Jun 9;270(23):13766-70.

Sabolich J and Guth T. Below-Knee prosthesis with total flexible socket (T.F.S.): A Preliminary report. Clin Prosth and Orthotics1986; 10(2):93-99.

Sastry SK, Burridge K. Focal adhesions: a nexus for intracellular signaling and cytoskeletal dynamics. Exp Cell Res2000 Nov 25;261(1):25-36.

Scheideler L, Rupp F, Wendel HP, Sathe S, Geis-Gerstorfer J. Photocoupling of fibronectin to titanium surfaces influences keratinocyte adhesion, pellicle formation and thrombogenicity. Dent Mater2007 Apr;23(4):469-78.

Schliephake H, Scharnweber D, Dard M, Rossler S, Sewing A, Meyer J, et al. Effect of RGD peptide coating of titanium implants on periimplant bone formation in the alveolar crest. An experimental pilot study in dogs. Clin Oral Implants Res2002 Jun;13(3):312-9.

Shen JW, Wu T, Wang Q, Pan HH. Molecular simulation of protein adsorption and desorption on hydroxyapatite surfaces. Biomaterials2008 Feb;29(5):513-32.

Sousa SR, Lamghari M, Sampaio P, Moradas-Ferreira P, Barbosa MA. Osteoblast adhesion and morphology on TiO2 depends on the competitive preadsorption of albumin and fibronectin. J Biomed Mater Res A2008 Feb;84(2):281-90.

Stigter M, de Groot K, Layrolle P. Incorporation of tobramycin into biomimetic hydroxyapatite coating on titanium. Biomaterials2002 Oct;23(20):4143-53.

Sullivan J, Uden M, Robinson KP, Sooriakumaran S. Rehabilitation of the trans-femoral amputee with an osseointegrated prosthesis: the United Kingdom experience. Prosthet Orthot Int2003 Aug;27(2):114-20.

Tamura RN, Oda D, Quaranta V, Plopper G, Lambert R, Glaser S, et al. Coating of titanium alloy with soluble laminin-5 promotes cell attachment and hemidesmosome assembly in gingival epithelial cells: potential application to dental implants. J Periodontal Res1997 Apr;32(3):287-94.

Tillander J, Hagberg K, Hagberg L, Branemark R. Osseointegrated titanium implants for limb prostheses attachments: infectious complications. Clin Orthop Relat Res Oct;468(10):2781-8.

Tosatti S, Schwartz Z, Campbell C, Cochran DL, VandeVondele S, Hubbell JA, et al. RGD-containing peptide GCRGYGRGDSPG reduces enhancement of osteoblast differentiation by poly(L-lysine)-graft-poly(ethylene glycol)-coated titanium surfaces. J Biomed Mater Res A2004 Mar 1;68(3):458-72.

Tsuruta D, Hashimoto T, Hamill KJ, Jones JC. Hemidesmosomes and focal contact proteins: functions and cross-talk in keratinocytes, bullous diseases and wound healing. J Dermatol Sci Apr;62(1):1-7.

Ulbrich R, Golbik R, Schellenberger A. Protein adsorption and leakage in carrier-enzyme systems. Biotechnol Bioeng1991 Feb 5;37(3):280-7.

Ulerich JP, Ionescu LC, Chen J, Soboyejo W, Arnold C, editors. Modifications of Ti-6Al-4V surfaces by direct-write laser machining of linear grooves. Proceedings of International society of optics and photonics; 2007.

Van den Dolder J, Bancroft GN, Sikavitsas VI, Spauwen PH, Mikos AG, Jansen JA. Effect of fibronectin- and collagen I-coated titanium fiber mesh on proliferation and differentiation of osteogenic cells. Tissue Eng2003 Jun;9(3):505-15.

Vroman L, Adams AL, Fischer GC, Munoz PC. Interaction of high molecular weight kininogen, factor XII, and fibrinogen in plasma at interfaces. Blood1980 Jan;55(1):156-9.

Walboomers XF, Croes HJ, Ginsel LA, Jansen JA. Contact guidance of rat fibroblasts on various implant materials. J Biomed Mater Res1999 Nov;47(2):204-12.

Weetall HH. Covalent coupling methods for inorganic support materials. Methods Enzymol1976;44:134-48.

Weetall HH. Preparation of immobilized proteins covalently coupled through silane coupling agents to inorganic supports. Appl Biochem Biotechnol1993 Jun;41(3):157-88.

Weiner S, Traub W, Wagner HD. Lamellar bone: structure-function relations. J Struct Biol1999 Jun 30;126(3):241-55.

Winter GD. Transcutaneous implants: reactions of the skin-implant interface. J Biomed Mater Res1974;8(3):99-113.

Xiao SJ, Textor M, Spencer ND, Wieland M, Keller B, Sigrist H. Immobilization of the cell-adhesive peptide Arg-Gly-Asp-Cys (RGDC) on titanium surfaces by covalent chemical attachment. J Mater Sci Mater Med1997 Dec;8(12):867-72.

Ysander M, Branemark R, Olmarker K, Myers RR. Intramedullary osseointegration: development of a rodent model and study of histology and neuropeptide changes around titanium implants. J Rehabil Res Dev2001 Mar-Apr;38(2):183-90.

Ziegler WH, Liddington RC, Critchley DR. The structure and regulation of vinculin. Trends Cell Biol2006 Sep;16(9):453-60.

Ziegler-Graham K, MacKenzie EJ, Ephraim PL, Travison TG, Brookmeyer R. Estimating the prevalence of limb loss in the United States: 2005 to 2050. Arch Phys Med Rehabil2008 Mar;89(3):422-9.

APPENDIX

7.1:Polished surfaces fibroblast cell area descriptives

	Polished Surface			Statistic	Std. Error
Cell Area (micrometres squared)	Pol 1hr	Mean		352.2083	18.44742
		95% Confidence Interval for Mean	Lower Bound	304.7877	
			Upper Bound	399.6289	
		5% Trimmed Mean		353.3315	
		Median		363.5650	
		Variance		2041.844	
		Std. Deviation		45.18677	
		Minimum		288.67	
		Maximum		395.53	
		Range		106.86	
		Interquartile Range		86.76	
		Skewness		-.507	.845
		Kurtosis		-1.884	1.741
	Pol 4hrs	Mean		487.0717	13.10684
		95% Confidence Interval for Mean	Lower Bound	453.3795	
			Upper Bound	520.7639	
		5% Trimmed Mean		487.5363	
		Median		491.1200	
		Variance		1030.735	
		Std. Deviation		32.10507	
		Minimum		440.49	
		Maximum		525.29	
		Range		84.80	
		Interquartile Range		60.85	
		Skewness		-.394	.845
		Kurtosis		-1.089	1.741
	Pol 24hrs	Mean		680.9733	15.59293
		95% Confidence Interval for Mean	Lower Bound	640.8904	

		Interval for Mean	Upper Bound	721.0562	
		5% Trimmed Mean		681.1165	
		Median		676.0800	
		Variance		1458.837	
		Std. Deviation		38.19473	
		Minimum		631.70	
		Maximum		727.67	
		Range		95.97	
		Interquartile Range		71.82	
		Skewness		.067	.845
		Kurtosis		-1.842	1.741
AdFn 1hr		Mean		1221.4433	10.80285
		95% Confidence	Lower Bound	1193.6737	
		Interval for Mean	Upper Bound	1249.2129	
		5% Trimmed Mean		1221.6787	
		Median		1225.3900	
		Variance		700.209	
		Std. Deviation		26.46147	
		Minimum		1186.56	
		Maximum		1252.09	
		Range		65.53	
		Interquartile Range		54.73	
		Skewness		-.336	.845
		Kurtosis		-1.619	1.741
AdFn 4hrs		Mean		1442.1417	24.17230
		95% Confidence	Lower Bound	1380.0048	
		Interval for Mean	Upper Bound	1504.2785	
		5% Trimmed Mean		1441.6330	
		Median		1437.5350	
		Variance		3505.801	
		Std. Deviation		59.20980	
		Minimum		1377.01	

		Maximum	1516.43	
		Range	139.42	
		Interquartile Range	127.95	
		Skewness	.193	.845
		Kurtosis	-1.801	1.741
AdFn 24hrs		Mean	1759.4550	18.80587
	95% Confidence	Lower Bound	1711.1130	
	Interval for Mean	Upper Bound	1807.7970	
		5% Trimmed Mean	1758.7561	
		Median	1756.8750	
		Variance	2121.964	
		Std. Deviation	46.06479	
		Minimum	1698.16	
		Maximum	1833.33	
		Range	135.17	
		Interquartile Range	72.77	
		Skewness	.484	.845
		Kurtosis	.734	1.741
AdLn 1hr		Mean	1069.5200	28.87035
	95% Confidence	Lower Bound	995.3064	
	Interval for Mean	Upper Bound	1143.7336	
		5% Trimmed Mean	1065.2933	
		Median	1036.4050	
		Variance	5000.982	
		Std. Deviation	70.71762	
		Minimum	1016.59	
		Maximum	1198.53	
		Range	181.94	
		Interquartile Range	106.51	
		Skewness	1.592	.845
		Kurtosis	1.958	1.741
AdLn 4hrs		Mean	1199.7567	33.44907
	95% Confidence	Lower Bound	1113.7731	

	Interval for Mean	Upper Bound	1285.7403	
	5% Trimmed Mean		1200.2396	
	Median		1215.5300	
	Variance		6713.044	
	Std. Deviation		81.93317	
	Minimum		1099.06	
	Maximum		1291.76	
	Range		192.70	
	Interquartile Range		172.56	
	Skewness		-.375	.845
	Kurtosis		-1.890	1.741
AdLn 24hrs	Mean		1587.3417	25.32817
	95% Confidence	Lower Bound	1522.2335	
	Interval for Mean	Upper Bound	1652.4498	
	5% Trimmed Mean		1588.3202	
	Median		1609.5650	
	Variance		3849.096	
	Std. Deviation		62.04108	
	Minimum		1506.12	
	Maximum		1650.95	
	Range		144.83	
	Interquartile Range		125.18	
	Skewness		-.666	.845
	Kurtosis		-1.834	1.741
AdFn/Ln 1hr	Mean		1572.7683	25.78516
	95% Confidence	Lower Bound	1506.4855	
	Interval for Mean	Upper Bound	1639.0512	
	5% Trimmed Mean		1572.2215	
	Median		1571.2400	
	Variance		3989.248	
	Std. Deviation		63.16049	
	Minimum		1499.19	

	Maximum		1656.19	
	Range		157.00	
	Interquartile Range		130.86	
	Skewness		.126	.845
	Kurtosis		-1.584	1.741
AdFn/Ln 4hrs	Mean		1821.9600	28.40093
	95% Confidence	Lower Bound	1748.9531	
	Interval for Mean	Upper Bound	1894.9669	
	5% Trimmed Mean		1821.5611	
	Median		1818.8900	
	Variance		4839.677	
	Std. Deviation		69.56778	
	Minimum		1754.32	
	Maximum		1896.78	
	Range		142.46	
	Interquartile Range		131.66	
	Skewness		.038	.845
	Kurtosis		-3.169	1.741
AdFn/Ln 24hrs	Mean		2206.6517	20.90016
	95% Confidence	Lower Bound	2152.9261	
	Interval for Mean	Upper Bound	2260.3772	
	5% Trimmed Mean		2206.8607	
	Median		2206.2350	
	Variance		2620.899	
	Std. Deviation		51.19472	
	Minimum		2145.07	
	Maximum		2264.47	
	Range		119.40	
	Interquartile Range		105.96	
	Skewness		-.013	.845
	Kurtosis		-2.245	1.741

7.2: Polished surfaces fibroblast vinculin per cell

descriptives

	Polished Surface			Statistic	Std. Error
Vinculin/Cell	Pol 1hr	Mean		1.833	.4014
		95% Confidence	Lower Bound	.802	
		Interval for Mean	Upper Bound	2.865	
		5% Trimmed Mean		1.815	
		Median		1.500	
		Variance		.967	
		Std. Deviation		.9832	
		Minimum		1.0	
		Maximum		3.0	
		Range		2.0	
		Interquartile Range		2.0	
		Skewness		.456	.845
		Kurtosis		-2.390	1.741
	Pol 4hrs	Mean		5.333	.3333
		95% Confidence	Lower Bound	4.476	
		Interval for Mean	Upper Bound	6.190	
		5% Trimmed Mean		5.370	
		Median		5.500	
		Variance		.667	
		Std. Deviation		.8165	
		Minimum		4.0	
		Maximum		6.0	
		Range		2.0	
		Interquartile Range		1.3	
		Skewness		-.857	.845
		Kurtosis		-.300	1.741
	Pol 24hrs	Mean		5.667	.2108
		95% Confidence	Lower Bound	5.125	

	Interval for Mean	Upper Bound	6.209	
	5% Trimmed Mean		5.685	
	Median		6.000	
	Variance		.267	
	Std. Deviation		.5164	
	Minimum		5.0	
	Maximum		6.0	
	Range		1.0	
	Interquartile Range		1.0	
	Skewness		-.968	.845
	Kurtosis		-1.875	1.741
AdFn 1hr	Mean		56.167	2.2274
	95% Confidence	Lower Bound	50.441	
	Interval for Mean	Upper Bound	61.892	
	5% Trimmed Mean		56.185	
	Median		56.500	
	Variance		29.767	
	Std. Deviation		5.4559	
	Minimum		49.0	
	Maximum		63.0	
	Range		14.0	
	Interquartile Range		11.0	
	Skewness		-.136	.845
	Kurtosis		-1.449	1.741
AdFn 4hrs	Mean		80.833	3.1981
	95% Confidence	Lower Bound	72.612	
	Interval for Mean	Upper Bound	89.054	
	5% Trimmed Mean		80.926	
	Median		80.500	
	Variance		61.367	
	Std. Deviation		7.8337	
	Minimum		70.0	

	Maximum		90.0	
	Range		20.0	
	Interquartile Range		15.5	
	Skewness		-.100	.845
	Kurtosis		-1.333	1.741
AdFn 24hrs	Mean		93.833	3.6462
	95% Confidence	Lower Bound	84.461	
	Interval for Mean	Upper Bound	103.206	
	5% Trimmed Mean		93.648	
	Median		92.500	
	Variance		79.767	
	Std. Deviation		8.9312	
	Minimum		84.0	
	Maximum		107.0	
	Range		23.0	
	Interquartile Range		17.0	
	Skewness		.490	.845
	Kurtosis		-1.187	1.741
AdLn 1hr	Mean		38.500	1.6073
	95% Confidence	Lower Bound	34.368	
	Interval for Mean	Upper Bound	42.632	
	5% Trimmed Mean		38.500	
	Median		38.500	
	Variance		15.500	
	Std. Deviation		3.9370	
	Minimum		34.0	
	Maximum		43.0	
	Range		9.0	
	Interquartile Range		7.5	
	Skewness		.000	.845
	Kurtosis		-2.758	1.741
AdLn 4hrs	Mean		40.333	2.0276
	95% Confidence	Lower Bound	35.121	

	Interval for Mean	Upper Bound	45.545	
	5% Trimmed Mean		40.370	
	Median		41.000	
	Variance		24.667	
	Std. Deviation		4.9666	
	Minimum		34.0	
	Maximum		46.0	
	Range		12.0	
	Interquartile Range		10.5	
	Skewness		-.298	.845
	Kurtosis		-1.736	1.741
AdLn 24hrs	Mean		81.667	2.9963
	95% Confidence	Lower Bound	73.964	
	Interval for Mean	Upper Bound	89.369	
	5% Trimmed Mean		81.852	
	Median		85.000	
	Variance		53.867	
	Std. Deviation		7.3394	
	Minimum		71.0	
	Maximum		89.0	
	Range		18.0	
	Interquartile Range		13.5	
	Skewness		-.830	.845
	Kurtosis		-1.419	1.741
AdFn/Ln 1hr	Mean		93.500	2.3488
	95% Confidence	Lower Bound	87.462	
	Interval for Mean	Upper Bound	99.538	
	5% Trimmed Mean		93.778	
	Median		94.500	
	Variance		33.100	
	Std. Deviation		5.7533	
	Minimum		83.0	

	Maximum		99.0	
	Range		16.0	
	Interquartile Range		8.5	
	Skewness		-1.418	.845
	Kurtosis		2.369	1.741
AdFn/Ln 4hrs	Mean		130.833	2.5615
	95% Confidence	Lower Bound	124.249	
	Interval for Mean	Upper Bound	137.418	
	5% Trimmed Mean		130.704	
	Median		129.500	
	Variance		39.367	
	Std. Deviation		6.2743	
	Minimum		124.0	
	Maximum		140.0	
	Range		16.0	
	Interquartile Range		11.5	
	Skewness		.512	.845
	Kurtosis		-1.409	1.741
AdFn/Ln 24hrs	Mean		153.333	2.8245
	95% Confidence	Lower Bound	146.073	
	Interval for Mean	Upper Bound	160.594	
	5% Trimmed Mean		153.426	
	Median		154.000	
	Variance		47.867	
	Std. Deviation		6.9186	
	Minimum		144.0	
	Maximum		161.0	
	Range		17.0	
	Interquartile Range		12.5	
	Skewness		-.242	.845
	Kurtosis		-2.131	1.741

7.3: Polished surfaces fibroblast vinculin per cell area descriptives

	Polished Surface			Statistic	Std. Error
Vinculin/Cell Area	Pol 1hr	Mean		.00513	.001038
		95% Confidence	Lower Bound	.00246	
		Interval for Mean	Upper Bound	.00779	
		5% Trimmed Mean		.00507	
		Median		.00426	
		Variance		.000	
		Std. Deviation		.002543	
		Minimum		.003	
		Maximum		.009	
		Range		.006	
		Interquartile Range		.005	
		Skewness		.660	.845
		Kurtosis		-1.658	1.741
	Pol 4hrs	Mean		.01092	.000505
		95% Confidence	Lower Bound	.00962	
		Interval for Mean	Upper Bound	.01222	
		5% Trimmed Mean		.01098	
		Median		.01139	
		Variance		.000	
		Std. Deviation		.001238	
		Minimum		.009	
		Maximum		.012	
		Range		.003	
		Interquartile Range		.002	
		Skewness		-1.471	.845
		Kurtosis		1.873	1.741
	Pol 24hrs	Mean		.00834	.000350
		95% Confidence	Lower Bound	.00744	

	Interval for Mean	Upper Bound	.00924	
	5% Trimmed Mean		.00834	
	Median		.00829	
	Variance		.000	
	Std. Deviation		.000857	
	Minimum		.007	
	Maximum		.009	
	Range		.002	
	Interquartile Range		.002	
	Skewness		.113	.845
	Kurtosis		-1.136	1.741
AdFn 1hr	Mean		.04598	.001751
	95% Confidence	Lower Bound	.04148	
	Interval for Mean	Upper Bound	.05048	
	5% Trimmed Mean		.04602	
	Median		.04687	
	Variance		.000	
	Std. Deviation		.004290	
	Minimum		.041	
	Maximum		.051	
	Range		.010	
	Interquartile Range		.009	
	Skewness		-.394	.845
	Kurtosis		-2.043	1.741
AdFn 4hrs	Mean		.05608	.002184
	95% Confidence	Lower Bound	.05046	
	Interval for Mean	Upper Bound	.06169	
	5% Trimmed Mean		.05590	
	Median		.05460	
	Variance		.000	
	Std. Deviation		.005351	
	Minimum		.051	

		Maximum	.064	
		Range	.014	
		Interquartile Range	.009	
		Skewness	.759	.845
		Kurtosis	-.771	1.741
AdFn 24hrs	Mean		.05340	.002362
	95% Confidence	Lower Bound	.04733	
	Interval for Mean	Upper Bound	.05947	
	5% Trimmed Mean		.05318	
	Median		.05192	
	Variance		.000	
	Std. Deviation		.005787	
	Minimum		.048	
	Maximum		.063	
	Range		.015	
	Interquartile Range		.010	
	Skewness		.953	.845
	Kurtosis		.102	1.741
AdLn 1hr	Mean		.03697	.001605
	95% Confidence	Lower Bound	.03285	
	Interval for Mean	Upper Bound	.04110	
	5% Trimmed Mean		.03722	
	Median		.03920	
	Variance		.000	
	Std. Deviation		.003931	
	Minimum		.030	
	Maximum		.039	
	Range		.009	
	Interquartile Range		.006	
	Skewness		-1.457	.845
	Kurtosis		1.045	1.741
AdLn 4hrs	Mean		.03358	.001236
	95% Confidence	Lower Bound	.03040	

	Interval for Mean	Upper Bound	.03675	
	5% Trimmed Mean		.03352	
	Median		.03205	
	Variance		.000	
	Std. Deviation		.003027	
	Minimum		.031	
	Maximum		.037	
	Range		.007	
	Interquartile Range		.006	
	Skewness		.850	.845
	Kurtosis		-1.838	1.741
AdLn 24hrs	Mean		.05149	.001926
	95% Confidence	Lower Bound	.04654	
	Interval for Mean	Upper Bound	.05644	
	5% Trimmed Mean		.05156	
	Median		.05226	
	Variance		.000	
	Std. Deviation		.004717	
	Minimum		.045	
	Maximum		.057	
	Range		.012	
	Interquartile Range		.009	
	Skewness		-.437	.845
	Kurtosis		-1.412	1.741
AdFn/Ln 1hr	Mean		.05948	.001405
	95% Confidence	Lower Bound	.05586	
	Interval for Mean	Upper Bound	.06309	
	5% Trimmed Mean		.05951	
	Median		.06040	
	Variance		.000	
	Std. Deviation		.003441	
	Minimum		.055	

		Maximum	.063	
		Range	.008	
		Interquartile Range	.007	
		Skewness	-.508	.845
		Kurtosis	-1.711	1.741
AdFn/Ln 4hrs		Mean	.07180	.000596
	95% Confidence	Lower Bound	.07026	
	Interval for Mean	Upper Bound	.07333	
		5% Trimmed Mean	.07178	
		Median	.07204	
		Variance	.000	
		Std. Deviation	.001461	
		Minimum	.070	
		Maximum	.074	
		Range	.004	
		Interquartile Range	.003	
		Skewness	-.045	.845
		Kurtosis	-1.196	1.741
AdFn/Ln 24hrs		Mean	.06951	.001416
	95% Confidence	Lower Bound	.06587	
	Interval for Mean	Upper Bound	.07315	
		5% Trimmed Mean	.06947	
		Median	.06853	
		Variance	.000	
		Std. Deviation	.003469	
		Minimum	.066	
		Maximum	.074	
		Range	.007	
		Interquartile Range	.007	
		Skewness	.473	.845
		Kurtosis	-2.272	1.741

7.4: Silanized non-passivated fibroblast cell area descriptives

	Silanized, non-Passivated Surface			Statistic	Std. Error
Cell Area (μm^2)	Si- 1hr	Mean		605.4150	21.64380
		95% Confidence Interval for Mean	Lower Bound	549.7778	
			Upper Bound	661.0522	
		5% Trimmed Mean		605.3728	
		Median		593.8750	
		Variance		2810.724	
		Std. Deviation		53.01627	
		Minimum		534.21	
		Maximum		677.38	
		Range		143.17	
		Interquartile Range		95.44	
		Skewness		.227	.845
		Kurtosis		-.928	1.741
	Si-4 hrs	Mean		757.1700	19.03333
		95% Confidence Interval for Mean	Lower Bound	708.2433	
			Upper Bound	806.0967	
		5% Trimmed Mean		755.0406	
		Median		735.5450	
		Variance		2173.606	
		Std. Deviation		46.62195	
		Minimum		721.03	
		Maximum		831.64	

		Range	110.61	
		Interquartile Range	84.01	
		Skewness	1.038	.845
		Kurtosis	-.663	1.741
Si- 24hrs	Mean		945.3100	24.21491
	95% Confidence Interval for Mean	Lower Bound	883.0636	
		Upper Bound	1007.5564	
	5% Trimmed Mean		945.8389	
	Median		955.1500	
	Variance		3518.170	
	Std. Deviation		59.31417	
	Minimum		863.01	
	Maximum		1018.09	
	Range		155.08	
	Interquartile Range		114.79	
	Skewness		-.351	.845
	Kurtosis		-1.271	1.741
SiFn- 1hr	Mean		1387.1367	22.92987
	95% Confidence Interval for Mean	Lower Bound	1328.1936	
		Upper Bound	1446.0798	
	5% Trimmed Mean		1387.0774	
	Median		1384.0650	
	Variance		3154.674	
	Std. Deviation		56.16648	
	Minimum		1322.45	
	Maximum		1452.89	
	Range		130.44	
	Interquartile Range		100.93	
	Skewness		.028	.845

		Kurtosis		-2.740	1.741
	SiFn- 4hrs	Mean		1686.7350	16.56526
		95% Confidence Interval for Mean	Lower Bound	1644.1527	
			Upper Bound	1729.3173	
		5% Trimmed Mean		1687.8594	
		Median		1705.5950	
		Variance		1646.446	
		Std. Deviation		40.57642	
		Minimum		1632.96	
		Maximum		1720.27	
		Range		87.31	
		Interquartile Range		83.23	
		Skewness		-.869	.845
		Kurtosis		-1.849	1.741
	SiFn- 24hrs	Mean		1990.4117	27.45996
		95% Confidence Interval for Mean	Lower Bound	1919.8236	
			Upper Bound	2060.9997	
		5% Trimmed Mean		1992.0157	
		Median		1999.8500	
		Variance		4524.296	
		Std. Deviation		67.26289	
		Minimum		1894.52	
		Maximum		2057.43	
		Range		162.91	
		Interquartile Range		120.92	
		Skewness		-.403	.845
		Kurtosis		-1.873	1.741
	SiLn- 1hr	Mean		1183.4950	23.52899
		95% Confidence Interval for Mean	Lower	1123.0118	

		Bound		
		Upper Bound	1243.9782	
	5% Trimmed Mean		1183.7317	
	Median		1185.2500	
	Variance		3321.681	
	Std. Deviation		57.63403	
	Minimum		1115.22	
	Maximum		1247.51	
	Range		132.29	
	Interquartile Range		103.89	
	Skewness		-.052	.845
	Kurtosis		-2.808	1.741
SiLn- 4hrs	Mean		1550.7567	43.04557
	95% Confidence Interval for Mean	Lower Bound	1440.1045	
		Upper Bound	1661.4088	
	5% Trimmed Mean		1549.6452	
	Median		1566.2800	
	Variance		11117.528	
	Std. Deviation		105.43969	
	Minimum		1428.04	
	Maximum		1693.48	
	Range		265.44	
	Interquartile Range		202.53	
	Skewness		-.036	.845
	Kurtosis		-1.450	1.741
SiLn- 24hrs	Mean		1810.3583	22.91183
	95% Confidence Interval for Mean	Lower Bound	1751.4616	
		Upper Bound	1869.2551	

		5% Trimmed Mean		1810.8698	
		Median		1824.0300	
		Variance		3149.712	
		Std. Deviation		56.12230	
		Minimum		1726.54	
		Maximum		1884.97	
		Range		158.43	
		Interquartile Range		93.86	
		Skewness		-.409	.845
		Kurtosis		-.242	1.741
SiFnLn- 1hr		Mean		1780.9733	25.78016
		95% Confidence Interval for Mean	Lower Bound	1714.7033	
			Upper Bound	1847.2433	
		5% Trimmed Mean		1779.8093	
		Median		1769.8350	
		Variance		3987.699	
		Std. Deviation		63.14823	
		Minimum		1700.75	
		Maximum		1882.15	
		Range		181.40	
		Interquartile Range		103.29	
		Skewness		.621	.845
		Kurtosis		.385	1.741
SiFnLn- 4hrs		Mean		2061.8400	25.53214
		95% Confidence Interval for Mean	Lower Bound	1996.2075	
			Upper Bound	2127.4725	
		5% Trimmed Mean		2060.4933	
		Median		2049.8350	
		Variance		3911.342	

	Std. Deviation		62.54072	
	Minimum		1997.11	
	Maximum		2150.81	
	Range		153.70	
	Interquartile Range		116.85	
	Skewness		.450	.845
	Kurtosis		-1.761	1.741
SiFnLn- 24hrs	Mean		2456.8950	33.79463
	95% Confidence Interval for Mean	Lower Bound	2370.0231	
		Upper Bound	2543.7669	
	5% Trimmed Mean		2456.8683	
	Median		2477.9100	
	Variance		6852.461	
	Std. Deviation		82.77959	
	Minimum		2355.84	
	Maximum		2558.43	
	Range		202.59	
	Interquartile Range		159.52	
	Skewness		-.301	.845
	Kurtosis		-1.775	1.741

7.5: Silanized non-passivated fibroblast vinculin per cell descriptives

Silanized, non-Passivated Surface			Statistic	Std. Error
Vinculin/Cell Si- 1hr	Mean		6.500	.7188
	95% Confidence Interval for Mean	Lower Bound	4.652	
		Upper Bound	8.348	
	5% Trimmed Mean		6.444	
	Median		6.000	
	Variance		3.100	
	Std. Deviation		1.7607	
	Minimum		5.0	
	Maximum		9.0	
	Range		4.0	
	Interquartile Range		3.3	
	Skewness		.495	.845
	Kurtosis		-1.925	1.741
Si-4 hrs	Mean		10.667	.3333
	95% Confidence Interval for Mean	Lower Bound	9.810	
		Upper Bound	11.524	
	5% Trimmed Mean		10.630	
	Median		10.500	
	Variance		.667	
	Std. Deviation		.8165	
	Minimum		10.0	
	Maximum		12.0	
	Range		2.0	
	Interquartile Range		1.3	
	Skewness		.857	.845
	Kurtosis		-.300	1.741
Si- 24hrs	Mean		16.333	1.5202

		95% Confidence	Lower Bound	12.425	
		Interval for Mean	Upper Bound	20.241	
		5% Trimmed Mean		16.259	
		Median		15.000	
		Variance		13.867	
		Std. Deviation		3.7238	
		Minimum		13.0	
		Maximum		21.0	
		Range		8.0	
		Interquartile Range		8.0	
		Skewness		.723	.845
		Kurtosis		-1.875	1.741
SiFn- 1hr	Mean			77.667	2.7406
		95% Confidence	Lower Bound	70.622	
		Interval for Mean	Upper Bound	84.712	
		5% Trimmed Mean		77.519	
		Median		77.000	
		Variance		45.067	
		Std. Deviation		6.7132	
		Minimum		70.0	
		Maximum		88.0	
		Range		18.0	
		Interquartile Range		12.0	
		Skewness		.531	.845
		Kurtosis		-.634	1.741
SiFn- 4hrs	Mean			103.333	3.5182
		95% Confidence	Lower Bound	94.289	
		Interval for Mean	Upper Bound	112.377	
		5% Trimmed Mean		103.370	
		Median		101.500	
		Variance		74.267	
		Std. Deviation		8.6178	

		Minimum	92.0	
		Maximum	114.0	
		Range	22.0	
		Interquartile Range	16.8	
		Skewness	.232	.845
		Kurtosis	-1.298	1.741
SiFn- 24hrs		Mean	132.333	5.3583
	95% Confidence	Lower Bound	118.559	
	Interval for Mean	Upper Bound	146.107	
		5% Trimmed Mean	132.648	
		Median	136.000	
		Variance	172.267	
		Std. Deviation	13.1250	
		Minimum	114.0	
		Maximum	145.0	
		Range	31.0	
		Interquartile Range	25.0	
		Skewness	-.518	.845
		Kurtosis	-1.920	1.741
SiLn- 1hr		Mean	56.833	2.6257
	95% Confidence	Lower Bound	50.084	
	Interval for Mean	Upper Bound	63.583	
		5% Trimmed Mean	56.926	
		Median	57.000	
		Variance	41.367	
		Std. Deviation	6.4317	
		Minimum	47.0	
		Maximum	65.0	
		Range	18.0	
		Interquartile Range	9.8	
		Skewness	-.392	.845
		Kurtosis	-.389	1.741
SiLn- 4hrs		Mean	78.000	2.6331

	95% Confidence Interval for Mean	Lower Bound	71.231	
		Upper Bound	84.769	
	5% Trimmed Mean		77.889	
	Median		79.000	
	Variance		41.600	
	Std. Deviation		6.4498	
	Minimum		70.0	
	Maximum		88.0	
	Range		18.0	
	Interquartile Range		10.5	
	Skewness		.322	.845
	Kurtosis		-.011	1.741
SiLn- 24hrs	Mean		104.500	2.6677
	95% Confidence Interval for Mean	Lower Bound	97.642	
		Upper Bound	111.358	
	5% Trimmed Mean		104.389	
	Median		103.500	
	Variance		42.700	
	Std. Deviation		6.5345	
	Minimum		97.0	
	Maximum		114.0	
	Range		17.0	
	Interquartile Range		12.5	
	Skewness		.452	.845
	Kurtosis		-1.191	1.741
SiFnLn- 1hr	Mean		129.333	2.6034
	95% Confidence Interval for Mean	Lower Bound	122.641	
		Upper Bound	136.026	
	5% Trimmed Mean		129.426	
	Median		130.500	
	Variance		40.667	
	Std. Deviation		6.3770	

		Minimum	120.0	
		Maximum	137.0	
		Range	17.0	
		Interquartile Range	11.8	
		Skewness	-.455	.845
		Kurtosis	-1.011	1.741
SiFnLn- 4hrs		Mean	162.000	3.4351
	95% Confidence	Lower Bound	153.170	
	Interval for Mean	Upper Bound	170.830	
		5% Trimmed Mean	161.944	
		Median	163.500	
		Variance	70.800	
		Std. Deviation	8.4143	
		Minimum	151.0	
		Maximum	174.0	
		Range	23.0	
		Interquartile Range	14.8	
		Skewness	-.012	.845
		Kurtosis	-.691	1.741
SiFnLn- 24hrs		Mean	220.167	3.4100
	95% Confidence	Lower Bound	211.401	
	Interval for Mean	Upper Bound	228.932	
		5% Trimmed Mean	219.963	
		Median	219.500	
		Variance	69.767	
		Std. Deviation	8.3526	
		Minimum	211.0	
		Maximum	233.0	
		Range	22.0	
		Interquartile Range	14.5	
		Skewness	.535	.845
		Kurtosis	-.823	1.741

7.6: Silanized non-passivated fibroblast vinculin per cell area descriptives

Silanized, non-Passivated Surface			Statistic	Std. Error
Vinculin/Cell Area	Si- 1hr	Mean	.01076	.001188
		95% Confidence Interval for Mean Lower Bound	.00771	
		Upper Bound	.01382	
		5% Trimmed Mean	.01071	
		Median	.00985	
		Variance	.000	
		Std. Deviation	.002911	
		Minimum	.008	
		Maximum	.015	
		Range	.007	
		Interquartile Range	.006	
		Skewness	.662	.845
		Kurtosis	-1.382	1.741
	Si-4 hrs	Mean	.01416	.000666
		95% Confidence Interval for Mean Lower Bound	.01244	
		Upper Bound	.01587	
		5% Trimmed Mean	.01417	
		Median	.01452	
		Variance	.000	
		Std. Deviation	.001632	
		Minimum	.012	
		Maximum	.016	
		Range	.004	
		Interquartile Range	.003	
		Skewness	-.296	.845
		Kurtosis	-1.933	1.741
	Si- 24hrs	Mean	.01725	.001500

	95% Confidence Interval for Mean	Lower Bound	.01340	
		Upper Bound	.02111	
	5% Trimmed Mean		.01713	
	Median		.01510	
	Variance		.000	
	Std. Deviation		.003674	
	Minimum		.015	
	Maximum		.022	
	Range		.008	
	Interquartile Range		.007	
	Skewness		.961	.845
	Kurtosis		-1.846	1.741
SiFn- 1hr	Mean		.05597	.001580
	95% Confidence Interval for Mean	Lower Bound	.05191	
		Upper Bound	.06003	
	5% Trimmed Mean		.05597	
	Median		.05611	
	Variance		.000	
	Std. Deviation		.003871	
	Minimum		.051	
	Maximum		.061	
	Range		.011	
	Interquartile Range		.007	
	Skewness		-.048	.845
	Kurtosis		-.625	1.741
SiFn- 4hrs	Mean		.06123	.001754
	95% Confidence Interval for Mean	Lower Bound	.05672	
		Upper Bound	.06573	
	5% Trimmed Mean		.06122	
	Median		.06052	
	Variance		.000	
	Std. Deviation		.004296	

		Minimum	.056	
		Maximum	.066	
		Range	.010	
		Interquartile Range	.009	
		Skewness	.295	.845
		Kurtosis	-2.020	1.741
SiFn- 24hrs		Mean	.06645	.002340
	95% Confidence	Lower Bound	.06043	
	Interval for Mean	Upper Bound	.07246	
		5% Trimmed Mean	.06651	
		Median	.06798	
		Variance	.000	
		Std. Deviation	.005731	
		Minimum	.059	
		Maximum	.073	
		Range	.014	
		Interquartile Range	.011	
		Skewness	-.501	.845
		Kurtosis	-1.710	1.741
SiLn- 1hr		Mean	.04806	.002209
	95% Confidence	Lower Bound	.04238	
	Interval for Mean	Upper Bound	.05374	
		5% Trimmed Mean	.04810	
		Median	.04841	
		Variance	.000	
		Std. Deviation	.005412	
		Minimum	.042	
		Maximum	.053	
		Range	.011	
		Interquartile Range	.010	
		Skewness	-.046	.845
		Kurtosis	-3.170	1.741
SiLn- 4hrs		Mean	.05043	.001881

	95% Confidence Interval for Mean	Lower Bound	.04560	
		Upper Bound	.05527	
	5% Trimmed Mean		.05049	
	Median		.05073	
	Variance		.000	
	Std. Deviation		.004607	
	Minimum		.044	
	Maximum		.056	
	Range		.012	
	Interquartile Range		.009	
	Skewness		-.285	.845
	Kurtosis		-1.154	1.741
SiLn- 24hrs	Mean		.05781	.001959
	95% Confidence Interval for Mean	Lower Bound	.05278	
		Upper Bound	.06285	
	5% Trimmed Mean		.05765	
	Median		.05655	
	Variance		.000	
	Std. Deviation		.004798	
	Minimum		.053	
	Maximum		.066	
	Range		.014	
	Interquartile Range		.007	
	Skewness		1.047	.845
	Kurtosis		.975	1.741
SiFnLn- 1hr	Mean		.07267	.001603
	95% Confidence Interval for Mean	Lower Bound	.06855	
		Upper Bound	.07679	
	5% Trimmed Mean		.07263	
	Median		.07274	
	Variance		.000	
	Std. Deviation		.003926	

		Minimum	.069	
		Maximum	.078	
		Range	.009	
		Interquartile Range	.007	
		Skewness	.102	.845
		Kurtosis	-2.564	1.741
SiFnLn- 4hrs		Mean	.07855	.001018
	95% Confidence	Lower Bound	.07593	
	Interval for Mean	Upper Bound	.08116	
		5% Trimmed Mean	.07859	
		Median	.07895	
		Variance	.000	
		Std. Deviation	.002494	
		Minimum	.075	
		Maximum	.081	
		Range	.006	
		Interquartile Range	.005	
		Skewness	-.384	.845
		Kurtosis	-1.897	1.741
SiFnLn- 24hrs		Mean	.08963	.001033
	95% Confidence	Lower Bound	.08697	
	Interval for Mean	Upper Bound	.09229	
		5% Trimmed Mean	.08964	
		Median	.08952	
		Variance	.000	
		Std. Deviation	.002531	
		Minimum	.086	
		Maximum	.093	
		Range	.007	
		Interquartile Range	.005	
		Skewness	-.035	.845
		Kurtosis	-.805	1.741

7.7: Silanized passivated fibroblast cell area

descriptives

	Silanized, Passivated Surface			Statistic	Std. Error
Cell Area (micrometres squared)	Si+ 1hr	Mean		536.2733	18.22227
		95% Confidence Interval for Mean	Lower Bound	489.4315	
			Upper Bound	583.1152	
		5% Trimmed Mean		535.8537	
		Median		529.7450	
		Variance		1992.308	
		Std. Deviation		44.63527	
		Minimum		491.27	
		Maximum		588.83	
		Range		97.56	
		Interquartile Range		95.15	
		Skewness		.263	.845
		Kurtosis		-2.336	1.741
	Si+ 4hrs	Mean		707.1800	8.21385
		95% Confidence Interval for Mean	Lower Bound	686.0656	
			Upper Bound	728.2944	
		5% Trimmed Mean		707.0961	
		Median		702.1500	
		Variance		404.804	
		Std. Deviation		20.11974	
		Minimum		684.26	
		Maximum		731.61	
		Range		47.35	
		Interquartile Range		41.11	
		Skewness		.420	.845
		Kurtosis		-1.905	1.741

Si+ 24hrs	Mean		742.7583	11.71889
	95% Confidence Interval for Mean	Lower Bound	712.6340	
		Upper Bound	772.8827	
	5% Trimmed Mean		741.9031	
	Median		728.6650	
	Variance		823.994	
	Std. Deviation		28.70530	
	Minimum		719.40	
	Maximum		781.51	
	Range		62.11	
	Interquartile Range		56.59	
	Skewness		.826	.845
	Kurtosis		-1.875	1.741
SiFn+ 1hr	Mean		978.3817	26.84955
	95% Confidence Interval for Mean	Lower Bound	909.3627	
		Upper Bound	1047.4006	
	5% Trimmed Mean		978.1185	
	Median		976.2750	
	Variance		4325.391	
	Std. Deviation		65.76770	
	Minimum		907.57	
	Maximum		1053.93	
	Range		146.36	
	Interquartile Range		136.82	
	Skewness		.060	.845
	Kurtosis		-2.524	1.741
SiFn+ 4hrs	Mean		1120.0800	22.83380
	95% Confidence Interval for Mean	Lower Bound	1061.3838	
		Upper Bound	1178.7762	
	5% Trimmed Mean		1120.0289	
	Median		1131.4550	
	Variance		3128.296	

		Std. Deviation	55.93117	
		Minimum	1049.84	
		Maximum	1191.24	
		Range	141.40	
		Interquartile Range	103.53	
		Skewness	-.172	.845
		Kurtosis	-1.723	1.741
SiFn+ 24hrs		Mean	1267.4967	18.06021
	95% Confidence	Lower Bound	1221.0714	
	Interval for Mean	Upper Bound	1313.9219	
		5% Trimmed Mean	1268.0319	
		Median	1275.8800	
		Variance	1957.027	
		Std. Deviation	44.23830	
		Minimum	1210.11	
		Maximum	1315.25	
		Range	105.14	
		Interquartile Range	83.33	
		Skewness	-.281	.845
		Kurtosis	-2.300	1.741
SiLn+ 1hr		Mean	829.3567	19.68192
	95% Confidence	Lower Bound	778.7627	
	Interval for Mean	Upper Bound	879.9507	
		5% Trimmed Mean	828.4530	
		Median	813.4000	
		Variance	2324.269	
		Std. Deviation	48.21067	
		Minimum	774.53	
		Maximum	900.45	
		Range	125.92	
		Interquartile Range	86.95	
		Skewness	.649	.845
		Kurtosis	-1.096	1.741

SiLn+ 4hrs	Mean		993.4333	22.35985
	95% Confidence Interval for Mean	Lower Bound	935.9555	
		Upper Bound	1050.9112	
	5% Trimmed Mean		994.5509	
	Median		1004.4250	
	Variance		2999.779	
	Std. Deviation		54.77023	
	Minimum		923.45	
	Maximum		1043.30	
	Range		119.85	
	Interquartile Range		102.80	
	Skewness		-.259	.845
	Kurtosis		-2.610	1.741
SiLn+ 24hrs	Mean		1169.9000	29.02984
	95% Confidence Interval for Mean	Lower Bound	1095.2764	
		Upper Bound	1244.5236	
	5% Trimmed Mean		1166.9044	
	Median		1150.4900	
	Variance		5056.390	
	Std. Deviation		71.10830	
	Minimum		1101.89	
	Maximum		1291.83	
	Range		189.94	
	Interquartile Range		117.36	
	Skewness		1.127	.845
	Kurtosis		.734	1.741
SiFnLn+ 1hr	Mean		1152.8983	10.67110
	95% Confidence Interval for Mean	Lower Bound	1125.4674	
		Upper Bound	1180.3293	
	5% Trimmed Mean		1151.8193	
	Median		1144.0300	
	Variance		683.234	

		Std. Deviation	26.13875	
		Minimum	1128.83	
		Maximum	1196.39	
		Range	67.56	
		Interquartile Range	46.43	
		Skewness	1.086	.845
		Kurtosis	.101	1.741
SiFnLn+ 4hrs		Mean	1249.9650	16.71188
	95% Confidence	Lower Bound	1207.0057	
	Interval for Mean	Upper Bound	1292.9243	
		5% Trimmed Mean	1250.4822	
		Median	1249.7450	
		Variance	1675.723	
		Std. Deviation	40.93559	
		Minimum	1190.63	
		Maximum	1299.99	
		Range	109.36	
		Interquartile Range	76.87	
		Skewness	-.226	.845
		Kurtosis	-.926	1.741
SiFnLn+ 24hrs		Mean	1286.2583	24.86839
	95% Confidence	Lower Bound	1222.3321	
	Interval for Mean	Upper Bound	1350.1846	
		5% Trimmed Mean	1285.8276	
		Median	1278.9650	
		Variance	3710.622	
		Std. Deviation	60.91487	
		Minimum	1213.63	
		Maximum	1366.64	
		Range	153.01	
		Interquartile Range	116.92	
		Skewness	.220	.845
		Kurtosis	-1.869	1.741

7.8: Silanized passivated fibroblast vinculin per cell descriptives

Silanized, Passivated Surface			Statistic	Std. Error
Vinculin/Cell	Si+ 1hr	Mean	2.500	.2236
		95% Confidence Interval for Mean — Lower Bound	1.925	
		95% Confidence Interval for Mean — Upper Bound	3.075	
		5% Trimmed Mean	2.500	
		Median	2.500	
		Variance	.300	
		Std. Deviation	.5477	
		Minimum	2.0	
		Maximum	3.0	
		Range	1.0	
		Interquartile Range	1.0	
		Skewness	.000	.845
		Kurtosis	-3.333	1.741
	Si+ 4hrs	Mean	4.500	.4282
		95% Confidence Interval for Mean — Lower Bound	3.399	
		95% Confidence Interval for Mean — Upper Bound	5.601	
		5% Trimmed Mean	4.500	
		Median	4.500	
		Variance	1.100	
		Std. Deviation	1.0488	
		Minimum	3.0	
		Maximum	6.0	
		Range	3.0	
		Interquartile Range	1.5	
		Skewness	.000	.845
		Kurtosis	-.248	1.741
	Si+ 24hrs	Mean	3.833	.7491

	95% Confidence Interval for Mean	Lower Bound	1.908	
		Upper Bound	5.759	
	5% Trimmed Mean		3.815	
	Median		3.500	
	Variance		3.367	
	Std. Deviation		1.8348	
	Minimum		2.0	
	Maximum		6.0	
	Range		4.0	
	Interquartile Range		4.0	
	Skewness		.362	.845
	Kurtosis		-2.103	1.741
SiFn+ 1hr	Mean		13.000	.5774
	95% Confidence Interval for Mean	Lower Bound	11.516	
		Upper Bound	14.484	
	5% Trimmed Mean		13.000	
	Median		13.000	
	Variance		2.000	
	Std. Deviation		1.4142	
	Minimum		11.0	
	Maximum		15.0	
	Range		4.0	
	Interquartile Range		2.5	
	Skewness		.000	.845
	Kurtosis		-.300	1.741
SiFn+ 4hrs	Mean		15.500	1.7654
	95% Confidence Interval for Mean	Lower Bound	10.962	
		Upper Bound	20.038	
	5% Trimmed Mean		15.611	
	Median		17.500	
	Variance		18.700	
	Std. Deviation		4.3243	

		Minimum	10.0	
		Maximum	19.0	
		Range	9.0	
		Interquartile Range	9.0	
		Skewness	-.846	.845
		Kurtosis	-1.897	1.741
SiFn+ 24hrs		Mean	17.333	1.9264
	95% Confidence	Lower Bound	12.381	
	Interval for Mean	Upper Bound	22.285	
		5% Trimmed Mean	17.426	
		Median	19.000	
		Variance	22.267	
		Std. Deviation	4.7188	
		Minimum	11.0	
		Maximum	22.0	
		Range	11.0	
		Interquartile Range	9.5	
		Skewness	-.673	.845
		Kurtosis	-1.840	1.741
SiLn+ 1hr		Mean	9.333	.4216
	95% Confidence	Lower Bound	8.249	
	Interval for Mean	Upper Bound	10.417	
		5% Trimmed Mean	9.315	
		Median	9.000	
		Variance	1.067	
		Std. Deviation	1.0328	
		Minimum	8.0	
		Maximum	11.0	
		Range	3.0	
		Interquartile Range	1.5	
		Skewness	.666	.845
		Kurtosis	.586	1.741
SiLn+ 4hrs		Mean	16.500	1.4549

	95% Confidence Interval for Mean	Lower Bound	12.760	
		Upper Bound	20.240	
	5% Trimmed Mean		16.556	
	Median		18.000	
	Variance		12.700	
	Std. Deviation		3.5637	
	Minimum		12.0	
	Maximum		20.0	
	Range		8.0	
	Interquartile Range		7.3	
	Skewness		-.776	.845
	Kurtosis		-1.826	1.741
SiLn+ 24hrs	Mean		10.667	1.5846
	95% Confidence Interval for Mean	Lower Bound	6.593	
		Upper Bound	14.740	
	5% Trimmed Mean		10.630	
	Median		10.500	
	Variance		15.067	
	Std. Deviation		3.8816	
	Minimum		6.0	
	Maximum		16.0	
	Range		10.0	
	Interquartile Range		7.8	
	Skewness		.193	.845
	Kurtosis		-1.354	1.741
SiFnLn+ 1hr	Mean		24.833	2.0235
	95% Confidence Interval for Mean	Lower Bound	19.632	
		Upper Bound	30.035	
	5% Trimmed Mean		24.815	
	Median		24.500	
	Variance		24.567	
	Std. Deviation		4.9565	

		Minimum	19.0	
		Maximum	31.0	
		Range	12.0	
		Interquartile Range	10.5	
		Skewness	.149	.845
		Kurtosis	-1.770	1.741
SiFnLn+ 4hrs		Mean	29.667	1.5846
	95% Confidence	Lower Bound	25.593	
	Interval for Mean	Upper Bound	33.740	
		5% Trimmed Mean	29.685	
		Median	30.500	
		Variance	15.067	
		Std. Deviation	3.8816	
		Minimum	25.0	
		Maximum	34.0	
		Range	9.0	
		Interquartile Range	8.3	
		Skewness	-.423	.845
		Kurtosis	-1.847	1.741
SiFnLn+ 24hrs		Mean	24.500	1.3844
	95% Confidence	Lower Bound	20.941	
	Interval for Mean	Upper Bound	28.059	
		5% Trimmed Mean	24.444	
		Median	24.000	
		Variance	11.500	
		Std. Deviation	3.3912	
		Minimum	21.0	
		Maximum	29.0	
		Range	8.0	
		Interquartile Range	7.3	
		Skewness	.369	.845
		Kurtosis	-1.696	1.741

7.9: Silanized passivated- fibroblast vinculin per cell area descriptives

	Silanized, Passivated Surface			Statistic	Std. Error
Vinculin/Cell Area	Si+ 1hr	Mean		.00466	.000383
		95% Confidence Interval for Mean	Lower Bound	.00367	
			Upper Bound	.00564	
		5% Trimmed Mean		.00463	
		Median		.00458	
		Variance		.000	
		Std. Deviation		.000938	
		Minimum		.004	
		Maximum		.006	
		Range		.002	
		Interquartile Range		.002	
		Skewness		.562	.845
		Kurtosis		-.951	1.741
	Si+ 4hrs	Mean		.00635	.000590
		95% Confidence Interval for Mean	Lower Bound	.00484	
			Upper Bound	.00787	
		5% Trimmed Mean		.00635	
		Median		.00631	
		Variance		.000	
		Std. Deviation		.001445	
		Minimum		.004	
		Maximum		.008	
		Range		.004	
		Interquartile Range		.002	
		Skewness		.175	.845
		Kurtosis		-.332	1.741

Si+ 24hrs	Mean		.00521	.001065
	95% Confidence Interval for Mean	Lower Bound	.00247	
		Upper Bound	.00795	
	5% Trimmed Mean		.00518	
	Median		.00464	
	Variance		.000	
	Std. Deviation		.002609	
	Minimum		.003	
	Maximum		.008	
	Range		.006	
	Interquartile Range		.006	
	Skewness		.415	.845
	Kurtosis		-2.140	1.741
SiFn+ 1hr	Mean		.01327	.000363
	95% Confidence Interval for Mean	Lower Bound	.01234	
		Upper Bound	.01420	
	5% Trimmed Mean		.01328	
	Median		.01315	
	Variance		.000	
	Std. Deviation		.000889	
	Minimum		.012	
	Maximum		.014	
	Range		.002	
	Interquartile Range		.002	
	Skewness		.039	.845
	Kurtosis		-1.451	1.741
SiFn+ 4hrs	Mean		.01382	.001539
	95% Confidence Interval for Mean	Lower Bound	.00987	
		Upper Bound	.01778	
	5% Trimmed Mean		.01393	
	Median		.01534	
	Variance		.000	

		Std. Deviation	.003769	
		Minimum	.009	
		Maximum	.017	
		Range	.008	
		Interquartile Range	.008	
		Skewness	-.784	.845
		Kurtosis	-1.801	1.741
SiFn+ 24hrs		Mean	.01368	.001505
	95% Confidence	Lower Bound	.00981	
	Interval for Mean	Upper Bound	.01755	
		5% Trimmed Mean	.01376	
		Median	.01527	
		Variance	.000	
		Std. Deviation	.003688	
		Minimum	.009	
		Maximum	.017	
		Range	.008	
		Interquartile Range	.008	
		Skewness	-.755	.845
		Kurtosis	-1.970	1.741
SiLn+ 1hr		Mean	.01096	.000351
	95% Confidence	Lower Bound	.01006	
	Interval for Mean	Upper Bound	.01186	
		5% Trimmed Mean	.01096	
		Median	.01115	
		Variance	.000	
		Std. Deviation	.000859	
		Minimum	.010	
		Maximum	.012	
		Range	.002	
		Interquartile Range	.001	
		Skewness	-.128	.845
		Kurtosis	.140	1.741

SiLn+ 4hrs	Mean		.01676	.001706
	95% Confidence Interval for Mean	Lower Bound	.01237	
		Upper Bound	.02114	
	5% Trimmed Mean		.01680	
	Median		.01840	
	Variance		.000	
	Std. Deviation		.004178	
	Minimum		.012	
	Maximum		.021	
	Range		.010	
	Interquartile Range		.008	
	Skewness		-.696	.845
	Kurtosis		-1.766	1.741
SiLn+ 24hrs	Mean		.00923	.001496
	95% Confidence Interval for Mean	Lower Bound	.00538	
		Upper Bound	.01307	
	5% Trimmed Mean		.00918	
	Median		.00880	
	Variance		.000	
	Std. Deviation		.003664	
	Minimum		.005	
	Maximum		.014	
	Range		.009	
	Interquartile Range		.007	
	Skewness		.289	.845
	Kurtosis		-1.816	1.741
SiFnLn+ 1hr	Mean		.02147	.001562
	95% Confidence Interval for Mean	Lower Bound	.01746	
		Upper Bound	.02549	
	5% Trimmed Mean		.02149	
	Median		.02141	
	Variance		.000	

		Std. Deviation	.003826	
		Minimum	.017	
		Maximum	.026	
		Range	.009	
		Interquartile Range	.008	
		Skewness	.007	.845
		Kurtosis	-1.798	1.741
SiFnLn+ 4hrs		Mean	.02373	.001246
	95% Confidence	Lower Bound	.02053	
	Interval for Mean	Upper Bound	.02694	
		5% Trimmed Mean	.02375	
		Median	.02357	
		Variance	.000	
		Std. Deviation	.003053	
		Minimum	.020	
		Maximum	.027	
		Range	.008	
		Interquartile Range	.006	
		Skewness	.060	.845
		Kurtosis	-1.661	1.741
SiFnLn+ 24hrs		Mean	.01911	.001246
	95% Confidence	Lower Bound	.01591	
	Interval for Mean	Upper Bound	.02231	
		5% Trimmed Mean	.01908	
		Median	.01799	
		Variance	.000	
		Std. Deviation	.003052	
		Minimum	.016	
		Maximum	.023	
		Range	.007	
		Interquartile Range	.006	
		Skewness	.592	.845
		Kurtosis	-1.644	1.741

7.10: Fibroblast cell area descriptives on different surfaces at 1 hour

	Surface at One Hour		Statistic	Std. Error
Cell Area (micrometres squared)	Pol 1hr	Mean	352.2083	18.44742
		95% Confidence Interval for Mean Lower Bound	304.7877	
		Upper Bound	399.6289	
		5% Trimmed Mean	353.3315	
		Median	363.5650	
		Variance	2041.844	
		Std. Deviation	45.18677	
		Minimum	288.67	
		Maximum	395.53	
		Range	106.86	
		Interquartile Range	86.76	
		Skewness	-.507	.845
		Kurtosis	-1.884	1.741
	AdFn 1hr	Mean	1221.4433	10.80285
		95% Confidence Interval for Mean Lower Bound	1193.6737	
		Upper Bound	1249.2129	
		5% Trimmed Mean	1221.6787	
		Median	1225.3900	
		Variance	700.209	
		Std. Deviation	26.46147	
		Minimum	1186.56	
		Maximum	1252.09	
		Range	65.53	
		Interquartile Range	54.73	
		Skewness	-.336	.845
		Kurtosis	-1.619	1.741
	AdLn 1hr	Mean	1069.5200	28.87035

		95% Confidence Interval for Mean	Lower Bound	995.3064	
			Upper Bound	1143.7336	
		5% Trimmed Mean		1065.2933	
		Median		1036.4050	
		Variance		5000.982	
		Std. Deviation		70.71762	
		Minimum		1016.59	
		Maximum		1198.53	
		Range		181.94	
		Interquartile Range		106.51	
		Skewness		1.592	.845
		Kurtosis		1.958	1.741
	AdFnLn 1hr	Mean		1572.7683	25.78516
		95% Confidence Interval for Mean	Lower Bound	1506.4855	
			Upper Bound	1639.0512	
		5% Trimmed Mean		1572.2215	
		Median		1571.2400	
		Variance		3989.248	
		Std. Deviation		63.16049	
		Minimum		1499.19	
		Maximum		1656.19	
		Range		157.00	
		Interquartile Range		130.86	
		Skewness		.126	.845
		Kurtosis		-1.584	1.741
	Si- 1hr	Mean		605.4150	21.64380
		95% Confidence Interval for Mean	Lower Bound	549.7778	
			Upper Bound	661.0522	
		5% Trimmed Mean		605.3728	
		Median		593.8750	
		Variance		2810.724	
		Std. Deviation		53.01627	

		Minimum	534.21	
		Maximum	677.38	
		Range	143.17	
		Interquartile Range	95.44	
		Skewness	.227	.845
		Kurtosis	-.928	1.741
SiFn- 1hr		Mean	1387.1367	22.92987
	95% Confidence	Lower Bound	1328.1936	
	Interval for Mean	Upper Bound	1446.0798	
		5% Trimmed Mean	1387.0774	
		Median	1384.0650	
		Variance	3154.674	
		Std. Deviation	56.16648	
		Minimum	1322.45	
		Maximum	1452.89	
		Range	130.44	
		Interquartile Range	100.93	
		Skewness	.028	.845
		Kurtosis	-2.740	1.741
SiLn- 1hr		Mean	1183.4950	23.52899
	95% Confidence	Lower Bound	1123.0118	
	Interval for Mean	Upper Bound	1243.9782	
		5% Trimmed Mean	1183.7317	
		Median	1185.2500	
		Variance	3321.681	
		Std. Deviation	57.63403	
		Minimum	1115.22	
		Maximum	1247.51	
		Range	132.29	
		Interquartile Range	103.89	
		Skewness	-.052	.845
		Kurtosis	-2.808	1.741
SiFnLn- 1hr		Mean	1780.9733	25.78016

	95% Confidence	Lower Bound	1714.7033	
	Interval for Mean	Upper Bound	1847.2433	
	5% Trimmed Mean		1779.8093	
	Median		1769.8350	
	Variance		3987.699	
	Std. Deviation		63.14823	
	Minimum		1700.75	
	Maximum		1882.15	
	Range		181.40	
	Interquartile Range		103.29	
	Skewness		.621	.845
	Kurtosis		.385	1.741
Si+ 1hr	Mean		536.2733	18.22227
	95% Confidence	Lower Bound	489.4315	
	Interval for Mean	Upper Bound	583.1152	
	5% Trimmed Mean		535.8537	
	Median		529.7450	
	Variance		1992.308	
	Std. Deviation		44.63527	
	Minimum		491.27	
	Maximum		588.83	
	Range		97.56	
	Interquartile Range		95.15	
	Skewness		.263	.845
	Kurtosis		-2.336	1.741
SiFn+ 1hr	Mean		978.3817	26.84955
	95% Confidence	Lower Bound	909.3627	
	Interval for Mean	Upper Bound	1047.4006	
	5% Trimmed Mean		978.1185	
	Median		976.2750	
	Variance		4325.391	
	Std. Deviation		65.76770	

		Minimum	907.57	
		Maximum	1053.93	
		Range	146.36	
		Interquartile Range	136.82	
		Skewness	.060	.845
		Kurtosis	-2.524	1.741
SiLn+ 1hr		Mean	829.3567	19.68192
	95% Confidence Interval for Mean	Lower Bound	778.7627	
		Upper Bound	879.9507	
		5% Trimmed Mean	828.4530	
		Median	813.4000	
		Variance	2324.269	
		Std. Deviation	48.21067	
		Minimum	774.53	
		Maximum	900.45	
		Range	125.92	
		Interquartile Range	86.95	
		Skewness	.649	.845
		Kurtosis	-1.096	1.741
SiFnLn+ 1hr		Mean	1152.8983	10.67110
	95% Confidence Interval for Mean	Lower Bound	1125.4674	
		Upper Bound	1180.3293	
		5% Trimmed Mean	1151.8193	
		Median	1144.0300	
		Variance	683.234	
		Std. Deviation	26.13875	
		Minimum	1128.83	
		Maximum	1196.39	
		Range	67.56	
		Interquartile Range	46.43	
		Skewness	1.086	.845
		Kurtosis	.101	1.741

7.11: Fibroblast vinculin per cell descriptives at 1 hour

	Surface at One Hour			Statistic	Std. Error
Vinculin/Cell	Pol 1hr	Mean		1.833	.4014
		95% Confidence	Lower Bound	.802	
		Interval for Mean	Upper Bound	2.865	
		5% Trimmed Mean		1.815	
		Median		1.500	
		Variance		.967	
		Std. Deviation		.9832	
		Minimum		1.0	
		Maximum		3.0	
		Range		2.0	
		Interquartile Range		2.0	
		Skewness		.456	.845
		Kurtosis		-2.390	1.741
	AdFn 1hr	Mean		56.167	2.2274
		95% Confidence	Lower Bound	50.441	
		Interval for Mean	Upper Bound	61.892	
		5% Trimmed Mean		56.185	
		Median		56.500	
		Variance		29.767	
		Std. Deviation		5.4559	
		Minimum		49.0	
		Maximum		63.0	
		Range		14.0	
		Interquartile Range		11.0	
		Skewness		-.136	.845
		Kurtosis		-1.449	1.741
	AdLn 1hr	Mean		38.500	1.6073
		95% Confidence	Lower Bound	34.368	
		Interval for Mean	Upper Bound	42.632	

		5% Trimmed Mean	38.500	
		Median	38.500	
		Variance	15.500	
		Std. Deviation	3.9370	
		Minimum	34.0	
		Maximum	43.0	
		Range	9.0	
		Interquartile Range	7.5	
		Skewness	.000	.845
		Kurtosis	-2.758	1.741
AdFnLn 1hr	Mean		93.500	2.3488
	95% Confidence	Lower Bound	87.462	
	Interval for Mean	Upper Bound	99.538	
		5% Trimmed Mean	93.778	
		Median	94.500	
		Variance	33.100	
		Std. Deviation	5.7533	
		Minimum	83.0	
		Maximum	99.0	
		Range	16.0	
		Interquartile Range	8.5	
		Skewness	-1.418	.845
		Kurtosis	2.369	1.741
Si- 1hr	Mean		6.500	.7188
	95% Confidence	Lower Bound	4.652	
	Interval for Mean	Upper Bound	8.348	
		5% Trimmed Mean	6.444	
		Median	6.000	
		Variance	3.100	
		Std. Deviation	1.7607	
		Minimum	5.0	
		Maximum	9.0	
		Range	4.0	

		Interquartile Range	3.3	
		Skewness	.495	.845
		Kurtosis	-1.925	1.741
SiFn- 1hr		Mean	77.667	2.7406
	95% Confidence	Lower Bound	70.622	
	Interval for Mean	Upper Bound	84.712	
		5% Trimmed Mean	77.519	
		Median	77.000	
		Variance	45.067	
		Std. Deviation	6.7132	
		Minimum	70.0	
		Maximum	88.0	
		Range	18.0	
		Interquartile Range	12.0	
		Skewness	.531	.845
		Kurtosis	-.634	1.741
SiLn- 1hr		Mean	56.833	2.6257
	95% Confidence	Lower Bound	50.084	
	Interval for Mean	Upper Bound	63.583	
		5% Trimmed Mean	56.926	
		Median	57.000	
		Variance	41.367	
		Std. Deviation	6.4317	
		Minimum	47.0	
		Maximum	65.0	
		Range	18.0	
		Interquartile Range	9.8	
		Skewness	-.392	.845
		Kurtosis	-.389	1.741
SiFnLn- 1hr		Mean	129.333	2.6034
	95% Confidence	Lower Bound	122.641	
	Interval for Mean	Upper Bound	136.026	

		5% Trimmed Mean	129.426	
		Median	130.500	
		Variance	40.667	
		Std. Deviation	6.3770	
		Minimum	120.0	
		Maximum	137.0	
		Range	17.0	
		Interquartile Range	11.8	
		Skewness	-.455	.845
		Kurtosis	-1.011	1.741
Si+ 1hr		Mean	2.500	.2236
	95% Confidence	Lower Bound	1.925	
	Interval for Mean	Upper Bound	3.075	
		5% Trimmed Mean	2.500	
		Median	2.500	
		Variance	.300	
		Std. Deviation	.5477	
		Minimum	2.0	
		Maximum	3.0	
		Range	1.0	
		Interquartile Range	1.0	
		Skewness	.000	.845
		Kurtosis	-3.333	1.741
SiFn+ 1hr		Mean	13.000	.5774
	95% Confidence	Lower Bound	11.516	
	Interval for Mean	Upper Bound	14.484	
		5% Trimmed Mean	13.000	
		Median	13.000	
		Variance	2.000	
		Std. Deviation	1.4142	
		Minimum	11.0	
		Maximum	15.0	
		Range	4.0	

	Interquartile Range		2.5	
	Skewness		.000	.845
	Kurtosis		-.300	1.741
SiLn+ 1hr	Mean		9.333	.4216
	95% Confidence	Lower Bound	8.249	
	Interval for Mean	Upper Bound	10.417	
	5% Trimmed Mean		9.315	
	Median		9.000	
	Variance		1.067	
	Std. Deviation		1.0328	
	Minimum		8.0	
	Maximum		11.0	
	Range		3.0	
	Interquartile Range		1.5	
	Skewness		.666	.845
	Kurtosis		.586	1.741
SiFnLn+ 1hr	Mean		24.833	2.0235
	95% Confidence	Lower Bound	19.632	
	Interval for Mean	Upper Bound	30.035	
	5% Trimmed Mean		24.815	
	Median		24.500	
	Variance		24.567	
	Std. Deviation		4.9565	
	Minimum		19.0	
	Maximum		31.0	
	Range		12.0	
	Interquartile Range		10.5	
	Skewness		.149	.845
	Kurtosis		-1.770	1.741

7.12: Fibroblast vinculin per cell area descriptives at 1 hour

	Surface at One Hour			Statistic	Std. Error
Vinculin/Cell Area	Pol 1hr	Mean		.00513	.001038
		95% Confidence Interval for Mean	Lower Bound	.00246	
			Upper Bound	.00779	
		5% Trimmed Mean		.00507	
		Median		.00426	
		Variance		.000	
		Std. Deviation		.002543	
		Minimum		.003	
		Maximum		.009	
		Range		.006	
		Interquartile Range		.005	
		Skewness		.660	.845
		Kurtosis		-1.658	1.741
	AdFn 1hr	Mean		.04598	.001751
		95% Confidence Interval for Mean	Lower Bound	.04148	
			Upper Bound	.05048	
		5% Trimmed Mean		.04602	
		Median		.04687	
		Variance		.000	
		Std. Deviation		.004290	
		Minimum		.041	
		Maximum		.051	
		Range		.010	
		Interquartile Range		.009	
		Skewness		-.394	.845
		Kurtosis		-2.043	1.741
	AdLn 1hr	Mean		.03697	.001605

	95% Confidence	Lower Bound	.03285	
	Interval for Mean	Upper Bound	.04110	
	5% Trimmed Mean		.03722	
	Median		.03920	
	Variance		.000	
	Std. Deviation		.003931	
	Minimum		.030	
	Maximum		.039	
	Range		.009	
	Interquartile Range		.006	
	Skewness		-1.457	.845
	Kurtosis		1.045	1.741
AdFnLn 1hr	Mean		.05948	.001405
	95% Confidence	Lower Bound	.05586	
	Interval for Mean	Upper Bound	.06309	
	5% Trimmed Mean		.05951	
	Median		.06040	
	Variance		.000	
	Std. Deviation		.003441	
	Minimum		.055	
	Maximum		.063	
	Range		.008	
	Interquartile Range		.007	
	Skewness		-.508	.845
	Kurtosis		-1.711	1.741
Si- 1hr	Mean		.01076	.001188
	95% Confidence	Lower Bound	.00771	
	Interval for Mean	Upper Bound	.01382	
	5% Trimmed Mean		.01071	
	Median		.00985	
	Variance		.000	
	Std. Deviation		.002911	

		Minimum	.008	
		Maximum	.015	
		Range	.007	
		Interquartile Range	.006	
		Skewness	.662	.845
		Kurtosis	-1.382	1.741
SiFn- 1hr	Mean		.05597	.001580
	95% Confidence	Lower Bound	.05191	
	Interval for Mean	Upper Bound	.06003	
	5% Trimmed Mean		.05597	
	Median		.05611	
	Variance		.000	
	Std. Deviation		.003871	
	Minimum		.051	
	Maximum		.061	
	Range		.011	
	Interquartile Range		.007	
	Skewness		-.048	.845
	Kurtosis		-.625	1.741
SiLn- 1hr	Mean		.04806	.002209
	95% Confidence	Lower Bound	.04238	
	Interval for Mean	Upper Bound	.05374	
	5% Trimmed Mean		.04810	
	Median		.04841	
	Variance		.000	
	Std. Deviation		.005412	
	Minimum		.042	
	Maximum		.053	
	Range		.011	
	Interquartile Range		.010	
	Skewness		-.046	.845
	Kurtosis		-3.170	1.741
SiFnLn- 1hr	Mean		.07267	.001603

	95% Confidence Interval for Mean	Lower Bound	.06855	
		Upper Bound	.07679	
	5% Trimmed Mean		.07263	
	Median		.07274	
	Variance		.000	
	Std. Deviation		.003926	
	Minimum		.069	
	Maximum		.078	
	Range		.009	
	Interquartile Range		.007	
	Skewness		.102	.845
	Kurtosis		-2.564	1.741
Si+ 1hr	Mean		.00466	.000383
	95% Confidence Interval for Mean	Lower Bound	.00367	
		Upper Bound	.00564	
	5% Trimmed Mean		.00463	
	Median		.00458	
	Variance		.000	
	Std. Deviation		.000938	
	Minimum		.004	
	Maximum		.006	
	Range		.002	
	Interquartile Range		.002	
	Skewness		.562	.845
	Kurtosis		-.951	1.741
SiFn+ 1hr	Mean		.01327	.000363
	95% Confidence Interval for Mean	Lower Bound	.01234	
		Upper Bound	.01420	
	5% Trimmed Mean		.01328	
	Median		.01315	
	Variance		.000	
	Std. Deviation		.000889	

		Minimum		.012	
		Maximum		.014	
		Range		.002	
		Interquartile Range		.002	
		Skewness		.039	.845
		Kurtosis		-1.452	1.741
SiLn+ 1hr		Mean		.01096	.000351
		95% Confidence	Lower Bound	.01006	
		Interval for Mean	Upper Bound	.01186	
		5% Trimmed Mean		.01096	
		Median		.01115	
		Variance		.000	
		Std. Deviation		.000859	
		Minimum		.010	
		Maximum		.012	
		Range		.002	
		Interquartile Range		.001	
		Skewness		-.128	.845
		Kurtosis		.140	1.741
SiFnLn+ 1hr		Mean		.02147	.001562
		95% Confidence	Lower Bound	.01746	
		Interval for Mean	Upper Bound	.02549	
		5% Trimmed Mean		.02149	
		Median		.02141	
		Variance		.000	
		Std. Deviation		.003826	
		Minimum		.017	
		Maximum		.026	
		Range		.009	
		Interquartile Range		.008	
		Skewness		.007	.845
		Kurtosis		-1.798	1.741

7.13: Fibroblast cell area descriptives on different surfaces at 4 hours

	Surface at Four Hours			Statistic	Std. Error
Cell Area (μm^2)	Pol 4hrs	Mean		487.0717	13.10684
		95% Confidence Interval for Mean	Lower Bound	453.3795	
			Upper Bound	520.7639	
		5% Trimmed Mean		487.5363	
		Median		491.1200	
		Variance		1030.735	
		Std. Deviation		32.10507	
		Minimum		440.49	
		Maximum		525.29	
		Range		84.80	
		Interquartile Range		60.85	
		Skewness		-.394	.845
		Kurtosis		-1.089	1.741
	AdFn 4hrs	Mean		1442.1417	24.17230
		95% Confidence Interval for Mean	Lower Bound	1380.0048	
			Upper Bound	1504.2785	
		5% Trimmed Mean		1441.6330	
		Median		1437.5350	
		Variance		3505.801	
		Std. Deviation		59.20980	
		Minimum		1377.01	
		Maximum		1516.43	
		Range		139.42	
		Interquartile Range		127.95	
		Skewness		.193	.845

		Kurtosis	-1.801	1.741
AdLn 4hrs	Mean		1199.7567	33.44907
	95% Confidence Interval for Mean	Lower Bound	1113.7731	
		Upper Bound	1285.7403	
	5% Trimmed Mean		1200.2396	
	Median		1215.5300	
	Variance		6713.044	
	Std. Deviation		81.93317	
	Minimum		1099.06	
	Maximum		1291.76	
	Range		192.70	
	Interquartile Range		172.56	
	Skewness		-.375	.845
	Kurtosis		-1.890	1.741
AdFnLn 4hrs	Mean		1821.9600	28.40093
	95% Confidence Interval for Mean	Lower Bound	1748.9531	
		Upper Bound	1894.9669	
	5% Trimmed Mean		1821.5611	
	Median		1818.8900	
	Variance		4839.677	
	Std. Deviation		69.56778	
	Minimum		1754.32	
	Maximum		1896.78	
	Range		142.46	
	Interquartile Range		131.66	
	Skewness		.038	.845
	Kurtosis		-3.169	1.741
Si- 4hrs	Mean		757.1700	19.03333
	95% Confidence Interval for Mean	Lower Bound	708.2433	

		Upper Bound	806.0967	
		5% Trimmed Mean	755.0406	
		Median	735.5450	
		Variance	2173.606	
		Std. Deviation	46.62195	
		Minimum	721.03	
		Maximum	831.64	
		Range	110.61	
		Interquartile Range	84.01	
		Skewness	1.038	.845
		Kurtosis	-.663	1.741
SiFn- 4hrs		Mean	1686.7350	16.56526
	95% Confidence Interval for Mean	Lower Bound	1644.1527	
		Upper Bound	1729.3173	
		5% Trimmed Mean	1687.8594	
		Median	1705.5950	
		Variance	1646.446	
		Std. Deviation	40.57642	
		Minimum	1632.96	
		Maximum	1720.27	
		Range	87.31	
		Interquartile Range	83.23	
		Skewness	-.869	.845
		Kurtosis	-1.849	1.741
SiLn- 4hrs		Mean	1550.7567	43.04557
	95% Confidence Interval for Mean	Lower Bound	1440.1045	
		Upper Bound	1661.4088	
		5% Trimmed Mean	1549.6452	
		Median	1566.2800	
		Variance	11117.528	

		Std. Deviation	105.43969	
		Minimum	1428.04	
		Maximum	1693.48	
		Range	265.44	
		Interquartile Range	202.53	
		Skewness	-.036	.845
		Kurtosis	-1.450	1.741
SiFnLn- 4hrs		Mean	2061.8400	25.53214
	95% Confidence Interval for Mean	Lower Bound	1996.2075	
		Upper Bound	2127.4725	
		5% Trimmed Mean	2060.4933	
		Median	2049.8350	
		Variance	3911.342	
		Std. Deviation	62.54072	
		Minimum	1997.11	
		Maximum	2150.81	
		Range	153.70	
		Interquartile Range	116.85	
		Skewness	.450	.845
		Kurtosis	-1.761	1.741
Si+ 4hrs		Mean	707.1800	8.21385
	95% Confidence Interval for Mean	Lower Bound	686.0656	
		Upper Bound	728.2944	
		5% Trimmed Mean	707.0961	
		Median	702.1500	
		Variance	404.804	
		Std. Deviation	20.11974	
		Minimum	684.26	
		Maximum	731.61	
		Range	47.35	
		Interquartile Range	41.11	

		Skewness	.420	.845
		Kurtosis	-1.905	1.741
SiFn+ 4hrs		Mean	1120.0800	22.83380
	95% Confidence Interval for Mean	Lower Bound	1061.3838	
		Upper Bound	1178.7762	
		5% Trimmed Mean	1120.0289	
		Median	1131.4550	
		Variance	3128.296	
		Std. Deviation	55.93117	
		Minimum	1049.84	
		Maximum	1191.24	
		Range	141.40	
		Interquartile Range	103.53	
		Skewness	-.172	.845
		Kurtosis	-1.723	1.741
SiLn+ 4hrs		Mean	993.4333	22.35985
	95% Confidence Interval for Mean	Lower Bound	935.9555	
		Upper Bound	1050.9112	
		5% Trimmed Mean	994.5509	
		Median	1004.4250	
		Variance	2999.779	
		Std. Deviation	54.77023	
		Minimum	923.45	
		Maximum	1043.30	
		Range	119.85	
		Interquartile Range	102.80	
		Skewness	-.259	.845
		Kurtosis	-2.610	1.741
SiFnLn+ 4hrs		Mean	1249.9650	16.71188
	95% Confidence Interval for Mean	Lower Bound	1207.0057	

		Upper Bound	1292.9243	
		5% Trimmed Mean	1250.4822	
		Median	1249.7450	
		Variance	1675.723	
		Std. Deviation	40.93559	
		Minimum	1190.63	
		Maximum	1299.99	
		Range	109.36	
		Interquartile Range	76.87	
		Skewness	-.226	.845
		Kurtosis	-.926	1.741

7.14: Fibroblast vinculin per cell descriptives at

4 hours

	Surface at Four Hours		Statistic	Std. Error
Vinculin/Cell	Pol 4hrs	Mean	5.333	.3333
		95% Confidence Interval for Mean Lower Bound	4.476	
		Upper Bound	6.190	
		5% Trimmed Mean	5.370	
		Median	5.500	
		Variance	.667	
		Std. Deviation	.8165	
		Minimum	4.0	
		Maximum	6.0	
		Range	2.0	
		Interquartile Range	1.3	
		Skewness	-.857	.845
		Kurtosis	-.300	1.741
	AdFn 4hrs	Mean	80.833	3.1981

	95% Confidence Interval for Mean	Lower Bound	72.612	
		Upper Bound	89.054	
	5% Trimmed Mean		80.926	
	Median		80.500	
	Variance		61.367	
	Std. Deviation		7.8337	
	Minimum		70.0	
	Maximum		90.0	
	Range		20.0	
	Interquartile Range		15.5	
	Skewness		-.100	.845
	Kurtosis		-1.333	1.741
AdLn 4hrs	Mean		40.333	2.0276
	95% Confidence Interval for Mean	Lower Bound	35.121	
		Upper Bound	45.545	
	5% Trimmed Mean		40.370	
	Median		41.000	
	Variance		24.667	
	Std. Deviation		4.9666	
	Minimum		34.0	
	Maximum		46.0	
	Range		12.0	
	Interquartile Range		10.5	
	Skewness		-.298	.845
	Kurtosis		-1.736	1.741
AdFnLn 4hrs	Mean		130.833	2.5615
	95% Confidence Interval for Mean	Lower Bound	124.249	
		Upper Bound	137.418	
	5% Trimmed Mean		130.704	
	Median		129.500	
	Variance		39.367	
	Std. Deviation		6.2743	

		Minimum	124.0	
		Maximum	140.0	
		Range	16.0	
		Interquartile Range	11.5	
		Skewness	.512	.845
		Kurtosis	-1.409	1.741
Si- 4hrs		Mean	10.667	.3333
	95% Confidence	Lower Bound	9.810	
	Interval for Mean	Upper Bound	11.524	
		5% Trimmed Mean	10.630	
		Median	10.500	
		Variance	.667	
		Std. Deviation	.8165	
		Minimum	10.0	
		Maximum	12.0	
		Range	2.0	
		Interquartile Range	1.3	
		Skewness	.857	.845
		Kurtosis	-.300	1.741
SiFn- 4hrs		Mean	103.333	3.5182
	95% Confidence	Lower Bound	94.289	
	Interval for Mean	Upper Bound	112.377	
		5% Trimmed Mean	103.370	
		Median	101.500	
		Variance	74.267	
		Std. Deviation	8.6178	
		Minimum	92.0	
		Maximum	114.0	
		Range	22.0	
		Interquartile Range	16.8	
		Skewness	.232	.845
		Kurtosis	-1.298	1.741
SiLn- 4hrs		Mean	78.000	2.6331

	95% Confidence Interval for Mean	Lower Bound	71.231	
		Upper Bound	84.769	
	5% Trimmed Mean		77.889	
	Median		79.000	
	Variance		41.600	
	Std. Deviation		6.4498	
	Minimum		70.0	
	Maximum		88.0	
	Range		18.0	
	Interquartile Range		10.5	
	Skewness		.322	.845
	Kurtosis		-.011	1.741
SiFnLn- 4hrs	Mean		162.000	3.4351
	95% Confidence Interval for Mean	Lower Bound	153.170	
		Upper Bound	170.830	
	5% Trimmed Mean		161.944	
	Median		163.500	
	Variance		70.800	
	Std. Deviation		8.4143	
	Minimum		151.0	
	Maximum		174.0	
	Range		23.0	
	Interquartile Range		14.8	
	Skewness		-.012	.845
	Kurtosis		-.691	1.741
Si+ 4hrs	Mean		4.500	.4282
	95% Confidence Interval for Mean	Lower Bound	3.399	
		Upper Bound	5.601	
	5% Trimmed Mean		4.500	
	Median		4.500	
	Variance		1.100	
	Std. Deviation		1.0488	

		Minimum	3.0	
		Maximum	6.0	
		Range	3.0	
		Interquartile Range	1.5	
		Skewness	.000	.845
		Kurtosis	-.248	1.741
SiFn+ 4hrs		Mean	15.500	1.7654
	95% Confidence	Lower Bound	10.962	
	Interval for Mean	Upper Bound	20.038	
		5% Trimmed Mean	15.611	
		Median	17.500	
		Variance	18.700	
		Std. Deviation	4.3243	
		Minimum	10.0	
		Maximum	19.0	
		Range	9.0	
		Interquartile Range	9.0	
		Skewness	-.846	.845
		Kurtosis	-1.897	1.741
SiLn+ 4hrs		Mean	16.500	1.4549
	95% Confidence	Lower Bound	12.760	
	Interval for Mean	Upper Bound	20.240	
		5% Trimmed Mean	16.556	
		Median	18.000	
		Variance	12.700	
		Std. Deviation	3.5637	
		Minimum	12.0	
		Maximum	20.0	
		Range	8.0	
		Interquartile Range	7.3	
		Skewness	-.776	.845
		Kurtosis	-1.826	1.741
SiFnLn+ 4hrs		Mean	29.667	1.5846

				Statistic	Std. Error
	95% Confidence	Lower Bound		25.593	
	Interval for Mean	Upper Bound		33.740	
	5% Trimmed Mean			29.685	
	Median			30.500	
	Variance			15.067	
	Std. Deviation			3.8816	
	Minimum			25.0	
	Maximum			34.0	
	Range			9.0	
	Interquartile Range			8.3	
	Skewness			-.423	.845
	Kurtosis			-1.847	1.741

7.15: Fibroblast vinculin per cell area descriptives at 4 hours

	Surface at Four Hours			Statistic	Std. Error
Vinculin/Cell Area	Pol 4hrs	Mean		.01092	.000505
		95% Confidence	Lower Bound	.00962	
		Interval for Mean	Upper Bound	.01222	
		5% Trimmed Mean		.01098	
		Median		.01139	
		Variance		.000	
		Std. Deviation		.001238	
		Minimum		.009	
		Maximum		.012	
		Range		.003	
		Interquartile Range		.002	
		Skewness		-1.471	.845
		Kurtosis		1.873	1.741

AdFn 4hrs	Mean			.05608	.002184
	95% Confidence	Lower Bound		.05046	
	Interval for Mean	Upper Bound		.06169	
	5% Trimmed Mean			.05590	
	Median			.05460	
	Variance			.000	
	Std. Deviation			.005351	
	Minimum			.051	
	Maximum			.064	
	Range			.014	
	Interquartile Range			.009	
	Skewness			.759	.845
	Kurtosis			-.771	1.741
AdLn 4hrs	Mean			.03358	.001236
	95% Confidence	Lower Bound		.03040	
	Interval for Mean	Upper Bound		.03675	
	5% Trimmed Mean			.03352	
	Median			.03205	
	Variance			.000	
	Std. Deviation			.003027	
	Minimum			.031	
	Maximum			.037	
	Range			.007	
	Interquartile Range			.006	
	Skewness			.850	.845
	Kurtosis			-1.838	1.741
AdFnLn 4hrs	Mean			.07180	.000596
	95% Confidence	Lower Bound		.07026	
	Interval for Mean	Upper Bound		.07333	
	5% Trimmed Mean			.07178	
	Median			.07204	
	Variance			.000	

		Std. Deviation	.001461	
		Minimum	.070	
		Maximum	.074	
		Range	.004	
		Interquartile Range	.003	
		Skewness	-.045	.845
		Kurtosis	-1.196	1.741
Si- 4hrs		Mean	.01416	.000666
	95% Confidence	Lower Bound	.01244	
	Interval for Mean	Upper Bound	.01587	
		5% Trimmed Mean	.01417	
		Median	.01452	
		Variance	.000	
		Std. Deviation	.001632	
		Minimum	.012	
		Maximum	.016	
		Range	.004	
		Interquartile Range	.003	
		Skewness	-.296	.845
		Kurtosis	-1.933	1.741
SiFn- 4hrs		Mean	.06123	.001754
	95% Confidence	Lower Bound	.05672	
	Interval for Mean	Upper Bound	.06573	
		5% Trimmed Mean	.06122	
		Median	.06052	
		Variance	.000	
		Std. Deviation	.004296	
		Minimum	.056	
		Maximum	.066	
		Range	.010	
		Interquartile Range	.009	
		Skewness	.295	.845
		Kurtosis	-2.020	1.741

SiLn- 4hrs	Mean		.05043	.001881
	95% Confidence Interval for Mean	Lower Bound	.04560	
		Upper Bound	.05527	
	5% Trimmed Mean		.05049	
	Median		.05073	
	Variance		.000	
	Std. Deviation		.004607	
	Minimum		.044	
	Maximum		.056	
	Range		.012	
	Interquartile Range		.009	
	Skewness		-.285	.845
	Kurtosis		-1.154	1.741
SiFnLn- 4hrs	Mean		.07855	.001018
	95% Confidence Interval for Mean	Lower Bound	.07593	
		Upper Bound	.08116	
	5% Trimmed Mean		.07859	
	Median		.07895	
	Variance		.000	
	Std. Deviation		.002494	
	Minimum		.075	
	Maximum		.081	
	Range		.006	
	Interquartile Range		.005	
	Skewness		-.384	.845
	Kurtosis		-1.897	1.741
Si+ 4hrs	Mean		.00635	.000590
	95% Confidence Interval for Mean	Lower Bound	.00484	
		Upper Bound	.00787	
	5% Trimmed Mean		.00635	
	Median		.00631	
	Variance		.000	

		Std. Deviation		.001445	
		Minimum		.004	
		Maximum		.008	
		Range		.004	
		Interquartile Range		.002	
		Skewness		.175	.845
		Kurtosis		-.332	1.741
SiFn+ 4hrs		Mean		.01382	.001539
		95% Confidence	Lower Bound	.00987	
		Interval for Mean	Upper Bound	.01778	
		5% Trimmed Mean		.01393	
		Median		.01534	
		Variance		.000	
		Std. Deviation		.003769	
		Minimum		.009	
		Maximum		.017	
		Range		.008	
		Interquartile Range		.008	
		Skewness		-.784	.845
		Kurtosis		-1.801	1.741
SiLn+ 4hrs		Mean		.01676	.001706
		95% Confidence	Lower Bound	.01237	
		Interval for Mean	Upper Bound	.02114	
		5% Trimmed Mean		.01680	
		Median		.01840	
		Variance		.000	
		Std. Deviation		.004178	
		Minimum		.012	
		Maximum		.021	
		Range		.010	
		Interquartile Range		.008	
		Skewness		-.696	.845
		Kurtosis		-1.766	1.741

SiFnLn+ 4hrs	Mean		.02373	.001246
	95% Confidence Interval for Mean	Lower Bound	.02053	
		Upper Bound	.02694	
	5% Trimmed Mean		.02375	
	Median		.02357	
	Variance		.000	
	Std. Deviation		.003053	
	Minimum		.020	
	Maximum		.027	
	Range		.008	
	Interquartile Range		.006	
	Skewness		.060	.845
	Kurtosis		-1.661	1.741

7.16: Fibroblast cell area descriptives at 24 hours

	Surface at Twenty Four Hours		Statistic	Std. Error
Cell Area (micrometres squared)	Pol 24hrs	Mean	680.9733	15.59293
		95% Confidence Interval for Mean Lower Bound	640.8904	
		Upper Bound	721.0562	
		5% Trimmed Mean	681.1165	
		Median	676.0800	
		Variance	1458.837	
		Std. Deviation	38.19473	
		Minimum	631.70	
		Maximum	727.67	
		Range	95.97	
		Interquartile Range	71.82	
		Skewness	.067	.845
		Kurtosis	-1.842	1.741

AdFn 24hrs	Mean		1759.4550	18.80587
	95% Confidence Interval for Mean	Lower Bound	1711.1130	
		Upper Bound	1807.7970	
	5% Trimmed Mean		1758.7561	
	Median		1756.8750	
	Variance		2121.964	
	Std. Deviation		46.06479	
	Minimum		1698.16	
	Maximum		1833.33	
	Range		135.17	
	Interquartile Range		72.77	
	Skewness		.484	.845
	Kurtosis		.734	1.741
AdLn 24hrs	Mean		1587.3417	25.32817
	95% Confidence Interval for Mean	Lower Bound	1522.2335	
		Upper Bound	1652.4498	
	5% Trimmed Mean		1588.3202	
	Median		1609.5650	
	Variance		3849.096	
	Std. Deviation		62.04108	
	Minimum		1506.12	
	Maximum		1650.95	
	Range		144.83	
	Interquartile Range		125.18	
	Skewness		-.666	.845
	Kurtosis		-1.834	1.741
AdFnLn 24hrs	Mean		2206.6517	20.90016
	95% Confidence Interval for Mean	Lower Bound	2152.9261	
		Upper Bound	2260.3772	
	5% Trimmed Mean		2206.8607	
	Median		2206.2350	
	Variance		2620.899	

		Std. Deviation	51.19472	
		Minimum	2145.07	
		Maximum	2264.47	
		Range	119.40	
		Interquartile Range	105.96	
		Skewness	-.013	.845
		Kurtosis	-2.245	1.741
Si- 24hrs		Mean	945.3100	24.21491
	95% Confidence	Lower Bound	883.0636	
	Interval for Mean	Upper Bound	1007.5564	
		5% Trimmed Mean	945.8389	
		Median	955.1500	
		Variance	3518.170	
		Std. Deviation	59.31417	
		Minimum	863.01	
		Maximum	1018.09	
		Range	155.08	
		Interquartile Range	114.79	
		Skewness	-.351	.845
		Kurtosis	-1.271	1.741
SiFn- 24hrs		Mean	1990.4117	27.45996
	95% Confidence	Lower Bound	1919.8236	
	Interval for Mean	Upper Bound	2060.9997	
		5% Trimmed Mean	1992.0157	
		Median	1999.8500	
		Variance	4524.296	
		Std. Deviation	67.26289	
		Minimum	1894.52	
		Maximum	2057.43	
		Range	162.91	
		Interquartile Range	120.92	
		Skewness	-.403	.845
		Kurtosis	-1.873	1.741

SiLn- 24hrs	Mean		1810.3583	22.91183
	95% Confidence Interval for Mean	Lower Bound	1751.4616	
		Upper Bound	1869.2551	
	5% Trimmed Mean		1810.8698	
	Median		1824.0300	
	Variance		3149.712	
	Std. Deviation		56.12230	
	Minimum		1726.54	
	Maximum		1884.97	
	Range		158.43	
	Interquartile Range		93.86	
	Skewness		-.409	.845
	Kurtosis		-.242	1.741
SiFnLn- 24hrs	Mean		2456.8950	33.79463
	95% Confidence Interval for Mean	Lower Bound	2370.0231	
		Upper Bound	2543.7669	
	5% Trimmed Mean		2456.8683	
	Median		2477.9100	
	Variance		6852.461	
	Std. Deviation		82.77959	
	Minimum		2355.84	
	Maximum		2558.43	
	Range		202.59	
	Interquartile Range		159.52	
	Skewness		-.301	.845
	Kurtosis		-1.775	1.741
Si+ 24hrs	Mean		742.7583	11.71889
	95% Confidence Interval for Mean	Lower Bound	712.6340	
		Upper Bound	772.8827	
	5% Trimmed Mean		741.9031	
	Median		728.6650	
	Variance		823.994	

		Std. Deviation	28.70530	
		Minimum	719.40	
		Maximum	781.51	
		Range	62.11	
		Interquartile Range	56.59	
		Skewness	.826	.845
		Kurtosis	-1.875	1.741
SiFn+ 24hrs		Mean	1267.4967	18.06021
	95% Confidence	Lower Bound	1221.0714	
	Interval for Mean	Upper Bound	1313.9219	
		5% Trimmed Mean	1268.0319	
		Median	1275.8800	
		Variance	1957.027	
		Std. Deviation	44.23830	
		Minimum	1210.11	
		Maximum	1315.25	
		Range	105.14	
		Interquartile Range	83.33	
		Skewness	-.281	.845
		Kurtosis	-2.300	1.741
SiLn+ 24hrs		Mean	1169.9000	29.02984
	95% Confidence	Lower Bound	1095.2764	
	Interval for Mean	Upper Bound	1244.5236	
		5% Trimmed Mean	1166.9044	
		Median	1150.4900	
		Variance	5056.390	
		Std. Deviation	71.10830	
		Minimum	1101.89	
		Maximum	1291.83	
		Range	189.94	
		Interquartile Range	117.36	
		Skewness	1.127	.845
		Kurtosis	.734	1.741

			Statistic	Std. Error
SiFnLn+ 24hrs	Mean		1286.2583	24.86839
	95% Confidence Interval for Mean	Lower Bound	1222.3321	
		Upper Bound	1350.1846	
	5% Trimmed Mean		1285.8276	
	Median		1278.9650	
	Variance		3710.622	
	Std. Deviation		60.91487	
	Minimum		1213.63	
	Maximum		1366.64	
	Range		153.01	
	Interquartile Range		116.92	
	Skewness		.220	.845
	Kurtosis		-1.869	1.741

7.17: Fibroblast vinculin per cell descriptives at

24 hours

	Surface at Twenty Four Hours		Statistic	Std. Error
Vinculin/Cell	Pol 24hrs	Mean	5.667	.2108
		95% Confidence Interval for Mean	Lower Bound	5.125	
		Upper Bound	6.209	
		5% Trimmed Mean	5.685	
		Median	6.000	
		Variance	.267	
		Std. Deviation	.5164	
		Minimum	5.0	
		Maximum	6.0	
		Range	1.0	
		Interquartile Range	1.0	
		Skewness	-.968	.845

		Kurtosis		-1.875	1.741
AdFn 24hrs	Mean		93.833	3.6462
	95% Confidence Interval for Mean	Lower Bound	84.461	
		Upper Bound	103.206	
	5% Trimmed Mean		93.648	
	Median		92.500	
	Variance		79.767	
	Std. Deviation		8.9312	
	Minimum		84.0	
	Maximum		107.0	
	Range		23.0	
	Interquartile Range		17.0	
	Skewness		.490	.845
	Kurtosis		-1.187	1.741
AdLn 24hrs	Mean		81.667	2.9963
	95% Confidence Interval for Mean	Lower Bound	73.964	
		Upper Bound	89.369	
	5% Trimmed Mean		81.852	
	Median		85.000	
	Variance		53.867	
	Std. Deviation		7.3394	
	Minimum		71.0	
	Maximum		89.0	
	Range		18.0	
	Interquartile Range		13.5	
	Skewness		-.830	.845
	Kurtosis		-1.419	1.741
AdFnLn 24hrs	Mean		153.333	2.8245
	95% Confidence Interval for Mean	Lower Bound	146.073	
		Upper Bound	160.594	
	5% Trimmed Mean		153.426	
	Median		154.000	

		Variance	47.867	
		Std. Deviation	6.9186	
		Minimum	144.0	
		Maximum	161.0	
		Range	17.0	
		Interquartile Range	12.5	
		Skewness	-.242	.845
		Kurtosis	-2.131	1.741
Si- 24hrs		Mean	16.333	1.5202
	95% Confidence	Lower Bound	12.425	
	Interval for Mean	Upper Bound	20.241	
		5% Trimmed Mean	16.259	
		Median	15.000	
		Variance	13.867	
		Std. Deviation	3.7238	
		Minimum	13.0	
		Maximum	21.0	
		Range	8.0	
		Interquartile Range	8.0	
		Skewness	.723	.845
		Kurtosis	-1.875	1.741
SiFn- 24hrs		Mean	132.333	5.3583
	95% Confidence	Lower Bound	118.559	
	Interval for Mean	Upper Bound	146.107	
		5% Trimmed Mean	132.648	
		Median	136.000	
		Variance	172.267	
		Std. Deviation	13.1250	
		Minimum	114.0	
		Maximum	145.0	
		Range	31.0	
		Interquartile Range	25.0	
		Skewness	-.518	.845

		Kurtosis		-1.920	1.741
SiLn- 24hrs	Mean		104.500	2.6677
	95% Confidence Interval for Mean	Lower Bound	97.642	
		Upper Bound	111.358	
	5% Trimmed Mean		104.389	
	Median		103.500	
	Variance		42.700	
	Std. Deviation		6.5345	
	Minimum		97.0	
	Maximum		114.0	
	Range		17.0	
	Interquartile Range		12.5	
	Skewness		.452	.845
	Kurtosis		-1.191	1.741
SiFnLn- 24hrs	Mean		220.167	3.4100
	95% Confidence Interval for Mean	Lower Bound	211.401	
		Upper Bound	228.932	
	5% Trimmed Mean		219.963	
	Median		219.500	
	Variance		69.767	
	Std. Deviation		8.3526	
	Minimum		211.0	
	Maximum		233.0	
	Range		22.0	
	Interquartile Range		14.5	
	Skewness		.535	.845
	Kurtosis		-.823	1.741
Si+ 24hrs	Mean		3.833	.7491
	95% Confidence Interval for Mean	Lower Bound	1.908	
		Upper Bound	5.759	
	5% Trimmed Mean		3.815	
	Median		3.500	

		Variance	3.367	
		Std. Deviation	1.8348	
		Minimum	2.0	
		Maximum	6.0	
		Range	4.0	
		Interquartile Range	4.0	
		Skewness	.362	.845
		Kurtosis	-2.103	1.741
SiFn+ 24hrs	Mean		17.333	1.9264
	95% Confidence	Lower Bound	12.381	
	Interval for Mean	Upper Bound	22.285	
		5% Trimmed Mean	17.426	
		Median	19.000	
		Variance	22.267	
		Std. Deviation	4.7188	
		Minimum	11.0	
		Maximum	22.0	
		Range	11.0	
		Interquartile Range	9.5	
		Skewness	-.673	.845
		Kurtosis	-1.840	1.741
SiLn+ 24hrs	Mean		10.667	1.5846
	95% Confidence	Lower Bound	6.593	
	Interval for Mean	Upper Bound	14.740	
		5% Trimmed Mean	10.630	
		Median	10.500	
		Variance	15.067	
		Std. Deviation	3.8816	
		Minimum	6.0	
		Maximum	16.0	
		Range	10.0	
		Interquartile Range	7.8	
		Skewness	.193	.845

				Statistic	Std. Error
			Kurtosis	-1.354	1.741
	SiFnLn+ 24hrs	Mean		24.500	1.3844
		95% Confidence	Lower Bound	20.941	
		Interval for Mean	Upper Bound	28.059	
		5% Trimmed Mean		24.444	
		Median		24.000	
		Variance		11.500	
		Std. Deviation		3.3912	
		Minimum		21.0	
		Maximum		29.0	
		Range		8.0	
		Interquartile Range		7.3	
		Skewness		.369	.845
		Kurtosis		-1.696	1.741

7.18: Fibroblast vinculin per cell area descriptives at 24 hours

	Surface at Twenty Four Hours			Statistic	Std. Error
Vinculin/Cell Area	Pol 24hrs	Mean		.00834	.000350
		95% Confidence	Lower Bound	.00744	
		Interval for Mean	Upper Bound	.00924	
		5% Trimmed Mean		.00834	
		Median		.00829	
		Variance		.000	
		Std. Deviation		.000857	
		Minimum		.007	
		Maximum		.009	
		Range		.002	

		Interquartile Range	.002	
		Skewness	.113	.845
		Kurtosis	-1.136	1.741
AdFn 24hrs	Mean		.05340	.002362
	95% Confidence	Lower Bound	.04733	
	Interval for Mean	Upper Bound	.05947	
	5% Trimmed Mean		.05318	
	Median		.05192	
	Variance		.000	
	Std. Deviation		.005787	
	Minimum		.048	
	Maximum		.063	
	Range		.015	
	Interquartile Range		.010	
	Skewness		.953	.845
	Kurtosis		.102	1.741
AdLn 24hrs	Mean		.05149	.001926
	95% Confidence	Lower Bound	.04654	
	Interval for Mean	Upper Bound	.05644	
	5% Trimmed Mean		.05156	
	Median		.05226	
	Variance		.000	
	Std. Deviation		.004717	
	Minimum		.045	
	Maximum		.057	
	Range		.012	
	Interquartile Range		.009	
	Skewness		-.437	.845
	Kurtosis		-1.412	1.741
AdFnLn 24hrs	Mean		.06951	.001416
	95% Confidence	Lower Bound	.06587	
	Interval for Mean	Upper Bound	.07315	

		5% Trimmed Mean	.06947	
		Median	.06853	
		Variance	.000	
		Std. Deviation	.003469	
		Minimum	.066	
		Maximum	.074	
		Range	.007	
		Interquartile Range	.007	
		Skewness	.473	.845
		Kurtosis	-2.272	1.741
Si- 24hrs	Mean		.01725	.001500
	95% Confidence	Lower Bound	.01340	
	Interval for Mean	Upper Bound	.02111	
		5% Trimmed Mean	.01713	
		Median	.01510	
		Variance	.000	
		Std. Deviation	.003674	
		Minimum	.015	
		Maximum	.022	
		Range	.008	
		Interquartile Range	.007	
		Skewness	.961	.845
		Kurtosis	-1.846	1.741
SiFn- 24hrs	Mean		.06645	.002340
	95% Confidence	Lower Bound	.06043	
	Interval for Mean	Upper Bound	.07246	
		5% Trimmed Mean	.06651	
		Median	.06798	
		Variance	.000	
		Std. Deviation	.005731	
		Minimum	.059	
		Maximum	.073	
		Range	.014	

		Interquartile Range	.011	
		Skewness	-.501	.845
		Kurtosis	-1.710	1.741
SiLn- 24hrs	Mean		.05781	.001959
	95% Confidence	Lower Bound	.05278	
	Interval for Mean	Upper Bound	.06285	
	5% Trimmed Mean		.05765	
	Median		.05655	
	Variance		.000	
	Std. Deviation		.004798	
	Minimum		.053	
	Maximum		.066	
	Range		.014	
	Interquartile Range		.007	
	Skewness		1.047	.845
	Kurtosis		.975	1.741
SiFnLn- 24hrs	Mean		.08963	.001033
	95% Confidence	Lower Bound	.08697	
	Interval for Mean	Upper Bound	.09229	
	5% Trimmed Mean		.08964	
	Median		.08952	
	Variance		.000	
	Std. Deviation		.002531	
	Minimum		.086	
	Maximum		.093	
	Range		.007	
	Interquartile Range		.005	
	Skewness		-.035	.845
	Kurtosis		-.805	1.741
Si+ 24hrs	Mean		.00521	.001065
	95% Confidence	Lower Bound	.00247	
	Interval for Mean	Upper Bound	.00795	

		5% Trimmed Mean	.00518	
		Median	.00464	
		Variance	.000	
		Std. Deviation	.002609	
		Minimum	.003	
		Maximum	.008	
		Range	.006	
		Interquartile Range	.006	
		Skewness	.415	.845
		Kurtosis	-2.140	1.741
SiFn+ 24hrs	Mean		.01368	.001505
	95% Confidence	Lower Bound	.00981	
	Interval for Mean	Upper Bound	.01755	
		5% Trimmed Mean	.01376	
		Median	.01527	
		Variance	.000	
		Std. Deviation	.003688	
		Minimum	.009	
		Maximum	.017	
		Range	.008	
		Interquartile Range	.008	
		Skewness	-.755	.845
		Kurtosis	-1.970	1.741
SiLn+ 24hrs	Mean		.00923	.001496
	95% Confidence	Lower Bound	.00538	
	Interval for Mean	Upper Bound	.01307	
		5% Trimmed Mean	.00918	
		Median	.00880	
		Variance	.000	
		Std. Deviation	.003664	
		Minimum	.005	
		Maximum	.014	
		Range	.009	

		Interquartile Range	.007	
		Skewness	.289	.845
		Kurtosis	-1.816	1.741
SiFnLn+ 24hrs		Mean	.01911	.001246
	95% Confidence	Lower Bound	.01591	
	Interval for Mean	Upper Bound	.02231	
		5% Trimmed Mean	.01908	
		Median	.01799	
		Variance	.000	
		Std. Deviation	.003052	
		Minimum	.016	
		Maximum	.023	
		Range	.007	
		Interquartile Range	.006	
		Skewness	.592	.845
		Kurtosis	-1.644	1.741

7.19: *p* values for fibroblast bioassay-cell area 1 hour

	Pol 1hr	AdFn 1hr	AdLn 1hr	AdFn Ln 1hr	Si- 1hr	SiFn - 1hr	SiLn - 1hr	SiFnL n- 1hr	Si+ 1hr	SiFn + 1hr	SiLn + 1hr	SiFnL n+ 1hr
Pol	-	0.00	0.00	0.004	0.0	0.00	0.00	0.004	0.0	0.00	0.00	0.004
AdFn	-	-	0.01	0.004	■	0.00	■	■	■	0.00	■	■
AdLn	-	-	-	0.004	■	■	0.01	■	■	■	0.00	■
AdFn	-	-	-	-	■	■	■	0.004	■	■	■	0.004
Si-	-	-	-	-	-	0.00	0.00	0.004	0.0	■	■	■
SiFn-	-	-	-	-	-	-	0.00	0.004	■	0.00	■	■
SiLn-	-	-	-	-	-	-	-	0.004	■	■	0.00	■
SiFnL	-	-	-	-	-	-	-	-	■	■	■	0.004
Si+	-	-	-	-	-	-	-	-	-	0.00	0.00	0.004
SiFn+	-	-	-	-	-	-	-	-	-	-	0.00	0.004
SiLn+	-	-	-	-	-	-	-	-	-	-	-	0.004

7.20: *p* values for fibroblast- vinculin per cell 1 hour

	Pol 1hr	AdFn 1hr	AdLn 1hr	AdFnLn 1hr	Si- 1hr	SiFn- 1hr	SiLn- 1hr	SiFnLn- 1hr	Si+ 1hr	SiFn+ 1hr	SiLn+ 1hr	SiFnLn+ 1hr
Pol 1hr	-	0.004	0.004	0.004	0.003	0.004	0.004	0.004	0.201	0.004	0.003	0.004
AdFn 1hr	-	-	0.004	0.004		0.004				0.004		
AdLn 1hr	-	-	-	0.004			0.004				0.004	
AdFnLn 1hr	-	-	-	-				0.004				0.004
Si- 1hr	-	-	-	-	-	0.004	0.004	0.004	0.003			
SiFn- 1hr	-	-	-	-	-	-	0.004	0.004		0.004		
SiLn- 1hr	-	-	-	-	-	-	-	0.004			0.004	
SiFnLn- 1hr	-	-	-	-	-	-	-	-				0.004
Si+ 1hr	-	-	-	-	-	-	-	-	-	0.003	0.003	0.003
SiFn+ 1hr	-	-	-	-	-	-	-	-	-	-	0.004	0.004
SiLn+ 1hr	-	-	-	-	-	-	-	-	-	-	-	0.004

7.21: *p* values for fibroblast bioassay-vinculin per cell area 1 hour

	Pol 1hr	AdFn 1hr	AdLn 1hr	AdFnLn 1hr	Si- 1hr	SiFn- 1hr	SiLn- 1hr	SiFnLn- 1hr	Si+ 1hr	SiFn+ 1hr	SiLn+ 1hr	SiFnLn+ 1hr
Pol 1hr	-	0.004	0.004	0.004	0.016	0.006	0.004	0.004	0.631	0.004	0.004	0.004
AdFn 1hr	-	-	0.004	0.004		0.004				0.004		
AdLn 1hr	-	-	-	0.004			0.004				0.004	
AdFnLn 1hr	-	-	-	-				0.004				0.004
Si- 1hr	-	-	-	-	-	0.004	0.004	0.004	0.004			
SiFn- 1hr	-	-	-	-	-	-	0.025	0.004		0.004		
SiLn- 1hr	-	-	-	-	-	-	-	0.004			0.004	
SiFnLn- 1hr	-	-	-	-	-	-	-	-				0.004
Si+ 1hr	-	-	-	-	-	-	-	-	-	0.004	0.004	0.004
SiFn+ 1hr	-	-	-	-	-	-	-	-	-	-	0.006	0.004
SiLn+ 1hr	-	-	-	-	-	-	-	-	-	-	-	0.004

7.22: *p* values for fibroblast bioassay-cell area 4 hours

	Pol 4hrs	AdFn 4hrs	AdLn 4hrs	AdFnLn 4hrs	Si- 4hrs	SiFn- 4hrs	SiLn- 4hrs	SiFnLn- 4hrs	Si+ 4hrs	SiFn+ 4hrs	SiLn+ 4hrs	SiFnLn+ 4hrs
Pol 4hrs	-	0.004	0.004	0.004	0.004	0.004	0.004	0.004	0.004	0.004	0.004	0.004
AdFn 4hrs	-	-	0.004	0.004		0.004				0.004		
AdLn 4hrs	-	-	-	0.004			0.004				0.004	
AdFnLn 4hrs	-	-	-	-				0.004				0.004
Si- 4hrs	-	-	-	-	-	0.004	0.004	0.004	0.055			
SiFn- 4hrs	-	-	-	-	-	-	0.01	0.004		0.004		
SiLn- 4hrs	-	-	-	-	-	-	-	0.004			0.004	
SiFnLn- 4hrs	-	-	-	-	-	-	-	-				0.004
Si+ 4hrs	-	-	-	-	-	-	-	-	-	0.004	0.004	0.004
SiFn+ 4hrs	-	-	-	-	-	-	-	-	-	-	0.004	0.006
SiLn+ 4hrs	-	-	-	-	-	-	-	-	-	-	-	0.004

7.23: *p* values for fibroblast bioassay-vinculin 4 hours

	Pol 4hrs	AdFn 4hrs	AdLn 4hrs	AdFnLn 4hrs	Si- 4hrs	SiFn- 4hrs	SiLn- 4hrs	SiFnLn- 4hrs	Si+ 4hrs	SiFn+ 4hrs	SiLn+ 4hrs	SiFnLn+ 4hrs
Pol 4hrs	-	0.004	0.004	0.004	0.004	0.004	0.004	0.004	0.004	0.004	0.004	0.004
AdFn 4hrs	-	-	0.004	0.004		0.004				0.004		
AdLn 4hrs	-	-	-	0.004			0.004				0.004	
AdFnLn 4hrs	-	-	-	-				0.004				0.004
Si- 4hrs	-	-	-	-	-	0.004	0.004	0.004	0.004			
SiFn- 4hrs	-	-	-	-	-	-	0.004	0.004		0.004		
SiLn- 4hrs	-	-	-	-	-	-	-	0.004			0.004	
SiFnLn- 4hrs	-	-	-	-	-	-	-	-				0.004
Si+ 4hrs	-	-	-	-	-	-	-	-	-	0.004	0.004	0.004
SiFn+ 4hrs	-	-	-	-	-	-	-	-	-	-	0.004	0.004
SiLn+ 4hrs	-	-	-	-	-	-	-	-	-	-	-	0.004

7.24: *p* values for fibroblast bioassay-vinculin per cell area 4 hours

	Pol 4hrs	AdFn 4hrs	AdLn 4hrs	AdFnLn 4hrs	Si- 4hrs	SiFn- 4hrs	SiLn- 4hrs	SiFnLn- 4hrs	Si+ 4hrs	SiFn+ 4hrs	SiLn+ 4hrs	SiFnLn+ 4hrs
Pol 4hrs	-	0.004	0.004	0.004	0.006	0.004	0.004	0.004	0.004	0.262	0.025	0.004
AdFn 4hrs	-	-	0.004	0.004		0.109				0.004		
AdLn 4hrs	-	-	-	0.004			0.004				0.004	
AdFnLn 4hrs	-	-	-	-				0.004				0.004
Si- 4hrs	-	-	-	-	-	0.004	0.004	0.004	0.004			
SiFn- 4hrs	-	-	-	-	-	-	0.004	0.004		0.004		
SiLn- 4hrs	-	-	-	-	-	-	-	0.004			0.004	
SiFnLn- 4hrs	-	-	-	-	-	-	-	-				0.004
Si+ 4hrs	-	-	-	-	-	-	-	-	-	0.004	0.004	0.004
SiFn+ 4hrs	-	-	-	-	-	-	-	-	-	-	0.109	0.004
SiLn+ 4hrs	-	-	-	-	-	-	-	-	-	-	-	0.004

7.25: *p* values for fibroblast bioassay- cell area 24 hours

	Pol 24hrs	AdFn 24hrs	AdLn 24hrs	AdFnLn 24hrs	Si- 24hrs	SiFn- 24hrs	SiLn- 24hrs	SiFnLn- 24hrs	Si+ 24hrs	SiFn+ 24hrs	SiLn+ 24hrs	SiFnLn+ 24hrs
Pol 24hrs	-	0.004	0.004	0.004	0.004	0.004	0.004	0.004	0.016	0.004	0.004	0.004
AdFn 24hrs	-	-	0.004	0.004	■	0.004	■	■	■	0.004	■	■
AdLn 24hrs	-	-	-	0.004	■	■	0.004	■	■	■	0.004	■
AdFnLn 24hrs	-	-	-	-	■	■	■	0.004	■	■	■	0.004
Si- 24hrs	-	-	-	-	-	0.004	0.004	0.004	0.004	■	■	■
SiFn- 24hrs	-	-	-	-	-	-	0.004	0.004	■	0.004	■	■
SiLn- 24hrs	-	-	-	-	-	-	-	0.004	■	■	0.004	■
SiFnLn- 24hrs	-	-	-	-	-	-	-	-	■	■	■	0.004
Si+ 24hrs	-	-	-	-	-	-	-	-	-	0.004	0.004	0.004
SiFn+ 24hrs	-	-	-	-	-	-	-	-	-	-	0.016	0.423
SiLn+ 24hrs	-	-	-	-	-	-	-	-	-	-	-	0.016

7.26: *p* values for fibroblast bioassay-vinculin 24 hours

	Pol 24hrs	AdFn 24hrs	AdLn 24hrs	AdFnLn 24hrs	Si- 24hrs	SiFn- 24hrs	SiLn- 24hrs	SiFnLn- 24hrs	Si+ 24hrs	SiFn+ 24hrs	SiLn+ 24hrs	SiFnLn+ 24hrs
Pol 24hrs	-	0.003	0.003	0.003	0.003	0.003	0.003	0.003	0.086	0.003	0.008	0.003
AdFn 24hrs	-	-	0.043	0.004	■	0.004	■	■	■	0.004	■	■
AdLn 24hrs	-	-	-	0.004	■	■	0.004	■	■	■	0.004	■
AdFnLn 24hrs	-	-	-	-	■	■	■	0.004	■	■	■	0.004
Si- 24hrs	-	-	-	-	-	0.004	0.004	0.004	0.004	■	■	■
SiFn- 24hrs	-	-	-	-	-	-	0.005	0.004	■	0.004	■	■
SiLn- 24hrs	-	-	-	-	-	-	-	0.004	■	■	0.004	■
SiFnLn- 24hrs	-	-	-	-	-	-	-	-	■	■	■	0.004
Si+ 24hrs	-	-	-	-	-	-	-	-	-	0.004	0.006	0.004
SiFn+ 24hrs	-	-	-	-	-	-	-	-	-	-	0.03	0.015
SiLn+ 24hrs	-	-	-	-	-	-	-	-	-	-	-	0.004

7.27: *p* values for fibroblast bioassay-vinculin per cell area 24 hours

	Pol 24hrs	AdFn 24hrs	AdLn 24hrs	AdFnLn 24hrs	Si- 24hrs	SiFn- 24hrs	SiLn- 24hrs	SiFnLn- 24hrs	Si+ 24hrs	SiFn+ 24hrs	SiLn+ 24hrs	SiFnLn+ 24hrs
Pol 24hrs	-	0.004	0.004	0.004	0.004	0.004	0.004	0.004	0.054	0.016	0.749	0.004
AdFn 24hrs	-	-	0.631	0.004		0.01				0.004		
AdLn 24hrs	-	-	-	0.004			0.078				0.004	
AdFnLn 24hrs	-	-	-	-				0.004				0.004
Si- 24hrs	-	-	-	-	-	0.004	0.004	0.004	0.004			
SiFn- 24hrs	-	-	-	-	-	-	0.025	0.004		0.004		
SiLn- 24hrs	-	-	-	-	-	-	-	0.004			0.004	
SiFnLn- 24hrs	-	-	-	-	-	-	-	-			.004	0.004
Si+ 24hrs	-	-	-	-	-	-	-	-	-	0.004	0.078	0.004
SiFn+ 24hrs	-	-	-	-	-	-	-	-	-	-	0.055	0.016
SiLn+ 24hrs	-	-	-	-	-	-	-	-	-	-	-	0.004

7.28: Keratinocyte cell area 1hour descriptives on different surfaces

	Surface at One Hour			Statistic	Std. Error
Cell Area (micrometres squared)	Pol 1hr	Mean		306.6867	11.75370
		95% Confidence Interval for Mean	Lower Bound	276.4728	
			Upper Bound	336.9005	
		5% Trimmed Mean		306.3991	
		Median		303.5550	
		Variance		828.897	
		Std. Deviation		28.79057	
		Minimum		272.02	
		Maximum		346.53	
		Range		74.51	
		Interquartile Range		56.23	
		Skewness		.287	.845
		Kurtosis		-1.396	1.741
	AdFn 1hr	Mean		524.1333	13.26125
		95% Confidence Interval for Mean	Lower Bound	490.0442	
			Upper Bound	558.2225	
		5% Trimmed Mean		522.5770	
		Median		520.1300	
		Variance		1055.165	
		Std. Deviation		32.48330	
		Minimum		494.27	
		Maximum		582.01	
		Range		87.74	
		Interquartile Range		48.76	
		Skewness		1.260	.845
		Kurtosis		1.706	1.741
	AdLn 1hr	Mean		462.9733	23.73728

		95% Confidence Interval for Mean	Lower Bound	401.9547	
			Upper Bound	523.9920	
		5% Trimmed Mean		461.9231	
		Median		473.3650	
		Variance		3380.751	
		Std. Deviation		58.14423	
		Minimum		394.29	
		Maximum		550.56	
		Range		156.27	
		Interquartile Range		101.78	
		Skewness		.194	.845
		Kurtosis		-.382	1.741
AdFnLn 1hr	Mean			856.0100	16.74587
		95% Confidence Interval for Mean	Lower Bound	812.9634	
			Upper Bound	899.0566	
		5% Trimmed Mean		855.3189	
		Median		846.5050	
		Variance		1682.544	
		Std. Deviation		41.01883	
		Minimum		813.70	
		Maximum		910.76	
		Range		97.06	
		Interquartile Range		85.67	
		Skewness		.512	.845
		Kurtosis		-1.779	1.741
Si- 1hr	Mean			289.4967	10.06019
		95% Confidence Interval for Mean	Lower Bound	263.6361	
			Upper Bound	315.3572	
		5% Trimmed Mean		289.4446	
		Median		287.3700	
		Variance		607.245	
		Std. Deviation		24.64234	

		Minimum	255.76	
		Maximum	324.17	
		Range	68.41	
		Interquartile Range	40.20	
		Skewness	.086	.845
		Kurtosis	-.767	1.741
SiFn- 1hr		Mean	585.8100	13.64070
	95% Confidence	Lower Bound	550.7455	
	Interval for Mean	Upper Bound	620.8745	
		5% Trimmed Mean	585.8156	
		Median	585.9400	
		Variance	1116.412	
		Std. Deviation	33.41274	
		Minimum	541.99	
		Maximum	629.53	
		Range	87.54	
		Interquartile Range	64.28	
		Skewness	-.007	.845
		Kurtosis	-1.404	1.741
SiLn- 1hr		Mean	467.8117	6.97137
	95% Confidence	Lower Bound	449.8912	
	Interval for Mean	Upper Bound	485.7321	
		5% Trimmed Mean	468.1135	
		Median	471.2200	
		Variance	291.600	
		Std. Deviation	17.07629	
		Minimum	440.48	
		Maximum	489.71	
		Range	49.23	
		Interquartile Range	26.66	
		Skewness	-.601	.845
		Kurtosis	.398	1.741
SiFnLn- 1hr		Mean	810.4000	23.41552

	95% Confidence	Lower Bound	750.2085	
	Interval for Mean	Upper Bound	870.5915	
	5% Trimmed Mean		810.4061	
	Median		821.0850	
	Variance		3289.718	
	Std. Deviation		57.35607	
	Minimum		743.04	
	Maximum		877.65	
	Range		134.61	
	Interquartile Range		112.54	
	Skewness		-.211	.845
	Kurtosis		-2.234	1.741
Si+ 1hr	Mean		399.1367	9.08381
	95% Confidence	Lower Bound	375.7860	
	Interval for Mean	Upper Bound	422.4873	
	5% Trimmed Mean		398.0819	
	Median		387.7700	
	Variance		495.094	
	Std. Deviation		22.25070	
	Minimum		381.14	
	Maximum		436.12	
	Range		54.98	
	Interquartile Range		37.58	
	Skewness		1.204	.845
	Kurtosis		-.088	1.741
SiFn+ 1hr	Mean		533.4133	16.11953
	95% Confidence	Lower Bound	491.9768	
	Interval for Mean	Upper Bound	574.8499	
	5% Trimmed Mean		533.2037	
	Median		531.3300	
	Variance		1559.035	
	Std. Deviation		39.48461	

		Minimum	490.96	
		Maximum	579.64	
		Range	88.68	
		Interquartile Range	82.35	
		Skewness	.099	.845
		Kurtosis	-2.445	1.741
SiLn+ 1hr		Mean	463.5100	23.79811
	95% Confidence	Lower Bound	402.3350	
	Interval for Mean	Upper Bound	524.6850	
		5% Trimmed Mean	461.6294	
		Median	449.3900	
		Variance	3398.101	
		Std. Deviation	58.29323	
		Minimum	405.83	
		Maximum	555.04	
		Range	149.21	
		Interquartile Range	111.26	
		Skewness	.800	.845
		Kurtosis	-.588	1.741
SiFnLn+ 1hr		Mean	582.5183	11.28956
	95% Confidence	Lower Bound	553.4976	
	Interval for Mean	Upper Bound	611.5391	
		5% Trimmed Mean	583.3237	
		Median	593.5200	
		Variance	764.725	
		Std. Deviation	27.65366	
		Minimum	541.29	
		Maximum	609.25	
		Range	67.96	
		Interquartile Range	52.10	
		Skewness	-.842	.845
		Kurtosis	-1.277	1.741

7.29: Keratinocyte Vinculin per cell descriptives on different surfaces

	Surface at One Hour			Statistic	Std. Error
Vinculin/Cell	Pol 1hr	Mean		1.0000	.36515
		95% Confidence	Lower Bound	.0614	
		Interval for Mean	Upper Bound	1.9386	
		5% Trimmed Mean		1.0000	
		Median		1.0000	
		Variance		.800	
		Std. Deviation		.89443	
		Minimum		.00	
		Maximum		2.00	
		Range		2.00	
		Interquartile Range		2.00	
		Skewness		.000	.845
		Kurtosis		-1.875	1.741
	AdFn 1hr	Mean		6.0000	.51640
		95% Confidence	Lower Bound	4.6726	
		Interval for Mean	Upper Bound	7.3274	
		5% Trimmed Mean		5.9444	
		Median		5.5000	
		Variance		1.600	
		Std. Deviation		1.26491	
		Minimum		5.00	
		Maximum		8.00	
		Range		3.00	
		Interquartile Range		2.25	
		Skewness		.889	.845
		Kurtosis		-.781	1.741
	AdLn 1hr	Mean		10.5000	.42817
		95% Confidence	Lower Bound	9.3993	

	Interval for Mean	Upper Bound	11.6007	
	5% Trimmed Mean		10.5000	
	Median		10.5000	
	Variance		1.100	
	Std. Deviation		1.04881	
	Minimum		9.00	
	Maximum		12.00	
	Range		3.00	
	Interquartile Range		1.50	
	Skewness		.000	.845
	Kurtosis		-.248	1.741
AdFnLn 1hr	Mean		39.0000	1.46059
	95% Confidence	Lower Bound	35.2454	
	Interval for Mean	Upper Bound	42.7546	
	5% Trimmed Mean		39.0000	
	Median		39.5000	
	Variance		12.800	
	Std. Deviation		3.57771	
	Minimum		34.00	
	Maximum		44.00	
	Range		10.00	
	Interquartile Range		6.25	
	Skewness		-.118	.845
	Kurtosis		-.491	1.741
Si- 1hr	Mean		.6667	.21082
	95% Confidence	Lower Bound	.1247	
	Interval for Mean	Upper Bound	1.2086	
	5% Trimmed Mean		.6852	
	Median		1.0000	
	Variance		.267	
	Std. Deviation		.51640	
	Minimum		.00	

		Maximum	1.00	
		Range	1.00	
		Interquartile Range	1.00	
		Skewness	-.968	.845
		Kurtosis	-1.875	1.741
SiFn- 1hr		Mean	7.5000	.42817
	95% Confidence	Lower Bound	6.3993	
	Interval for Mean	Upper Bound	8.6007	
		5% Trimmed Mean	7.5000	
		Median	7.5000	
		Variance	1.100	
		Std. Deviation	1.04881	
		Minimum	6.00	
		Maximum	9.00	
		Range	3.00	
		Interquartile Range	1.50	
		Skewness	.000	.845
		Kurtosis	-.248	1.741
SiLn- 1hr		Mean	11.6667	.66667
	95% Confidence	Lower Bound	9.9529	
	Interval for Mean	Upper Bound	13.3804	
		5% Trimmed Mean	11.6296	
		Median	11.5000	
		Variance	2.667	
		Std. Deviation	1.63299	
		Minimum	10.00	
		Maximum	14.00	
		Range	4.00	
		Interquartile Range	3.25	
		Skewness	.383	.845
		Kurtosis	-1.481	1.741
SiFnLn- 1hr		Mean	40.1667	.94575
	95% Confidence	Lower Bound	37.7355	

	Interval for Mean	Upper Bound	42.5978	
	5% Trimmed Mean		40.1296	
	Median		40.0000	
	Variance		5.367	
	Std. Deviation		2.31661	
	Minimum		37.00	
	Maximum		44.00	
	Range		7.00	
	Interquartile Range		3.25	
	Skewness		.568	.845
	Kurtosis		1.499	1.741
Si+ 1hr	Mean		.8333	.30732
	95% Confidence	Lower Bound	.0433	
	Interval for Mean	Upper Bound	1.6233	
	5% Trimmed Mean		.8148	
	Median		1.0000	
	Variance		.567	
	Std. Deviation		.75277	
	Minimum		.00	
	Maximum		2.00	
	Range		2.00	
	Interquartile Range		1.25	
	Skewness		.313	.845
	Kurtosis		-.104	1.741
SiFn+ 1hr	Mean		1.5000	.22361
	95% Confidence	Lower Bound	.9252	
	Interval for Mean	Upper Bound	2.0748	
	5% Trimmed Mean		1.5000	
	Median		1.5000	
	Variance		.300	
	Std. Deviation		.54772	
	Minimum		1.00	

		Maximum	2.00	
		Range	1.00	
		Interquartile Range	1.00	
		Skewness	.000	.845
		Kurtosis	-3.333	1.741
SiLn+ 1hr		Mean	.8333	.30732
	95% Confidence	Lower Bound	.0433	
	Interval for Mean	Upper Bound	1.6233	
		5% Trimmed Mean	.8148	
		Median	1.0000	
		Variance	.567	
		Std. Deviation	.75277	
		Minimum	.00	
		Maximum	2.00	
		Range	2.00	
		Interquartile Range	1.25	
		Skewness	.313	.845
		Kurtosis	-.104	1.741
SiFnLn+ 1hr		Mean	3.6667	.33333
	95% Confidence	Lower Bound	2.8098	
	Interval for Mean	Upper Bound	4.5235	
		5% Trimmed Mean	3.6296	
		Median	3.5000	
		Variance	.667	
		Std. Deviation	.81650	
		Minimum	3.00	
		Maximum	5.00	
		Range	2.00	
		Interquartile Range	1.25	
		Skewness	.857	.845
		Kurtosis	-.300	1.741

7.30: Keratinocyte vinculin per cell area descriptives on different surfaces at 1 hour

	Surface at One Hour			Statistic	Std. Error
Vinculin/Cell Area	Pol 1hr	Mean		.00323	.001143
		95% Confidence Interval for Mean	Lower Bound	.00029	
			Upper Bound	.00617	
		5% Trimmed Mean		.00323	
		Median		.00345	
		Variance		.000	
		Std. Deviation		.002799	
		Minimum		.000	
		Maximum		.006	
		Range		.006	
		Interquartile Range		.006	
		Skewness		-.166	.845
		Kurtosis		-1.841	1.741
	AdFn 1hr	Mean		.01143	.000864
		95% Confidence Interval for Mean	Lower Bound	.00920	
			Upper Bound	.01365	
		5% Trimmed Mean		.01139	
		Median		.01093	
		Variance		.000	
		Std. Deviation		.002116	
		Minimum		.009	
		Maximum		.014	
		Range		.005	
		Interquartile Range		.004	
		Skewness		.426	.845
		Kurtosis		-2.214	1.741
	AdLn 1hr	Mean		.02280	.000790

	95% Confidence Interval for Mean	Lower Bound	.02077	
		Upper Bound	.02483	
	5% Trimmed Mean		.02284	
	Median		.02296	
	Variance		.000	
	Std. Deviation		.001935	
	Minimum		.020	
	Maximum		.025	
	Range		.005	
	Interquartile Range		.004	
	Skewness		-.392	.845
	Kurtosis		-1.075	1.741
AdFnLn 1hr	Mean		.04553	.001272
	95% Confidence Interval for Mean	Lower Bound	.04226	
		Upper Bound	.04880	
	5% Trimmed Mean		.04557	
	Median		.04558	
	Variance		.000	
	Std. Deviation		.003116	
	Minimum		.042	
	Maximum		.049	
	Range		.007	
	Interquartile Range		.006	
	Skewness		-.108	.845
	Kurtosis		-2.175	1.741
Si- 1hr	Mean		.00240	.000764
	95% Confidence Interval for Mean	Lower Bound	.00044	
		Upper Bound	.00436	
	5% Trimmed Mean		.00245	
	Median		.00343	
	Variance		.000	
	Std. Deviation		.001871	

		Minimum	.000	
		Maximum	.004	
		Range	.004	
		Interquartile Range	.004	
		Skewness	-.916	.845
		Kurtosis	-1.877	1.741
SiFn- 1hr		Mean	.01281	.000687
	95% Confidence	Lower Bound	.01104	
	Interval for Mean	Upper Bound	.01457	
		5% Trimmed Mean	.01277	
		Median	.01258	
		Variance	.000	
		Std. Deviation	.001684	
		Minimum	.011	
		Maximum	.015	
		Range	.004	
		Interquartile Range	.003	
		Skewness	.378	.845
		Kurtosis	-1.679	1.741
SiLn- 1hr		Mean	.02500	.001612
	95% Confidence	Lower Bound	.02085	
	Interval for Mean	Upper Bound	.02914	
		5% Trimmed Mean	.02484	
		Median	.02461	
		Variance	.000	
		Std. Deviation	.003948	
		Minimum	.021	
		Maximum	.032	
		Range	.011	
		Interquartile Range	.007	
		Skewness	1.009	.845
		Kurtosis	1.058	1.741
SiFnLn- 1hr		Mean	.04970	.001376

	95% Confidence Interval for Mean	Lower Bound	.04616		
		Upper Bound	.05323		
	5% Trimmed Mean		.04971		
	Median		.05001		
	Variance		.000		
	Std. Deviation		.003369		
	Minimum		.046		
	Maximum		.054		
	Range		.008		
	Interquartile Range		.006		
	Skewness		-.122	.845	
	Kurtosis		-2.488	1.741	
Si+ 1hr	Mean		.00174	.000622	
	95% Confidence Interval for Mean	Lower Bound	.00015		
		Upper Bound	.00334		
	5% Trimmed Mean		.00172		
	Median		.00206		
	Variance		.000		
	Std. Deviation		.001523		
	Minimum		.000		
	Maximum		.004		
	Range		.004		
	Interquartile Range		.003		
	Skewness		.039	.845	
	Kurtosis		-.733	1.741	
SiFn+ 1hr	Mean		.00276	.000342	
	95% Confidence Interval for Mean	Lower Bound	.00189		
		Upper Bound	.00364		
	5% Trimmed Mean		.00276		
	Median		.00274		
	Variance		.000		
	Std. Deviation		.000837		

		Minimum	.002	
		Maximum	.004	
		Range	.002	
		Interquartile Range	.002	
		Skewness	.019	.845
		Kurtosis	-3.243	1.741
SiLn+ 1hr		Mean	.00185	.000684
	95% Confidence Interval for Mean	Lower Bound	.00009	
		Upper Bound	.00361	
		5% Trimmed Mean	.00181	
		Median	.00210	
		Variance	.000	
		Std. Deviation	.001675	
		Minimum	.000	
		Maximum	.004	
		Range	.004	
		Interquartile Range	.003	
		Skewness	.310	.845
		Kurtosis	-.220	1.741
SiFnLn+ 1hr		Mean	.00628	.000517
	95% Confidence Interval for Mean	Lower Bound	.00495	
		Upper Bound	.00761	
		5% Trimmed Mean	.00622	
		Median	.00605	
		Variance	.000	
		Std. Deviation	.001266	
		Minimum	.005	
		Maximum	.008	
		Range	.003	
		Interquartile Range	.002	
		Skewness	1.162	.845
		Kurtosis	1.234	1.741

7.31: Keratinocyte cell area descriptives on different surfaces at 4 hours

Surface at Four Hours			Statistic	Std. Error
Cell Area (micrometres squared)	Pol 4hrs	Mean	367.9600	17.44037
		95% Confidence Interval for Mean Lower Bound	323.1281	
		Upper Bound	412.7919	
		5% Trimmed Mean	369.0250	
		Median	376.0200	
		Variance	1825.000	
		Std. Deviation	42.72002	
		Minimum	300.98	
		Maximum	415.77	
		Range	114.79	
		Interquartile Range	78.59	
		Skewness	-.692	.845
		Kurtosis	-.398	1.741
	AdFn 4hrs	Mean	860.9650	18.21252
		95% Confidence Interval for Mean Lower Bound	814.1482	
		Upper Bound	907.7818	
		5% Trimmed Mean	861.6528	
		Median	864.4200	
		Variance	1990.175	
		Std. Deviation	44.61137	
		Minimum	804.81	
		Maximum	904.74	

		Range	99.93	
		Interquartile Range	85.72	
		Skewness	-.169	.845
		Kurtosis	-2.632	1.741
AdLn 4hrs		Mean	799.4717	18.87334
	95% Confidence Interval for Mean	Lower Bound	750.9562	
		Upper Bound	847.9871	
		5% Trimmed Mean	800.1763	
		Median	801.7100	
		Variance	2137.217	
		Std. Deviation	46.23005	
		Minimum	725.02	
		Maximum	861.24	
		Range	136.22	
		Interquartile Range	71.95	
		Skewness	-.489	.845
		Kurtosis	.834	1.741
AdFnLn 4hrs		Mean	1120.7217	26.36353
	95% Confidence Interval for Mean	Lower Bound	1052.9520	
		Upper Bound	1188.4913	
		5% Trimmed Mean	1121.9235	
		Median	1132.1400	
		Variance	4170.215	
		Std. Deviation	64.57720	
		Minimum	1023.77	
		Maximum	1196.04	
		Range	172.27	
		Interquartile Range	120.87	

		Skewness		-.542	.845
		Kurtosis		-.809	1.741
Si- 4hrs	Mean			412.2250	8.86341
	95% Confidence Interval for Mean	Lower Bound		389.4409	
		Upper Bound		435.0091	
	5% Trimmed Mean			412.6306	
	Median			412.9400	
	Variance			471.360	
	Std. Deviation			21.71084	
	Minimum			382.27	
	Maximum			434.88	
	Range			52.61	
	Interquartile Range			42.72	
	Skewness			-.236	.845
	Kurtosis			-1.768	1.741
SiFn- 4hrs	Mean			998.1817	22.97408
	95% Confidence Interval for Mean	Lower Bound		939.1249	
		Upper Bound		1057.2384	
	5% Trimmed Mean			998.1613	
	Median			988.7300	
	Variance			3166.850	
	Std. Deviation			56.27477	
	Minimum			923.42	
	Maximum			1073.31	
	Range			149.89	
	Interquartile Range			106.58	
	Skewness			.209	.845
	Kurtosis			-1.062	1.741

SiLn- 4hrs	Mean		879.0783	17.08980
	95% Confidence Interval for Mean	Lower Bound	835.1476	
		Upper Bound	923.0091	
	5% Trimmed Mean		877.8704	
	Median		867.3750	
	Variance		1752.367	
	Std. Deviation		41.86129	
	Minimum		839.83	
	Maximum		940.07	
	Range		100.24	
	Interquartile Range		76.12	
	Skewness		.561	.845
	Kurtosis		-1.667	1.741
SiFnLn- 4hrs	Mean		1193.5683	10.11880
	95% Confidence Interval for Mean	Lower Bound	1167.5571	
		Upper Bound	1219.5795	
	5% Trimmed Mean		1192.9437	
	Median		1195.2800	
	Variance		614.341	
	Std. Deviation		24.78590	
	Minimum		1167.15	
	Maximum		1231.23	
	Range		64.08	
	Interquartile Range		44.39	
	Skewness		.376	.845
	Kurtosis		-.682	1.741
Si+ 4hrs	Mean		475.3283	14.08938

	95% Confidence Interval for Mean	Lower Bound	439.1104	
		Upper Bound	511.5462	
	5% Trimmed Mean		476.4798	
	Median		477.6800	
	Variance		1191.064	
	Std. Deviation		34.51179	
	Minimum		418.44	
	Maximum		511.49	
	Range		93.05	
	Interquartile Range		57.90	
	Skewness		-.793	.845
	Kurtosis		.263	1.741
SiFn+ 4hrs	Mean		609.0933	9.81691
	95% Confidence Interval for Mean	Lower Bound	583.8582	
		Upper Bound	634.3285	
	5% Trimmed Mean		609.3254	
	Median		608.8600	
	Variance		578.231	
	Std. Deviation		24.04643	
	Minimum		575.05	
	Maximum		638.96	
	Range		63.91	
	Interquartile Range		46.30	
	Skewness		-.153	.845
	Kurtosis		-1.017	1.741
SiLn+ 4hrs	Mean		562.5917	15.32493
	95% Confidence Interval for Mean	Lower Bound	523.1977	

		Upper Bound	601.9856	
	5% Trimmed Mean		562.0896	
	Median		560.9000	
	Variance		1409.120	
	Std. Deviation		37.53825	
	Minimum		516.61	
	Maximum		617.61	
	Range		101.00	
	Interquartile Range		59.37	
	Skewness		.319	.845
	Kurtosis		-1.106	1.741
SiFnLn+ 4hrs	Mean		657.5183	9.95511
	95% Confidence Interval for Mean	Lower Bound	631.9279	
		Upper Bound	683.1088	
	5% Trimmed Mean		657.4070	
	Median		656.7300	
	Variance		594.625	
	Std. Deviation		24.38493	
	Minimum		628.18	
	Maximum		688.86	
	Range		60.68	
	Interquartile Range		42.25	
	Skewness		.083	.845
	Kurtosis		-2.223	1.741

7.32: Keratinocyte vinculin per cell descriptives on different surfaces at 4 hours

Surface at Four Hours			Statistic	Std. Error
Vinculin/Cell Pol 4hrs	Mean		1.5000	.22361
	95% Confidence Interval for Mean	Lower Bound	.9252	
		Upper Bound	2.0748	
	5% Trimmed Mean		1.5000	
	Median		1.5000	
	Variance		.300	
	Std. Deviation		.54772	
	Minimum		1.00	
	Maximum		2.00	
	Range		1.00	
	Interquartile Range		1.00	
	Skewness		.000	.845
	Kurtosis		-3.333	1.741
AdFn 4hrs	Mean		17.1667	.74907
	95% Confidence Interval for Mean	Lower Bound	15.2411	
		Upper Bound	19.0922	
	5% Trimmed Mean		17.1852	
	Median		17.5000	
	Variance		3.367	
	Std. Deviation		1.83485	
	Minimum		15.00	
	Maximum		19.00	

	Range		4.00	
	Interquartile Range		4.00	
	Skewness		-.362	.845
	Kurtosis		-2.103	1.741
AdLn 4hrs	Mean		24.6667	1.14504
	95% Confidence Interval for Mean	Lower Bound	21.7233	
		Upper Bound	27.6101	
	5% Trimmed Mean		24.6852	
	Median		25.0000	
	Variance		7.867	
	Std. Deviation		2.80476	
	Minimum		21.00	
	Maximum		28.00	
	Range		7.00	
	Interquartile Range		5.50	
	Skewness		-.224	.845
	Kurtosis		-1.864	1.741
AdFnLn 4hrs	Mean		52.6667	.80277
	95% Confidence Interval for Mean	Lower Bound	50.6031	
		Upper Bound	54.7303	
	5% Trimmed Mean		52.6852	
	Median		53.0000	
	Variance		3.867	
	Std. Deviation		1.96638	
	Minimum		50.00	
	Maximum		55.00	
	Range		5.00	
	Interquartile Range		3.50	

		Skewness	-.254	.845
		Kurtosis	-1.828	1.741
Si- 4hrs	Mean		1.3333	.21082
	95% Confidence Interval for Mean	Lower Bound	.7914	
		Upper Bound	1.8753	
	5% Trimmed Mean		1.3148	
	Median		1.0000	
	Variance		.267	
	Std. Deviation		.51640	
	Minimum		1.00	
	Maximum		2.00	
	Range		1.00	
	Interquartile Range		1.00	
	Skewness		.968	.845
	Kurtosis		-1.875	1.741
SiFn- 4hrs	Mean		25.1667	1.13774
	95% Confidence Interval for Mean	Lower Bound	22.2420	
		Upper Bound	28.0913	
	5% Trimmed Mean		25.1296	
	Median		25.5000	
	Variance		7.767	
	Std. Deviation		2.78687	
	Minimum		22.00	
	Maximum		29.00	
	Range		7.00	
	Interquartile Range		5.50	
	Skewness		-.006	.845
	Kurtosis		-1.274	1.741

SiLn- 4hrs	Mean		30.6667	1.08525
	95% Confidence Interval for Mean	Lower Bound	27.8769	
		Upper Bound	33.4564	
	5% Trimmed Mean		30.6852	
	Median		31.5000	
	Variance		7.067	
	Std. Deviation		2.65832	
	Minimum		27.00	
	Maximum		34.00	
	Range		7.00	
	Interquartile Range		4.75	
	Skewness		-.422	.845
	Kurtosis		-1.188	1.741
SiFnLn- 4hrs	Mean		61.5000	1.31022
	95% Confidence Interval for Mean	Lower Bound	58.1320	
		Upper Bound	64.8680	
	5% Trimmed Mean		61.5000	
	Median		62.0000	
	Variance		10.300	
	Std. Deviation		3.20936	
	Minimum		57.00	
	Maximum		66.00	
	Range		9.00	
	Interquartile Range		5.25	
	Skewness		-.082	.845
	Kurtosis		-.514	1.741
Si+ 4hrs	Mean		1.5000	.34157

	95% Confidence Interval for Mean	Lower Bound	.6220	
		Upper Bound	2.3780	
	5% Trimmed Mean		1.4444	
	Median		1.0000	
	Variance		.700	
	Std. Deviation		.83666	
	Minimum		1.00	
	Maximum		3.00	
	Range		2.00	
	Interquartile Range		1.25	
	Skewness		1.537	.845
	Kurtosis		1.429	1.741
SiFn+ 4hrs	Mean		4.5000	.22361
	95% Confidence Interval for Mean	Lower Bound	3.9252	
		Upper Bound	5.0748	
	5% Trimmed Mean		4.5000	
	Median		4.5000	
	Variance		.300	
	Std. Deviation		.54772	
	Minimum		4.00	
	Maximum		5.00	
	Range		1.00	
	Interquartile Range		1.00	
	Skewness		.000	.845
	Kurtosis		-3.333	1.741
SiLn+ 4hrs	Mean		1.5000	.34157
	95% Confidence Interval for Mean	Lower Bound	.6220	

		Upper Bound	2.3780	
	5% Trimmed Mean		1.5556	
	Median		2.0000	
	Variance		.700	
	Std. Deviation		.83666	
	Minimum		.00	
	Maximum		2.00	
	Range		2.00	
	Interquartile Range		1.25	
	Skewness		-1.537	.845
	Kurtosis		1.429	1.741
SiFnLn+ 4hrs	Mean		5.5000	.76376
	95% Confidence Interval for Mean	Lower Bound	3.5367	
		Upper Bound	7.4633	
	5% Trimmed Mean		5.5000	
	Median		5.5000	
	Variance		3.500	
	Std. Deviation		1.87083	
	Minimum		3.00	
	Maximum		8.00	
	Range		5.00	
	Interquartile Range		3.50	
	Skewness		.000	.845
	Kurtosis		-1.200	1.741

7.33: Keratinocyte vinculin per cell area descriptives on different surfaces at 4 hours

Surface at Four Hours			Statistic	Std. Error
Vinculin/Cell Area	Pol 4hrs	Mean	.00409	.000600
		95% Confidence Interval for Mean	Lower Bound	.00255	
			Upper Bound	.00563	
		5% Trimmed Mean	.00408	
		Median	.00407	
		Variance	.000	
		Std. Deviation	.001469	
		Minimum	.002	
		Maximum	.006	
		Range	.003	
		Interquartile Range	.003	
		Skewness	.102	.845
		Kurtosis	-2.345	1.741
	AdFn 4hrs	Mean	.01999	.000972
		95% Confidence Interval for Mean	Lower Bound	.01749	
			Upper Bound	.02248	
		5% Trimmed Mean	.02000	
		Median	.02051	
		Variance	.000	
		Std. Deviation	.002380	
		Minimum	.017	
		Maximum	.023	
		Range	.006	

		Interquartile Range	.004	
		Skewness	-.322	.845
		Kurtosis	-.863	1.741
AdLn 4hrs	Mean		.03096	.001683
	95% Confidence Interval for Mean	Lower Bound	.02664	
		Upper Bound	.03529	
	5% Trimmed Mean		.03099	
	Median		.03180	
	Variance		.000	
	Std. Deviation		.004123	
	Minimum		.026	
	Maximum		.036	
	Range		.010	
	Interquartile Range		.008	
	Skewness		-.277	.845
	Kurtosis		-1.888	1.741
AdFnLn 4hrs	Mean		.04713	.001397
	95% Confidence Interval for Mean	Lower Bound	.04354	
		Upper Bound	.05072	
	5% Trimmed Mean		.04707	
	Median		.04644	
	Variance		.000	
	Std. Deviation		.003421	
	Minimum		.043	
	Maximum		.053	
	Range		.010	
	Interquartile Range		.005	
	Skewness		.652	.845
	Kurtosis		.990	1.741
Si- 4hrs	Mean		.00243	.000053

	95% Confidence Interval for Mean	Lower Bound	.00230	
		Upper Bound	.00257	
	5% Trimmed Mean		.00243	
	Median		.00242	
	Variance		.000	
	Std. Deviation		.000129	
	Minimum		.002	
	Maximum		.003	
	Range		.000	
	Interquartile Range		.000	
	Skewness		.340	.845
	Kurtosis		-1.577	1.741
SiFn- 4hrs	Mean		.02531	.001362
	95% Confidence Interval for Mean	Lower Bound	.02180	
		Upper Bound	.02881	
	5% Trimmed Mean		.02536	
	Median		.02614	
	Variance		.000	
	Std. Deviation		.003337	
	Minimum		.020	
	Maximum		.029	
	Range		.009	
	Interquartile Range		.006	
	Skewness		-.498	.845
	Kurtosis		-1.220	1.741
SiLn- 4hrs	Mean		.03490	.001152
	95% Confidence Interval for Mean	Lower Bound	.03194	
		Upper Bound	.03786	
	5% Trimmed Mean		.03491	

	Median		.03534	
	Variance		.000	
	Std. Deviation		.002821	
	Minimum		.032	
	Maximum		.038	
	Range		.007	
	Interquartile Range		.006	
	Skewness		-.217	.845
	Kurtosis		-2.320	1.741
SiFnLn-4hrs	Mean		.05154	.001095
	95% Confidence Interval for Mean	Lower Bound	.04872	
		Upper Bound	.05435	
	5% Trimmed Mean		.05160	
	Median		.05215	
	Variance		.000	
	Std. Deviation		.002682	
	Minimum		.048	
	Maximum		.054	
	Range		.006	
	Interquartile Range		.005	
	Skewness		-.370	.845
	Kurtosis		-2.346	1.741
Si+ 4hrs	Mean		.00381	.000913
	95% Confidence Interval for Mean	Lower Bound	.00146	
		Upper Bound	.00616	
	5% Trimmed Mean		.00367	
	Median		.00259	
	Variance		.000	
	Std. Deviation		.002236	

		Minimum	.002	
		Maximum	.008	
		Range	.005	
		Interquartile Range	.003	
		Skewness	1.495	.845
		Kurtosis	1.252	1.741
SiFn+ 4hrs		Mean	.00741	.000441
	95% Confidence Interval for Mean	Lower Bound	.00628	
		Upper Bound	.00855	
		5% Trimmed Mean	.00741	
		Median	.00747	
		Variance	.000	
		Std. Deviation	.001081	
		Minimum	.006	
		Maximum	.009	
		Range	.002	
		Interquartile Range	.002	
		Skewness	.016	.845
		Kurtosis	-2.744	1.741
SiLn+ 4hrs		Mean	.00267	.000599
	95% Confidence Interval for Mean	Lower Bound	.00113	
		Upper Bound	.00421	
		5% Trimmed Mean	.00276	
		Median	.00334	
		Variance	.000	
		Std. Deviation	.001466	
		Minimum	.000	
		Maximum	.004	
		Range	.004	

		Interquartile Range	.002	
		Skewness	-1.580	.845
		Kurtosis	1.939	1.741
SiFnLn+ 4hrs	Mean		.00841	.001221
	95% Confidence Interval for Mean	Lower Bound	.00527	
		Upper Bound	.01155	
	5% Trimmed Mean		.00841	
	Median		.00816	
	Variance		.000	
	Std. Deviation		.002992	
	Minimum		.004	
	Maximum		.012	
	Range		.008	
	Interquartile Range		.005	
	Skewness		.082	.845
	Kurtosis		-.980	1.741

7.34: Keratinocyte cell area descriptives on different surfaces at 24 hours

	Surface at Twenty Four Hours			Statistic	Std. Error
Cell Area (micrometres squared)	Pol 24hrs	Mean		751.6933	17.33588
		95% Confidence Interval for Mean	Lower Bound	707.1300	
			Upper Bound	796.2566	
		5% Trimmed Mean		753.4204	
		Median		761.0300	
		Variance		1803.197	
		Std. Deviation		42.46407	
		Minimum		676.83	
		Maximum		795.47	
		Range		118.64	
		Interquartile Range		66.29	
		Skewness		-1.214	.845
		Kurtosis		1.525	1.741
	AdFn 24hrs	Mean		1127.9967	12.24533
		95% Confidence Interval for Mean	Lower Bound	1096.5191	
			Upper Bound	1159.4743	
		5% Trimmed Mean		1127.4457	
		Median		1121.5300	
		Variance		899.688	
		Std. Deviation		29.99480	
		Minimum		1097.22	

		Maximum	1168.69	
		Range	71.47	
		Interquartile Range	59.15	
		Skewness	.432	.845
		Kurtosis	-1.989	1.741
AdLn 24hrs	Mean		996.2900	18.16759
	95% Confidence Interval for Mean	Lower Bound	949.5887	
		Upper Bound	1042.9913	
	5% Trimmed Mean		996.3211	
	Median		1001.6900	
	Variance		1980.369	
	Std. Deviation		44.50133	
	Minimum		937.46	
	Maximum		1054.56	
	Range		117.10	
	Interquartile Range		85.75	
	Skewness		-.162	.845
	Kurtosis		-1.253	1.741
AdFnLn 24hrs	Mean		1476.6867	16.62267
	95% Confidence Interval for Mean	Lower Bound	1433.9567	
		Upper Bound	1519.4166	
	5% Trimmed Mean		1477.0513	
	Median		1484.9250	
	Variance		1657.878	
	Std. Deviation		40.71705	
	Minimum		1421.40	

		Maximum	1525.41	
		Range	104.01	
		Interquartile Range	80.35	
		Skewness	-.401	.845
		Kurtosis	-1.451	1.741
Si- 24hrs		Mean	812.8950	23.10229
	95% Confidence Interval for Mean	Lower Bound	753.5087	
		Upper Bound	872.2813	
		5% Trimmed Mean	812.9128	
		Median	821.3450	
		Variance	3202.294	
		Std. Deviation	56.58882	
		Minimum	744.62	
		Maximum	880.85	
		Range	136.23	
		Interquartile Range	110.67	
		Skewness	-.170	.845
		Kurtosis	-2.146	1.741
SiFn- 24hrs		Mean	1267.2500	16.66207
	95% Confidence Interval for Mean	Lower Bound	1224.4188	
		Upper Bound	1310.0812	
		5% Trimmed Mean	1266.9122	
		Median	1260.1900	
		Variance	1665.747	
		Std. Deviation	40.81356	
		Minimum	1220.98	

		Maximum	1319.60	
		Range	98.62	
		Interquartile Range	80.80	
		Skewness	.295	.845
		Kurtosis	-2.067	1.741
SiLn- 24hrs	Mean		1186.4417	11.18697
	95% Confidence Interval for Mean	Lower Bound	1157.6846	
		Upper Bound	1215.1987	
	5% Trimmed Mean		1186.1841	
	Median		1185.9500	
	Variance		750.890	
	Std. Deviation		27.40237	
	Minimum		1152.69	
	Maximum		1224.83	
	Range		72.14	
	Interquartile Range		53.26	
	Skewness		.175	.845
	Kurtosis		-1.159	1.741
SiFnLn-24hrs	Mean		1464.9717	12.21750
	95% Confidence Interval for Mean	Lower Bound	1433.5656	
		Upper Bound	1496.3777	
	5% Trimmed Mean		1464.9685	
	Median		1467.7600	
	Variance		895.603	
	Std. Deviation		29.92664	
	Minimum		1425.49	

		Maximum	1504.51	
		Range	79.02	
		Interquartile Range	58.24	
		Skewness	-.121	.845
		Kurtosis	-1.185	1.741
Si+ 24hrs		Mean	494.2233	13.47255
	95% Confidence Interval for Mean	Lower Bound	459.5911	
		Upper Bound	528.8556	
		5% Trimmed Mean	495.4259	
		Median	502.4750	
		Variance	1089.057	
		Std. Deviation	33.00086	
		Minimum	439.17	
		Maximum	527.63	
		Range	88.46	
		Interquartile Range	56.86	
		Skewness	-.987	.845
		Kurtosis	.297	1.741
SiFn+ 24hrs		Mean	616.5250	14.86409
	95% Confidence Interval for Mean	Lower Bound	578.3156	
		Upper Bound	654.7344	
		5% Trimmed Mean	614.8972	
		Median	601.5450	
		Variance	1325.646	
		Std. Deviation	36.40943	
		Minimum	584.92	

		Maximum	677.43	
		Range	92.51	
		Interquartile Range	62.45	
		Skewness	1.148	.845
		Kurtosis	.099	1.741
SiLn+ 24hrs	Mean		693.1450	24.56269
	95% Confidence Interval for Mean	Lower Bound	630.0046	
		Upper Bound	756.2854	
	5% Trimmed Mean		693.0294	
	Median		705.0700	
	Variance		3619.956	
	Std. Deviation		60.16607	
	Minimum		619.32	
	Maximum		769.05	
	Range		149.73	
	Interquartile Range		116.92	
	Skewness		-.222	.845
	Kurtosis		-1.699	1.741
SiFnLn+ 24hrs	Mean		855.6567	19.41475
	95% Confidence Interval for Mean	Lower Bound	805.7495	
		Upper Bound	905.5639	
	5% Trimmed Mean		856.2730	
	Median		870.7150	
	Variance		2261.594	
	Std. Deviation		47.55622	
	Minimum		796.64	

			Statistic	Std. Error
	Maximum		903.58	
	Range		106.94	
	Interquartile Range		96.04	
	Skewness		-.513	.845
	Kurtosis		-2.144	1.741

7.35: Keratinocyte vinculin per cell descriptives on different surfaces at 24 hours

Surface at Twenty Four Hours			Statistic	Std. Error
Vinculin/Cell Pol 24hrs	Mean		4.0000	.36515
	95% Confidence Interval for Mean	Lower Bound	3.0614	
		Upper Bound	4.9386	
	5% Trimmed Mean		4.0000	
	Median		4.0000	
	Variance		.800	
	Std. Deviation		.89443	
	Minimum		3.00	
	Maximum		5.00	
	Range		2.00	
	Interquartile Range		2.00	
	Skewness		.000	.845
	Kurtosis		-1.875	1.741
AdFn 24hrs	Mean		38.1667	1.01379
	95% Confidence Interval for Mean	Lower Bound	35.5606	
		Upper Bound	40.7727	

316

	5% Trimmed Mean		38.1296	
	Median		38.5000	
	Variance		6.167	
	Std. Deviation		2.48328	
	Minimum		35.00	
	Maximum		42.00	
	Range		7.00	
	Interquartile Range		4.00	
	Skewness		.305	.845
	Kurtosis		-.001	1.741
AdLn 24hrs	Mean		44.5000	1.54380
	95% Confidence Interval for Mean	Lower Bound	40.5315	
		Upper Bound	48.4685	
	5% Trimmed Mean		44.3333	
	Median		44.0000	
	Variance		14.300	
	Std. Deviation		3.78153	
	Minimum		41.00	
	Maximum		51.00	
	Range		10.00	
	Interquartile Range		6.25	
	Skewness		1.049	.845
	Kurtosis		.923	1.741
AdFnLn 24hrs	Mean		92.3333	.76012
	95% Confidence Interval for Mean	Lower Bound	90.3794	
		Upper Bound	94.2873	
	5% Trimmed Mean		92.3148	

	Median		92.0000	
	Variance		3.467	
	Std. Deviation		1.86190	
	Minimum		90.00	
	Maximum		95.00	
	Range		5.00	
	Interquartile Range		3.50	
	Skewness		.392	.845
	Kurtosis		-.943	1.741
Si- 24hrs	Mean		5.5000	.42817
	95% Confidence Interval for Mean	Lower Bound	4.3993	
		Upper Bound	6.6007	
	5% Trimmed Mean		5.5000	
	Median		5.5000	
	Variance		1.100	
	Std. Deviation		1.04881	
	Minimum		4.00	
	Maximum		7.00	
	Range		3.00	
	Interquartile Range		1.50	
	Skewness		.000	.845
	Kurtosis		-.248	1.741
SiFn- 24hrs	Mean		53.6667	2.20101
	95% Confidence Interval for Mean	Lower Bound	48.0088	
		Upper Bound	59.3245	
	5% Trimmed Mean		53.6852	
	Median		54.0000	

		Variance	29.067	
		Std. Deviation	5.39135	
		Minimum	46.00	
		Maximum	61.00	
		Range	15.00	
		Interquartile Range	9.00	
		Skewness	-.116	.845
		Kurtosis	-.708	1.741
SiLn- 24hrs	Mean		60.6667	2.09231
	95% Confidence Interval for Mean	Lower Bound	55.2882	
		Upper Bound	66.0451	
	5% Trimmed Mean		60.5741	
	Median		60.5000	
	Variance		26.267	
	Std. Deviation		5.12510	
	Minimum		55.00	
	Maximum		68.00	
	Range		13.00	
	Interquartile Range		9.25	
	Skewness		.315	.845
	Kurtosis		-1.582	1.741
SiFnLn- 24hrs	Mean		108.8333	1.85143
	95% Confidence Interval for Mean	Lower Bound	104.0741	
		Upper Bound	113.5926	
	5% Trimmed Mean		108.7037	
	Median		108.0000	
	Variance		20.567	

	Std. Deviation		4.53505	
	Minimum		104.00	
	Maximum		116.00	
	Range		12.00	
	Interquartile Range		8.25	
	Skewness		.722	.845
	Kurtosis		-.439	1.741
Si+ 24hrs	Mean		.6667	.21082
	95% Confidence Interval for Mean	Lower Bound	.1247	
		Upper Bound	1.2086	
	5% Trimmed Mean		.6852	
	Median		1.0000	
	Variance		.267	
	Std. Deviation		.51640	
	Minimum		.00	
	Maximum		1.00	
	Range		1.00	
	Interquartile Range		1.00	
	Skewness		-.968	.845
	Kurtosis		-1.875	1.741
SiFn+ 24hrs	Mean		8.8333	.47726
	95% Confidence Interval for Mean	Lower Bound	7.6065	
		Upper Bound	10.0602	
	5% Trimmed Mean		8.8704	
	Median		9.0000	
	Variance		1.367	
	Std. Deviation		1.16905	

	Minimum		7.00	
	Maximum		10.00	
	Range		3.00	
	Interquartile Range		2.25	
	Skewness		-.668	.845
	Kurtosis		-.446	1.741
SiLn+ 24hrs	Mean		5.5000	.56273
	95% Confidence Interval for Mean	Lower Bound	4.0535	
		Upper Bound	6.9465	
	5% Trimmed Mean		5.5000	
	Median		5.5000	
	Variance		1.900	
	Std. Deviation		1.37840	
	Minimum		4.00	
	Maximum		7.00	
	Range		3.00	
	Interquartile Range		3.00	
	Skewness		.000	.845
	Kurtosis		-2.299	1.741
SiFnLn+ 24hrs	Mean		9.1667	.70317
	95% Confidence Interval for Mean	Lower Bound	7.3591	
		Upper Bound	10.9742	
	5% Trimmed Mean		9.1296	
	Median		9.0000	
	Variance		2.967	
	Std. Deviation		1.72240	
	Minimum		7.00	

		Statistic	Std. Error
Maximum		12.00	
Range		5.00	
Interquartile Range		2.75	
Skewness		.678	.845
Kurtosis		.814	1.741

7.36: Keratinocyte vinculin per cell area descriptives on different surfaces at 24 hours

Surface at Twenty Four Hours			Statistic	Std. Error
Vinculin/Cell Area	Pol 24hrs	Mean	.00536	.000564
		95% Confidence Interval for Mean	Lower Bound	.00391	
			Upper Bound	.00681	
		5% Trimmed Mean	.00533	
		Median	.00507	
		Variance	.000	
		Std. Deviation	.001382	
		Minimum	.004	
		Maximum	.007	
		Range	.003	
		Interquartile Range	.003	
		Skewness	.596	.845
		Kurtosis	-1.192	1.741
	AdFn 24hrs	Mean	.03385	.000929
		95% Confidence Interval for Mean	Lower Bound	.03146	
			Upper Bound	.03624	

	5% Trimmed Mean		.03384	
	Median		.03398	
	Variance		.000	
	Std. Deviation		.002275	
	Minimum		.031	
	Maximum		.037	
	Range		.006	
	Interquartile Range		.004	
	Skewness		.020	.845
	Kurtosis		-.735	1.741
AdLn 24hrs	Mean		.04464	.001117
	95% Confidence Interval for Mean	Lower Bound	.04177	
		Upper Bound	.04751	
	5% Trimmed Mean		.04466	
	Median		.04480	
	Variance		.000	
	Std. Deviation		.002736	
	Minimum		.041	
	Maximum		.048	
	Range		.008	
	Interquartile Range		.004	
	Skewness		-.173	.845
	Kurtosis		-.453	1.741
AdFnLn 24hrs	Mean		.06255	.000607
	95% Confidence Interval for Mean	Lower Bound	.06099	
		Upper Bound	.06411	

		5% Trimmed Mean	.06255	
		Median	.06247	
		Variance	.000	
		Std. Deviation	.001486	
		Minimum	.061	
		Maximum	.064	
		Range	.003	
		Interquartile Range	.003	
		Skewness	.076	.845
		Kurtosis	-2.773	1.741
Si- 24hrs	Mean		.00682	.000606
	95% Confidence Interval for Mean	Lower Bound	.00526	
		Upper Bound	.00838	
	5% Trimmed Mean		.00687	
	Median		.00712	
	Variance		.000	
	Std. Deviation		.001484	
	Minimum		.005	
	Maximum		.008	
	Range		.004	
	Interquartile Range		.003	
	Skewness		-.633	.845
	Kurtosis		-1.156	1.741
SiFn- 24hrs	Mean		.04240	.001897
	95% Confidence Interval for Mean	Lower Bound	.03752	
		Upper Bound	.04728	

	5% Trimmed Mean		.04238	
	Median		.04237	
	Variance		.000	
	Std. Deviation		.004646	
	Minimum		.037	
	Maximum		.048	
	Range		.011	
	Interquartile Range		.009	
	Skewness		.027	.845
	Kurtosis		-2.672	1.741
SiLn- 24hrs	Mean		.05116	.001821
	95% Confidence Interval for Mean	Lower Bound	.04648	
		Upper Bound	.05584	
	5% Trimmed Mean		.05118	
	Median		.05223	
	Variance		.000	
	Std. Deviation		.004460	
	Minimum		.046	
	Maximum		.056	
	Range		.011	
	Interquartile Range		.009	
	Skewness		-.305	.845
	Kurtosis		-2.125	1.741
SiFnLn- 24hrs	Mean		.07431	.001393
	95% Confidence Interval for Mean	Lower Bound	.07073	
		Upper Bound	.07790	

	5% Trimmed Mean		.07425	
	Median		.07288	
	Variance		.000	
	Std. Deviation		.003413	
	Minimum		.071	
	Maximum		.079	
	Range		.009	
	Interquartile Range		.006	
	Skewness		.727	.845
	Kurtosis		-1.416	1.741
Si+ 24hrs	Mean		.00133	.000422
	95% Confidence Interval for Mean	Lower Bound	.00025	
		Upper Bound	.00242	
	5% Trimmed Mean		.00136	
	Median		.00193	
	Variance		.000	
	Std. Deviation		.001034	
	Minimum		.000	
	Maximum		.002	
	Range		.002	
	Interquartile Range		.002	
	Skewness		-.948	.845
	Kurtosis		-1.874	1.741
SiFn+ 24hrs	Mean		.01443	.001018
	95% Confidence Interval for Mean	Lower Bound	.01181	
		Upper Bound	.01705	

	5% Trimmed Mean		.01449	
	Median		.01526	
	Variance		.000	
	Std. Deviation		.002495	
	Minimum		.011	
	Maximum		.017	
	Range		.006	
	Interquartile Range		.005	
	Skewness		-.728	.845
	Kurtosis		-1.525	1.741
SiLn+ 24hrs	Mean		.00812	.001091
	95% Confidence Interval for Mean	Lower Bound	.00531	
		Upper Bound	.01092	
	5% Trimmed Mean		.00810	
	Median		.00779	
	Variance		.000	
	Std. Deviation		.002673	
	Minimum		.005	
	Maximum		.011	
	Range		.006	
	Interquartile Range		.006	
	Skewness		.258	.845
	Kurtosis		-1.976	1.741
SiFnLn+ 24hrs	Mean		.01071	.000745
	95% Confidence Interval for Mean	Lower Bound	.00879	
		Upper Bound	.01262	

		Statistic	Std. Error
5% Trimmed Mean		.01070	
Median		.01123	
Variance		.000	
Std. Deviation		.001826	
Minimum		.008	
Maximum		.013	
Range		.005	
Interquartile Range		.003	
Skewness		-.152	.845
Kurtosis		-.476	1.741

7.37: Keratinocyte cell area descriptives on different surfaces

Polished Surface			Statistic	Std. Error
Cell Area (micrometres squared)	Pol 1hr	Mean	306.6867	11.75370
		95% Confidence Interval for Mean — Lower Bound	276.4728	
		95% Confidence Interval for Mean — Upper Bound	336.9005	
		5% Trimmed Mean	306.3991	
		Median	303.5550	
		Variance	828.897	
		Std. Deviation	28.79057	
		Minimum	272.02	
		Maximum	346.53	
		Range	74.51	

		Interquartile Range	56.23	
		Skewness	.287	.845
		Kurtosis	-1.396	1.741
Pol 4hrs		Mean	367.9600	17.44037
	95% Confidence Interval for Mean	Lower Bound	323.1281	
		Upper Bound	412.7919	
		5% Trimmed Mean	369.0250	
		Median	376.0200	
		Variance	1825.000	
		Std. Deviation	42.72002	
		Minimum	300.98	
		Maximum	415.77	
		Range	114.79	
		Interquartile Range	78.59	
		Skewness	-.692	.845
		Kurtosis	-.398	1.741
Pol 24hrs		Mean	751.6933	17.33588
	95% Confidence Interval for Mean	Lower Bound	707.1300	
		Upper Bound	796.2566	
		5% Trimmed Mean	753.4204	
		Median	761.0300	
		Variance	1803.197	
		Std. Deviation	42.46407	
		Minimum	676.83	
		Maximum	795.47	
		Range	118.64	

		Interquartile Range	66.29	
		Skewness	-1.214	.845
		Kurtosis	1.525	1.741
AdFn 1hr		Mean	524.1333	13.26125
	95% Confidence Interval for Mean	Lower Bound	490.0442	
		Upper Bound	558.2225	
		5% Trimmed Mean	522.5770	
		Median	520.1300	
		Variance	1055.165	
		Std. Deviation	32.48330	
		Minimum	494.27	
		Maximum	582.01	
		Range	87.74	
		Interquartile Range	48.76	
		Skewness	1.260	.845
		Kurtosis	1.706	1.741
AdFn 4hrs		Mean	860.9650	18.21252
	95% Confidence Interval for Mean	Lower Bound	814.1482	
		Upper Bound	907.7818	
		5% Trimmed Mean	861.6528	
		Median	864.4200	
		Variance	1990.175	
		Std. Deviation	44.61137	
		Minimum	804.81	
		Maximum	904.74	
		Range	99.93	

		Interquartile Range	85.72	
		Skewness	-.169	.845
		Kurtosis	-2.632	1.741
AdFn 24hrs	Mean		1127.9967	12.24533
	95% Confidence Interval for Mean	Lower Bound	1096.5191	
		Upper Bound	1159.4743	
	5% Trimmed Mean		1127.4457	
	Median		1121.5300	
	Variance		899.688	
	Std. Deviation		29.99480	
	Minimum		1097.22	
	Maximum		1168.69	
	Range		71.47	
	Interquartile Range		59.15	
	Skewness		.432	.845
	Kurtosis		-1.989	1.741
AdLn 1hr	Mean		462.9733	23.73728
	95% Confidence Interval for Mean	Lower Bound	401.9547	
		Upper Bound	523.9920	
	5% Trimmed Mean		461.9231	
	Median		473.3650	
	Variance		3380.751	
	Std. Deviation		58.14423	
	Minimum		394.29	
	Maximum		550.56	
	Range		156.27	

		Interquartile Range	101.78	
		Skewness	.194	.845
		Kurtosis	-.382	1.741
AdLn 4hrs	Mean		799.4717	18.87334
	95% Confidence Interval for Mean	Lower Bound	750.9562	
		Upper Bound	847.9871	
	5% Trimmed Mean		800.1763	
	Median		801.7100	
	Variance		2137.217	
	Std. Deviation		46.23005	
	Minimum		725.02	
	Maximum		861.24	
	Range		136.22	
	Interquartile Range		71.95	
	Skewness		-.489	.845
	Kurtosis		.834	1.741
AdLn 24hrs	Mean		996.2900	18.16759
	95% Confidence Interval for Mean	Lower Bound	949.5887	
		Upper Bound	1042.9913	
	5% Trimmed Mean		996.3211	
	Median		1001.6900	
	Variance		1980.369	
	Std. Deviation		44.50133	
	Minimum		937.46	
	Maximum		1054.56	
	Range		117.10	

		Interquartile Range	85.75	
		Skewness	-.162	.845
		Kurtosis	-1.253	1.741
AdFn/Ln 1hr		Mean	856.0100	16.74587
	95% Confidence Interval for Mean	Lower Bound	812.9634	
		Upper Bound	899.0566	
		5% Trimmed Mean	855.3189	
		Median	846.5050	
		Variance	1682.544	
		Std. Deviation	41.01883	
		Minimum	813.70	
		Maximum	910.76	
		Range	97.06	
		Interquartile Range	85.67	
		Skewness	.512	.845
		Kurtosis	-1.779	1.741
AdFn/Ln 4hrs		Mean	1120.7217	26.36353
	95% Confidence Interval for Mean	Lower Bound	1052.9520	
		Upper Bound	1188.4913	
		5% Trimmed Mean	1121.9235	
		Median	1132.1400	
		Variance	4170.215	
		Std. Deviation	64.57720	
		Minimum	1023.77	
		Maximum	1196.04	
		Range	172.27	

				Statistic	Std. Error
		Interquartile Range		120.87	
		Skewness		-.542	.845
		Kurtosis		-.809	1.741
	AdFn/Ln 24hrs	Mean		1476.6867	16.62267
		95% Confidence Interval for Mean	Lower Bound	1433.9567	
			Upper Bound	1519.4166	
		5% Trimmed Mean		1477.0513	
		Median		1484.9250	
		Variance		1657.878	
		Std. Deviation		40.71705	
		Minimum		1421.40	
		Maximum		1525.41	
		Range		104.01	
		Interquartile Range		80.35	
		Skewness		-.401	.845
		Kurtosis		-1.451	1.741

7.38: Keratinocyte vinculin per cell descriptives on different surfaces

Polished Surface				Statistic	Std. Error
Vinculin/Cell	Pol 1hr	Mean		1.0000	.36515
		95% Confidence Interval for Mean	Lower Bound	.0614	
			Upper Bound	1.9386	
		5% Trimmed Mean		1.0000	
		Median		1.0000	

	Variance		.800	
	Std. Deviation		.89443	
	Minimum		.00	
	Maximum		2.00	
	Range		2.00	
	Interquartile Range		2.00	
	Skewness		.000	.845
	Kurtosis		-1.875	1.741
Pol 4hrs	Mean		1.5000	.22361
	95% Confidence Interval for Mean	Lower Bound	.9252	
		Upper Bound	2.0748	
	5% Trimmed Mean		1.5000	
	Median		1.5000	
	Variance		.300	
	Std. Deviation		.54772	
	Minimum		1.00	
	Maximum		2.00	
	Range		1.00	
	Interquartile Range		1.00	
	Skewness		.000	.845
	Kurtosis		-3.333	1.741
Pol 24hrs	Mean		4.0000	.36515
	95% Confidence Interval for Mean	Lower Bound	3.0614	
		Upper Bound	4.9386	
	5% Trimmed Mean		4.0000	
	Median		4.0000	

		Variance	.800	
		Std. Deviation	.89443	
		Minimum	3.00	
		Maximum	5.00	
		Range	2.00	
		Interquartile Range	2.00	
		Skewness	.000	.845
		Kurtosis	-1.875	1.741
AdFn 1hr	Mean		6.0000	.51640
	95% Confidence Interval for Mean	Lower Bound	4.6726	
		Upper Bound	7.3274	
	5% Trimmed Mean		5.9444	
	Median		5.5000	
	Variance		1.600	
	Std. Deviation		1.26491	
	Minimum		5.00	
	Maximum		8.00	
	Range		3.00	
	Interquartile Range		2.25	
	Skewness		.889	.845
	Kurtosis		-.781	1.741
AdFn 4hrs	Mean		17.1667	.74907
	95% Confidence Interval for Mean	Lower Bound	15.2411	
		Upper Bound	19.0922	
	5% Trimmed Mean		17.1852	
	Median		17.5000	

		Variance	3.367	
		Std. Deviation	1.83485	
		Minimum	15.00	
		Maximum	19.00	
		Range	4.00	
		Interquartile Range	4.00	
		Skewness	-.362	.845
		Kurtosis	-2.103	1.741
AdFn 24hrs		Mean	38.1667	1.01379
	95% Confidence Interval for Mean	Lower Bound	35.5606	
		Upper Bound	40.7727	
		5% Trimmed Mean	38.1296	
		Median	38.5000	
		Variance	6.167	
		Std. Deviation	2.48328	
		Minimum	35.00	
		Maximum	42.00	
		Range	7.00	
		Interquartile Range	4.00	
		Skewness	.305	.845
		Kurtosis	-.001	1.741
AdLn 1hr		Mean	10.5000	.42817
	95% Confidence Interval for Mean	Lower Bound	9.3993	
		Upper Bound	11.6007	
		5% Trimmed Mean	10.5000	
		Median	10.5000	

		Variance	1.100	
		Std. Deviation	1.04881	
		Minimum	9.00	
		Maximum	12.00	
		Range	3.00	
		Interquartile Range	1.50	
		Skewness	.000	.845
		Kurtosis	-.248	1.741
AdLn 4hrs		Mean	24.6667	1.14504
	95% Confidence Interval for Mean	Lower Bound	21.7233	
		Upper Bound	27.6101	
		5% Trimmed Mean	24.6852	
		Median	25.0000	
		Variance	7.867	
		Std. Deviation	2.80476	
		Minimum	21.00	
		Maximum	28.00	
		Range	7.00	
		Interquartile Range	5.50	
		Skewness	-.224	.845
		Kurtosis	-1.864	1.741
AdLn 24hrs		Mean	44.5000	1.54380
	95% Confidence Interval for Mean	Lower Bound	40.5315	
		Upper Bound	48.4685	
		5% Trimmed Mean	44.3333	
		Median	44.0000	

338

		Variance		14.300	
		Std. Deviation		3.78153	
		Minimum		41.00	
		Maximum		51.00	
		Range		10.00	
		Interquartile Range		6.25	
		Skewness		1.049	.845
		Kurtosis		.923	1.741
AdFn/Ln 1hr	Mean		39.0000	1.46059
	95% Confidence Interval for Mean	Lower Bound	35.2454	
		Upper Bound	42.7546	
	5% Trimmed Mean		39.0000	
	Median		39.5000	
	Variance		12.800	
	Std. Deviation		3.57771	
	Minimum		34.00	
	Maximum		44.00	
	Range		10.00	
	Interquartile Range		6.25	
	Skewness		-.118	.845
	Kurtosis		-.491	1.741
AdFn/Ln 4hrs	Mean		52.6667	.80277
	95% Confidence Interval for Mean	Lower Bound	50.6031	
		Upper Bound	54.7303	
	5% Trimmed Mean		52.6852	
	Median		53.0000	

		Variance	3.867	
		Std. Deviation	1.96638	
		Minimum	50.00	
		Maximum	55.00	
		Range	5.00	
		Interquartile Range	3.50	
		Skewness	-.254	.845
		Kurtosis	-1.828	1.741
AdFn/Ln 24hrs		Mean	92.3333	.76012
	95% Confidence Interval for Mean	Lower Bound	90.3794	
		Upper Bound	94.2873	
		5% Trimmed Mean	92.3148	
		Median	92.0000	
		Variance	3.467	
		Std. Deviation	1.86190	
		Minimum	90.00	
		Maximum	95.00	
		Range	5.00	
		Interquartile Range	3.50	
		Skewness	.392	.845
		Kurtosis	-.943	1.741

7.39: Keratinocyte vinculin per cell area descriptives on different surfaces

	Polished Surface			Statistic	Std. Error
Vinculin/Cell Area	Pol 1hr	Mean		.00323	.001143
		95% Confidence	Lower Bound	.00029	
		Interval for Mean	Upper Bound	.00617	
		5% Trimmed Mean		.00323	
		Median		.00345	
		Variance		.000	
		Std. Deviation		.002799	
		Minimum		.000	
		Maximum		.006	
		Range		.006	
		Interquartile Range		.006	
		Skewness		-.166	.845
		Kurtosis		-1.841	1.741
	Pol 4hrs	Mean		.00409	.000600
		95% Confidence	Lower Bound	.00255	
		Interval for Mean	Upper Bound	.00563	
		5% Trimmed Mean		.00408	
		Median		.00407	
		Variance		.000	
		Std. Deviation		.001469	
		Minimum		.002	
		Maximum		.006	
		Range		.003	
		Interquartile Range		.003	
		Skewness		.102	.845
		Kurtosis		-2.345	1.741
	Pol 24hrs	Mean		.00536	.000564
		95% Confidence	Lower Bound	.00391	

	Interval for Mean	Upper Bound	.00681	
	5% Trimmed Mean		.00533	
	Median		.00507	
	Variance		.000	
	Std. Deviation		.001382	
	Minimum		.004	
	Maximum		.007	
	Range		.003	
	Interquartile Range		.003	
	Skewness		.596	.845
	Kurtosis		-1.192	1.741
AdFn 1hr	Mean		.01143	.000864
	95% Confidence	Lower Bound	.00920	
	Interval for Mean	Upper Bound	.01365	
	5% Trimmed Mean		.01139	
	Median		.01093	
	Variance		.000	
	Std. Deviation		.002116	
	Minimum		.009	
	Maximum		.014	
	Range		.005	
	Interquartile Range		.004	
	Skewness		.426	.845
	Kurtosis		-2.214	1.741
AdFn 4hrs	Mean		.03464	.000768
	95% Confidence	Lower Bound	.03266	
	Interval for Mean	Upper Bound	.03661	
	5% Trimmed Mean		.03468	
	Median		.03470	
	Variance		.000	
	Std. Deviation		.001881	
	Minimum		.032	

		Maximum	.036	
		Range	.004	
		Interquartile Range	.003	
		Skewness	-.317	.845
		Kurtosis	-1.985	1.741
AdFn 24hrs	Mean		.04035	.002041
	95% Confidence	Lower Bound	.03510	
	Interval for Mean	Upper Bound	.04559	
	5% Trimmed Mean		.04044	
	Median		.04112	
	Variance		.000	
	Std. Deviation		.004998	
	Minimum		.033	
	Maximum		.046	
	Range		.013	
	Interquartile Range		.009	
	Skewness		-.435	.845
	Kurtosis		-1.476	1.741
AdLn 1hr	Mean		.02280	.000790
	95% Confidence	Lower Bound	.02077	
	Interval for Mean	Upper Bound	.02483	
	5% Trimmed Mean		.02284	
	Median		.02296	
	Variance		.000	
	Std. Deviation		.001935	
	Minimum		.020	
	Maximum		.025	
	Range		.005	
	Interquartile Range		.004	
	Skewness		-.392	.845
	Kurtosis		-1.075	1.741
AdLn 4hrs	Mean		.03096	.001683
	95% Confidence	Lower Bound	.02664	

	Interval for Mean	Upper Bound	.03529	
	5% Trimmed Mean		.03099	
	Median		.03180	
	Variance		.000	
	Std. Deviation		.004123	
	Minimum		.026	
	Maximum		.036	
	Range		.010	
	Interquartile Range		.008	
	Skewness		-.277	.845
	Kurtosis		-1.888	1.741
AdLn 24hrs	Mean		.04464	.001117
	95% Confidence	Lower Bound	.04177	
	Interval for Mean	Upper Bound	.04751	
	5% Trimmed Mean		.04466	
	Median		.04480	
	Variance		.000	
	Std. Deviation		.002736	
	Minimum		.041	
	Maximum		.048	
	Range		.008	
	Interquartile Range		.004	
	Skewness		-.173	.845
	Kurtosis		-.453	1.741
AdFn/Ln 1hr	Mean		.04553	.001272
	95% Confidence	Lower Bound	.04226	
	Interval for Mean	Upper Bound	.04880	
	5% Trimmed Mean		.04557	
	Median		.04558	
	Variance		.000	
	Std. Deviation		.003116	
	Minimum		.042	

		Maximum	.049	
		Range	.007	
		Interquartile Range	.006	
		Skewness	-.108	.845
		Kurtosis	-2.175	1.741
AdFn/Ln 4hrs	Mean		.04713	.001397
	95% Confidence	Lower Bound	.04354	
	Interval for Mean	Upper Bound	.05072	
	5% Trimmed Mean		.04707	
	Median		.04644	
	Variance		.000	
	Std. Deviation		.003421	
	Minimum		.043	
	Maximum		.053	
	Range		.010	
	Interquartile Range		.005	
	Skewness		.652	.845
	Kurtosis		.990	1.741
AdFn/Ln 24hrs	Mean		.06255	.000607
	95% Confidence	Lower Bound	.06099	
	Interval for Mean	Upper Bound	.06411	
	5% Trimmed Mean		.06255	
	Median		.06247	
	Variance		.000	
	Std. Deviation		.001486	
	Minimum		.061	
	Maximum		.064	
	Range		.003	
	Interquartile Range		.003	
	Skewness		.076	.845
	Kurtosis		-2.773	1.741

7.40: Keratinocyte cell area descriptives on salinized non-passivated surfaces

	Silanized, non-Passivated Surface		Statistic	Std. Error
Cell Area (micrometres squared)	Si- 1hr	Mean	289.4967	10.06019
		95% Confidence Interval for Mean — Lower Bound	263.6361	
		95% Confidence Interval for Mean — Upper Bound	315.3572	
		5% Trimmed Mean	289.4446	
		Median	287.3700	
		Variance	607.245	
		Std. Deviation	24.64234	
		Minimum	255.76	
		Maximum	324.17	
		Range	68.41	
		Interquartile Range	40.20	
		Skewness	.086	.845
		Kurtosis	-.767	1.741
	Si-4 hrs	Mean	412.2250	8.86341
		95% Confidence Interval for Mean — Lower Bound	389.4409	
		95% Confidence Interval for Mean — Upper Bound	435.0091	
		5% Trimmed Mean	412.6306	
		Median	412.9400	
		Variance	471.360	
		Std. Deviation	21.71084	
		Minimum	382.27	
		Maximum	434.88	

		Range	52.61	
		Interquartile Range	42.72	
		Skewness	-.236	.845
		Kurtosis	-1.768	1.741
Si- 24hrs		Mean	812.8950	23.10229
	95% Confidence Interval for Mean	Lower Bound	753.5087	
		Upper Bound	872.2813	
		5% Trimmed Mean	812.9128	
		Median	821.3450	
		Variance	3202.294	
		Std. Deviation	56.58882	
		Minimum	744.62	
		Maximum	880.85	
		Range	136.23	
		Interquartile Range	110.67	
		Skewness	-.170	.845
		Kurtosis	-2.146	1.741
SiFn- 1hr		Mean	585.8100	13.64070
	95% Confidence Interval for Mean	Lower Bound	550.7455	
		Upper Bound	620.8745	
		5% Trimmed Mean	585.8156	
		Median	585.9400	
		Variance	1116.412	
		Std. Deviation	33.41274	
		Minimum	541.99	
		Maximum	629.53	
		Range	87.54	
		Interquartile Range	64.27	

		Skewness	-.007	.845
		Kurtosis	-1.404	1.741
SiFn- 4hrs		Mean	998.1817	22.97408
	95% Confidence Interval for Mean	Lower Bound	939.1249	
		Upper Bound	1057.2384	
		5% Trimmed Mean	998.1613	
		Median	988.7300	
		Variance	3166.850	
		Std. Deviation	56.27477	
		Minimum	923.42	
		Maximum	1073.31	
		Range	149.89	
		Interquartile Range	106.58	
		Skewness	.209	.845
		Kurtosis	-1.062	1.741
SiFn- 24hrs		Mean	1267.2500	16.66207
	95% Confidence Interval for Mean	Lower Bound	1224.4188	
		Upper Bound	1310.0812	
		5% Trimmed Mean	1266.9122	
		Median	1260.1900	
		Variance	1665.747	
		Std. Deviation	40.81356	
		Minimum	1220.98	
		Maximum	1319.60	
		Range	98.62	
		Interquartile Range	80.80	
		Skewness	.295	.845
		Kurtosis	-2.067	1.741

SiLn- 1hr	Mean		467.8117	6.97137
	95% Confidence Interval for Mean	Lower Bound	449.8912	
		Upper Bound	485.7321	
	5% Trimmed Mean		468.1135	
	Median		471.2200	
	Variance		291.600	
	Std. Deviation		17.07629	
	Minimum		440.48	
	Maximum		489.71	
	Range		49.23	
	Interquartile Range		26.66	
	Skewness		-.601	.845
	Kurtosis		.398	1.741
SiLn- 4hrs	Mean		879.0783	17.08980
	95% Confidence Interval for Mean	Lower Bound	835.1476	
		Upper Bound	923.0091	
	5% Trimmed Mean		877.8704	
	Median		867.3750	
	Variance		1752.367	
	Std. Deviation		41.86129	
	Minimum		839.83	
	Maximum		940.07	
	Range		100.24	
	Interquartile Range		76.12	
	Skewness		.561	.845
	Kurtosis		-1.667	1.741
SiLn- 24hrs	Mean		1186.4417	11.18697

	95% Confidence Interval for Mean	Lower Bound	1157.6846	
		Upper Bound	1215.1987	
	5% Trimmed Mean		1186.1841	
	Median		1185.9500	
	Variance		750.890	
	Std. Deviation		27.40237	
	Minimum		1152.69	
	Maximum		1224.83	
	Range		72.14	
	Interquartile Range		53.26	
	Skewness		.175	.845
	Kurtosis		-1.159	1.741
SiFnLn- 1hr	Mean		810.4000	23.41552
	95% Confidence Interval for Mean	Lower Bound	750.2085	
		Upper Bound	870.5915	
	5% Trimmed Mean		810.4061	
	Median		821.0850	
	Variance		3289.718	
	Std. Deviation		57.35607	
	Minimum		743.04	
	Maximum		877.65	
	Range		134.61	
	Interquartile Range		112.54	
	Skewness		-.211	.845
	Kurtosis		-2.234	1.741
SiFnLn- 4hrs	Mean		1193.5683	10.11880
	95% Confidence Interval	Lower Bound	1167.5571	

		Interval for Mean Upper Bound	1219.5795	
		5% Trimmed Mean	1192.9437	
		Median	1195.2800	
		Variance	614.341	
		Std. Deviation	24.78590	
		Minimum	1167.15	
		Maximum	1231.23	
		Range	64.08	
		Interquartile Range	44.39	
		Skewness	.376	.845
		Kurtosis	-.682	1.741
SiFnLn-24hrs		Mean	1464.9717	12.21750
	95% Confidence Interval for Mean	Lower Bound	1433.5656	
		Upper Bound	1496.3777	
		5% Trimmed Mean	1464.9685	
		Median	1467.7600	
		Variance	895.603	
		Std. Deviation	29.92664	
		Minimum	1425.49	
		Maximum	1504.51	
		Range	79.02	
		Interquartile Range	58.24	
		Skewness	-.121	.845
		Kurtosis	-1.185	1.741

7.41: Keratinocyte vinculin per cell descriptives on salinized non-passivated surfaces

Silanized, non-Passivated Surface			Statistic	Std. Error
Vinculin/Cell Si- 1hr	Mean		.6667	.21082
	95% Confidence Interval for Mean	Lower Bound	.1247	
		Upper Bound	1.2086	
	5% Trimmed Mean		.6852	
	Median		1.0000	
	Variance		.267	
	Std. Deviation		.51640	
	Minimum		.00	
	Maximum		1.00	
	Range		1.00	
	Interquartile Range		1.00	
	Skewness		-.968	.845
	Kurtosis		-1.875	1.741
Si-4 hrs	Mean		1.3333	.21082
	95% Confidence Interval for Mean	Lower Bound	.7914	
		Upper Bound	1.8753	
	5% Trimmed Mean		1.3148	
	Median		1.0000	
	Variance		.267	
	Std. Deviation		.51640	
	Minimum		1.00	
	Maximum		2.00	

	Range		1.00	
	Interquartile Range		1.00	
	Skewness		.968	.845
	Kurtosis		-1.875	1.741
Si- 24hrs	Mean		5.5000	.42817
	95% Confidence Interval for Mean	Lower Bound	4.3993	
		Upper Bound	6.6007	
	5% Trimmed Mean		5.5000	
	Median		5.5000	
	Variance		1.100	
	Std. Deviation		1.04881	
	Minimum		4.00	
	Maximum		7.00	
	Range		3.00	
	Interquartile Range		1.50	
	Skewness		.000	.845
	Kurtosis		-.248	1.741
SiFn- 1hr	Mean		7.5000	.42817
	95% Confidence Interval for Mean	Lower Bound	6.3993	
		Upper Bound	8.6007	
	5% Trimmed Mean		7.5000	
	Median		7.5000	
	Variance		1.100	
	Std. Deviation		1.04881	
	Minimum		6.00	
	Maximum		9.00	
	Range		3.00	

		Interquartile Range	1.50	
		Skewness	.000	.845
		Kurtosis	-.248	1.741
SiFn- 4hrs	Mean		25.1667	1.13774
	95% Confidence Interval for Mean	Lower Bound	22.2420	
		Upper Bound	28.0913	
	5% Trimmed Mean		25.1296	
	Median		25.5000	
	Variance		7.767	
	Std. Deviation		2.78687	
	Minimum		22.00	
	Maximum		29.00	
	Range		7.00	
	Interquartile Range		5.50	
	Skewness		-.006	.845
	Kurtosis		-1.274	1.741
SiFn- 24hrs	Mean		53.6667	2.20101
	95% Confidence Interval for Mean	Lower Bound	48.0088	
		Upper Bound	59.3245	
	5% Trimmed Mean		53.6852	
	Median		54.0000	
	Variance		29.067	
	Std. Deviation		5.39135	
	Minimum		46.00	
	Maximum		61.00	
	Range		15.00	
	Interquartile Range		9.00	

		Skewness	-.116	.845
		Kurtosis	-.708	1.741
SiLn- 1hr	Mean		11.6667	.66667
	95% Confidence Interval for Mean	Lower Bound	9.9529	
		Upper Bound	13.3804	
	5% Trimmed Mean		11.6296	
	Median		11.5000	
	Variance		2.667	
	Std. Deviation		1.63299	
	Minimum		10.00	
	Maximum		14.00	
	Range		4.00	
	Interquartile Range		3.25	
	Skewness		.383	.845
	Kurtosis		-1.481	1.741
SiLn- 4hrs	Mean		30.6667	1.08525
	95% Confidence Interval for Mean	Lower Bound	27.8769	
		Upper Bound	33.4564	
	5% Trimmed Mean		30.6852	
	Median		31.5000	
	Variance		7.067	
	Std. Deviation		2.65832	
	Minimum		27.00	
	Maximum		34.00	
	Range		7.00	
	Interquartile Range		4.75	
	Skewness		-.422	.845
	Kurtosis		-1.188	1.741

SiLn- 24hrs	Mean		60.6667	2.09231
	95% Confidence Interval for Mean	Lower Bound	55.2882	
		Upper Bound	66.0451	
	5% Trimmed Mean		60.5741	
	Median		60.5000	
	Variance		26.267	
	Std. Deviation		5.12510	
	Minimum		55.00	
	Maximum		68.00	
	Range		13.00	
	Interquartile Range		9.25	
	Skewness		.315	.845
	Kurtosis		-1.582	1.741
SiFnLn- 1hr	Mean		40.1667	.94575
	95% Confidence Interval for Mean	Lower Bound	37.7355	
		Upper Bound	42.5978	
	5% Trimmed Mean		40.1296	
	Median		40.0000	
	Variance		5.367	
	Std. Deviation		2.31661	
	Minimum		37.00	
	Maximum		44.00	
	Range		7.00	
	Interquartile Range		3.25	
	Skewness		.568	.845
	Kurtosis		1.499	1.741
SiFnLn- 4hrs	Mean		61.5000	1.31022

	95% Confidence Interval for Mean	Lower Bound	58.1320	
		Upper Bound	64.8680	
	5% Trimmed Mean		61.5000	
	Median		62.0000	
	Variance		10.300	
	Std. Deviation		3.20936	
	Minimum		57.00	
	Maximum		66.00	
	Range		9.00	
	Interquartile Range		5.25	
	Skewness		-.082	.845
	Kurtosis		-.514	1.741
SiFnLn-24hrs	Mean		108.8333	1.85143
	95% Confidence Interval for Mean	Lower Bound	104.0741	
		Upper Bound	113.5926	
	5% Trimmed Mean		108.7037	
	Median		108.0000	
	Variance		20.567	
	Std. Deviation		4.53505	
	Minimum		104.00	
	Maximum		116.00	
	Range		12.00	
	Interquartile Range		8.25	
	Skewness		.722	.845
	Kurtosis		-.439	1.741

7.42: Keratinocyte vinculin per cell area descriptives on salinized non-passivated surfaces

Silanized, non-Passivated Surface				Statistic	Std. Error
Vinculin/Cell Area	Si- 1hr	Mean		.00240	.000764
		95% Confidence Interval for Mean	Lower Bound	.00044	
			Upper Bound	.00436	
		5% Trimmed Mean		.00245	
		Median		.00343	
		Variance		.000	
		Std. Deviation		.001871	
		Minimum		.000	
		Maximum		.004	
		Range		.004	
		Interquartile Range		.004	
		Skewness		-.916	.845
		Kurtosis		-1.877	1.741
	Si-4 hrs	Mean		.00243	.000053
		95% Confidence Interval for Mean	Lower Bound	.00230	
			Upper Bound	.00257	
		5% Trimmed Mean		.00243	
		Median		.00242	
		Variance		.000	
		Std. Deviation		.000129	
		Minimum		.002	

		Maximum	.003	
		Range	.000	
		Interquartile Range	.000	
		Skewness	.340	.845
		Kurtosis	-1.577	1.741
Si- 24hrs		Mean	.00682	.000606
	95% Confidence Interval for Mean	Lower Bound	.00526	
		Upper Bound	.00838	
		5% Trimmed Mean	.00687	
		Median	.00712	
		Variance	.000	
		Std. Deviation	.001484	
		Minimum	.005	
		Maximum	.008	
		Range	.004	
		Interquartile Range	.003	
		Skewness	-.633	.845
		Kurtosis	-1.156	1.741
SiFn- 1hr		Mean	.01281	.000687
	95% Confidence Interval for Mean	Lower Bound	.01104	
		Upper Bound	.01457	
		5% Trimmed Mean	.01277	
		Median	.01258	
		Variance	.000	
		Std. Deviation	.001684	
		Minimum	.011	

	Maximum		.015	
	Range		.004	
	Interquartile Range		.003	
	Skewness		.378	.845
	Kurtosis		-1.679	1.741
SiFn- 4hrs	Mean		.02531	.001362
	95% Confidence Interval for Mean	Lower Bound	.02180	
		Upper Bound	.02881	
	5% Trimmed Mean		.02536	
	Median		.02614	
	Variance		.000	
	Std. Deviation		.003337	
	Minimum		.020	
	Maximum		.029	
	Range		.009	
	Interquartile Range		.006	
	Skewness		-.498	.845
	Kurtosis		-1.220	1.741
SiFn- 24hrs	Mean		.04240	.001897
	95% Confidence Interval for Mean	Lower Bound	.03752	
		Upper Bound	.04728	
	5% Trimmed Mean		.04238	
	Median		.04237	
	Variance		.000	
	Std. Deviation		.004646	
	Minimum		.037	

		Maximum	.048	
		Range	.011	
		Interquartile Range	.009	
		Skewness	.027	.845
		Kurtosis	-2.672	1.741
SiLn- 1hr	Mean		.02500	.001612
	95% Confidence Interval for Mean	Lower Bound	.02085	
		Upper Bound	.02914	
	5% Trimmed Mean		.02484	
	Median		.02461	
	Variance		.000	
	Std. Deviation		.003948	
	Minimum		.021	
	Maximum		.032	
	Range		.011	
	Interquartile Range		.007	
	Skewness		1.009	.845
	Kurtosis		1.058	1.741
SiLn- 4hrs	Mean		.03490	.001152
	95% Confidence Interval for Mean	Lower Bound	.03194	
		Upper Bound	.03786	
	5% Trimmed Mean		.03491	
	Median		.03534	
	Variance		.000	
	Std. Deviation		.002821	
	Minimum		.032	

	Maximum		.038	
	Range		.007	
	Interquartile Range		.006	
	Skewness		-.217	.845
	Kurtosis		-2.320	1.741
SiLn- 24hrs	Mean		.05116	.001821
	95% Confidence Interval for Mean	Lower Bound	.04648	
		Upper Bound	.05584	
	5% Trimmed Mean		.05118	
	Median		.05223	
	Variance		.000	
	Std. Deviation		.004460	
	Minimum		.046	
	Maximum		.056	
	Range		.011	
	Interquartile Range		.009	
	Skewness		-.305	.845
	Kurtosis		-2.125	1.741
SiFnLn- 1hr	Mean		.04970	.001376
	95% Confidence Interval for Mean	Lower Bound	.04616	
		Upper Bound	.05323	
	5% Trimmed Mean		.04971	
	Median		.05001	
	Variance		.000	
	Std. Deviation		.003369	
	Minimum		.046	

	Maximum		.054	
	Range		.008	
	Interquartile Range		.006	
	Skewness		-.122	.845
	Kurtosis		-2.488	1.741
SiFnLn- 4hrs	Mean		.05154	.001095
	95% Confidence Interval for Mean	Lower Bound	.04872	
		Upper Bound	.05435	
	5% Trimmed Mean		.05160	
	Median		.05215	
	Variance		.000	
	Std. Deviation		.002682	
	Minimum		.048	
	Maximum		.054	
	Range		.006	
	Interquartile Range		.005	
	Skewness		-.370	.845
	Kurtosis		-2.346	1.741
SiFnLn- 24hrs	Mean		.07431	.001393
	95% Confidence Interval for Mean	Lower Bound	.07073	
		Upper Bound	.07790	
	5% Trimmed Mean		.07425	
	Median		.07288	
	Variance		.000	
	Std. Deviation		.003413	
	Minimum		.071	

			Statistic	Std. Error
		Maximum	.079	
		Range	.009	
		Interquartile Range	.006	
		Skewness	.727	.845
		Kurtosis	-1.416	1.741

7.43: Keratinocyte cell area descriptives on salinized passivated surfaces

	Silanized, Passivated Surface			Statistic	Std. Error
Cell Area (micrometres squared)	Si+ 1hr	Mean		306.6867	11.75370
		95% Confidence Interval for Mean	Lower Bound	276.4728	
			Upper Bound	336.9005	
		5% Trimmed Mean		306.3991	
		Median		303.5550	
		Variance		828.897	
		Std. Deviation		28.79057	
		Minimum		272.02	
		Maximum		346.53	
		Range		74.51	
		Interquartile Range		56.23	
		Skewness		.287	.845
		Kurtosis		-1.396	1.741
	Si+ 4hrs	Mean		367.9600	17.44037
		95% Confidence Interval for Mean	Lower Bound	323.1281	
			Upper Bound	412.7919	
		5% Trimmed Mean		369.0250	
		Median		376.0200	
		Variance		1825.000	

		Std. Deviation	42.72002	
		Minimum	300.98	
		Maximum	415.77	
		Range	114.79	
		Interquartile Range	78.60	
		Skewness	-.692	.845
		Kurtosis	-.398	1.741
Si+ 24hrs		Mean	751.6933	17.33588
	95% Confidence	Lower Bound	707.1300	
	Interval for Mean	Upper Bound	796.2566	
		5% Trimmed Mean	753.4204	
		Median	761.0300	
		Variance	1803.197	
		Std. Deviation	42.46407	
		Minimum	676.83	
		Maximum	795.47	
		Range	118.64	
		Interquartile Range	66.29	
		Skewness	-1.214	.845
		Kurtosis	1.525	1.741
SiFn+ 1hr		Mean	524.1333	13.26125
	95% Confidence	Lower Bound	490.0442	
	Interval for Mean	Upper Bound	558.2225	
		5% Trimmed Mean	522.5770	
		Median	520.1300	
		Variance	1055.165	
		Std. Deviation	32.48330	
		Minimum	494.27	
		Maximum	582.01	
		Range	87.74	
		Interquartile Range	48.76	
		Skewness	1.260	.845
		Kurtosis	1.706	1.741

SiFn+ 4hrs	Mean		860.9650	18.21252
	95% Confidence Interval for Mean	Lower Bound	814.1482	
		Upper Bound	907.7818	
	5% Trimmed Mean		861.6528	
	Median		864.4200	
	Variance		1990.175	
	Std. Deviation		44.61137	
	Minimum		804.81	
	Maximum		904.74	
	Range		99.93	
	Interquartile Range		85.72	
	Skewness		-.169	.845
	Kurtosis		-2.632	1.741
SiFn+ 24hrs	Mean		1161.3300	32.54592
	95% Confidence Interval for Mean	Lower Bound	1077.6680	
		Upper Bound	1244.9920	
	5% Trimmed Mean		1158.9272	
	Median		1121.5300	
	Variance		6355.421	
	Std. Deviation		79.72090	
	Minimum		1097.22	
	Maximum		1268.69	
	Range		171.47	
	Interquartile Range		159.16	
	Skewness		.877	.845
	Kurtosis		-1.850	1.741
SiLn+ 1hr	Mean		462.9733	23.73728
	95% Confidence Interval for Mean	Lower Bound	401.9547	
		Upper Bound	523.9920	
	5% Trimmed Mean		461.9231	
	Median		473.3650	
	Variance		3380.751	

		Std. Deviation		58.14423	
		Minimum		394.29	
		Maximum		550.56	
		Range		156.27	
		Interquartile Range		101.78	
		Skewness		.194	.845
		Kurtosis		-.382	1.741
SiLn+ 4hrs	Mean		799.4717	18.87334
	95% Confidence	Lower Bound	750.9562	
	Interval for Mean	Upper Bound	847.9871	
	5% Trimmed Mean		800.1763	
	Median		801.7100	
	Variance		2137.217	
	Std. Deviation		46.23005	
	Minimum		725.02	
	Maximum		861.24	
	Range		136.22	
	Interquartile Range		71.95	
	Skewness		-.489	.845
	Kurtosis		.834	1.741
SiLn+ 24hrs	Mean		996.2900	18.16759
	95% Confidence	Lower Bound	949.5887	
	Interval for Mean	Upper Bound	1042.9913	
	5% Trimmed Mean		996.3211	
	Median		1001.6900	
	Variance		1980.369	
	Std. Deviation		44.50133	
	Minimum		937.46	
	Maximum		1054.56	
	Range		117.10	
	Interquartile Range		85.75	
	Skewness		-.162	.845
	Kurtosis		-1.253	1.741

SiFnLn+ 1hr	Mean		856.0100	16.74587
	95% Confidence Interval for Mean	Lower Bound	812.9634	
		Upper Bound	899.0566	
	5% Trimmed Mean		855.3189	
	Median		846.5050	
	Variance		1682.544	
	Std. Deviation		41.01883	
	Minimum		813.70	
	Maximum		910.76	
	Range		97.06	
	Interquartile Range		85.67	
	Skewness		.512	.845
	Kurtosis		-1.779	1.741
SiFnLn+ 4hrs	Mean		1120.7217	26.36353
	95% Confidence Interval for Mean	Lower Bound	1052.9520	
		Upper Bound	1188.4913	
	5% Trimmed Mean		1121.9235	
	Median		1132.1400	
	Variance		4170.215	
	Std. Deviation		64.57720	
	Minimum		1023.77	
	Maximum		1196.04	
	Range		172.27	
	Interquartile Range		120.87	
	Skewness		-.542	.845
	Kurtosis		-.809	1.741
SiFnLn+ 24hrs	Mean		1476.6867	16.62267
	95% Confidence Interval for Mean	Lower Bound	1433.9567	
		Upper Bound	1519.4166	
	5% Trimmed Mean		1477.0513	
	Median		1484.9250	
	Variance		1657.878	

			Std. Error
Std. Deviation		40.71705	
Minimum		1421.40	
Maximum		1525.41	
Range		104.01	
Interquartile Range		80.35	
Skewness		-.401	.845
Kurtosis		-1.451	1.741

7.44: Keratinocyte vinculin per cell descriptives on salinized passivated surfaces

	Silanized, Passivated Surface			Statistic	Std. Error
Vinculin/Cell	Si+ 1hr	Mean		1.0000	.36515
		95% Confidence Interval for Mean	Lower Bound	.0614	
			Upper Bound	1.9386	
		5% Trimmed Mean		1.0000	
		Median		1.0000	
		Variance		.800	
		Std. Deviation		.89443	
		Minimum		.00	
		Maximum		2.00	
		Range		2.00	
		Interquartile Range		2.00	
		Skewness		.000	.845
		Kurtosis		-1.875	1.741
	Si+ 4hrs	Mean		1.5000	.22361
		95% Confidence Interval for Mean	Lower Bound	.9252	
			Upper Bound	2.0748	
		5% Trimmed Mean		1.5000	
		Median		1.5000	

		Variance	.300	
		Std. Deviation	.54772	
		Minimum	1.00	
		Maximum	2.00	
		Range	1.00	
		Interquartile Range	1.00	
		Skewness	.000	.845
		Kurtosis	-3.333	1.741
Si+ 24hrs		Mean	4.0000	.36515
	95% Confidence	Lower Bound	3.0614	
	Interval for Mean	Upper Bound	4.9386	
		5% Trimmed Mean	4.0000	
		Median	4.0000	
		Variance	.800	
		Std. Deviation	.89443	
		Minimum	3.00	
		Maximum	5.00	
		Range	2.00	
		Interquartile Range	2.00	
		Skewness	.000	.845
		Kurtosis	-1.875	1.741
SiFn+ 1hr		Mean	6.0000	.51640
	95% Confidence	Lower Bound	4.6726	
	Interval for Mean	Upper Bound	7.3274	
		5% Trimmed Mean	5.9444	
		Median	5.5000	
		Variance	1.600	
		Std. Deviation	1.26491	
		Minimum	5.00	
		Maximum	8.00	
		Range	3.00	
		Interquartile Range	2.25	
		Skewness	.889	.845

	Kurtosis		-.781	1.741
SiFn+ 4hrs	Mean		31.3333	1.62617
	95% Confidence	Lower Bound	27.1531	
	Interval for Mean	Upper Bound	35.5135	
	5% Trimmed Mean		31.2037	
	Median		31.0000	
	Variance		15.867	
	Std. Deviation		3.98330	
	Minimum		27.00	
	Maximum		38.00	
	Range		11.00	
	Interquartile Range		6.50	
	Skewness		.857	.845
	Kurtosis		.597	1.741
SiFn+ 24hrs	Mean		46.6667	1.89150
	95% Confidence	Lower Bound	41.8044	
	Interval for Mean	Upper Bound	51.5289	
	5% Trimmed Mean		46.7407	
	Median		48.5000	
	Variance		21.467	
	Std. Deviation		4.63321	
	Minimum		40.00	
	Maximum		52.00	
	Range		12.00	
	Interquartile Range		8.25	
	Skewness		-.659	.845
	Kurtosis		-1.205	1.741
SiLn+ 1hr	Mean		10.5000	.42817
	95% Confidence	Lower Bound	9.3993	
	Interval for Mean	Upper Bound	11.6007	
	5% Trimmed Mean		10.5000	
	Median		10.5000	

		Variance	1.100	
		Std. Deviation	1.04881	
		Minimum	9.00	
		Maximum	12.00	
		Range	3.00	
		Interquartile Range	1.50	
		Skewness	.000	.845
		Kurtosis	-.248	1.741
SiLn+ 4hrs		Mean	24.6667	1.14504
	95% Confidence	Lower Bound	21.7233	
	Interval for Mean	Upper Bound	27.6101	
		5% Trimmed Mean	24.6852	
		Median	25.0000	
		Variance	7.867	
		Std. Deviation	2.80476	
		Minimum	21.00	
		Maximum	28.00	
		Range	7.00	
		Interquartile Range	5.50	
		Skewness	-.224	.845
		Kurtosis	-1.864	1.741
SiLn+ 24hrs		Mean	44.5000	1.54380
	95% Confidence	Lower Bound	40.5315	
	Interval for Mean	Upper Bound	48.4685	
		5% Trimmed Mean	44.3333	
		Median	44.0000	
		Variance	14.300	
		Std. Deviation	3.78153	
		Minimum	41.00	
		Maximum	51.00	
		Range	10.00	
		Interquartile Range	6.25	
		Skewness	1.049	.845

		Kurtosis		.923	1.741
SiFnLn+ 1hr	Mean		39.0000	1.46059
	95% Confidence Interval for Mean	Lower Bound	35.2454	
		Upper Bound	42.7546	
	5% Trimmed Mean		39.0000	
	Median		39.5000	
	Variance		12.800	
	Std. Deviation		3.57771	
	Minimum		34.00	
	Maximum		44.00	
	Range		10.00	
	Interquartile Range		6.25	
	Skewness		-.118	.845
	Kurtosis		-.491	1.741
SiFnLn+ 4hrs	Mean		52.6667	.80277
	95% Confidence Interval for Mean	Lower Bound	50.6031	
		Upper Bound	54.7303	
	5% Trimmed Mean		52.6852	
	Median		53.0000	
	Variance		3.867	
	Std. Deviation		1.96638	
	Minimum		50.00	
	Maximum		55.00	
	Range		5.00	
	Interquartile Range		3.50	
	Skewness		-.254	.845
	Kurtosis		-1.828	1.741
SiFnLn+ 24hrs	Mean		92.3333	.76012
	95% Confidence Interval for Mean	Lower Bound	90.3794	
		Upper Bound	94.2873	
	5% Trimmed Mean		92.3148	
	Median		92.0000	

			Statistic	Std. Error
		Variance	3.467	
		Std. Deviation	1.86190	
		Minimum	90.00	
		Maximum	95.00	
		Range	5.00	
		Interquartile Range	3.50	
		Skewness	.392	.845
		Kurtosis	-.943	1.741

7.45: Keratinocyte vinculin per cell area descriptives on salinized passivated surfaces

	Silanized, Passivated Surface			Statistic	Std. Error
Vinculin/Cell Area	Si+ 1hr	Mean		.00174	.000622
		95% Confidence Interval for Mean	Lower Bound	.00015	
			Upper Bound	.00334	
		5% Trimmed Mean		.00172	
		Median		.00206	
		Variance		.000	
		Std. Deviation		.001523	
		Minimum		.000	
		Maximum		.004	
		Range		.004	
		Interquartile Range		.003	
		Skewness		.039	.845
		Kurtosis		-.733	1.741
	Si+ 4hrs	Mean		.00381	.000913
		95% Confidence Interval for Mean	Lower Bound	.00146	
			Upper Bound	.00616	

		5% Trimmed Mean	.00367	
		Median	.00259	
		Variance	.000	
		Std. Deviation	.002236	
		Minimum	.002	
		Maximum	.008	
		Range	.005	
		Interquartile Range	.003	
		Skewness	1.495	.845
		Kurtosis	1.252	1.741
Si+ 24hrs		Mean	.00133	.000422
	95% Confidence	Lower Bound	.00025	
	Interval for Mean	Upper Bound	.00242	
		5% Trimmed Mean	.00136	
		Median	.00193	
		Variance	.000	
		Std. Deviation	.001034	
		Minimum	.000	
		Maximum	.002	
		Range	.002	
		Interquartile Range	.002	
		Skewness	-.948	.845
		Kurtosis	-1.874	1.741
SiFn+ 1hr		Mean	.00276	.000342
	95% Confidence	Lower Bound	.00189	
	Interval for Mean	Upper Bound	.00364	
		5% Trimmed Mean	.00276	
		Median	.00274	
		Variance	.000	
		Std. Deviation	.000837	
		Minimum	.002	
		Maximum	.004	
		Range	.002	

		Interquartile Range		.002	
		Skewness		.019	.845
		Kurtosis		-3.243	1.741
SiFn+ 4hrs		Mean		.00741	.000441
		95% Confidence	Lower Bound	.00628	
		Interval for Mean	Upper Bound	.00855	
		5% Trimmed Mean		.00741	
		Median		.00747	
		Variance		.000	
		Std. Deviation		.001081	
		Minimum		.006	
		Maximum		.009	
		Range		.002	
		Interquartile Range		.002	
		Skewness		.016	.845
		Kurtosis		-2.744	1.741
SiFn+ 24hrs		Mean		.01443	.001018
		95% Confidence	Lower Bound	.01181	
		Interval for Mean	Upper Bound	.01705	
		5% Trimmed Mean		.01449	
		Median		.01526	
		Variance		.000	
		Std. Deviation		.002495	
		Minimum		.011	
		Maximum		.017	
		Range		.006	
		Interquartile Range		.005	
		Skewness		-.728	.845
		Kurtosis		-1.525	1.741
SiLn+ 1hr		Mean		.00185	.000684
		95% Confidence	Lower Bound	.00009	
		Interval for Mean	Upper Bound	.00361	

		5% Trimmed Mean	.00181	
		Median	.00210	
		Variance	.000	
		Std. Deviation	.001675	
		Minimum	.000	
		Maximum	.004	
		Range	.004	
		Interquartile Range	.003	
		Skewness	.310	.845
		Kurtosis	-.220	1.741
SiLn+ 4hrs		Mean	.00267	.000599
	95% Confidence	Lower Bound	.00113	
	Interval for Mean	Upper Bound	.00421	
		5% Trimmed Mean	.00276	
		Median	.00334	
		Variance	.000	
		Std. Deviation	.001466	
		Minimum	.000	
		Maximum	.004	
		Range	.004	
		Interquartile Range	.002	
		Skewness	-1.580	.845
		Kurtosis	1.939	1.741
SiLn+ 24hrs		Mean	.00812	.001091
	95% Confidence	Lower Bound	.00531	
	Interval for Mean	Upper Bound	.01092	
		5% Trimmed Mean	.00810	
		Median	.00779	
		Variance	.000	
		Std. Deviation	.002673	
		Minimum	.005	
		Maximum	.011	
		Range	.006	

		Interquartile Range	.006	
		Skewness	.258	.845
		Kurtosis	-1.976	1.741
SiFnLn+ 1hr		Mean	.00628	.000517
	95% Confidence	Lower Bound	.00495	
	Interval for Mean	Upper Bound	.00761	
		5% Trimmed Mean	.00622	
		Median	.00605	
		Variance	.000	
		Std. Deviation	.001266	
		Minimum	.005	
		Maximum	.008	
		Range	.003	
		Interquartile Range	.002	
		Skewness	1.162	.845
		Kurtosis	1.234	1.741
SiFnLn+ 4hrs		Mean	.00841	.001221
	95% Confidence	Lower Bound	.00527	
	Interval for Mean	Upper Bound	.01155	
		5% Trimmed Mean	.00841	
		Median	.00816	
		Variance	.000	
		Std. Deviation	.002992	
		Minimum	.004	
		Maximum	.012	
		Range	.008	
		Interquartile Range	.005	
		Skewness	.082	.845
		Kurtosis	-.980	1.741
SiFnLn+ 24hrs		Mean	.01071	.000745
	95% Confidence	Lower Bound	.00879	
	Interval for Mean	Upper Bound	.01262	

5% Trimmed Mean	.01070	
Median	.01123	
Variance	.000	
Std. Deviation	.001826	
Minimum	.008	
Maximum	.013	
Range	.005	
Interquartile Range	.003	
Skewness	-.152	.845
Kurtosis	-.476	1.741

7.46: *p* values for keratinocyte bioassay-cell area

1 hour

	Pol 1hr	AdFn 1hr	AdLn 1hr	AdFnLn 1hr	Si- 1hr	SiFn- 1hr	SiLn- 1hr	SiFnLn - 1hr	Si+ 1hr	SiFn+ 1hr	SiLn+ 1hr	SiFnLn + 1hr
Pol 1hr	-	0.004	0.004	0.004	0.337	0.004	0.004	0.004	0.004	0.004	0.004	0.004
AdFn 1hr	-	-	0.037	0.004	■	0.016	■	■	■	0.001	■	■
AdLn 1hr	-	-	-	0.004	■	■	0.001	■	■	■	0.873	■
AdFnLn 1hr	-	-	-	-	■	■	■	0.2	■	■	■	0.004
Si- 1hr	-	-	-	-	-	0.004	0.004	0.004	0.004	■	■	■
SiFn- 1hr	-	-	-	-	-	-	0.004	0.004	■	0.055	■	■
SiLn- 1hr	-	-	-	-	-	-	-	0.004	■	■	0.522	■
SiFnLn - 1hr	-	-	-	-	-	-	-	-	■	■	■	0.004
Si+ 1hr	-	-	-	-	-	-	-	-	-	0.004	0.025	0.004
SiFn+ 1hr	-	-	-	-	-	-	-	-	-	-	0.055	0.037
SiLn+ 1hr	-	-	-	-	-	-	-	-	-	-	-	0.006

7.47: *p* values for keratinocyte bioassay-vinculin per cell 1 hour

	Pol 1hr	AdFn 1hr	AdLn 1hr	AdFnLn 1hr	Si- 1hr	SiFn- 1hr	SiLn- 1hr	SiFnLn - 1hr	Si+ 1hr	SiFn+ 1hr	SiLn+ 1hr	SiFnLn + 1hr
Pol 1hr	-	0.004	0.004	0.004	0.484	0.004	0.004	0.004	0.733	0.299	0.733	0.003
AdFn 1hr	-	-	0.004	0.004		0.059				0.003		
AdLn 1hr	-	-	-	0.004			0.217				0.004	
AdFnLn 1hr	-	-	-	-				0.57				0.004
Si- 1hr	-	-	-	-	-	0.003	0.003	0.003	0.715			
SiFn- 1hr	-	-	-	-	-	-	0.004	0.004		0.003		
SiLn- 1hr	-	-	-	-	-	-	-	0.004			0.004	
SiFnLn - 1hr	-	-	-	-	-	-	-	-				0.004
Si+ 1hr	-	-	-	-	-	-	-	-	-	0.116	0.001	0.003
SiFn+ 1hr	-	-	-	-	-	-	-	-	-	-	0.116	0.003
SiLn+ 1hr	-	-	-	-	-	-	-	-	-	-	-	0.003

7.48: *p* values for keratinocyte bioassay-vinculin per cell area 1 hour

	Pol 1hr	AdFn 1hr	AdLn 1hr	AdFnLn 1hr	Si- 1hr	SiFn- 1hr	SiLn- 1hr	SiFnLn - 1hr	Si+ 1hr	SiFn+ 1hr	SiLn+ 1hr	SiFnLn + 1hr
Pol 1hr	-	0.004	0.004	0.004	0.744	0.004	0.004	0.004	0.328	0.748	0.328	0.054
AdFn 1hr	-	-	0.004	0.004		0.2				0.004		
AdLn 1hr	-	-	-	0.004			0.262				0.004	
AdFnLn 1hr	-	-	-	-				0.109				0.004
Si- 1hr	-	-	-	-	-	0.004	0.004	0.004	0.514			
SiFn- 1hr	-	-	-	-	-	-	0.004	0.004		0.004		
SiLn- 1hr	-	-	-	-	-	-	-	0.004			0.004	
SiFnLn - 1hr	-	-	-	-	-	-	-	-				0.004
Si+ 1hr	-	-	-	-	-	-	-	-	-	0.423	0.744	0.004
SiFn+ 1hr	-	-	-	-	-	-	-	-	-	-	0.423	0.004
SiLn+ 1hr	-	-	-	-	-	-	-	-	-	-	-	0.004

7.49: *p* values for keratinocyte bioassay-vinculin per cell area 4 hours

	Pol 4hrs	AdFn 4hrs	AdLn 4hrs	AdFnLn 4hrs	Si- 4hrs	SiFn- 4hrs	SiLn- 4hrs	SiFnLn - 4hrs	Si+ 4hrs	SiFn+ 4hrs	SiLn+ 4hrs	SiFnLn + 4hrs
Pol 4hrs	-	0.004	0.004	0.004	0.037	0.004	0.004	0.004	0.004	0.004	0.004	0.004
AdFn 4hrs	-	-	0.037	0.004		0.004				0.004		
AdLn 4hrs	-	-	-	0.004			0.016				0.004	
AdFnLn 4hrs	-	-	-	-				0.037				0.004
Si- 4hrs	-	-	-	-	-	0.004	0.004	0.004	0.016			
SiFn- 4hrs	-	-	-	-	-	-	0.006	0.004		0.004		
SiLn- 4hrs	-	-	-	-	-	-	-	0.004			0.004	
SiFnLn - 4hrs	-	-	-	-	-	-	-	-				0.004
Si+ 4hrs	-	-	-	-	-	-	-	-	-	0.004	0.004	0.004
SiFn+ 4hrs	-	-	-	-	-	-	-	-	-	-	0.055	0.01
SiLn+ 4hrs	-	-	-	-	-	-	-	-	-	-	-	0.004

7.50: *p* values for keratinocyte bioassay-vinculin 4 hours

	Pol 4hrs	AdFn 4hrs	AdLn 4hrs	AdFnLn 4hrs	Si-4hrs	SiFn-4hrs	SiLn-4hrs	SiFnLn-4hrs	Si+4hrs	SiFn+4hrs	SiLn+4hrs	SiFnLn+4hrs
Pol 4hrs	-	0.003	0.003	0.003	0.575	0.003	0.003	0.003	0.784	0.003	0.784	0.003
AdFn 4hrs	-	-	0.004	0.004		0.004				0.003		
AdLn 4hrs	-	-	-	0.004			0.01				0.003	
AdFnLn 4hrs	-	-	-	-				0.004				0.004
Si-4hrs	-	-	-	-	-	0.003	0.003	0.003	0.847			
SiFn-4hrs	-	-	-	-	-	-	0.013	0.004		0.003		
SiLn-4hrs	-	-	-	-	-	-	-	0.004			0.003	
SiFnLn-4hrs	-	-	-	-	-	-	-	-				0.004
Si+4hrs	-	-	-	-	-	-	-	-	-	0.003	0.73	0.004
SiFn+4hrs	-	-	-	-	-	-	-	-	-	-	0.003	0.319
SiLn+4hrs	-	-	-	-	-	-	-	-	-	-	-	0.003

7.51: *p* values for keratinocyte bioassayvinculin per cell area 4 hours

	Pol 4hrs	AdFn 4hrs	AdLn 4hrs	AdFnLn 4hrs	Si-4hrs	SiFn-4hrs	SiLn-4hrs	SiFnLn-4hrs	Si+4hrs	SiFn+4hrs	SiLn+4hrs	SiFnLn+4hrs
Pol 4hrs	-	0.004	0.004	0.004	0.01	0.004	0.004	0.004	0.337	0.004	0.262	0.016
AdFn 4hrs	-	-	0.004	0.004		0.025				0.004		
AdLn 4hrs	-	-	-	0.004			0.078				0.004	
AdFnLn 4hrs	-	-	-	-				0.025				0.004
Si-4hrs	-	-	-	-	-	0.004	0.004	0.004	0.2			
SiFn-4hrs	-	-	-	-	-	-	0.004	0.004		0.004		
SiLn-4hrs	-	-	-	-	-	-	-	0.004			0.004	
SiFnLn-4hrs	-	-	-	-	-	-	-	-				0.004
Si+4hrs	-	-	-	-	-	-	-	-	-	0.016	0.749	0.025
SiFn+4hrs	-	-	-	-	-	-	-	-	-	-	0.004	0.423
SiLn+4hrs	-	-	-	-	-	-	-	-	-	-	-	0.004

7.52: *p* values for keratinocyte bioassay-cell area 24 hours

	Pol 24hrs	AdFn 24hrs	AdLn 24hrs	AdFnLn 24hrs	Si- 24hrs	SiFn- 24hrs	SiLn- 24hrs	SiFnLn- 24hrs	Si+ 24hrs	SiFn+ 24hrs	SiLn+ 24hrs	SiFnLn+ 24hrs
Pol 24hrs	-	0.004	0.004	0.004	0.109	0.004	0.004	0.004	0.004	0.006	0.078	0.004
AdFn 24hrs	-	-	0.004	0.004	█	0.004	█	█	█	0.004	█	█
AdLn 24hrs	-	-	-	0.004	█	█	0.004	█	█	█	0.004	█
AdFnLn 24hrs	-	-	-	-	█	█	█	0.522	█	█	█	0.004
Si- 24hrs	-	-	-	-	-	0.004	0.004	0.004	0.004	█	█	█
SiFn- 24hrs	-	-	-	-	-	-	0.006	0.004	█	0.004	█	█
SiLn- 24hrs	-	-	-	-	-	-	-	0.004	█	█	0.004	█
SiFnLn- 24hrs	-	-	-	-	-	-	-	-	█	█	█	0.004
Si+ 24hrs	-	-	-	-	-	-	-	-	-	0.004	0.004	0.004
SiFn+ 24hrs	-	-	-	-	-	-	-	-	-	-	0.025	0.004
SiLn+ 24hrs	-	-	-	-	-	-	-	-	-	-	-	0.004

7.53: *p* values for keratinocyte bioassay-vinculin 24 hours

	Pol 24hrs	AdFn 24hrs	AdLn 24hrs	AdFnLn 24hrs	Si- 24hrs	SiFn- 24hrs	SiLn- 24hrs	SiFnLn- 24hrs	Si+ 24hrs	SiFn+ 24hrs	SiLn+ 24hrs	SiFnLn+ 24hrs
Pol 24hrs	-	0.004	0.004	0.004	0.032	0.004	0.004	0.004	0.003	0.004	0.07	0.004
AdFn 24hrs	-	-	0.01	0.004	█	0.004	█	█	█	0.004	█	█
AdLn 24hrs	-	-	-	0.004	█	█	0.004	█	█	█	0.004	█
AdFnLn 24hrs	-	-	-	-	█	█	█	0.004	█	█	█	0.004
Si- 24hrs	-	-	-	-	-	0.004	0.004	0.004	0.003	█	█	█
SiFn- 24hrs	-	-	-	-	-	-	0.065	0.004	█	0.004	█	█
SiLn- 24hrs	-	-	-	-	-	-	-	0.004	█	█	0.004	█
SiFnLn- 24hrs	-	-	-	-	-	-	-	-	█	█	█	0.004
Si+ 24hrs	-	-	-	-	-	-	-	-	-	0.003	0.003	0.003
SiFn+ 24hrs	-	-	-	-	-	-	-	-	-	-	0.006	0.869
SiLn+ 24hrs	-	-	-	-	-	-	-	-	-	-	-	0.006

7.54: *p* values for keratinocyte bioassay-vinculin per cell area 24 hours

	Pol 24hrs	AdFn 24hrs	AdLn 24hrs	AdFnLn 24hrs	Si- 24hrs	SiFn- 24hrs	SiLn- 24hrs	SiFnLn- 24hrs	Si+ 24hrs	SiFn+ 24hrs	SiLn+ 24hrs	SiFnLn+ 24hrs
Pol 24hrs	-	0.004	0.004	0.004	0.109	0.004	0.004	0.004	0.004	0.004	0.037	0.004
AdFn 24hrs	-	-	0.004	0.004	■	0.004	■	■	■	0.004	■	■
AdLn 24hrs	-	-	-	0.004	■	■	0.037	■	■	■	0.004	■
AdFnLn 24hrs	-	-	-	-	■	■	■	0.004	■	■	■	0.004
Si- 24hrs	-	-	-	-	-	0.004	0.004	0.004	0.004	■	■	■
SiFn- 24hrs	-	-	-	-	-	-	0.025	0.004	■	0.004	■	■
SiLn- 24hrs	-	-	-	-	-	-	-	0.004	■	■	0.004	■
SiFnLn- 24hrs	-	-	-	-	-	-	-	-	■	■	.004	0.004
Si+ 24hrs	-	-	-	-	-	-	-	-	-	0.004	0.004	0.004
SiFn+ 24hrs	-	-	-	-	-	-	-	-	-	-	0.01	0.037
SiLn+ 24hrs	-	-	-	-	-	-	-	-	-	-	-	0.109